

CSDL-T-902

**AN ADAPTIVE GUIDANCE ALGORITHM
FOR AN AERODYNAMICALLY ASSISTED
ORBITAL PLANE CHANGE MANEUVER**

by

Capt. James A. Blissit

May 1986

{NASA-CR-177296) AN ADAPTIVE GUIDANCE
ALGORITHM FOR AN AERODYNAMICALLY ASSISTED
ORBITAL PLANE CHANGE MANEUVER M.S. Thesis
(Draper (Charles Stark) Lab., Inc.) 229 p
HC A13/MF A01

N86-26933

Unclas
43592

CSCL 09B G3/61



The Charles Stark Draper Laboratory, Inc.

Cambridge, Massachusetts 02139

AN ADAPTIVE GUIDANCE ALGORITHM FOR AN AERODYNAMICALLY ASSISTED
ORBITAL PLANE CHANGE MANEUVER

by

James A Blissit Jr.

B. S., United States Air Force Academy

(1975)

SUBMITTED IN PARTIAL FULFILLMENT
OF THE REQUIREMENTS FOR THE
DEGREE OF

MASTER OF SCIENCE IN
AERONAUTICS AND ASTRONAUTICS

at the

MASSACHUSETTS INSTITUTE OF TECHNOLOGY

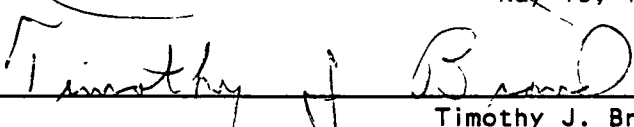
JUNE 1986

© James A. Blissit Jr., 1986

Signature of Author


Department of Aeronautics and Astronautics
May 16, 1986

Approved by


Timothy J. Brand
Technical Supervisor, CSDL

Certified by


Professor Antonio L. Elias
Thesis Supervisor,
Department of Aeronautics and Astronautics, MIT

Accepted by

Professor Harold Y. Wachman
Chairman, Department Graduate Committee

AN ADAPTIVE GUIDANCE ALGORITHM FOR AN AERODYNAMICALLY ASSISTED
ORBITAL PLANE CHANGE MANEUVER

BY

JAMES A. BLISSIT JR.

Submitted to the Department of Aeronautics and
Astronautics on 16 May 1986 in partial fulfillment of the
requirements for the Degree of Master of Science
in Aeronautics and Astronautics

ABSTRACT

Using analysis results from the POST trajectory optimization program, an adaptive guidance algorithm is developed to compensate for density, aerodynamic and thrust perturbations during an atmospheric orbital plane change maneuver. The maneuver offers increased mission flexibility along with potential fuel savings for future reentry vehicles. Although designed to guide a proposed NASA Entry Research Vehicle, the algorithm is sufficiently generic for a range of future entry vehicles. The plane change analysis provides insight suggesting a straight-forward algorithm based on an optimized nominal command profile. Bank angle, angle-of-attack, and engine thrust level, ignition and cutoff times are modulated to adjust the vehicle's trajectory to achieve the desired end-conditions. A performance evaluation of the scheme demonstrates a capability to guide to within 0.05 degrees of the desired plane change and five nautical miles of the desired apogee altitude while maintaining heating constraints. The algorithm is tested under off-nominal conditions of $\pm 30\%$ density biases, two density profile models, $\pm 15\%$ aerodynamic uncertainty, and a 33% thrust loss and for various combinations of these conditions. Based on fuel comparisons with results of the optimization program, the guidance scheme offers a nearoptimum solution without the complexity of real-time optimization.

Technical Supervisor: Mr. Timothy J. Brand
Title: Division Leader, Charles Stark Draper Laboratory,
Inc.

Thesis Advisor: Dr. Antonio L. Elias
Title: Assistant Professor of Aeronautics and Astronautics

ACKNOWLEDGEMENT

The production of this thesis was influenced by quite a few people and it is only fitting that I should start with an expression of my thanks and appreciation to them.

First and foremost, without the continuous support of my family (Maria, Carmen, and Jessica), I could have never made it to this satisfying point of my career. To them, I send my sincere thanks for everything and my love, always.

Thanks to my advisor, Professor Antonio Eliás, and my Draper Supervisor, Tim Brand, for their support, advice and guidance. To the rest of the technical staff at Draper, especially Bob Richards with his continuous willing assistance and advice, Bernie Kriegsman with his constant words of encouragement, Steve Bauer who got me out of the office often enough to keep my in-office time efficient and Florie Fabiano who is responsible for making this document look as great as it does, I say thanks for everything. Draper has certainly been an enlightening place to work and a highlight of my time at MIT.

Thanks to Howard Stone, Dick Powell, and the rest of the Vehicle Analysis Branch at NASA Langley Research Center who provided a great place to start my research experience and continued to provide assistance, support, and advice throughout my effort.

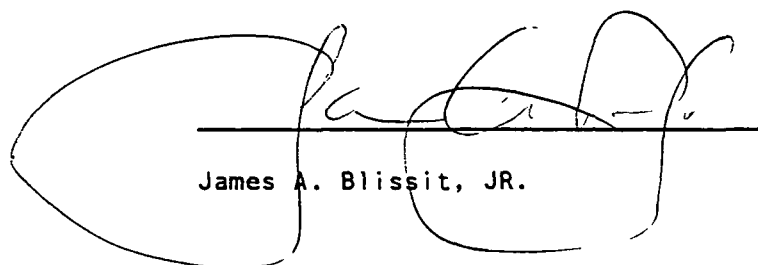
A special thanks to the men and women of our space program who through their efforts have provided a great deal of motivation to myself and I am sure, countless others. The price of their efforts can be quite high as the tragedy of "Challenger" has reminded us all, but the rewards of success can be truly sensational and beyond our imagination. Thus, I dedicate this paper to the crew of "Challenger" and all the men and women who follow them in our quest for the stars. Good luck!

Finally, I would like to extend a special thanks to one person in particular. Like most things I have encountered as I have moved along, this thesis is very much a product of the work and effort that was put into it. Whether it sinks or floats will be left to history, but the contribution that it has played in my overall education is already fixed and can not be modified or deleted. Therefore, I say thanks for the dedication and effort that I exerted to make this a worthwhile contribution, because this time has surely been a rewarding experience. Thanks!

This report was prepared at the Charles Stark Draper Laboratory, Inc. under Contract NAS1-18061.

Publication of this report does not constitute approval by the Draper Laboratory or the National Aeronautics and Space Administration (NASA) of the findings or conclusions contained herein.

I hereby assign my copyright of this thesis to The Charles Stark Draper Laboratory, Inc. Cambridge, Massachusetts.



James A. Blissit, JR.

Permission is hereby granted by the Charles Stark Draper Laboratory, Inc. to the Massachusetts Institute of Technology to reproduce any or all of this thesis.

TABLE OF CONTENTS

<u>CHAPTER</u>	<u>PAGE</u>
1. INTRODUCTION	16
1.1 Thesis Contribution and Scope	17
1.2 Thesis Overview	18
2. PROBLEM BACKGROUND	20
2.1 Introduction	20
2.2 Concept Justification	24
2.3 Vehicle Description	27
2.4 Baseline Trajectory	32
2.4.1 Background and Strategy	32
2.4.2 Trajectory Development and Understanding	34
2.5 Guidelines and Requirements	44
3. PROBLEM DEVELOPMENT	48
3.1 Introduction	48
3.2 Guidance Characteristics and Concepts	49
3.3 Control Variables and Pairings	53
4. TRAJECTORY ANALYSIS	56

<u>CHAPTER</u>	<u>PAGE</u>
4.1 Introduction	56
4.2 Method of Analysis	58
4.2.1 Objective	58
4.2.2 Specific Approach	59
4.2.3 Limitations	60
4.3 Overall Results	62
4.4 Detailed Results	64
4.4.1 Density Perturbations	66
4.4.2 Aerodynamic Uncertainties	74
4.4.3 Heat-Rate Variation	82
4.4.4 Single-Engine Failure	84
4.4.5 Multiple Off-Nominal Conditions	89
 5. GUIDANCE SCHEME	 108
5.1 Introduction	108
5.2 Guidance Algorithm	111
5.2.1 Entry Phase	111
5.2.2 Cruise Phase	113
5.2.3 Exit Phase	116
5.3 Guidance Rationale	119
5.3.1 Entry Phase	119
5.3.2 Cruise Phase	120
5.3.3 Exit Phase	122

CHAPTER

PAGE

6. GUIDANCE ALGORITHM TESTING 124

 6.1 Introduction 124

 6.2 Evaluation Criteria and the Nominal Simulation 125

 6.3 Simulation Test Results 129

 6.3.1 Single Off-Nominal Condition Tests 129

 6.3.2 Multiple Off-Nominal Condition Tests 163

7. SUMMARY, CONCLUSIONS, AND TOPICS FOR FURTHER RESEARCH 177

 7.1 Summary 177

 7.2 Conclusions 178

 7.3 Topics for Further Research 179

 7.3.1 Node Control 180

 7.3.2 Plane Change Trajectory Improvements 180

 7.3.3 Heat-Rate Control 181

 7.3.4 Minimum Fuel 181

 7.3.5 Apogee Control 182

LIST OF REFERENCES 183

APPENDIX

A. POST 187

 A.1 Introduction 187

 A.2 POST Description 187

<u>CHAPTER</u>	<u>PAGE</u>
A.3 Trajectory Generation Example	190
A.3.1 Input File Description	206
A.3.2 Output Description	209
B. DRAPER ERV COMPUTER SIMULATOR AND GUIDANCE ALGORITHM	224
B.1 Simulator Description	224
B.2 Simulator and Guidance Algorithm Computer Program .	224

List Of Illustrations

<u>FIGURE</u>	<u>PAGE</u>
2-1 Candidate missions for the entry research vehicle	23
2-2 Typical entry profile for an ERV synergetic plane change followed by reentry	23
2-3 Comparison of fuel requirements for all-propulsive maneuvers and synergetic maneuvers to produce an orbital inclination change of the ERV	26
2-4 Comparison of ΔV requirements for all-propulsive maneuvers and synergetic maneuvers to produce an orbital inclination change of the ERV	26
2-5 Optimum convective heat-rate for synergetic orbital inclination change using the ERV	28
2-6 Artist's concept of the ERV	28
2-7 Three-view drawing of the ERV	31
2-8 Inboard profile of the ERV	31
2-9 Altitude profiles for synergetic plane changes using the ERV	36
2-10 Angle-of-attack profiles for synergetic plane change using the ERV	36
2-11 Bank profiles for synergetic plane change using the ERV	37
2-12 Engine throttling profiles for synergetic plane change using the ERV	37
2-13 Heat-rate profiles for synergetic plane change using the ERA	38
2-14 Heat-load profiles for synergetic plane change using the ERV	38
2-15 POST synergetic plane change altitude profile and generic	

<u>FIGURE</u>	<u>PAGE</u>
phase names	39
4-1 Heat-rate profiles for +30% density, -15% CL and +15% CD ...	94
4-2 Dynamic pressure profiles for +30% density, -15% CL and +15% CD	96
4-3 Bank angle profiles for +30% density, -15% CL and +15% CD ..	98
4-4 Engine throttling profiles for +30% density, -15% CL and +15% CD	99
4-5 Heat-rate profiles for -30% density, -15% CL and +15% CD ...	101
5-1 Guidance algorithm phases	110
5-2 Synergetic plane change guidance system summary	112
6-1 Altitude profiles for QDOT = 80 and 125, nominal conditions	130
6-2 Vehicle velocity profiles for QDOT = 80 and 125, nominal conditions	131
6-3 Angle-of-attack profiles for QDOT = 80 and 125, nominal conditions	132
6-4 Bank angle profiles for QDOT = 80 and 125, nominal conditions	133
6-5 Engine throttling profiles for QDOT = 80 and 125, nominal conditions	134
6-6 Heat-rate profiles for QDOT = 80 and 125, nominal conditions	135
6-7 Inclination change profiles for QDOT = 80 and 125, nominal conditions	136
6-8 Apogee and perigee altitude profiles for QDOT = 80 and 125, nominal conditions	137
6-9 Altitude and vehicle velocity profiles for QDOT = 80, +50% density bias	141
6-10 Angle-of-attack and bank angle profiles for QDOT = 80, +50% density bias	142
6-11 Engine throttling and heat-rate profiles for QDOT = 80, +50% density bias	143
6-12 Inclination change, apogee and perigee altitude profiles for QDOT = 80, +50% density bias	144

<u>FIGURE</u>	<u>PAGE</u>
6-13 STS-4 density profile	147
6-14 CSDL density shear model profile	148
6-15 Altitude and vehicle velocity profiles for QDOT = 125, sts-4 density shear profile	151
6-16 Angle-of-attack and bank angle profiles for QDOT = 125, STS-4 density profile	152
6-17 Engine throttling and heat-rate profiles for QDOT = 125, STS-4 density profile	153
6-18 Inclination change, and density perturbation profiles for QDOT = 125, STS-4 density profile	154
6-19 Altitude and vehicle velocity profiles for QDOT = 125, -25% CL and +25% CD	158
6-20 Angle-of-attack and bank angle profiles for QDOT = 125, -25% CL and +25% CD	159
6-21 Engine throttling and heat-rate profiles for QDOT = 125, -25% CL and +25% CD	160
6-22 Inclination change, apogee and perigee altitude profiles for QDOT = 125, -25% CL and +25% CD	161
6-23 Altitude and vehicle velocity profiles for QDOT = 125, single-engine failure at level-off	165
6-24 Angle-of-attack and bank angle profiles for QDOT = 125, single-engine failure at level-off	166
6-25 Engine throttling and heat-rate profiles for QDOT = 125, single-engine failure at level-off	167
6-26 Inclination change, apogee and perigee altitude profiles for QDOT = 125, single-engine failure at level-off	168
6-27 Altitude and vehicle velocity profiles for QDOT = 125, -30% density, -15% CL and +15% CD, single-engine failure at level-off	171
6-28 Angle-of-attack and bank angle profiles for QDOT = 125, -30% density, -15% CL and +15% CD, single-engine failure at level-off	172
6-29 Engine throttling and heat-rate profiles for QDOT = 125, -30% density, -15% CL and +15% CD, single-engine failure at level-off	173
6-30 Inclination change, apogee and perigee altitude profiles for QDOT = 125, -30% density, -15% CL and +15% CD,	

<u>FIGURE</u>	<u>PAGE</u>
single-engine failure at level-off	174
A-1 Sample of POST output data for cruise phase	211
A-2 Sample of POST output data for circularization phase	212
A-3 Sample of POST trajectory summary	213
A-4 Baseline altitude profiles	215
A-5 Baseline vehicle velocity relative to the atmosphere profile	216
A-6 Baseline angle-of-attack profiles	217
A-7 Baseline bank angle profiles	218
A-8 Baseline engine throttling profiles	219
A-9 Baseline heat-rate profiles	220
A-10 Baseline heat-load profiles	221
A-11 Baseline dynamic Pressure profiles	222
A-12 Baseline inclination angle profiles	223
B-1 ERV top-level computer simulation and guidance algorithm flowchart	228

List of Tables

<u>TABLE</u>		<u>PAGE</u>
4-1	Density bias "Open-Loop" results with POST	68
4-2	Density bias optimization results for QDOT = 80	70
4-3	Density bias optimization results for QDOT = 125	71
4-4	Density bias optimization results for QDOT = 125 with entry parameters fixed	72
4-5	Aerodynamic uncertainty "Open-Loop" results with POST	76
4-6	Aerodynamic uncertainty optimization results for QDOT = 80	77
4-7	Aerodynamic uncertainty optimization results for QDOT = 125	78
4-8	Aerodynamic uncertainty optimization results for QDOT = 125 with entry parameters fixed	79
4-9	Single-engine failure "Open-Loop" results with POST for QDOT = 125	86
4-10	Single-engine failure optimization results for QDOT = 125 ..	88
4-11	Multiple off-nominal "Open-Loop" results with POST for QDOT = 125	91
4-12	Multiple off-nominal optimization results for QDOT = 125 with entry parameters fixed	93
4-13	Multiple off-nominal optimization results for QDOT = 125 with entry parameters fixed	102
4-14	Multiple off-nominal optimization results for QDOT = 125 ...	105
4-15	Multiple off-nominal optimization results for QDOT = 125 ...	106
6-1	Density bias test results for QDOT = 80	139
6-2	Density bias test results for QDOT = 125	140
6-3	Density shear test results for QDOT = 125	150
6-4	Aerodynamic uncertainty test results for QDOT = 80	156
6-5	Aerodynamic uncertainty test results for QDOT = 125	157
6-6	Single-engine failure test results	164

TABLE

PAGE

6-7	Multiple off-nominal test results for QDOT = 80	169
6-8	Multiple off-nominal test results for QDOT = 125	170

CHAPTER 1

INTRODUCTION

A potential joint NASA/Air Force atmospheric reentry research flight experiment is being considered for the 1990 time frame. This flight experiment will help provide the technology base for development of future reusable earth-to-orbit transportation systems and Air Force aero/space vehicles. The experimental vehicle is envisioned to be carried aloft and deployed in orbit by the Space Shuttle. After executing a deorbit procedure, the vehicle will reenter the atmosphere to perform a variety of maneuvers and experiments and eventually glide to a landing site.

One of the more interesting maneuvers is the synergetic orbital plane change. A synergetic plane change is a maneuver in which a change in the orbital inclination is accomplished through a combination of aerodynamic and propulsive forces rather than through propulsion alone (17). The guidance system presented here is designed to guide a winged vehicle such as the proposed NASA Entry Research Vehicle (ERV) during the atmospheric phase of a synergetic plane change mission. This mission involves a deorbit maneuver and aerodynamic turn in the atmosphere combined with a powered cruise and exit back into orbit. The guidance

system takes the vehicle from entry interface (400,000 feet), through the atmospheric maneuvering turn and back to orbit.

1.1 THESIS CONTRIBUTION AND SCOPE

This thesis presents the problem analysis, development, and testing of a guidance algorithm for a synergetic plane change maneuver for NASA's ERV. The motivation for this effort was the design analysis requirements for the development of the guidance scheme. The major contribution is the new level of insight on how to efficiently perform this maneuver in the presence of density and vehicular perturbations. The guidance algorithm is a summation of this insight and satisfies NASA's requirement for a generic guidance scheme. The testing of the algorithm demonstrates the effectiveness of the scheme and indirectly adds support or proof to the analysis results. Hence the parts fit nicely together as a complete monograph with each part both resting on and supporting the other parts.

The guidance algorithm is only one possibility of many guidance schemes that could and will, as demand requires, be developed to satisfy the mission. However, it completely satisfies the stated NASA requirements at this conceptual phase of ERV development. In addition, the algorithm offers a basic scheme to modify and refine as the ERV program

progresses and a standard to measure future schemes against. In short, the guidance algorithm is a simple straight-forward application of the results from the synergetic plane change trajectory analysis.

The algorithm testing was conducted on a three degree of freedom computer simulator developed at The Charles Stark Draper Laboratory (CSDL) for the NASA ERV contract. The algorithm testing is by no means exhaustive but for the time and money constraints, it does offer a good validation of the guidance algorithm.

1.2 Thesis Overview

In the remaining six chapters, this thesis details the problem development and analysis along with guidance algorithm development and testing. Chapter 2 presents background information for the ERV and synergetic plane change problem to include concept justification, vehicle description, an explanation of the baseline trajectories, and basic NASA guidelines and requirements. Chapter 3 contains a brief discussion of the initial problem development and formulation. Chapter 4 details the problem analysis with a computer optimization program called "POST". This analysis provides insight into the difficulty of the guidance problem along with specific means of handling density, aerodynamic and propulsive uncertainties. Chapter 5 presents our final iteration of the guidance scheme along with rationale leading to the scheme.

The evaluation criteria and test results for the algorithm are contained in Chapter 6. Chapter 7 summarizes the work covered in this thesis and discusses what can be done to expand on the analysis insight and possible algorithm improvements. Appendix A provides a brief explanation of "POST" along with an example trajectory generation. A brief description and flowchart for the Draper Laboratory ERV simulator and guidance algorithm computer programs are presented in Appendix B.

CHAPTER 2

PROBLEM BACKGROUND

2.1 Introduction

During the past few years, there has been resurgence of national interest in vehicles that can maneuver in the atmosphere while returning from orbit and vehicles that can fly in the atmosphere at hypersonic speeds for sustained periods of time. This rebirth of interest in hypersonics has resulted both from the success of the Space Shuttle and from a developing awareness of the potential benefits that can be derived from vehicles with the capability to operate between the limits of existing aircraft and spacecraft. Examples of the types of maneuvers that are projected for this new class of vehicles are presented in Figure 2-1. Most of the projected requirements are dictated by either a need for flexibility offered by a large landing footprint or by a requirement for specific entry maneuvers such as a synergetic plane change (4).

For vehicles that operate in space or in the upper reaches of the atmosphere, an orbital plane change offers significant flexibility for

Earth overflight and space operations. Specifically, the studies of the late 1960's indicated that the same type of high lift-to-drag ratio (L/D) vehicle required for the synergetic plane change maneuver could also perform Earth-return missions with large cross range capability, could perform evasive maneuvers, and could have considerable military as well as civilian uses (17). This new class of vehicles will dictate new requirements for the vehicle's thermal protection systems (TPS) and thermo-structures design. The plane change maneuver will require a TPS designed for a high heat-rate while the large landing foot print will require a high heat-rate and heat-load capability (6). The Space Shuttle provides a good starting point but to achieve the potential fuel efficiency and large landing foot print will require an improvement in TPS capability.

Addressing the technology deficiencies for these future systems will provide a significant challenge for the aerospace community. The synergetic or atmospheric plane change will be one of the more difficult missions for future entry vehicles. Analysis to date have shown that performance of the maneuver will require sustained flight at or near entry mach numbers at altitudes over 200,000 feet. This is the flight regime where the predicted aerodynamic trim of the Space Shuttle orbiter was in error by as much as nine degrees body-flap deflection (4). Whereas the shuttle currently flies a tightly tailored trajectory, the flight envelope for the ERV will be broadened to allow the vehicle to

maneuver during entry. The results from Space Shuttle flights presented in Reference 4 have shown density variations as large as 60 percent in the altitude regime where the synergetic plane change maneuver occurs. This large density variation is random, can not be predicted and must, therefore, be treated as an uncertainty in the estimated aerodynamics and aeroheating used in the vehicle design.

With the ERV, NASA is attempting to address these issues and develop a building block approach to handling the difficulties. The ERV is designed to demonstrate atmospheric maneuvers that are beyond the capability of existing spacecraft and aircraft. Presented in Figure 2-2 is a typical altitude time profile for an entry research vehicle flight where first a synergetic turn is performed, and then the vehicle performs a normal entry (4). As shown in the figure, the entry vehicle is released from the shuttle, performs a deorbit burn, and then descends into the atmosphere to an altitude of approximately 220,000 feet. There the engines are started, and the vehicle cruises at a mach number of 25 until its exit point. It then uses a combination of angle-of-attack and throttle to reboost into orbit while completing the plane change. After remaining on orbit for several revolutions, the vehicle deorbits and performs an entry and landing.

In order to accommodate the large density variations and vehicle aerodynamic uncertainties referred to earlier, the new vehicle will be

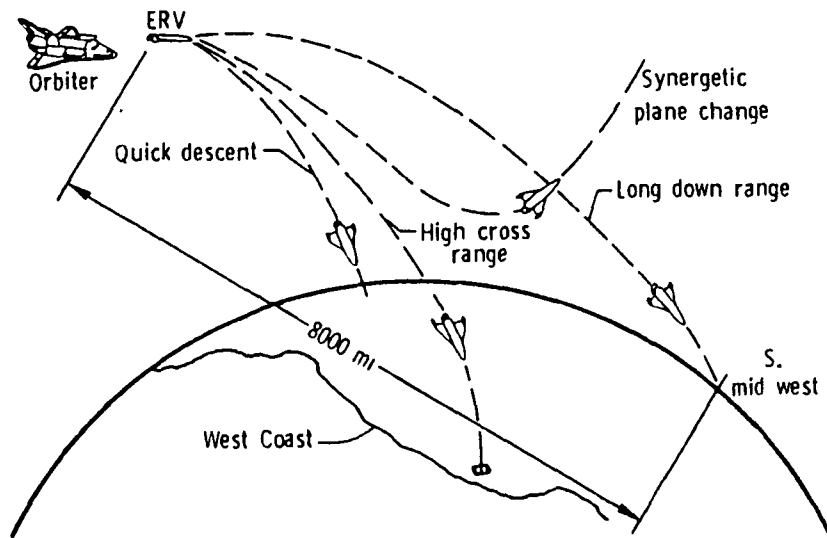


Figure 2-1. Candidate missions for the entry research vehicle [4].

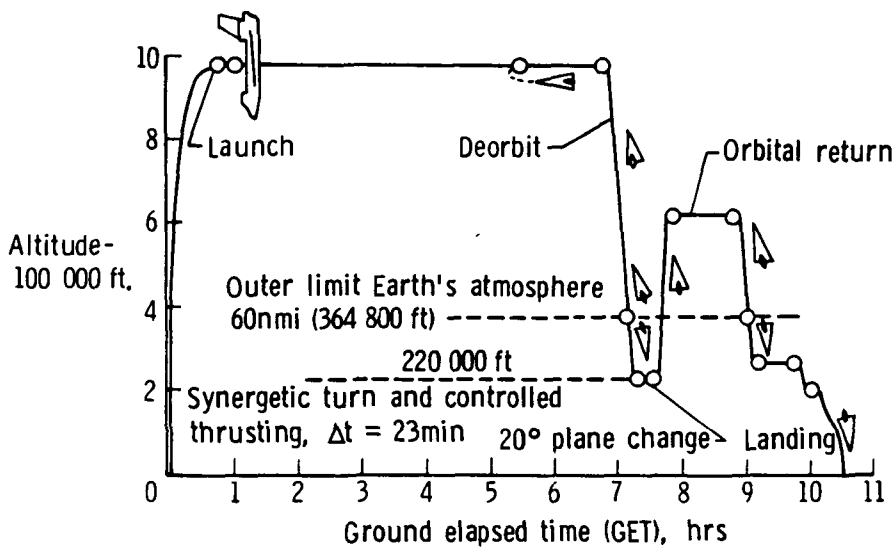


Figure 2-2. Typical entry profile for an ERV synergetic plane change followed by reentry [4].

required to have a sophisticated adaptive guidance and navigation system. This system must be able to sense the atmospheric conditions and provide necessary control inputs in real-time to enable the vehicle to accurately achieve its end-conditions and remain within the vehicle's flight boundaries. The best previous example is the Space Shuttle. However, the shuttle worked around these uncertainties by designing into the guidance algorithm large margins for error. This resulted in a reentry trajectory with less concern for maneuvering efficiency than is possible with the ERV and often the solution to handling the uncertainties (e.g., roll reversals) resulted in other problems like attitude instability of the vehicle (8). The ERV is designed to demonstrate the technologies required to perform a synergetic plane change mission and other maneuvering entries. Thus, an acceptable guidance system must be able to efficiently compensate for the discussed uncertainties while safely executing the maneuver.

2.2 Concept Justification

The strongest argument for a synergetic plane change is the opportunity for a significant reduction in the amount of fuel required for an orbital plane change maneuver. Many studies have shown that for a large plane change in low-earth orbit, a synergetic plane change will use less fuel than an all-propulsive maneuver. The initial motivation for this work was the recognition that orbital plane changes required very large

characteristic velocities (ΔV). As pointed out by Caudra and Arthur (18), the ΔV required for a single-impulse 60 degree plane change is as large as that required to place a satellite in low earth orbit in the first place. The fuel required for the 12,000 pound ERV to perform a 20-degree orbital inclination change is shown in Figure 2-3, and the corresponding velocity change requirement is shown in Figure 2-4. Results are shown for an in-orbit, all-propulsive maneuver and for two synergetic plane change maneuvers, one constrained to a maximum convective heat-rate referenced to a one-foot radius sphere of 80 BTU/ft²-sec and one constrained to a maximum heat-rate of 125 BTU/ft²-sec. For the ERV to perform an all-propulsive plane change requires 7100 pounds (lbs) of propellant. The same plane change using an aerodynamic turn limited by heating to 80 BTU/ft²-sec requires 6400 pounds of propellant. If the ERV can withstand a heating rate of 125 BTU/ft²-sec, the fuel savings are even greater, and only 5500 lbs of fuel would be required (6). It should be kept in mind however, that significant fuel savings are only realized for a vehicle that already requires the added weight for TPS and wings. Or as Maslau concluded "... the results indicate that the synergetic mode can be more desirable than in-orbit propulsion only if the aerodynamic performance must be provided for other reasons..." (20).

Further analysis done at NASA Langley Research Center (LaRC), determined that there is an optimum heat-rate depending on the amount of desired plane change. Figure 2-5 provides a curve of this heat-rate

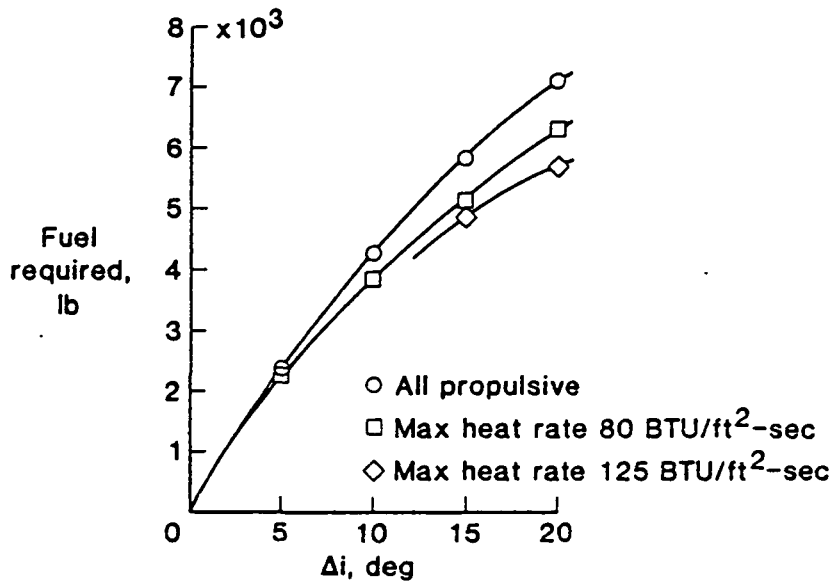


Figure 2-3. Comparison of fuel requirements for all-propulsive maneuvers and synergetic maneuvers to produce an orbital inclination change of the ERV [4].

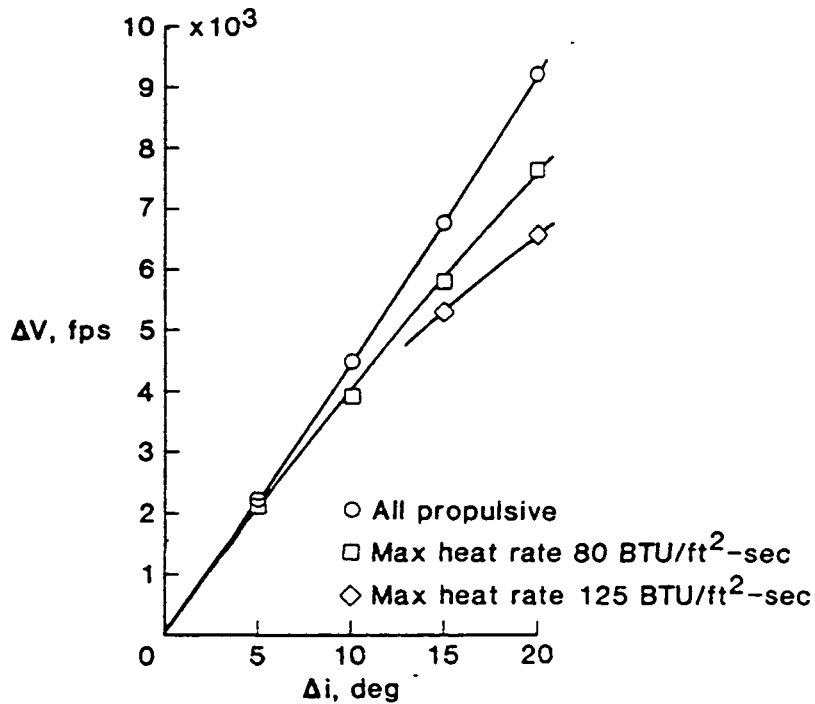


Figure 2-4. Comparison of Delta V requirements for all-propulsive maneuvers and synergetic maneuvers to produce an orbital inclination change of the ERV [4].

verses inclination relationship for the ERV for angles through 20 degrees. Specifically, the results indicated that 125 BTU/ft²-sec was nearly the optimum heat-rate for a 20 degree plane change and a higher heat-rate of say 135 BTU/ft²-sec will actually require more fuel (6). Thus, the maximum allowable heat-rate will significantly influence the vehicle's fuel efficiency and, as it will be shown later, the vehicle's trajectory and response to perturbations.

2.3 Vehicle Description

The candidate Entry Research Vehicle shown in Figure 2-6 is 25 feet long with a wing span of 13.9 feet. It is designed to occupy half of the Shuttle cargo bay which is 60 feet long and 15 feet in diameter. The vehicle has a distinct wing-body design with a blended wing-body interface to increase the overall hypersonic performance of the vehicle. The wing has a reference area of 177.4 square feet. Conventional elevons are used for pitch and roll control, and tip-fin controllers provide the yaw stability augmentation and control. A body flap assists in trimming the vehicle hypersonically. Reaction control system jets are used to control the vehicle in the upper atmosphere. The jets are placed in the nose of the vehicle and in the tip fins. Figure 2-7 is a three-view drawing of the ERV with the basic vehicle dimensions and relationship with the Shuttle payload bay envelope. The fineness ratio of the fuselage is approximately six, and its volume is 300 cubic feet.

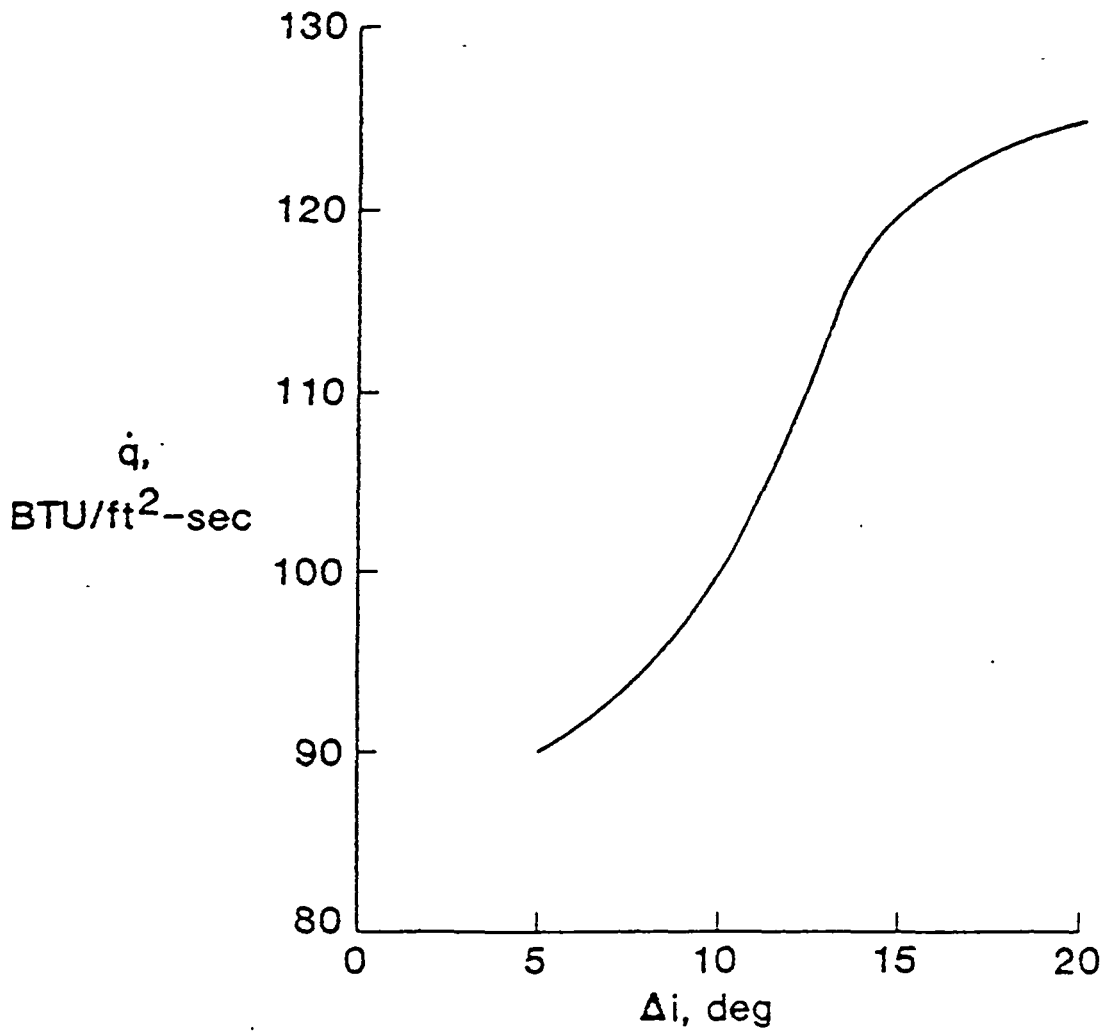


Figure 2-5. Optimum convective heat-rate for synergetic orbital inclination change using the ERV [6].

ORIGINAL PAGE IS
OF POOR QUALITY

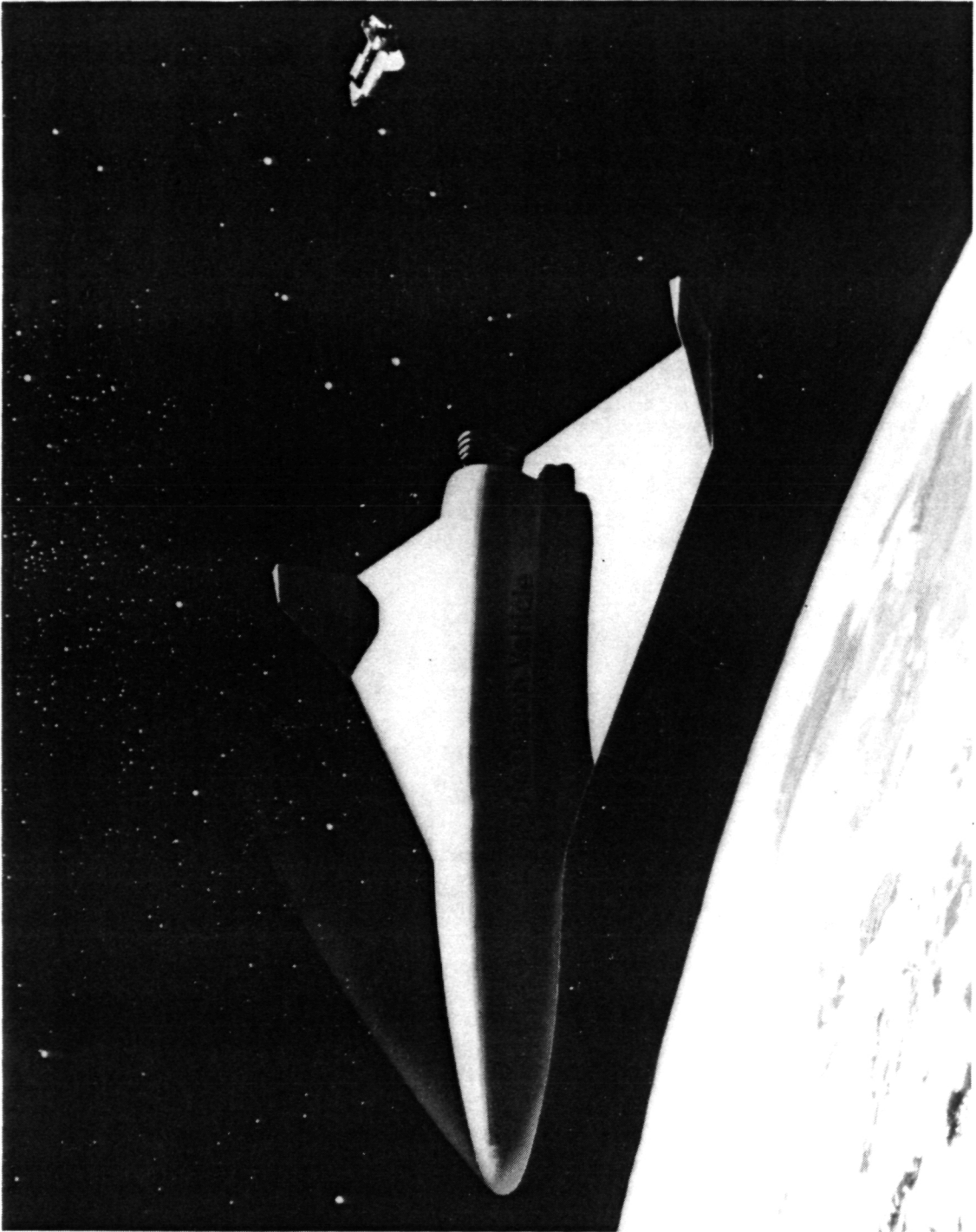


Figure 2-6. Artist's concept of the ERV [5].

Figure 2-8 shows an inboard profile of the ERV. The payload bay housing many of the experiments is located in the nose of the vehicle where atmospheric sensing can be performed with minimal engine combustion by-product contamination. The avionics are located behind the payload compartment. To minimize the center-of-gravity shift as propellant is depleted, the fuel and oxidizer tanks are positioned around the center of gravity which is located at 67 percent of the body length. The electrical system and batteries are positioned between the fuel tanks, approximately at the center of gravity. Propulsion is provided by three Marquardt R-40-B rocket motors, each providing 1100 pounds of thrust with an ISP of 295 seconds. The engines are aligned with the vehicle's longitudinal axis and thrust through the vehicle's center of gravity.

The vehicle's launch weight from the Shuttle is estimated to be 11,430 pounds. 6000 pounds of propellant is carried to provide the nearly 7000 feet-per-second ΔV required for a 20 degree synergetic plane change maneuver with the Marquardt engines. The leading-edge sweep angle is 72.5 degrees. An NACA four-digit series symmetrical airfoil section is used for the wing and its hypersonic maximum L/D is approximately two. Complete coefficient of lift (CL) and drag (CD) data is provided in Appendix A. The thickness ratio was varied to maintain a half-inch radius over the entire leading edge of the wing. The geometric shape of the wing was designed with the intention of reducing the aerothermodynamic heating on entry. A heat pipe, in addition to new

Theoretical wing area = 177.40 ft²
 Body flap area = 7.50 ft²
 Elevon area per side = 6.07 ft²
 Aileron area per side = 0.88 ft²
 Tip fin area per side = 4.16 ft²

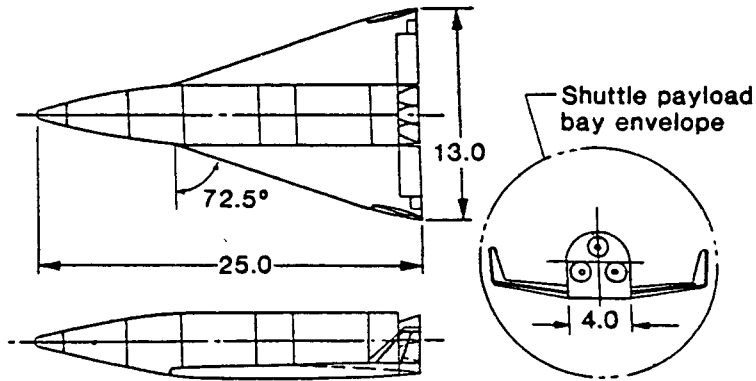
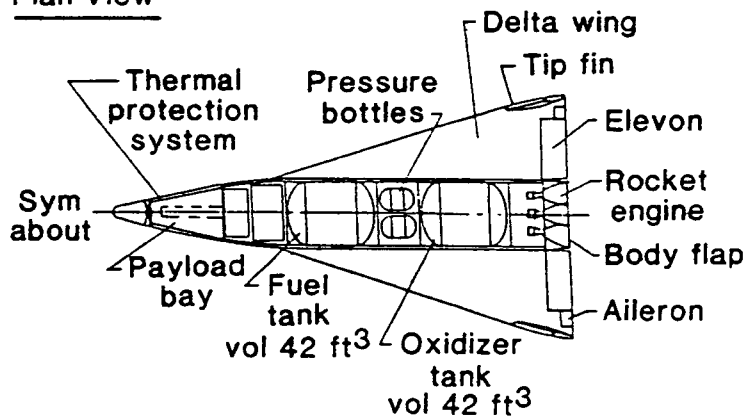


Figure 2-7. Three-view drawing of the ERV [5].

Plan View



Side View

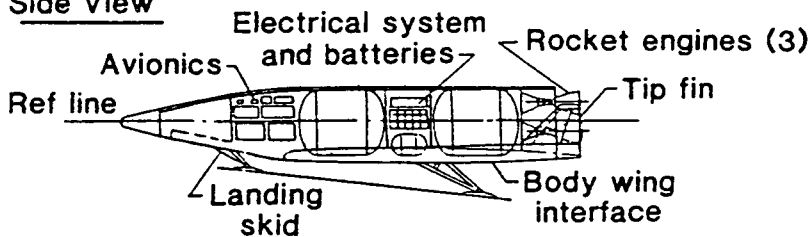


Figure 2-8. Inboard profile of the ERV [5].

thermal protection systems and materials, will be used to accommodate excessive temperatures (6).

2.4 Baseline Trajectory

2.4.1 Background and Strategy

The vehicle analysis branch at LaRC defined a baseline or nominal synergetic plane change trajectory. This baseline trajectory was developed by combining the best ideas and concepts that have emerged since 1961 when London's paper first convincingly demonstrated a significant performance gain with a synergetic plane change. A brief listing of these basic concepts are shown below as an aid to understanding the vehicle's design and baseline trajectory. A more detailed discussion of these concepts are in reference 17.

1. For plane changes of less than 15 degrees, the all-propulsive maneuver is generally more efficient.
2. An L/D of at least two is required to offer a significant advantage over the all-propulsive plane change, and it is desirable to maximize vehicle L/D.

3. Turns made at maximum CL (i.e., high angle-of-attack) are quicker and hence more fuel efficient than the more gradual maximum L/D turns. This improved efficiency is primarily a result of orbital mechanics. A plane change made at the intersection of two orbits (i.e., the node) produces all inclination change whereas a turn at the orbit apex (90 degree from node) produces no inclination change, only a node shift. Hence, for maximum inclination change and minimum node shift, the turn should be centered over the node in the shortest duration possible.
4. A large reduction in total heat load can be achieved by carrying out a short duration, high angle-of-attack maneuver rather than the slower maximum L/D turn.
5. A thrusting turn (aerocruise) offers significant advantages over the gliding turn (aeroglide) when the desired plane change is more than 10 degrees. This relationship is especially true when lower wall temperature (heat-rate) limits are imposed.
6. Aerocruise vehicles use continuous thrusting sufficient to balance aerodynamic drag and maintain an altitude high enough to allow optimum bank angles throughout the turn without exceeding heat-rate limits.

7. For the high angle-of-attack aerocruise vehicle, assuming thrust along the longitudinal axis, a significant portion of the plane change results from out-of-plane thrust due to the high angle-of-attack and bank attitude of the vehicle during the turn.
8. For the quick, high angle-of-attack turn, the vehicle is banking throughout the maneuver, and the exit should be timed such that the plane change is accomplished just as the vehicle exits the atmosphere to minimize fuel.
9. For each amount of plane change, there is a heat-rate that offers optimum fuel efficiency. If this heat-rate can be achieved, the resulting trajectory is more a combination aeroglide-aerocruise. A part of the turn is achieved on the gliding entry and the remaining plane change is achieved during the powered exit with almost no level-flight phase.

2.4.2 Trajectory Development and Understanding

Using these basic concepts, R.W. Powell and J.C. Naftel of NASA Langley Research Center developed a baseline synergetic plane change trajectory for a reference heating rate of both 80 and 125 BTU/ft²-sec. These trajectories were generated on their three-degree-of-freedom Program to Optimize Simulated Trajectories (POST). References 1,2, and 3

offer a detailed description of this program while Appendix A provides a brief description of POST along with an example of trajectory generation for the synergetic plane change maneuver.

The strategy for both baseline plane change trajectories are similar. First a deorbit burn is performed. Once the vehicles enters the atmosphere and the heating rate reaches the desired cruise value, the engines are restarted and throttled to maintain a nearly constant vehicle velocity. At the end of this cruising phase the engines are commanded to maximum thrust, and the vehicle exits the atmosphere. Bank angle and angle-of-attack are used during the entire atmospheric phase so that the required inclination change occurs during the entry, cruise and exit legs. Figures 2-9 thru 14 show profile plots for altitude, angle-of-attack, bank angle, engine throttling, heat-rate (QDOT), and heat load histories for both the 80 and 125 BTU/ft²-sec 20 degree synergetic plane change trajectories (6). Figure 2-15 shows a typical POST-generated altitude plot and the generic phase names that will be used during the plane change trajectory discussion. These profiles are presented here as basic reference material that should be helpful during the discussion in the remainder of this chapter. Appendix A provides more details into the generation of these trajectories while Chapter 4 will cover these trajectories and their plots in detail.

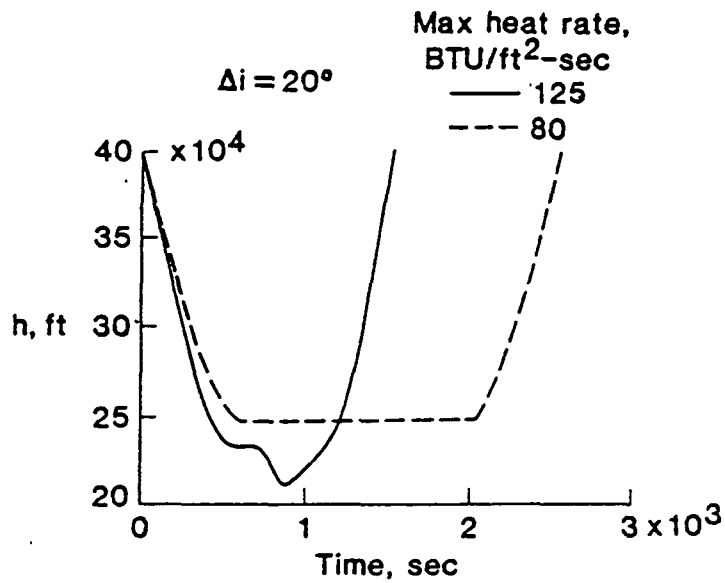


Figure 2-9. Altitude profiles for synergetic plane change using the ERV [6].

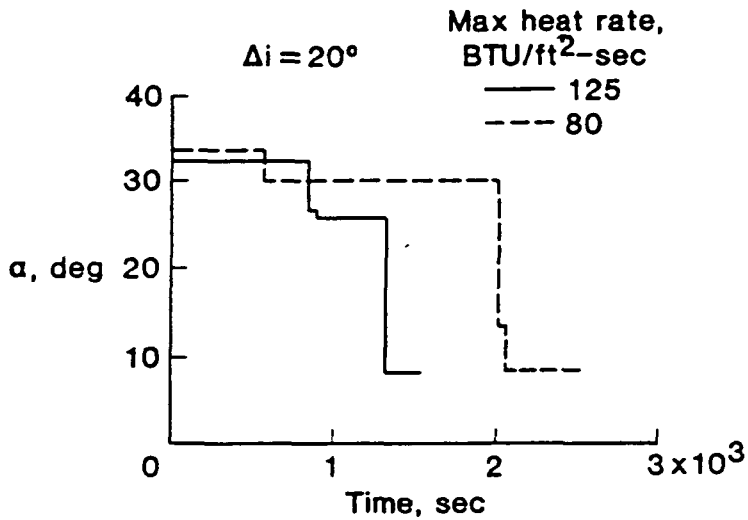


Figure 2-10. Angle-of-attack profiles for synergetic plane change using the ERV [6].

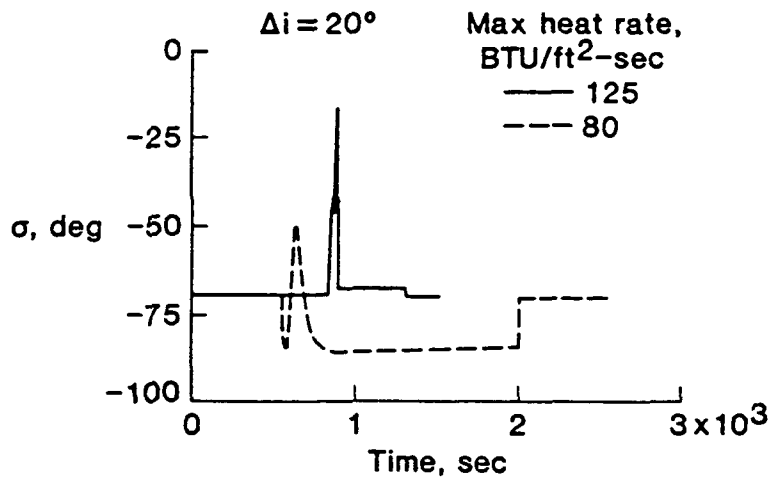


Figure 2-11. Bank angle profiles for synergetic plane change using the ERV [6].

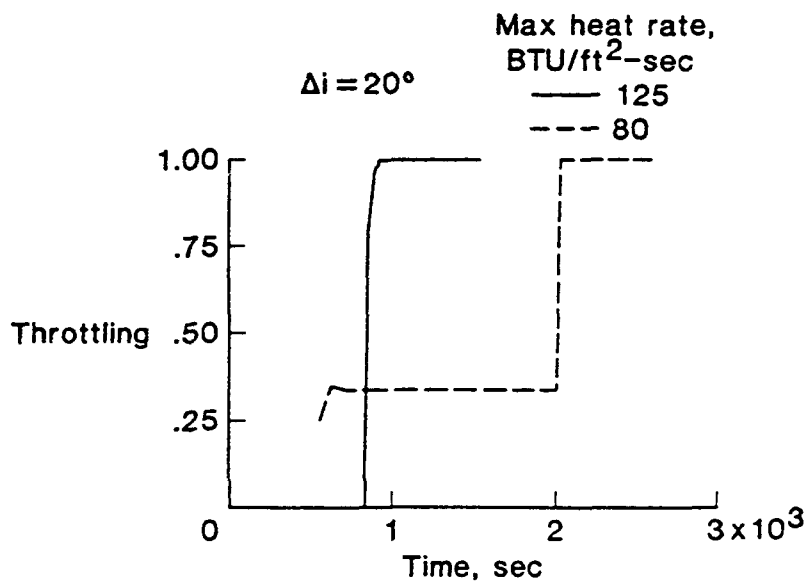


Figure 2-12. Engine throttling profiles for synergetic plane change using the ERV (0-off, 1 maximum) [6].

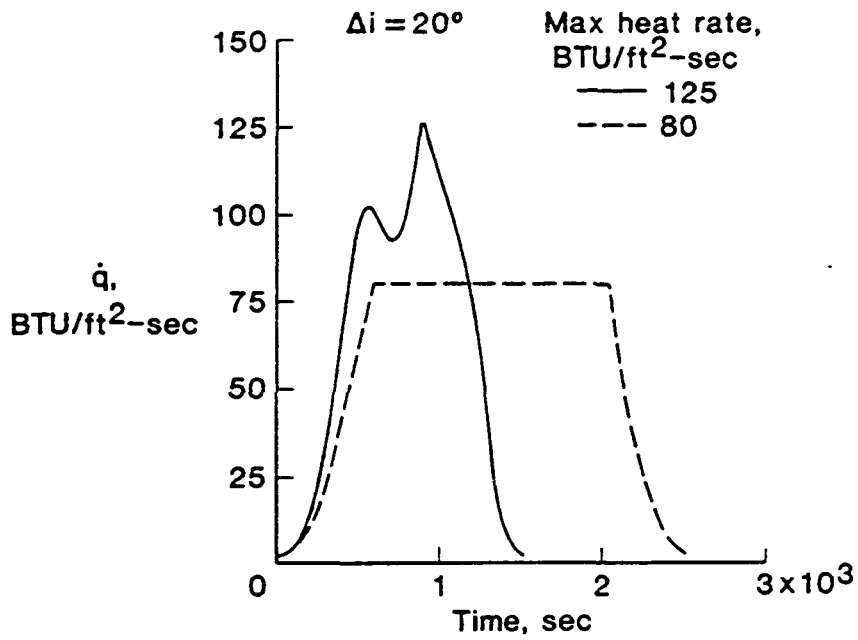


Figure 2-13. Heat-rate profiles for synergetic plane change using the ERV [6].

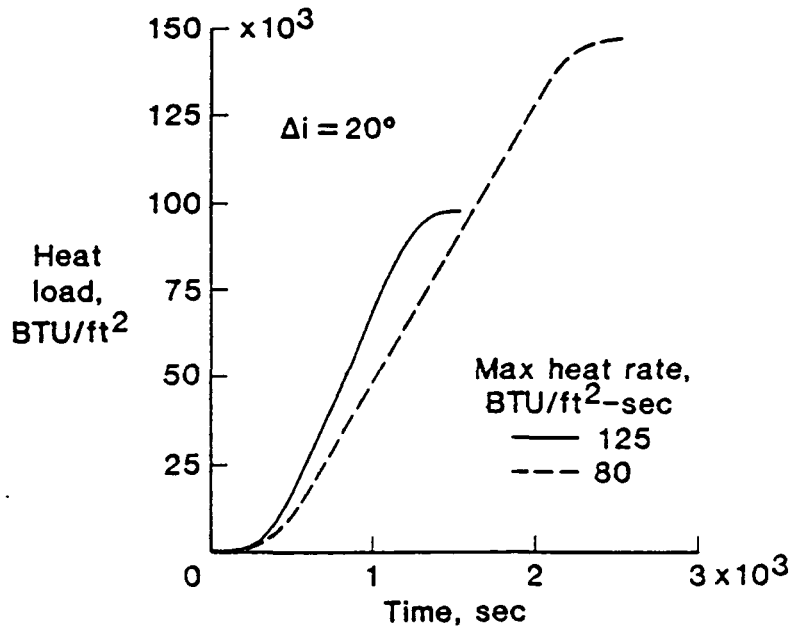


Figure 2-14. Heat load profile for synergetic plane change using the ERV [6].

ERV CRUISING SYNERGISTIC PLANE CHANGE $Q\text{-DOT}=125$

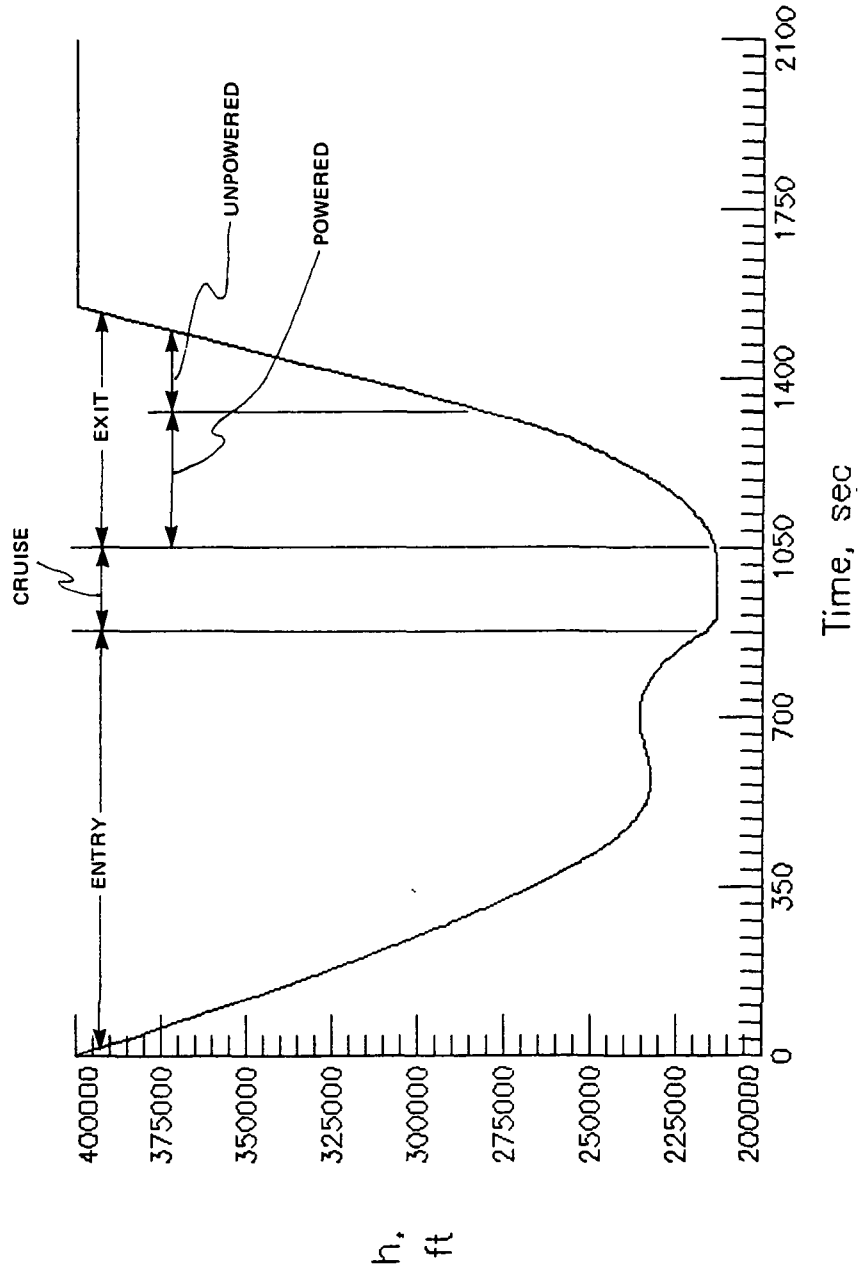


Figure 2-15. Post synergistic plane change altitude profile and generic phase names.

Langley's objective was to obtain the most fuel efficient plane change trajectory (within the adopted strategy) by allowing POST to find optimum values for carefully selected guidance parameters (independent variables). The 12 independent variables used for the baseline trajectories are listed below with a brief description of how POST uses the parameter.

1. Geocentric Latitude: The latitude at which a deorbit burn is started.
2. Perigee Altitude: The conically predicted orbital parameter which determines when the deorbit burn is stopped. This determines the ΔV of the deorbit burn and thus the position and velocity of the vehicle at entry interface.
3. Entry Angle-of-Attack: Angle-of-attack from atmospheric entry to level-off.
4. Entry Bank Angle: The bank angle from atmospheric entry to level-off.
5. Cruise Angle-of-Attack: Angle-of-attack for the cruise phase of flight.

6. Cruise Acceleration: The acceleration maintained during the cruise phase of flight.

7. Exit Inclination: The inclination angle where the exit is started.

8. Exit Bank Angle: The bank angle during the powered part of the exit.

9. Exit Angle-of-Attack: The angle-of-attack during the powered part of the exit.

10. Apogee Altitude: The conically predicted orbital parameter which determines when the rocket engines are cutoff. This determines when the vehicle can fly unpowered back to the desired orbital altitude.

11. Unpowered Exit Angle-of-Attack: The angle-of-attack after the engines are cutoff during the exit phase.

12. Unpowered Exit Bank Angle: The bank angle after the engines are cutoff during the exit phase.

The constraints and targeting parameters include:

1. Maximum heat-rate
2. Desired inclination angle
3. Desired final orbital apogee altitude
4. Maximum throttle setting

It should be noted that total heat-load is not considered a constraint for the relatively short plane change maneuver.

The optimizing parameter is final vehicle weight in the desired final circular orbit. Thus, POST attempts to minimize the amount of fuel used from the start of the deorbit burn until the ERV is back in the desired circular orbit. During this time, the 12 guidance parameters (free parameters) are adjusted to achieve the targeting parameters of inclination angle, apogee altitude, and maximum throttle setting. In addition, as a means of controlling heat-rate and achieving the cruise acceleration, POST can respectively vary bank angle and throttle setting during the level-off and cruise phase.

To simplify discussion here and throughout the remainder of this thesis, an abbreviated notation will be used to represent a heat-rate of 80 or 125 BTU/ft²-sec. Typically, the numbers 80 or 125 will be used

without units as stand-alone adjectives to describe trajectories or cases, or as objects (e.g., heat-rate of 80 or heating rate of 125). The more complete notation will be used where any uncertainty of meaning might exist or occasionally as a reminder.

To provide additional understanding of the baseline trajectories, a more detailed explanation of the previously presented trajectory plots will be made. Figure 2-9 provides an altitude versus time profile starting and ending at 400,000 feet (maximum extent of atmosphere). For the synergetic plane change with a design maximum convective heat-rate of 80, the ERV initiates level-off approaching the design heat-rate, and the engines are ignited. However, for the case with the design maximum heat-rate of 125 BTU/ft²-sec, the ERV phugoids at a heat-rate of approximately 100 BTU/ft²-sec and then continues to glide (engines off) until the design maximum heat-rate is reached. Once the design maximum heat-rate is reached, the level-off is started and the engines are ignited. For the 125 case, the exit maneuver begins almost immediately. For the 80 case the cruise phase continues significantly longer before throttling to 100% and boosting back into orbit. These differences are the result of a higher heat-rate allowing the vehicle to fly deeper into the atmosphere, thus generating higher lift to turn the vehicle quicker. As stated earlier, the quicker the maneuver can be performed, allowing the vehicle to remain close to the orbital node, the more efficient the maneuver.

Figure 2-10 presents angle-of-attack profiles that are reasonably similar for the 80 and 125 cases with length of the cruise phase making the biggest difference. The bank profiles in Figure 2-11 are again similar for the two cases with the spike just prior to 1000 seconds due to the ERV's heat-rate controller adjusting the bank angle to maintain the designed maximum heat-rate during level-off. Figure 2-12, the engine throttling profiles, displays the high percentage of maximum throttle required for level-off and cruise for the 125 case as compared to the relatively low throttle setting required for the 80 case. In Figure 2-13, the "double-peaked" heat-rate (QDOT) curve for the 125 case stands out quite clearly from the "Table-top" curve of the 80 case. Finally, the heat-load profiles in Figure 2-14 demonstrate the significantly higher total heat-load for the 80 case.

2.5 Guidelines and Requirements

NASA contracted with the Charles Stark Draper Laboratory to develop a guidance algorithm to satisfy the broad requirements for a future entry vehicle. As stated earlier, the new class of vehicles will require a sophisticated adaptive guidance and navigation system. This system must be able to sense the actual conditions and provide necessary control inputs in real-time to enable the vehicle to accurately achieve its end-conditions and remain within the vehicle's flight boundaries.

A primary objective in the development of the guidance system for the ERV was that it be flexible. Many past guidance algorithms have lacked flexibility because of severe computational constraints. With the availability of more advanced flight computers, the intent is to devise a guidance law offering more flexibility even if it is more computationally intensive.

In addition, the guidance system should not require exhaustive pre-mission planning. It should explicitly calculate on-board the desired trajectory or guidance commands instead of relying on elaborate tables which are highly mission dependent. Overall, this desire for greater flexibility and independence is in response to the need for increased operational performance to go along with the improved capabilities of future space vehicles.

Other general guidelines include:

1. Explicit control of vehicle heat-rate
2. Maximum ability to handle dispersions
3. High accuracy

4. Investigate the use of both angle-of-attack and bank angle as control variables.
5. Control capability for powered and unpowered maneuvering during the atmospheric flight phase.
6. Minimize fuel usage
7. Usable in vehicles with low roll rates
8. Transportable between vehicles.

Specifically, the plane change guidance system should be able to:

1. Achieve an inclination change of 20 ± 0.1 degrees and a final apogee altitude of 160 ± 5 nautical miles (nm).
2. Demonstrate acceptable performance for a heat-rate constraint of either 80 or 125 BTU/ft²-sec.
3. Demonstrate acceptable performance with atmospheric dispersions ($\pm 30\%$ density biases along with density shear models), aerodyna-

mic uncertainties ($\pm 15\%$ for all CL and CD combinations), and propulsion performance loss of one of its three engines.

One caveat should be pointed out concerning the requirements. The longitude of the ascending node (LAN) is not specifically required to be controlled. It is important to remember that an orbital plane is usually defined in terms of inclination and longitude of the ascending node. This defines a single orbital plane with respect to the equator and the vernal equinox. Thus, a change from one orbital plane to another orbital plane will, in general, cause a change in both of these parameters. However, for the purpose of this thesis, only an inclination change will be controlled. Longitude of the ascending node will be monitored to determine the magnitude of any shift.

CHAPTER 3

PROBLEM DEVELOPMENT

3.1 Introduction

The objective is to develop a guidance system to take the ERV through the atmospheric phase of a synergetic plane change mission. The powered flight guidance for accomplishing the deorbit and recircularization burns is well developed and documented. Starting with a well-defined reference trajectory, a specific set of end-condition requirements, one limiting constraint (maximum heat rate), and a large number of control parameters, the problem of developing a guidance scheme seemed rather straight forward. However, it was not immediately clear as to which combination of control variables provided the most efficient solution. Some type of analysis was done for each combination considered. However, some of the decisions made about the nominal guidance scheme were based on heuristic arguments rather than precise numerical comparisons. Naturally, where possible, both means were used to arrive at conclusions, however, numerical results alone can be misleading if they are not fully understood. Where appropriate, information

from other sources was used and referenced, rather than data generated specifically for this study.

Still, with the nominal baseline trajectories that are presented in Chapter 2, the problem is quite simply: how to develop an algorithm to use the vehicle's control variables to achieve a 20 degree plane change and a 160 nm apogee altitude in the presence of dispersions? Thus, it was a matter of choosing a basic guidance concept and a pairing of available control variables with the conditions to be controlled.

3.2 Guidance Characteristics and Concepts

Guidance systems span a spectrum of adaptability or flexibility from very rigid like an open-loop guidance system to a highly flexible system which continually generates an optimum trajectory from the current position to the desired end-conditions based on the latest knowledge. As stated in the previous chapter, the task was to develop a guidance system that is as flexible as possible within the constraints of the expected flight computer capability.

In addition, NASA desired an explicit type of guidance system not based on a reference trajectory requiring a great deal of pre-mission planning and loading of data. In terms of explicit guidance concepts, three general types of systems are available:

1. Perturbation
2. Predictor/Corrector
3. Real-time Optimization

Perturbation guidance generally relies on the explicit solution of simplified equations of motion. Typical perturbation guidance trajectories are equilibrium glide, constant drag, and constant heating rate. Often a relationship between the end-condition and the type of trajectory can be determined. For perturbation guidance, guidance commands are composed of two parts--nominal and perturbed. In a broader sense, the nominal could be a nominal reference command or a nominal reference trajectory profile. In either case, a nominal is calculated each guidance cycle to achieve mission objectives. The perturbed part is used as feedback to bring the vehicle back to the nominal. This has been used by the Johnson Space Center for Shuttle entry and various aerobraking schemes to force a vehicle to fly a drag acceleration profile to meet mission objectives. The advantages for this type of scheme are:

1. Lower sensitivity to initial conditions than an open-loop scheme
2. Guidance parameters are calculated explicitly

3. Low computational load
4. Flight experience on Shuttle

While the disadvantages include:

1. No direct control on the end conditions
2. A lack of mission flexibility
3. Scheme is usually very vehicle specific

A predictor/corrector scheme on the other hand, generally works with more accurate equations of motion. The guidance continuously computes a new trajectory to go from the present position to the end-conditions. The sensitivity of the end-conditions to changes in the control variables is determined by multiple numerical integrations of the trajectory. Once the sensitivity is determined, the current control profile can be corrected to satisfy the end-conditions. Advantages for this type of scheme are:

1. Sensed dispersions can be easily incorporated into the predictor to improve the performance during the remaining part the mission.

2. The scheme is less vehicle specific and thus can be transferred between vehicles more easily because changes in the vehicle model or aerodynamic data base do not change the guidance scheme.
3. The predictor can use a conservative vehicle model to allow additional margin for dispersions.
4. Very flexible in terms of using different control variables

While the disadvantages include:

1. A higher computational load
2. Possible convergence problems
3. Not especially useful for control of boundary conditions (like heating rate) that are unrelated to end-conditions
4. More difficult to verify and validate

Real-time optimization provides the most desirable guidance solution. At each guidance cycle a trajectory is calculated to hit the end-conditions and minimize a cost function such as fuel usage. The advantages include extreme flexibility and dispersion compensation capa-

bility while minimizing the costs. The disadvantages are just a magnification of the predictor/corrector disadvantages of high computational load along with reliability and convergence concerns.

In the final analysis, a hybrid offered the best hope of satisfying all of NASA's guidelines. A perturbation guidance scheme is used to maintain the heat-rate boundary while a predictor/corrector is used to achieve the end-conditions. As a means of achieving at least a nearly optimum solution, insight gained from our trajectory analysis that will be covered in Chapter 4 is used to develop techniques which allow efficient handling of perturbed situations.

3.3 Control Variables and Pairings

As a final step of breaking down the guidance problem, the degrees of freedom and the constraints or end conditions that must be satisfied with these control variables should be discussed. The objectives for the plane change are:

1. Final orbital inclination angle control
2. Final apogee altitude control
3. Heat-rate constraint

4. Minimization of fuel usage

While the parameters available to handle these conditions are:

1. Angle-of-attack
2. Bank angle
3. Engine thrust level (adjustable throttle setting)
4. Engine start time
5. Engine cutoff time

Simple accounting points out the fact that there are more control variables than trajectory objectives. Our approach to the problem was to explore the use of all parameters but use only what was necessary. This provides a straight forward scheme that can be more easily modified for later developments or other vehicles.

Based on several sensitivity studies conducted by R. Richards of CSDL (19), the effectiveness of angle-of-attack and bank angle was determined to be very similar during the last two-thirds of the plane change trajectory in controlling inclination. In addition, either con-

trol variable was shown to be capable of correcting inclination errors of up to 30% during the exit phase. The same group of studies indicated that final apogee altitude could be easily control with engine cutoff time. It is important to remember however, that because of the relatively high angles-of-attack during the powered flight phases, a significant amount of the turn and hence inclination change is directly attributable to engine thrust. Therefore, engine cutoff time displays a large coupling effect on final inclination. In-spite of this effect, the pairing of bank or angle-of-attack with inclination change and engine cutoff with apogee altitude offered a simple, reasonable approach to the problem.

For control of heating rate and fuel usage no simple study offered a clear indication of what control pairings offered the best means of control. However, based on the author's experience with POST, it seemed possible to gain the additional insight into the problem through this avenue.

CHAPTER 4

TRAJECTORY ANALYSIS

4.1 Introduction

Although the concept of performing an orbital plane change maneuver by using aerodynamic forces has been seriously considered and worked on since the early 1960's(17), this thesis offers a new level of knowledge for the optimum control of the maneuver in the presence of density and vehicular perturbations.

As discussed in Chapter 3, it became quickly apparent that some method was needed to provide insight into which of the various options was the preferred way to guide the ERV. Having some experience with POST, it was felt that at least a certain amount of that insight could be gained by simply perturbing the nominal conditions (POST initial conditions) and studying the initial and the optimized trajectory generated by POST. If nothing else, we could obtain the scope of the problem (i.e., the net effect of the perturbations on the end-conditions) for the required density, aerodynamic, and thrust perturbation/uncertainty

criteria. Furthermore, analysis of the optimized solutions generated by POST could help determine a generalized method for correcting the perturbation errors in an optimum manner without the complexity of continuously determining the optimum solution. That is, a means to optimize the guidance process without using real-time optimization. As it turned out, not only did the work with POST offer a simple means to size the problem, but it offered enough insight to logically and directly develop a guidance law which easily met all the required conditions stated in Chapter 2.

Overall, the basic plane change strategy and the analysis results obtained with POST appear to be generally applicable and sound. The performance evaluation results of Chapter 6 strongly validate most of the conclusions reached during our analysis. Still, it is important to remember that our trajectory analysis is based on POST and the nominal plane change trajectories that Langley developed with POST. Thus, any unique properties of how POST optimized or any changes or errors in the basic plane change strategy could effect the results and conclusions contained herein.

The remaining part of this chapter will discuss the methods and results of our trajectory analysis with POST. After discussing the methods, overall analysis results will be covered. This will be followed by a detailed discussion of the scope of the problem and the

optimization/compensation results for density perturbations aerodynamic uncertainties, single-engine failure and various combinations of these conditions on the nominal trajectory.

4.2 Method of Analysis

4.2.1 Objective

As previously discussed, our objective with POST was to obtain the type and size of trajectory errors that were caused by changes in density, aerodynamic characteristics and available thrust. In addition, we were seeking ways to optimize or compensate for these changes. To achieve this objective, we started with the nominal guidance parameters (independent variables) but off-nominal conditions and observed the initial and final trajectory generated by POST during its optimization process.

As an aid to understanding this method, a brief explanation of how POST operates is in order. Using POST as an optimum trajectory generator, it goes through an iteration process to determine the best solution. Starting with the initial conditions and guidance parameters it generates an initial trajectory based solely on those inputs. POST then tries to improve the trajectory by changing the independent variables based on numerically determined partial derivatives. On each successive

iteration, it repeats the process of changing the guidance parameters based on the partial derivatives and compares the resulting end-conditions with the desired conditions. This process continues until the desired conditions are obtained. At the same time, POST is trying to minimize or maximize a cost function. Thus, the final trajectory will not only achieve the desired end-conditions but do it in an optimum manner.

4.2.2 Specific Approach

All the trajectory analysis discussed in this chapter was performed with the POST computer program. The program was started with the ERV in a 160 nm circular orbit. The specific trajectory objective was to achieve a 20 degree synergetic inclination change using a maximum heat-rate of either 80 or 125 BTU/ft²-sec and return to a 160 nm circular orbit with the maximum vehicle weight (i.e., minimum amount of fuel consumed).

Starting with the 12 optimum independent variables for the nominal/baseline trajectories (see Chapter 2 and Appendix A for additional information), various amounts and combinations of density and aerodynamic perturbations and/or single engine failure were added to the nominal conditions. During the first cycle through (first iteration of the optimization process), POST would use the nominal independent variables

to generate a trajectory. The end-condition results of this initial trajectory were the "qualified" open-loop results (not a true open-loop as will be discussed in the next subsection) caused by the perturbations. These results provide an indication of the net effect of the perturbation on the trajectory.

After the first iteration, the independent variables are adjusted to find an optimum trajectory for the off-nominal conditions. Analyzing the manner in which the independent variables were adjusted for various perturbations, certain trends stood out that offered insight into how the ERV could best be guided.

The final step in our analysis process was to systematically "fix" or "freeze" some of the guidance parameters (e.g., the four entry variables) at their nominal value. By fixing the entry variables we were able to gain insight into how to optimize under what we felt were "real-world" constraints. In other words, you should not be able to adjust your entry parameters before you have actually had time to sense that entry conditions are not nominal. Thus, insight was gained on how to optimize various sections of the trajectory in addition to the trajectory as a whole.

4.2.3 Limitations

Before discussing the results of our trajectory analysis, three limitations or qualifiers on POST should be covered. The first qualifier concerns the 12 free parameters (independent variables). The analysis discussed in this chapter used the same free parameters that were used in developing the baseline trajectories. Therefore, the plane change trajectories discussed are really only optimum to the degree that POST was allowed to adjust trajectory parameters. Still, based on the knowledge of how Langley developed the baseline trajectories and the work done for this thesis, the baseline trajectories do represent a very good approximation of the "true" optimum solution.

The second limitation deals with the manner in which POST optimized for off-nominal conditions. As POST iterates to an optimum trajectory, it has apriori knowledge of perturbations. This is in contrast to a real-time guidance system that can only estimate what future perturbations will be. Therefore, not all methods used by POST to optimize are directly applicable to a real-world guidance algorithm. The process of "freezing" the entry parameters as discussed in the last subsection, was one approach used to overcome this limitation.

The third qualifier deals with the way the baseline plane change trajectories were defined and how POST handles certain constraints. Specifically, the strategy for the baseline trajectories was to maintain a maximum design heat-rate and an optimum vehicle acceleration during

the cruise phase. It should be pointed out that the results of numerous POST runs indicated that the optimum vehicle acceleration in all practicality does not vary and is almost zero (0.0036 ft/sec^2). Thus, a near constant velocity is maintained which (as it will be shown later) implies a nearly constant altitude to maintain a constant heat-rate. To handle these constraints, POST is allowed to vary bank angle to control heat-rate and throttle setting to maintain vehicle velocity during the cruise phase. The heat-rate and constant velocity (actually a near zero acceleration) constraints are necessary to maintain the same type of trajectory from case to case, but they must be considered when interpreting the trajectory analysis results. Specifically, it is important to realize that POST will always be able to adjust bank angle and throttle setting during the cruise phase. Therefore, as suggested earlier, the initial trajectory generated by POST during its optimization process is not really a true open-loop trajectory. Still, even with these limitations, this initial trajectory offers some valuable insight on the effects of the perturbations, and the results will be labeled as "open-loop" results.

4.3 Overall Results

The results of our trajectory analysis with POST are listed below as a means of overview. Each specific point will be discussed in the following sections. It is important to remember that while the following

results are generally applicable to the plane change problem, they must be considered with the qualifiers and limitations discussed above. That is, while the listed results are not uniquely attributable to POST, they are restricted to the plane change problem as previously defined.

1. "Open-Loop" Results: The single-engine failure case caused the greatest error in end-conditions, with roughly a 25% error in final inclination, while the $\pm 15\%$ aerodynamic uncertainty produced a range of 5-20% error in final inclination. The $\pm 30\%$ density perturbations, surprisingly, caused almost no end-condition errors.

2. Heat-Rate Control: Proved to be very important for minimizing fuel usage and density compensation. In addition, the trajectory's sensitivity to perturbations was a function of its maximum heat-rate.

3. Angle-of-Attack: Remained almost nominal except during the cruise phase where it is adjusted to equalize the thrust-drag balance.

4. Cruise Acceleration: Does not significantly change under any tested conditions and is practically zero. Fixing it at zero (i.e., constant velocity) has no observable effect.

5. Early Corrections: From a fuel optimization standpoint, corrections should be made as early as possible. However, "fixing" the four entry

parameters only resulted in a maximum loss of 100 pounds of fuel efficiency.

6. Time-to-Exit: Significant variations in exit inclination were made to compensate for the various perturbations. With the entry parameters fixed, the overall trend was to adjust the exit point and then exit using nominal exit parameters.

7. Bank Angle Versus Angle-of-Attack: Typically bank was a more efficient (in terms of fuel usage) means of correcting for perturbations than angle-of-attack.

8. Fuel Usage: Several items significantly effect the fuel usage. Aerodynamic characteristics, not surprisingly, had the largest effect followed by the time-to-exit, maximum heat-rate, and the transition from entry to the heat-rate boundary during cruise.

9. Exit Parameters: Tended to remain at near nominal values. In fact, angle-of-attack and bank angle after engine cutoff never significantly changed from the nominal values.

4.4 DETAILED RESULTS

In the following subsections, the "open-loop" and optimization/compensation results for each perturbation type and perturbation combinations are discussed in detail. The "open-loops" results consist of the "open-loop" errors and the final vehicle weight for the specified conditions. The "open-loop" errors indicate how much deviation (from the desired value) in final inclination, apogee altitude or maximum throttle setting for a perturbed trajectory using nominal guidance parameter values (see Section 4.2). As a reminder, the desired end-conditions values are:

1. Final inclination change - 20 degrees
2. Final Apogee Altitude - 160 nm
3. Maximum throttle setting - 100%

The final vehicle weight provides an idea of how the perturbations affected fuel usage. However, significant "open-loop" errors will affect the usefulness of this result. As reference weights, the final vehicle weight (in a 160 nm circular orbit) for the baseline 80 and 125 trajectories is 5262 lbs and 5873 lbs respectively.

The optimization/compensation results consist of the optimized guidance parameter values and the best final vehicle weight for the speci-

fied conditions. Recall that these optimized guidance parameter values are the best independent variable values that POST can generate thru its optimization process for the specified conditons. Using these optimized independent variables as POST guidance parameters or commands will produce a trajectory to achieve to desired end-conditions with the best final vehicle weight. By comparing these off-nominal optimized guidance parameters with the nominal guidance-parameters (also optimized for nominal conditions), insight can be gained on how to compensate for the dispersions in an optimum manner. Comparing the final vehicle weights (nominal verses off-nominal conditions), the net effect of the perturbation in terms of fuel usage can be obtained.

4.4.1 Density Perturbations

Trajectory analysis results for density perturbations indicated that heat-rate control offered "automatic" density compensation. This result was the most surprising result of our analysis. From an initial study it was determined that density dispersions would cause significant inclination and apogee altitude errors (19). In fact, this earlier study suggested that the extreme cases of density perturbations ($\pm 30\%$) could result in 4 to 6 degrees (20-30%) of inclination error. However, as the results in the next subsection show, the $\pm 30\%$ density perturbations produced also no POST "open-loop" errors. This implies that either the trajectory is unaffected by density perturbations and our

initial study was incorrect or there is actually some automatic density compensator in the "open-loop" trajectory.

4.4.1.1 "Open-Loop" Results

To obtain the scope of the problem for density perturbations, POST runs were made using a 30% high density bias, a 30% low density bias and a "worst case" density situation where the density was 30% high until the start of the exit phase and then it switched to 30% low. The three cases were run for plane change missions using a maximum heat-rate of 80 and 125. Overall, as the results in Table 4-1 demonstrate, density variations had almost no effect on the end-condition results for the "open-loop" trajectory. In fact, for a heating rate of 80 BTU/ft²-sec with a 30% low density atmosphere, the resulting trajectory meets the desired end-conditions more accurately and with less fuel than under nominal (standard atmosphere) conditions. Even for the "worst case", the end-conditions were just outside of NASA's accuracy criteria.

One final point that warrants mention concerning the "open-loop" results shown Table 4-1. For two of the cases, the maximum throttle setting exceeded 100%. To understand the significance of this point, further discussion on how the throttle setting is determined is in order. Except during the cruise phase, the throttle is fixed at either 100% or zero. During the cruise phase, to maintain the cruise accerler-

Table 4-1. Density bias "open-loop" results with post.

Condition	Inclination Error (deg)	Apogee Altitude Error (nm)	Maximum Throttle Error (%)	Final Vehicle Weight (lbs)
QDOT = 80 Nominal	0.004	-0.27	0	5262
QDOT = 80 +30%	0.004	-0.28	0	5253
QDOT = 80 -30%	-0.001	0.07	0	5269
QDOT = 125 Nominal	0.001	0.20	0	5873
QDOT = 125 +30%	0.129	0.39	0.80	5847
QDOT = 125 -30%	-0.214	0.09	0	5904
QDOT = 125 +30% Until Exit Then -30%	-0.670	-5.38	0.83	5978

NOTE: A negative sign indicates the error was below the desired value.

ation, POST has the freedom to adjust the throttle. Initially, POST has the freedom to exceed 100% but during the optimization process it must eliminate the excess (real-world necessity) as one of its end-condition constraints. Therefore, the maximum throttle error is similar to inclination and apogee errors -- some sort of adjustment will be needed to compensate for the error. While in both cases shown in Table 4-1, the throttle error was less than 1%, it is the first hint that during cruise, nominal angle-of-attack and 100% thrust will not maintain a constant velocity under some conditions.

4.4.1.2 Optimization/Compensation Results

As might be expected the optimized trajectory results for density perturbations do not provide much insight since the "open-loop" errors were so small. As the summary of the results shown in Tables 4-2 thru 4 indicate, many of the parameters do not change at all. The few changes that are made do not really stand out until analyzing the data for a 125 heat-rate with the four entry parameters frozen (Table 4-4). In these cases, the data suggests that the best way to correct is with a variation in exit inclination or a "time-to-exit" routine. However, before dealing with smaller details of the results, the basic question of why such large density biases result in such small end-condition errors should be covered.

Table 4-2. Density bias optimization results for
 QDOT = 80 BTU/ft²-sec.

Guidance Parameter Name (Units)	Condition		
	Nominal	+30%	-30%
Geocentric Latitude (deg)	0.957	Same	Same
Perigee Altitude (nm)	30.0	Same	30.1
Entry Angle-of-Attack (deg)	32.2	Same	33.5
Entry Bank Angle (deg)	-67.8	Same	-63.5
Cruise Angle-of-Attack (deg)	30.8	Same	31.3
Cruise Acceleration (ft/s ²)	0.0036	Same	Same
Exit Inclination (deg)	47.4	Same	47.2
Exit Bank angle (deg)	-59.1	Same	-60.8
Exit Angle-of-Attack (deg)	21.8	Same	Same
Apogee Altitude (nm)	193	Same	192
Unpowered Exit Angle-of-Attack (deg)	8.03	Same	8.05
Unpowered Exit Bank Angle (deg)	-68.5	Same	-68.7
Final Vehicle Weight (lbs)	5262	5253	5293

- NOTE: (1) "Same" indicates the parameter value did not change from the nominal value.
 (2) "Fixed" indicates the parameter was not allowed to change during the optimization process.
 (3) A negative sign indicates a left bank angle.

Table 4-3. Density bias optimization results for QDOT = 125 BTU/ft²-sec.

Guidance Parameter Name (Units)	Condition			
	Nominal	+30%	-30%	+30% Until Exit Then -30%
Geocentric Latitude (deg)	-0.958	Same	Same	Same
Perigee Altitude (nm)	27.6	27.4	27.5	27.5
Entry Angle-of-Attack (deg)	27.2	26.8	26.8	27.4
Entry Bank Angle (deg)	-69.2	-71.1	-71.4	-69.4
Cruise Angle-of-Attack (deg)	25.4	25.3	25.3	25.1
Cruise Acceleration (ft/s ²)	0.0036	Same	Same	Same
Exit Inclination (deg)	40.6	40.1	40.5	40.9
Exit Bank angle (deg)	-65.7	-66.1	-66.4	-65.8
Exit Angle-of-Attack (deg)	20.4	20.3	Same	20.6
Apogee Altitude (nm)	165	Same	Same	169
Unpowered Exit Angle-of-Attack (deg)	8.13	Same	Same	8.12
Unpowered Exit Bank Angle (deg)	-69.8	Same	Same	-69.7
Final Vehicle Weight (lbs)	5873	5941	5943	5842

- NOTE: (1) "Same" indicates the parameter value did not change from the nominal value.
 (2) "Fixed" indicates the parameter was not allowed to change during the optimization process.
 (3) A negative sign indicates a left bank angle.

Table 4-4. Density bias optimization results for QDOT = 125 BTU/ft²-sec. with entry parameters fixed.

Guidance Parameter Name (Units)	Condition		
	Nominal	+30%	-30%
Geocentric Latitude (deg)	-0.958	Fixed	Fixed
Perigee Altitude (nm)	27.6	Fixed	Fixed
Entry Angle-of-Attack (deg)	27.2	Fixed	Fixed
Entry Bank Angle (deg)	-69.2	Fixed	Fixed
Cruise Angle-of-Attack (deg)	25.4	25.2	25.2
Cruise Acceleration (ft/s ²)	0.0036	Same	Same
Exit Inclination (deg)	40.6	39.2	40.2
Exit Bank angle (deg)	-65.7	-67.1	-67.3
Exit Angle-of-Attack (deg)	20.4	20.3	20.3
Apogee Altitude (nm)	165	166	166
Unpowered Exit Angle-of-Attack (deg)	8.13	Same	Same
Unpowered Exit Bank Angle (deg)	-69.8	Same	Same
Final Vehicle Weight (lbs)	5873	5893	5884

- NOTE: (1) "Same" indicates the parameter value did not change from the nominal value.
 (2) "Fixed" indicates the parameter was not allowed to change during the optimization process.
 (3) A negative sign indicates a left bank angle.

The most reasonable explanation is that POST is doing something automatically to control one thing and ends up also compensating automatically for density variations. Closer examination and tests clearly pointed out that the POST "heat-rate" controller (necessary to maintain the same plane change strategy) was also providing a built-in density compensator. Examination of Chapman's heat-rate (QDOT) equation

$$QDOT = 17600/Rn (\rho/\rho_{SL})^{0.5} (V_R/V_C)^3 \quad 15$$

where R_n is the vehicle's nose radius, ρ and ρ_{SL} are the current and sea level atmospheric density, V_C is the reference circular orbital velocity, and V_R is the relative vehicle velocity, offers an explanation. By controlling to a given heat-rate you are actually controlling to a density-velocity combination. There are infinite combinations of velocity and density to give the desired heat-rate, but with density providing the predominate deacceleration force during reentry, a straight change in density will only change the geometric altitude where the deacceleration profile occurs and eventually you will hit the heat-rate at roughly the same velocity-density combination. In other words, the vehicle will basically fly through the same density profile, but at a different geometric altitude. Thus, the heat-rate controller insures the same density profile which insures the same plane change results. So, while providing for safety of the vehicle, you are also getting compensation for density perturbations.

4.4.2 AERODYNAMIC UNCERTAINTIES

As discussed in Chapter 2, the ERV is expected to perform the plane change maneuver in the region where previous aerodynamic predictions have been significantly in error. Therefore, the capability to handle uncertainties in the predicted aerodynamics is important for an accurate guidance system. To obtain the "open-loop" and optimization/compensation results, the following four variations of aerodynamic characteristics were considered.

1. +15% CL and CD (Both High)
2. -15% CL and CD (Both Low)
3. +15% CL and -15% CD (High Aero)
4. -15% CL and +15% CD (Low Aero)

where CL is the coefficient of lift and CD is the coefficient of drag. These four cases represent the four possible extremes for a maximum aerodynamic uncertainty of $\pm 15\%$.

4.4.2.1 "OPEN-LOOP" RESULTS

The effects of the ERV's $\pm 15\%$ aerodynamic uncertainties produced a range of inclination errors of 5-20% depending of the combination of CL and CD as shown in Table 4-5. Overall, two important conclusions can be made. First, aerodynamic perturbations, unlike density perturbations, produce significant open-loop errors (e.g., fuel and final inclination) and will require some compensation to minimize their effects. Second, the problem of having sufficient power during level off was again highlighted as potentially serious because the +15% CL and CD case (QDOT = 125) required nearly 120% of maximum throttle to level-off using nominal guidance parameters. Some adjustment in a vehicle control parameter will be needed to correct this problem.

4.4.2.2 OPTIMIZAION/COMPENSATION RESULTS

Analyzing the results shown in Table 4-6 thru 8, four specific observations or insights are apparent concerning (1) fuel usage, (2) angle-of-attack (3) optimum location for corrections, and (4) sensitivity of the 80 and 125 heat-rate cases to the aerodynamic uncertainties.

On fuel usage, the results of Tables 4-6 thru 8 fall into two categories. For the case where CL and CD are either high or low (no net change of L/D), it is possible to compensate for the perturbations with-

Table 4-5. Aerodynamic uncertainty "open-loop" results with post.

Condition	Inclination Error (deg)	Apogee Altitude Error (nm)	Maximum Throttle Error (%)	Final Vehicle Weight (lbs)
QDOT = 80 Nominal	0.004	-0.27	0	5262
QDOT = 80 +15% CL & CD	0.322	7.52	0	5306
QDOT = 80 -15% CL & CD	-0.397	-3.33	0	5073
QDOT = 80 +15% CL -15% CD	-0.043	25.5	0	5996
QDOT = 80 -15% CL +15% CD	0.0387	-12.1	0	4543
QDOT = 125 Nominal	0.001	0.20	0	5873
QDOT = 125 +15% CL & CD	1.070	-0.50	19.7	5721
QDOT = 125 -15% CL & CD	-1.232	-0.86	0	6041
QDOT = 125 +15% CL -15% CD	-2.411	4.96	0	6926
QDOT = 125 -15% CL and +15% CD	-3.681	-7.00	0	5691

NOTE: A negative sign indicates the error was below the desired value.

Table 4-6. Aerodynamic uncertainty optimization results for
 QDOT = 80 BTU/ft²-sec.

Guidance Parameter Name (Units)	Condition		
	Nominal	+15% CL -15% CD	-15% CL +15% CD
Geocentric Latitude (deg)	0.957	0.956	0.959
Perigee Altitude (nm)	30.0	29.2	30.5
Entry Angle-of-Attack (deg)	32.2	32.1	32.5
Entry Bank Angle (deg)	-67.8	Same	-67.4
Cruise Angle-of-Attack (deg)	30.8	30.2	30.9
Cruise Acceleration (ft/s ²)	0.0036	Same	Same
Exit Inclination (deg)	47.4	47.5	47.3
Exit Bank angle (deg)	-59.1	-59.7	-58.3
Exit Angle-of-Attack (deg)	21.8	21.6	22.1
Apogee Altitude (nm)	193	186	201
Unpowered Exit Angle-of-Attack (deg)	8.03	8.04	8.00
Unpowered Exit Bank Angle (deg)	-68.5	-68.7	-68.4
Final Vehicle Weight (lbs)	5262	6029	4521

- NOTE: (1) "Same" indicates the parameter value did not change from the nominal value.
 (2) "Fixed" indicates the parameter was not allowed to change during the optimization process.
 (3) A negative sign indicates a left bank angle.

Table 4-7. Aerodynamic uncertainty optimization results for QDOT = 125 BTU/ft²-sec.

Guidance Parameter Name (Units)	Condition				
	Nominal	+15% CL & CD	-15% CL & CD	+15% CL -15% CD	-15% CL +15% CD
Geocentric Latitude (deg)	-0.958	Same	Same	-0.948	Same
Perigee Altitude (nm)	27.6	27.8	27.5	29.4	28.3
Entry Angle-of-Attack (deg)	27.2	26.2	27.4	26.7	27.7
Entry Bank Angle (deg)	-69.2	-68.5	-69.6	-73.3	-70.4
Cruise Angle-of-Attack (deg)	25.4	23.3	Same	25.3	Same
Cruise Acceleration (ft/s)	0.0036	Same	Same	Same	Same
Exit Inclination (deg)	40.6	Same	41.5	41.4	44.2
Exit Bank angle (deg)	-65.7	-65.3	-66.3	-69.8	-65.8
Exit Angle-of-Attack (deg)	20.4	Same	20.5	20.3	20.9
Apogee Altitude (nm)	165	164	166	166	172
Unpowered Exit Angle-of-Attack (deg)	8.13	8.12	Same	8.12	8.12
Unpowered Exit Bank Angle (deg)	-69.8	Same	Same	Same	-69.7
Final Vehicle Weight (lbs)	5873	5892	5819	6682	4886

- NOTE: (1) "Same" indicates the parameter value did not change from the nominal value.
(2) "Fixed" indicates the parameter was not allowed to change during the optimization process.
(3) A negative sign indicates a left bank angle.

Table 4-8. Aerodynamic uncertainty optimization results for QDOT = 125 BTU/ft²-sec. with entry parameters fixed.

Guidance Parameter Name (Units)	Condition		
	Nominal	+15% CL -15% CD	-15% CL +15% CD
Geocentric Latitude (deg)	-0.958	Fixed	Fixed
Perigee Altitude (nm)	27.6	Fixed	Fixed
Entry Angle-of-Attack (deg)	27.2	Fixed	Fixed
Entry Bank Angle (deg)	-69.2	Fixed	Fixed
Cruise Angle-of-Attack (deg)	25.4	24.8	24.6
Cruise Acceleration (ft/s ²)	0.0036	Same	Same
Exit Inclination (deg)	40.6	41.4	42.5
Exit Bank angle (deg)	-65.7	-72.1	-74.3
Exit Angle-of-Attack (deg)	20.4	20.1	21.3
Apogee Altitude (nm)	165	168	185
Unpowered Exit Angle-of-Attack (deg)	8.13	Same	8.11
Unpowered Exit Bank Angle (deg)	-69.8	Same	-69.7
Final Vehicle Weight (lbs)	5873	6584	4981

- NOTE: (1) "Same" indicates the parameter value did not change from the nominal value.
(2) "Fixed" indicates the parameter was not allowed to change during the optimization process.
(3) A negative sign indicates a left bank angle.

out a net effect on fuel usage. For the cases where you have either high aero or low aero, the optimized trajectory had a roughly 10-15% net increase or decrease in fuel usage or about 700 pounds of fuel. Neither of these observations are unexpected but should be kept in mind when evaluating the final guidance algorithm.

Concerning angle-of-attack (α) control, the results of Tables 4-6 thru 8 fall into two categories. First, for the case of both high CL and CD in Table 4-7, a change in α was able to eliminate the maximum throttle error (not shown in table). Thus, angle-of-attack is a good candidate for handling thrust deficiencies. Second, throughout the optimization process for aerodynamic uncertainties, bank angle was adjusted significantly more than α to eliminate inclination errors. This is especially apparent in Table 4-8 where the entry parameters are not allowed to change. Examination of the partial derivatives of inclination with respect to α and bank (not shown in tables), indicates that the effectiveness of α verses bank angle is about the same. However, the fuel efficiency is apparently not the same because the optimization process adjusts almost strictly with bank angle during entry and exit. For example, Table 4-8 shows that during the powered exit phase, bank and α for nominal conditions are respectively -65.7 and 20.4, while for the high aero case, bank and α are -72.1 and 20.1. In other words, a change of 6.4 degrees in bank but only 0.3 degrees in α is used to optimize for the off-nominal condition.

This implies that bank control is more fuel efficient for aerodynamic perturbation corrections than alpha.

Concerning the optimum location for corrections, one general trend runs through all the results thus far (density and aerodynamic). Looking at where POST modified its guidance parameters to correct for errors caused by perturbations, it is apparent that an "earlier-is-better" logic prevails. That is, most of the changes in the independent variables are made at the front end of the trajectory. In addition, the size of these changes tend to hide their true significance since the effectiveness of corrections (sensitivity) is much higher on the front end of the trajectory. Particularly surprising was how little the exit parameters were changed by the optimization process. This observation suggest that corrections for perturbations errors should be made early and then exit nominally. Bear in mind though that POST "knows" about the perturbations before hand and can correct early. This apriori knowledge is not normally available "real-world", thus the results are not completely applicable to a real situation. Table 4-8 shows the optimized parameters after "fixing" the first four. This requires POST to optimize for perturbations without the ability to adjust the entry parameters. Just as before though, the results show most of the adjustments were made as soon as possible (i.e., during the cruise phase), and then the exit is made with a near nominal command profile. Thus, for fuel conservation, corrections should be made as early as possible.

As a final observation, the 125 BTU/ft²-sec trajectories are much more sensitive to perturbations than the 80 BTU/ft²-sec trajectories. This trend is apparent in the density perturbation results, but is especially highlighted in the aerodynamic uncertainty results. This insight will be further expanded in the next subsection.

4.4.3 HEAT-RATE VARIATION

As discussed in Chapter 2, the guidance algorithm should be able to handle plane change maneuvers at a heating-rate of both 80 and 125. During the early trajectory analysis work, both 80 and 125 BTU/ft²-sec heat-rates were examined. However, a review of Table 4-1 and 4-5 indicates the relative insensitivity of a 20 degree plane change done at a heating rate of 80 versus 125 to both density and aerodynamic perturbations. Specifically, for the 80 case, the perturbations have almost no effect (i.e., less than 2%) on final inclination, little effect on fuel usage (10% in the most extreme cases) and only a moderate effect on the final apogee altitude. In contrast, the "open-loop" errors for the 125 case are significantly larger.

The only exception to this trend is with apogee altitude. However, the apparent exception to the sensitivity trend is not really as it appears. It can be explained by the large difference in engine cutoff altitudes for the two trajectories. Examination of Figures A-8 and A-1

shows that the engines were cutoff at 255,000 feet for the 80 BTU/ft²-sec trajectory but at 281,000 feet for the 125 trajectory. This difference in cutoff altitude magnifies the perturbation effects resulting in a much larger apogee error for the 80 trajectory. In other words, the perturbation effects are not really larger for the 80 case, they just have longer to propagate. While this particular difference in the trajectories must be considered in developing a guidance algorithm, the 125 heat-rate trajectory will drive most of the design requirements.

Actually, the sensitivity trend is not surprising in light of the work done earlier at NASA LaRC which demonstrated that each plane change had an optimum heat-rate (using fuel usage as an efficiency criterion) (6). From that study, it was shown that for a 20 degree plane change, a heating rate of 125 was near-optimum for the ERV, while a heating rate of 80 was significantly less efficient. Thus it is reasonable that density and aerodynamic perturbations would have a larger effect on the optimum heat-rate trajectory (125) than on other trajectories.

A more quantitative explanation can be made by comparing the dynamic pressure profiles shown in Figure A-11 for the 80 and 125 trajectories (nominal conditions). Not only does the 125 trajectory reach a much higher maximum value but the time-integrated total dynamic pressure is significantly higher (area under the curve). Considering the direct relationship between aerodynamic forces and dynamic pressure,

$$\begin{array}{ccccccc} \text{aerodynamic} & = & \text{dynamic} & \times & \text{aerodynamic} & \times & \text{surface} \\ \text{forces} & & \text{pressure} & & \text{coefficients} & & \text{area} \end{array}$$

the sensitivity differences between the 80 and 125 trajectories is straight forward. The 125 plane change uses less fuel because it uses more aerodynamic forces to assist in the plane change. Therefore, perturbations that effect the aerodynamic forces (e.g., density, CL or CD) will cause a more significant impact on the 125 trajectory.

The final guidance scheme must demonstrate satisfactory performance for both heat-rates, and Chapter 6 provides that demonstration. However, in the interest of clarity of discussion and because the 125 heat-rate is generally the more difficult case, the remaining discussion of this chapter will deal only with the 125 case.

4.4.4 SINGLE-ENGINE FAILURE

The purpose for considering engine failure is more a question of safety than anything else. That is, we do not expect to experience an engine failure as we do expect density and aerodynamic dispersions. So the first question is can the ERV be safely returned to orbit even if the desired plane change is not completed. To obtain that answer, two cases were considered that were thought to be the two worst possibilities for single-engine failure. The first case was where failure occurs at the start of the level off phase and the second case at the start of the exit phase. In both cases, the thrust from one of the ERV's three engines was eliminated for the duration of the mission.

4.4.4.1 "OPEN-LOOP" RESULTS

As might be expected, the loss of an engine during the plane change has by far the largest effect on end-condition errors, but the maneuver can still be accomplished. Table 4-9 shows the "open-loop" errors for the two, single-engine failure cases. The inclination and apogee errors are initially the same for both situations because the exit command is based on an inclination angle. However, the loss of an engine at the start of the level-off phase is the more difficult case because of the power deficiency as highlighted by the maximum throttle error of 50%. The other significant error is the roughly 25% error in final inclination. The fact that too much plane change was obtained might seem surprising unless you realized that, "open-loop", the exit will be at the same nominal inclination. Therefore, with a slower climb back to orbit (less power), the extra time in the atmosphere will produce a greater turn and hence a greater plane change.

4.4.4.2 OPTIMIZATION/COMPENSATION RESULTS

Table 4-10 presents the results for the optimized trajectory with a single-engine failure. Analysis of these results brings out two recurring observations and one new piece of insight.

Table 4-9. Single engine failure "open-loop" results with post for QDOT = 125 BTU/ft²-sec.

Condition	Inclination Error (deg)	Apogee Altitude Error (nm)	Maximum Throttle Error (%)	Final Vehicle Weight (lbs)
Nominal	0.001	0.20	0	5873
Single Engine Failure at Level Off	4.651	-2.82	49.9	5092
Single Engine Failure at Exit	4.651	-2.82	0	5092

NOTE: A negative sign indicates the error was below the desired value.

First of all, concerning angle-of-attack control, the results demonstrate that a thrust deficiency can be corrected with alpha. As stated before, some sort of scheme will be needed to correct a power deficiency, and angle-of-attack is capable of handling even this worst case of an engine out. Furthermore, this means of compensation for a loss of power is evidently fuel efficient since the optimized results for an engine failure (Table 4-10) show a final vehicle weight that is almost the same as for nominal conditions.

The second recurring trend is the preference for bank instead of alpha for inclination corrections. This trend is especially evident in Table 4-10 when comparing bank and alpha during the exit phase for an engine failure at level-off. When the entry parameters are fixed, the optimum means of compensation is to change the bank by 3.5 degrees but alpha by only 0.1 degrees. Again, the sensitivity of bank and alpha are almost the same (the partial derivatives are not shown), but evidently, the fuel efficiency is not, because bank is strongly favored.

Finally, the new bit of insight deals with determination of the time or point to exit. The results of Table 4-10 indicate that exit inclination was adjusted during the optimization process as much as 2.3 degrees. This represents a significant modification to the trajectory and can be explained by the basic plane change strategy. Recall from Chapter 2 that as much of the plane change should be done during entry

Table 4-10. Single engine failure optimization results for
 QDOT = 125 BTU/ft²-sec.

Guidance Parameter Name (Units)	Condition			
	Nominal	Single Engine Failure		
		At Level- Off	At Exit	At Level- Off
Geocentric Latitude (deg)	-0.958	-0.961	Same	Fixed
Perigee Altitude (nm)	27.6	28.7	27.7	Fixed
Entry Angle-of-Attack (deg)	27.2	25.6	26.6	Fixed
Entry Bank Angle (deg)	-69.2	-69.6	-68.0	Fixed
Cruise Angle-of-Attack (deg)	25.4	20.4	Same	20.6
Cruise Acceleration (ft/s ²)	0.0036	Same	Same	Same
Exit Inclination (deg)	40.6	38.3	39.7	38.8
Exit Bank angle (deg)	-65.7	-65.9	-62.8	-62.2
Exit Angle-of-Attack (deg)	20.4	Same	20.3	20.3
Apogee Altitude (nm)	165	166	167	Same
Unpowered Exit Angle-of-Attack (deg)	8.13	Same	Same	Same
Unpowered Exit Bank Angle (deg)	-69.8	Same	Same	Same
Final Vehicle Weight (lb)	5873	5827	5827	5732

- NOTE: (1) "Same" indicates the parameter value did not change from the nominal value.
 (2) "Fixed" indicates the parameter was not allowed to change during the optimization process.
 (3) A negative sign indicates a left bank angle.

and exit to minimize fuel usage. Thus, this shift in exit just represents the optimization process adjusting to achieve this objective. A similar capability will probably be needed for an efficient guidance scheme.

4.4.5 MULTIPLE OFF-NOMINAL CONDITIONS

Having discussed analysis results on each individual type of perturbation, it is also worthwhile to discuss various combinations of perturbations. Although, little additional insight was gained by combining various perturbations, the fact that these combinations did not cause any new problems is in itself, a very useful insight.

4.4.5.1 "OPEN-LOOP" RESULTS

Although a large number of perturbation combinations are possible, the following five combinations were chosen to scope the problem.

1. 30% high density and high aero
2. 30% high density and low aero
3. 30% low density and high aero

4. 30% low density and low aero

5. 30% low density, low aero, and single-engine failure at
level-off

The "open-loop" errors for these runs are summarized in Table 4-11. For these cases, the trajectory problems caused by the combination of perturbations did not produce any errors larger than had been seen previously and in some cases the perturbations seem to neutralize each other. Overall, inclination errors were within 25% of nominal, apogee errors within 10%, and maximum throttle errors within 23%.

4.4.5.2 OPTIMIZATION/COMPENSATION RESULTS

With but one exception, the insight gained from the results of optimizing the five cases are mainly a repeat of what was discussed in the previous sections. The new point will be discussed in detail while the old points will only be briefly covered.

4.4.5.2.1 HEAT-RATE CONTROL

4.4.5.2.1.1 TRANSITION TO CRUISE

Table 4-11. Multiple off-nominal "open-loop" results with post for
 QDOT = 125 BTU/ft²-sec.

Condition	Inclination Error (deg)	Apogee Altitude Error (nm)	Maximum Throttle Error (%)	Final Vehicle Weight (lbs)
Nominal	0.001	0.20	0	5873
+30% Density +15% CL -15% CD	-2.362	5.29	0	6922
+30% Density -15% CL +15% CD	-4.471	-13.1	0	5819
-30% Density +15% CL -15% CD	-2.523	4.34	0	6938
-30% Density -15% CL +15% CD	-0.166	-2.58	11.9	5158
-30% Density -15% CL +15% CD Single Engine Failure	-4.711	8.04	22.8	5915

NOTE: A negative sign indicates the error was below the desired value.

Our analysis showed that the transition from entry to the cruise phase could effect the plane change fuel efficiency by as much as seven or eight percent of the total fuel required for a plane change.

4.4.5.2.1.1.1 THE PROBLEM

While analyzing the results, for multiple off-nominal conditions, we realized that a couple of the trajectories had lost the characteristic (for the 125 case) "double-peak" in the heat-rate verse time curve. Further analysis indicated that if the "double-peak" (see Figure 2-13 or A-9) is eliminated or altered, extra fuel will be required to complete the mission. For example, the results in Table 4-12 show that the optimized trajectory for 30% high density and 15% low aero has a final vehicle weight at 4839 pounds. However, by slightly modifying the trajectory (the modification will be covered in the next subsection), the heat-rate "double-peak" is restored, and the final vehicle weight is now 5281 pounds for a net fuel savings of roughly 450 pounds. The heat-rate verses time profiles for the two cases are shown in Figure 4-1. Further study suggests two reasons for this fuel savings, both a benefit of the relatively high dynamic pressure during this phase of flight.

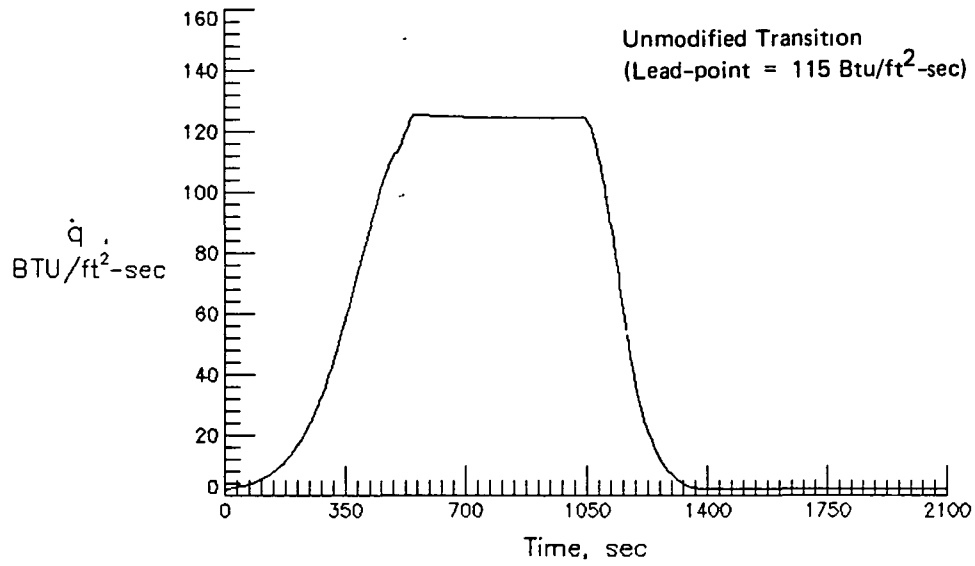
The first reason can be seen by comparing the plots in Figure 4-2 which show the dynamic pressure profiles for the unmodified (original) trajectory and the modified trajectory (both trajectories are optimized

Table 4-12. Multiple off-nominal optimization results for
 QDOT = 125 BTU/ft²-sec. with entry parameters fixed.

Guidance Parameter Name (Units)	Condition		
	Nominal	+30% Density -15% CL and +15% CD	
		Unmodified	Modified
Geocentric Latitude (deg)	-0.958	Fixed	Fixed
Perigee Altitude (nm)	27.6	Fixed	Fixed
Entry Angle-of-Attack (deg)	27.2	Fixed	Fixed
Entry Bank Angle (deg)	-69.2	Fixed	Fixed
Cruise Angle-of-Attack (deg)	25.4	25.3	23.1
Cruise Acceleration (ft/s ²)	0.0036	Same	Same
Exit Inclination (deg)	40.6	44.2	35.8
Exit Bank angle (deg)	-65.7	-69.2	-66.5
Exit Angle-of-Attack (deg)	20.4	21.4	Same
Apogee Altitude (nm)	165	180	168
Unpowered Exit Angle-of-Attack (deg)	8.13	8.12	Same
Unpowered Exit Bank Angle (deg)	-69.8	-69.7	Same
Final Vehicle Weight (lbs)	5873	4839	5281

- NOTE: (1) "Same" indicates the parameter value did not change from the nominal value.
 (2) "Fixed" indicates the parameter was not allowed to change during the optimization process.
 (3) A negative sign indicates a left bank angle.

ERV CRUISING SYNERGISTIC PLANE CHANGE Q-DOT=125



ERV CRUISING SYNERGISTIC PLANE CHANGE Q-DOT=125

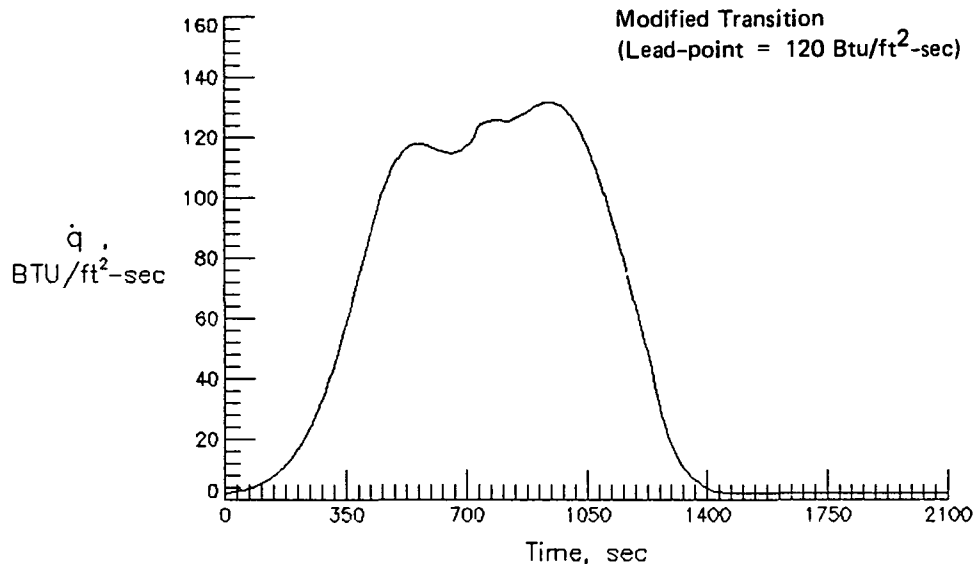


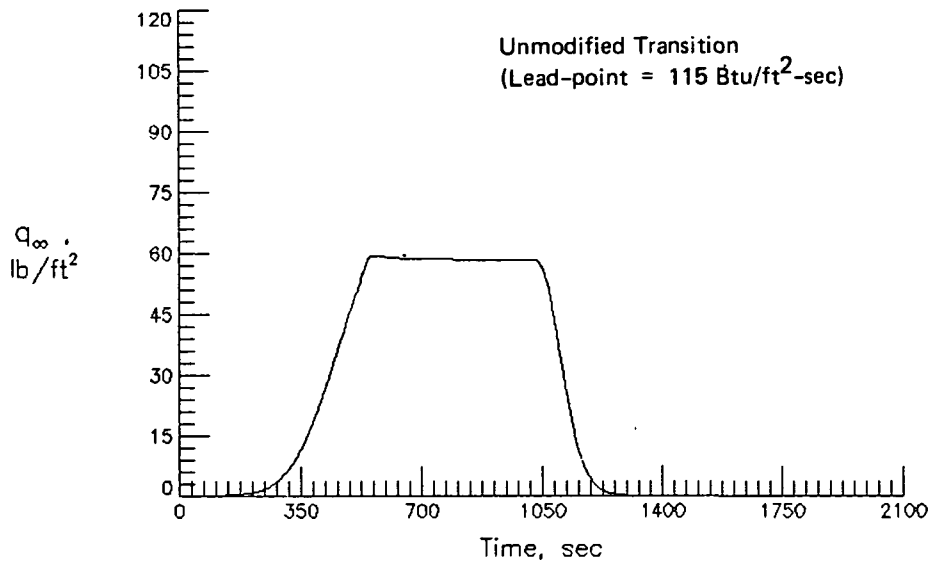
Figure 4-1. Heat-rate profiles for +30% density, -15% CL and +15% CD.

as previously explained for 30% high density and 15% low aero). The curves are similar except the first curve does not extend above 60 lbs/ft² in dynamic pressure, while the second curve has a section that goes almost to 85 lbs/ft². Overall, the maximum and the time-integrated total dynamic pressure is less for the unmodified trajectory. This situation is similar to the comparison between the 80 and 125 BTU/ft²-sec trajectories that was covered in Section 4.6. The lower dynamic pressure results in lower aerodynamic forces, hence less turning capability, which results in more of the plane change being done with propulsive forces. Thus, a similar fuel difference is seen between the unmodified and modified trajectories as between the 80 and 125 trajectories.

A second explanation for the fuel difference has to do with the plane change strategy itself. Recall from previous explanations of this strategy, that during entry as the vehicle approaches the maximum heat-rate, a level-off is started. For the unmodified trajectory, the level-off was started as the heat-rate curve was approaching what should have been its first heat-rate peak. In fact, closer examination of Figure 4-1 (unmodified plot) shows a slight change in the slope at 115 BTU/ft²-sec. For the modified trajectory the level-off was not started until the heat-rate curve was approaching a second peak.

By starting the level off at the first heat-rate peak, the vehicle reaches the maximum heat-rate boundary earlier than necessary, and the

ERV CRUISING SYNERGISTIC PLANE CHANGE Q-DOT=125



ERV CRUISING SYNERGISTIC PLANE CHANGE Q-DOT=125

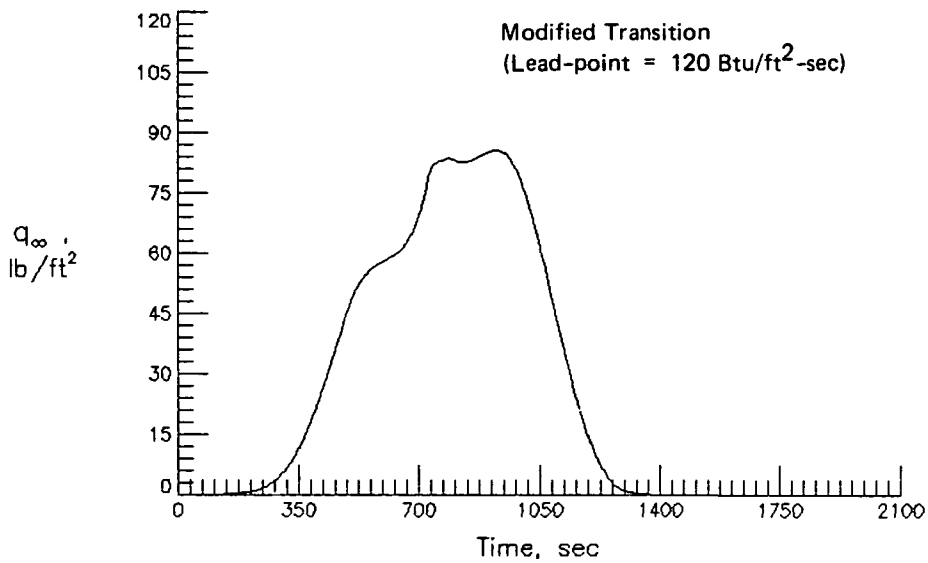


Figure 4-2. Dynamic pressure profiles for +30% density, -15% CL and +15% CD.

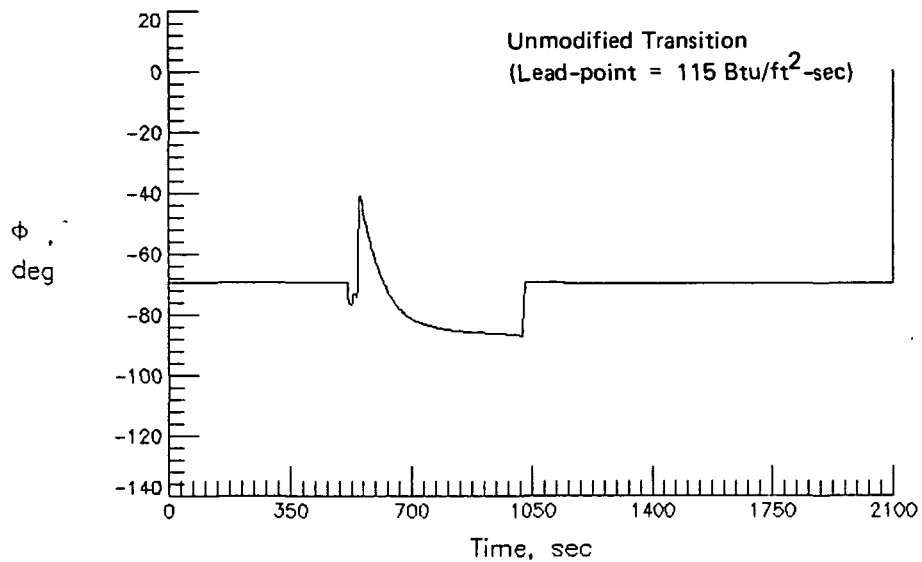
engines are used earlier than necessary. Recall that the engines are started as a part of the level-off. A comparison of the plots in Figure 4-3 shows how for the unmodified trajectory, the ERV is initially commanded to increase its bank angle (driven onto the heat boundary) before decreasing the bank angle to join the heat-rate boundary. A comparison of the plots in Figure 4-4 shows how the engines are started 210 seconds earlier for the unmodified trajectory but only cutoff 95 seconds earlier. This results in a larger time-integrated total, which translates into a fuel difference between the two trajectories. In essence, you are throwing away this phase of free, relatively high dynamic pressure which could be used to give a high turning rate at no cost in propellant. In addition, the higher dynamic pressures that are obtained by delaying your level-off (modified trajectory) are never obtained. Thus, the problem that was discussed in the first explanation.

It should be pointed out that this alteration of the heat-rate curve also occurred for the 15% low aero case. This helps explain the large decrease (from nominal) in final vehicle weight that is shown in Table 4-7. In other words, this transition to cruise problem is not restricted only to multiple off-nominal conditions.

4.4.5.2.1.1.2 THE SOLUTION

C-2

ERV CRUISING SYNERGISTIC PLANE CHANGE $\dot{Q}=125$



ERV CRUISING SYNERGISTIC PLANE CHANGE $\dot{Q}=125$

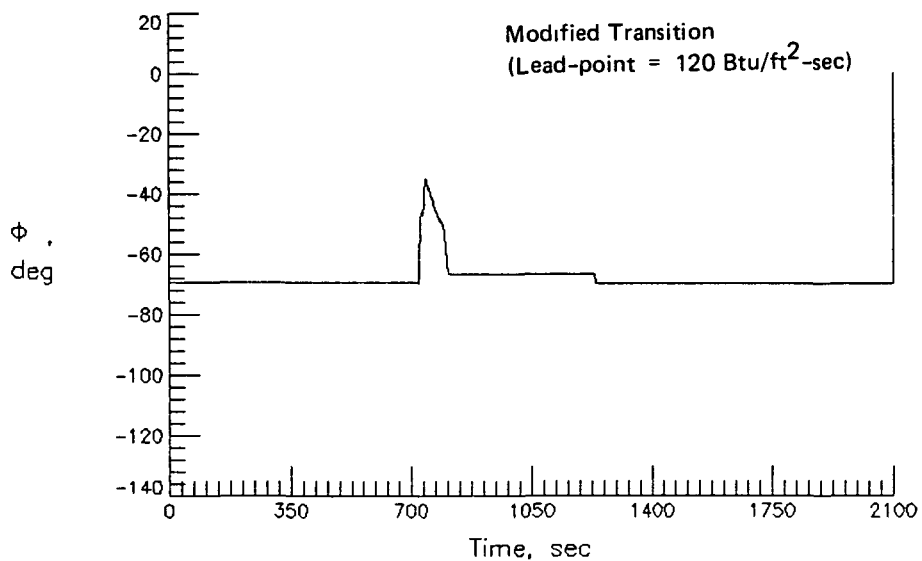
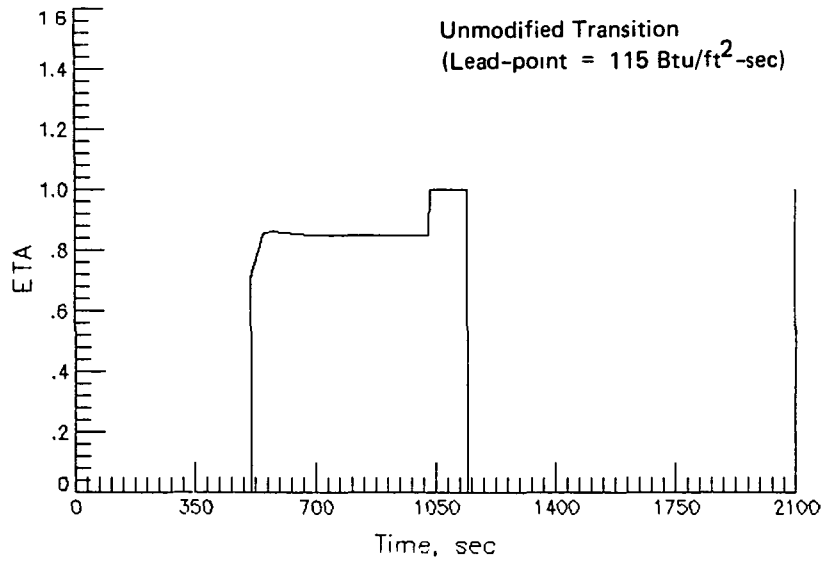


Figure 4-3. Bank angle profiles for +30% density, -15% CL and +15% CD.

ERV CRUISING SYNERGISTIC PLANE CHANGE Q-DOT=125



ERV CRUISING SYNERGISTIC PLANE CHANGE Q-DOT=125

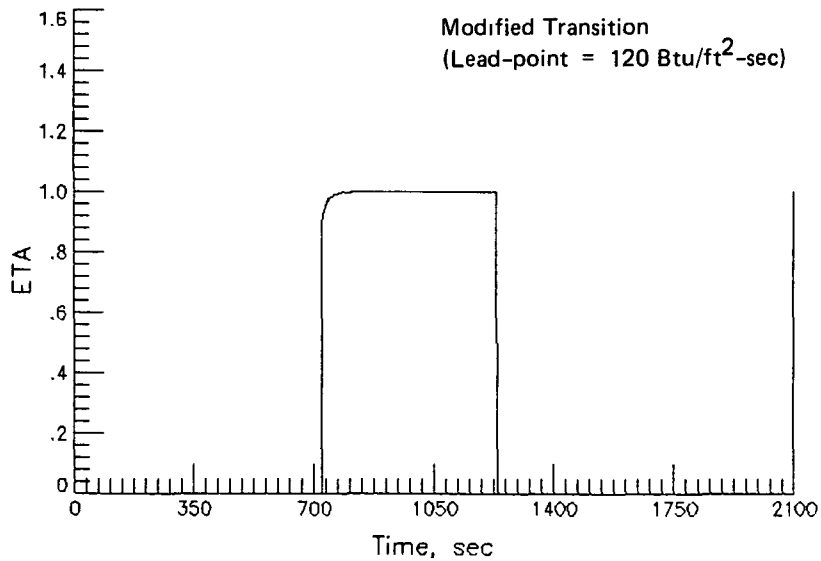


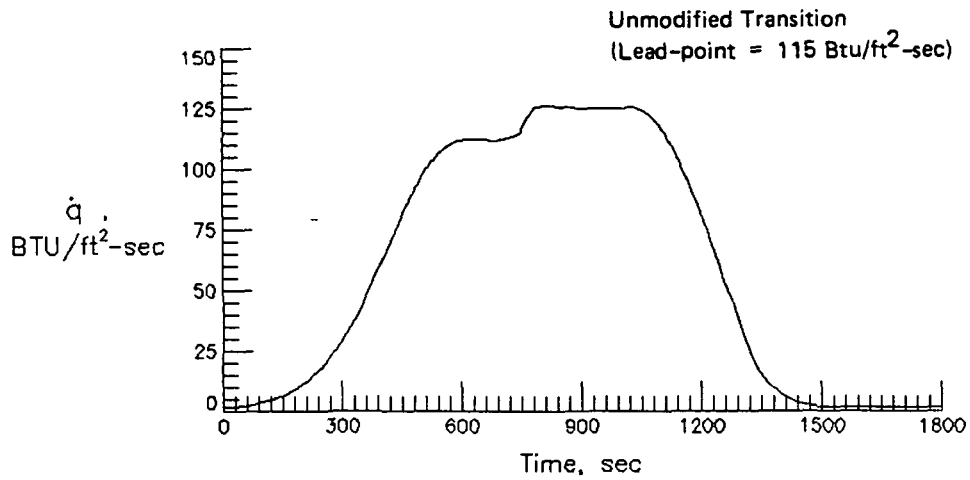
Figure 4-4. Engine throttling profiles for +30% density, -15% CL and +15% CD (0 - OFF, 1.0 - MAXIMUM).

The difference between the modified and unmodified trajectories was achieved by changing the lead-point used by the heat-rate controller. For a dynamic environment, to avoid overshooting the desired heat-rate, a controller uses a value that is different than the desired heat-rate. This value can be called the lead-point value or simply lead-point. For all previous 125 trajectories, the lead-point was set at 115 BTU/ft²-sec. The only change for the modified trajectory was to raise the lead-point to 120 BTU/ft²-sec. This allowed the restoration of the "double-peaked" heat-rate curve and the 450 pound fuel savings.

This simple lead-point modification could not fully restore the first heat-rate peak for all perturbation combinations, but it did provide a progressive improvement in fuel usage (i.e., the more restoration, the more fuel savings). Figure 4-5 provides a comparison of a modified and unmodified trajectory as an example of partial restoration. The scales for the plots are not the same so an exact comparison is difficult. However, it is evident that some restoration is made. A comparison of the final vehicle weights in Table 4-13 indicates that nearly 200 pounds of fuel was recovered for this example.

There is another possible modification that could be used since the lead-point modification does not always work. The loss of fuel efficiency is caused by either a lead-point that is too low or off-nominal conditions that raise the occurrence of the first heat peak up to the

ERV CRUISING SYNERGISTIC PLANE CHANGE $\dot{Q}=125$



ERV CRUISING SYNERGISTIC PLANE CHANGE $\dot{Q}=125$

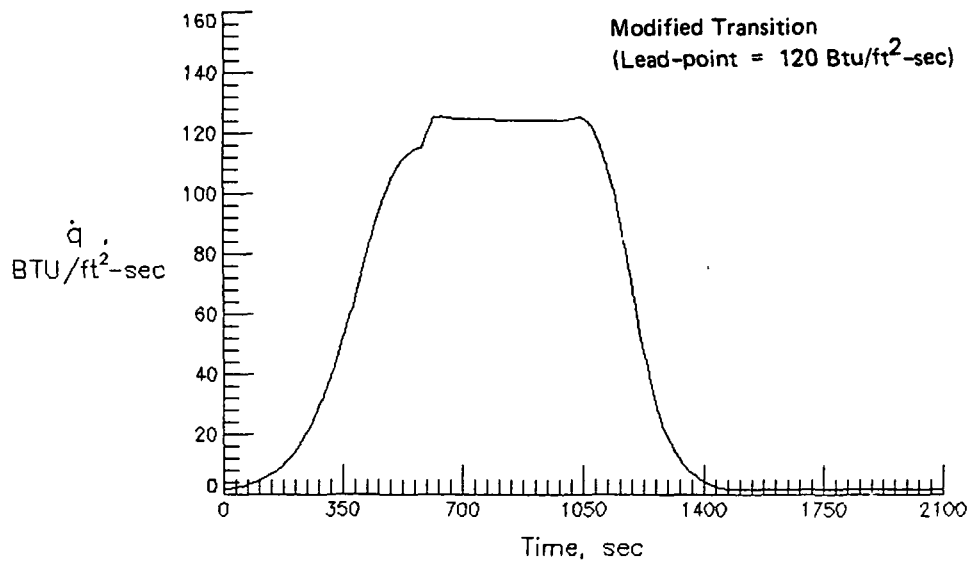


Figure 4-5. Heat-rate profiles for -30% density, -15% CL and +15% CD.

Table 4-13. Multiple off-nominal optimization results for
 QDOT = 125 BTU/ft²-sec. with entry parameters fixed.

Guidance Parameter Name (Units)	Condition		
	Nominal	-30% Density -15% CL and +15% CD	
		Unmodified	Modified
Geocentric Latitude (deg)	-0.958	Fixed	Fixed
Perigee Altitude (nm)	27.6	Fixed	Fixed
Entry Angle-of-Attack (deg)	27.2	Fixed	Fixed
Entry Bank Angle (deg)	-69.2	Fixed	Fixed
Cruise Angle-of-Attack (deg)	25.4	24.1	24.0
Cruise Acceleration (ft/s ²)	0.0036	Same	Same
Exit Inclination (deg)	40.6	41.2	37.2
Exit Bank angle (deg)	-65.7	-67.1	-70.9
Exit Angle-of-Attack (deg)	20.4	20.6	19.9
Apogee Altitude (nm)	165	168	173
Unpowered Exit Angle-of-Attack (deg)	8.13	Same	8.12
Unpowered Exit Bank Angle (deg)	-69.8	Same	Same
Final Vehicle Weight (lbs)	5873	5024	5222

- NOTE: (1) "Same" indicates the parameter value did not change from the nominal value.
 (2) "Fixed" indicates the parameter was not allowed to change during the optimization process.
 (3) A negative sign indicates a left bank angle.

nominal lead-point. Thus, the lead-point needs to be carefully chosen to avoid the maximum level of the first heat peak for off-nominal conditions. However, if this is not possible, active control to maintain the first heat peak below the lead-point might be possible. This option will be discussed in Chapter 7.

4.4.5.2.1.2 HEAT-RATE UNCERTAINTY

It has been shown several times that the efficiency of the synergetic plane change is very much a function of heat-rate and how accurately it can be controlled. In fact, for the latest example, a modification of the lead-point by only 5 BTU/ft²-sec offered a significant fuel savings. Chapman's equation, defines heat-rate as a function of velocity and density. Therefore, to achieve accurate heat-rate control, accurate velocity and density measurements are a necessity. Previous schemes have used other control boundaries such as constant drag because it can be measured quite accurately and avoids the uncertainty in density. However, flying a constant drag level does not insure that heat-rate is accurately controlled or constrained. To remain within a heat-rate constraint, a constant drag level still must be far enough from the heat-rate limit to account for the uncertainties. Therefore, no advantage is gained by using a controller other than heat-rate. The bottom line is you still must deal with the heat-rate uncertainty if you wish to

achieve the performance gains offered by a maneuver like the synergetic plane change.

4.4.5.2.2 ANGLE-OF-ATTACK CONTROL

Tables 4-12 thru 15 indicate, as have the previous optimized tables, that there is very little variation between the optimized angles-of-attack for nominal conditions and the perturbed conditions except during the cruise phase. However, during cruise, the angle-of-attack is significantly adjusted in the cases where there was an "open-loop" maximum throttle error. In all such cases, enough modification in the cruise alpha was made to eliminate the throttle error at no cost in terms of fuel usage.

4.4.5.2.3 BANK ANGLE VERSUS ANGLE-OF-ATTACK

The preference for bank angle over angle-at-attack for adjustments during entry or exit is again highlighted in Table 4-12 and 13. In all four off-nominal cases, the exit bank angle is increased anywhere from 0.8 to 5.2 degrees while angle-of-attack at most (except for one unmodified case) is decreased by 0.5 degrees. Again, the partial derivatives (not shown in the tables) indicate that the effectiveness of angle-of-attack and bank angle are about the same. Thus, the preference for bank

Table 4-14. Multiple off-nominal optimization results for QDOT = 125 BTU/ft²-sec.

Guidance Parameter Name (Units)	Condition		
	Nominal	+30% Density	
		+15% CL -15% CD	-15% CL +15% CD
Geocentric Latitude (deg)	-0.958	Same	Same
Perigee Altitude (nm)	27.6	Same	27.8
Entry Angle-of-Attack (deg)	27.2	27.4	28.0
Entry Bank Angle (deg)	-69.2	-70.1	-69.0
Cruise Angle-of-Attack (deg)	25.4	Same	24.6
Cruise Acceleration (ft/s ²)	0.0036	Same	Same
Exit Inclination (deg)	40.6	42.4	43.7
Exit Bank angle (deg)	-65.7	-66.7	-66.5
Exit Angle-of-Attack (deg)	20.4	Same	20.6
Apogee Altitude (nm)	165	163	171
Unpowered Exit Angle-of-Attack (deg)	8.13	Same	Same
Unpowered Exit Bank Angle (deg)	-69.8	Same	Same
Final Vehicle Weight (lbs)	5873	6559	4941

- NOTE: (1) "Same" indicates the parameter value did not change from the nominal value.
(2) "Fixed" indicates the parameter was not allowed to change during the optimization process.
(3) A negative sign indicates a left bank angle.

Table 4-15. Multiple off-nominal optimization results for
 QDOT = 125 BTU/ft²-sec.

Guidance Parameter Name (Units)	Condition			
	Nominal	-30% Density		
		+15% CL -15% CD	-15% CL and +15% CD	
			1 Engine Out	
Geocentric Latitude (deg)	-0.958	-0.960	Same	-0.959
Perigee Altitude (nm)	27.6	28.1	27.5	28.0
Entry Angle-of-Attack (deg)	27.2	27.2	26.7	21.8
Entry Bank Angle (deg)	-69.2	-69.0	Same	-68.3
Cruise Angle-of-Attack (deg)	25.4	25.5	24.1	22.8
Cruise Acceleration (ft/s ²)	0.0036	Same	Same	Same
Exit Inclination (deg)	40.6	42.9	40.6	44.9
Exit Bank angle (deg)	-65.7	-67.8	-67.1	-66.1
Exit Angle-of-Attack (deg)	20.4	20.5	20.5	20.8
Apogee Altitude (nm)	165	164	168	169
Unpowered Exit Angle-of-Attack (deg)	8.13	Same	Same	8.12
Unpowered Exit Bank Angle (deg)	-69.8	Same	Same	-69.7
Final Vehicle Weight (lb)	5873	6474	5124	4882

- NOTE: (1) "Same" indicates the parameter value did not change from the nominal value.
 (2) "Fixed" indicates the parameter was not allowed to change during the optimization process.
 (3) A negative sign indicates a left bank angle.

angle implies that bank angle is more fuel efficient in compensating for the perturbations in question.

4.4.5.2.4 EARLY CORRECTIONS

While the results of Table 4-12 thru 15 are not as clear as the previous results, there is still a trend of making adjustments early and flying the remaining trajectory with near nominal guidance parameters. Again the effectiveness of alpha and bank changes is much higher during entry so the preference for early changes is somewhat hidden by the size of the changes.

4.4.5.2.5 TIME-TO-EXIT

Tables 4-12 thru 15 show a significant variation in the exit inclination. Actually, this result is not especially surprising since the closer a plane change is done to the node and the quicker it is performed, the more efficient it tends to be. Therefore, the variation in exit inclination is just a result of the optimization program adjusting for changes in speed and location of the plane change for the perturbed conditions. Thus, a guidance scheme will certainly need to make similar types of adjustments to obtain a reasonable degree of fuel efficiency.

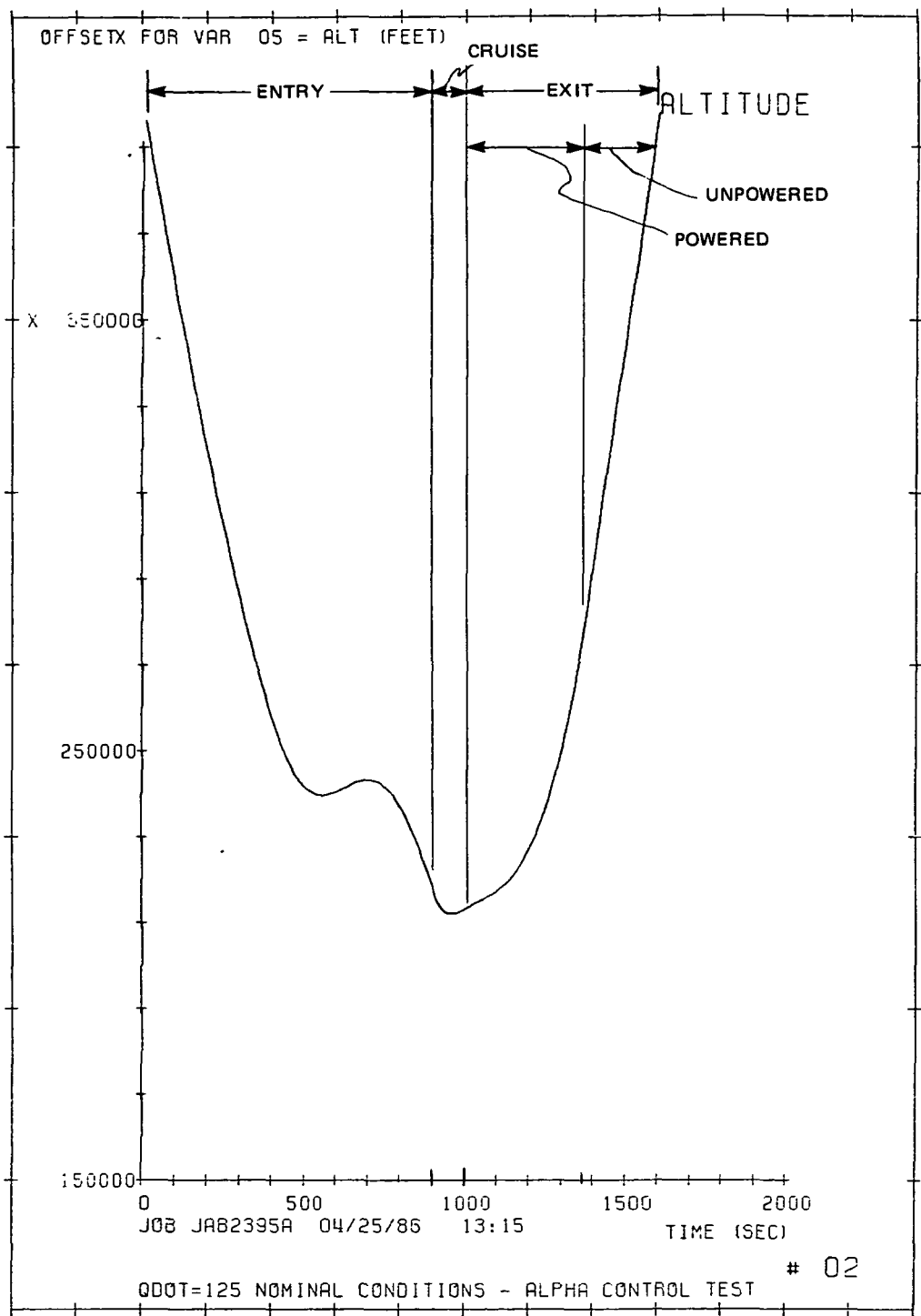
CHAPTER 5

GUIDANCE SCHEME

5.1 INTRODUCTION

Based on the guidance concepts discussed in Chapter 3 and the trajectory analysis covered in Chapter 4, a guidance scheme designed to guide the ERV through the atmospheric phase of a synergetic plane change maneuver is suggested. This guidance scheme by design produces a trajectory very similar to the plane change trajectory generated by POST. As shown in Chapter 4, this trajectory provides a very good baseline that requires relatively few modifications to maintain its optimality even in the presence of significant density and vehicular perturbations. Therefore, the suggested algorithm mirrors the strategy used in POST with a few simplifications (e.g., no optimization cycle) and several technique refinements. The resulting trajectory can be divided into three phases: (1) An entry phase where angle-of-attack and bank are held constant until pullout, (2) A powered cruise phase where the maximum heating rate is maintained and the time to start the exit phase is determined and (3) The exit phase where apogee and inclination angle are controlled with thrust and bank angle respectively. Figure 5-1

shows an altitude profile, for a target heat-rate of 125 BTU/ft²-sec and nominal conditions, with the three trajectory phases labeled. Within these three phases are three primary guidance controllers that form the hybrid guidance system discussed in Chapter 3. (1) A heat-rate controller using perturbation guidance techniques, (2) A time-to-exit controller using predictor logic, and (3) An end-condition controller using predictor/corrector techniques. Fuel is not explicitly optimized. The remaining two sections of this chapter will discuss in detail the guidance algorithm and the rationale for choosing the suggested scheme.



FRAME 003

Figure 5-1. Guidance algorithm phases.

5.2 GUIDANCE ALGORITHM

This section details the guidance algorithm by individually discussing each of the three trajectory phase. Figure 5-2 provides a summary of the guidance system and should be helpful as the algorithm is covered. All the symbols used in this chart are explained in the following subsections.

5.2.1 ENTRY PHASE

The entry phase is a constant attitude gliding maneuver that starts at atmosphere interface (400,00 feet) and ends at the pullout point for the cruise phase. A deorbit burn is made to achieve the desired velocity and position at 400,00 feet. The deorbit burn, perigee altitude, angle-of-attack, and bank angle are determined pre-mission to provide the most fuel efficient entry conditions for nominal conditions. The entry angle-of-attack and bank angle are set at 400,00 feet and remain constant throughout the entry phase. The pullout point is defined as the point where the vehicle reaches 90% of the desired heat-rate. Heat-rate (QDOT) is calculated on board using Chapman's equation.

$$QDOT = 17600 (\rho_m/\rho_{SL})^{0.5} (V_R/26000)^{3.15}$$

Phase Name	Entry	Cruise	Exit
Switching Criterion	QDOT = 0.9 QDOT	$i_p > i_D$	$\phi_c > \phi_p$ $H = 400,000'$ $ha_C \geq ha_D + ha_B$
Subphase Name	None	None	Powered Unpowered
Angle-of-Attack Logic	Nominal	Nominal If throttle > 1.0 Then $\alpha_C = \alpha_N - 0.5$ Else $\alpha_C = \alpha_{prev}$	Nominal
Bank Angle Logic	Nominal	$\phi_c = \phi_{prev}$ $- a_v (180/\pi) / (\tan(\phi_{prev}) a_{sv})$	$\phi_c = \phi_{prev} + \delta\phi_D$
Throttle Logic	Off	THRITTLE = DRAG/THRUST(cos α) If THRITTLE > 1.0 Then adjust α and THRITTLE = 1.0	Off
Function	Gliding	Heat-rate control and Time-to-exit prediction	Inclination and apogee control Inclination control
Targeting	None	Maximum heat-rate	Inclination angle and apogee altitude Final inclination angle

Note: See text for an explanation of the symbols.

Figure 5-2. Synergetic plane change guidance system summary.

where ρ_m is the measured atmospheric density, ρ_{SL} is the sea-level atmospheric density, and V_R is the vehicle's velocity relative to the atmosphere in feet/second². The density measurement is determined by direct measurement from an air data system like the Shuttle Entry Air Data System. Velocity is obtained from the inertial measurement unit (IMU).

5.2.2 CRUISE PHASE

The cruise phase begins when the heat-rate reaches 90% of the desired heat-rate and ends when exit is commanded by the time-to-exit predictor. During this phase, the ERV transitions from a descending glide to a powered, level-flight, constant-velocity cruise to maintain the desired heat-rate. The level-off is initiated by lowering the angle-of-attack to the nominal cruise value and adding power as necessary to offset drag. The cruise condition is maintained by modulating primarily engine thrust, but also angle-of-attack as necessary to maintain a constant velocity. Throttle setting is commanded such that thrust equals sensed drag or

$$\text{THRITTLE} = \text{DRAG} / (\text{THRUST} \times \text{COS}(\alpha))$$

where α is angle-of-attack. If thrust is insufficient to cancel drag (e.g., single-engine failure), then throttle is fixed at 100% and α is adjusted in 0.5 degree increments until thrust is able to offset drag.

5.2.2.1 HEAT-RATE CONTROL

With velocity fixed, altitude and hence heat-rate are controlled by modulating bank angle. Heat-rate is again defined by Chapman's equation. Heat-rate control is achieved by flying the vehicle at a density appropriate to the current velocity. The desired density is then

$$\rho_D = \rho_{SL} QDOT_D^2 / ((17600) (V_R/26000)^{3.15})^2$$

where the "D" subscripts represent desired values. So, given a velocity and desired heat-rate, a desired density can be calculated and converted to a desired density altitude (h_ρ) with a simple exponential model. The heat-rate controller equation is a standard second order controller defining a desired vertical acceleration (a_v) such that

$$a_v = k_1 \Delta h_\rho + k_2 \Delta h_\rho' + \Delta h_\rho''$$

where k_1 and k_2 are constants. Δh_ρ , $\Delta h_\rho'$, and $\Delta h_\rho''$ are the difference between desired and current density altitude, density altitude rate, and density altitude acceleration respectively. Desired altitude rate and altitude acceleration are determined by back differencing. The desired altitude acceleration is smoothed with a low pass filter. The current

altitude rate is the vertical component of the vehicle velocity and this is back differenced to determine current altitude acceleration.

Finally the desired vertical acceleration can be converted to a commanded bank angle (ϕ_c) such that

$$\phi_c = \phi_{prev} - a_v (180/\pi) / (\text{TAN}(\phi_{prev})) a_{sv}$$

where ϕ_{prev} is the previous bank angle and a_{sv} is the vertical component of the sensed nongravitational acceleration (19).

5.2.2.2 TIME-TO-EXIT

While the heat-rate controller is maintaining a constant heat-rate, a predictor is run every ten seconds to see how much of the desired plane change could be accomplished using nominal exit controls and conditions if the exit was begun at current time. Specifically, the guidance system integrates the vehicle state ahead to 400,000 feet assuming nominal alpha, bank and 100% thrust to determine the final inclination. When the predicted inclination angle (i_p) is greater than the desired inclination angle (i_D) then exit is started. There is an additional constraint on determining the time to begin the exit. For heat control, any bank angle greater than the current commanded bank angle will cause overheating of the vehicle. Thus when determining the time to begin the

exit, the algorithm uses the smaller of current or nominal exit bank angle in the integration to 400,000 feet.

5.2.3 EXIT PHASE

The exit phase begins when exit is commanded by the time-to-exit predictor and ends when the vehicles leaves the atmosphere at 400,000 feet. During this phase, thrust is increased to 100%, angle-of-attack is set at the nominal exit value, bank angle is modulated to achieve the desired final inclination, and final apogee altitude is controlled by engine cutoff. However, heat-rate control must be continued until the vehicle climbs to an altitude where heating is no longer a concern. Therefore, during the first minutes of exit, if heat control requires a smaller bank angle than inclination control, heat control takes priority. Once heat-rate commands a bank angle greater than inclination control, then inclination control takes priority (19).

5.2.3.1 INCLINATION CONTROL

During the final part of the exit phase, the inclination at 400,000 feet is controlled by modulating bank angle. A predictor/corrector guidance routine predicts a bank angle that, if held constantly throughout the remaining exit phase, will achieve the desired inclination angle.

The predicted bank angle is determined by finding a linear relationship between the final inclination and bank angle. The predictor algorithm numerically integrates the trajectory ahead to 400,000 feet to determine the final inclination (i_{oid}). Another integration is made with a slightly different bank profile ($\phi_{prev} + \delta\phi$) and the new inclination (i_{new}) is determined. A partial derivative of inclination with respect to bank angle ($\partial i/\partial\phi$) is calculated such that

$$\partial i/\partial\phi = (i_{new} - i_{oid})/\delta\phi$$

With the sensitivity of changes in inclination to changes in bank angle, the change in bank angle ($\delta\phi_D$) to achieve the final inclination (i_D) can be determined as

$$\delta\phi_D = (i_D - i_{oid})/(\partial i/\partial\phi)$$

Then the commanded bank angle is the previous bank angle plus the update or

$$\phi_c = \phi_{prev} + \delta\phi_D$$

If the update is large, then non-linear effects may require the process to be iterated.

5.2.3.2 APOGEE ALTITUDE CONTROL

The final apogee altitude is controlled by engine cutoff time. The engine cutoff is commanded when the vehicle has sufficient velocity to coast to the desired apogee altitude (ha_D). For simplicity, the initial apogee prediction is done assuming the vehicle is moving conically (point mass gravity and no atmosphere). The expression for the apogee of any conic orbit can be written in closed form. However, since the engine cutoff occurs in the atmosphere, the conic apogee (ha_c) cutoff altitude is biased to compensate for the residual atmospheric drag between cutoff and apogee. So, the cutoff time is when

$$ha_c = ha_D + ha_B$$

where ha_B is apogee bias. To compensate for perturbations, this bias must be adjusted using the predictor/corrector's estimation of apogee altitude (ha_p) at 400,000 feet such that

$$(ha)_\epsilon = ha_p - ha_D$$

$$ha_B = ha_B + K(ha)_\epsilon$$

where $(ha)_\epsilon$ is apogee error and k is a constant. This process is repeated if apogee error is greater than five nautical miles.

5.3 GUIDANCE RATIONALE

5.3.1 ENTRY PHASE

The reasoning for going with constant attitude or open-loop is based on the overall results of Chapter 4. Specifically, the results in Tables 4-8, 4-12 and 4-13, where the entry parameters were fixed, indicated that the cost was at most 100 pounds of fuel. In actuality, the possibility of achieving a 100 pound savings by adjusting entry parameters was remote since the optimization program achieved this result with a priori knowledge. In fact, we could visualize situations where a correction for one deviation is made on the front-end while it might be reversed on the tail-end of the trajectory. At the same time, allowing the errors to build up and trying to fix them at the end did not seem reasonable either. First, it goes completely against what our trajectory analysis indicated was the most fuel efficient method, and second, it might over tax the guidance system to try and compensate too late. Thus, we compromised and chose to begin closed loop guidance at the start of the cruise phase. The final consideration during entry was the lead-point for the heat-rate controller. Once again a compromise approach was chosen. To avoid exceeding the maximum heat-rate, an adequate lead-point for the heat-rate is needed. However, as shown in Chapter 4, if the lead-point is too low, it is possible to cutoff the

first heat-rate peak which can cost up to 450 pounds of fuel. Based on test results, 90% of the maximum heat-rate was determined to be a reasonable compromise (19).

5.3.2 CRUISE PHASE

The rationale for control of heat-rate and time-to-exit are a result of the baseline plane change strategy and our trajectory analysis. The optimization analysis showed that fuel could be minimized by doing the pullout and cruise at maximum heat-rate. Also, the time in the atmosphere could be reduced by doing as much of the plane change during the exit as possible.

5.3.2.1 HEAT-RATE CONTROL

The control of heat-rate during the cruise phase is very important. Overheating will jeopardize vehicle safety and underheating will cost additional fuel. In order to maintain tight control over heat-rate, perturbation guidance was chosen.

Heat-rate, based on Chapman's equation, is only a function of density and velocity. Therefore, of the available control parameters discussed in Chapter 3, only angle-of-attack, bank angle and engine thrust are possible controller candidates. Engine thrust has no direct effect

on density so it could only be paired with velocity. Bank angle and angle-of-attack can be used to control density or velocity. Analysis of the POST results indicated that bank angle was always able to control the heat-rate and hence density but the nominal angle-of-attack along with maximum thrust (e.g., single-engine failure) was not always able to maintain a constant velocity. Therefore, it was reasonable to use angle-of-attack and engine thrust to maintain velocity. Because of the multiple influence of angle-of-attack (affects CL,CD and the component of thrust aligned with drag) and for simplicity it seemed more appropriate to use angle-of-attack only as necessary and primarily modulate thrust to maintain velocity. Therefore, the final scheme sets a nominal angle-of-attack and adjusts thrust as necessary to maintain a constant velocity. If thrust is insufficient to cancel drag (i.e., maintain velocity), then angle-of-attack is adjusted until drag is offset. Recall that this reduction of alpha is beneficial for two reasons: (1) The CD is lowered as angle-of-attack is reduced, thereby reducing drag and (2) A reduced alpha increases the component of thrust in the direction of drag. Separately, bank angle is modulated to control altitude which controls density which in turn controls heat-rate.

5.3.2.2 TIME-TO-EXIT

The rationale for the time-to-exit predictor is a result of the trajectory analysis work in Chapter 4 and an earlier study by R. Richards

(19). The trajectory analysis results generally showed that fuel is minimized for the entire trajectory by adjusting the exit point and using near nominal parameters during exit. The study that Richards conducted showed that fuel was minimized for the exit phase when the ERV started the exit at a point where it could just make the end-conditions using approximately 90 degrees of bank and nearly nominal angle-of-attack. However, this study assumed no perturbations were encountered during exit and left very little room to compensate for any future perturbations. Recall from Chapter 4, optimum exit bank angles for all cases considered with POST ranged from 65-72 degrees. Thus, the scheme of exiting when the predictor concluded you could make the end-conditions with nominal exit controls and conditions seemed to offer a near optimum solution while providing some extra margin to compensate for future perturbations.

5.3.3 EXIT PHASE

The rationale for the end-condition controller during the exit phases is a result of the discussion in Chapter 3 on control variable pairings and analysis of the POST results covered in Chapter 4. For simplicity, we decided to make a one-to-one pairing of each control variable and targeting parameter and if possible, handle each pair separately even though there are coupling effects. Likewise, even though there is one more control variables than items to constrain, we chose not to go with

the added complexity and convergence concerns unless the extra variable was needed or offered some clear advantage. Recall from Chapter 4, angle-of-attack was hardly used during exit and consistently used less than bank angle for fuel efficiency reasons. Thus, we chose to use bank angle only as an inclination controller and engine cutoff for apogee control. Hence, angle-of-attack is left as an additional control variable, completely free for future guidance requirements.

CHAPTER 6

GUIDANCE ALGORITHM TESTING

6.1 INTRODUCTION

To evaluate the performance of the plane change guidance scheme discussed in Chapter 5, many simulations are made using various operating conditions. Although the guidance scheme is the same, the characteristic trajectory for a heating rate of 80 as compared to 125 BTU/ft²-sec is quite different. Therefore, they are treated as separate cases for the various operating conditions.

The entire plane change process entails using the Earth's atmosphere to change the orbital plane. Therefore, if the atmosphere is not a nominal atmosphere with standard density values, the guidance algorithm must still be able to do its job. Many test simulations are made with off-nominal atmospheric conditions to verify that the algorithm does, in fact, perform as desired. Among these tests are density bias tests, where the nominal density is increased or decreased by a constant factor, and density shears, where the trajectory passes through a varying

density profile model. Various values of density biases and different shear models are simulated to evaluate the algorithm's performance.

Another test of the algorithm is to change the aerodynamic characteristics of the ERV. This is done by using various combinations of CL and CD. A final test was made to determine the algorithm's response to a single-engine failure. This was done by eliminating the thrust produced by one of the three ERV engines.

After testing each off-nominal condition individually, several combinations are tested as well. For example, a thin atmosphere is tested in combination with low aerodynamic characteristics. Some of the combinations of off-nominal conditions yield a more realistic simulation overall, as there are bound to be multiple variations in a real environment at all times. However, some of the combinations probably provide a more severe test of the algorithm than would be reasonable to expect the ERV to encounter. The scheme was not specifically designed to handle these cases but are included to demonstrate its robustness.

6.2 EVALUATION CRITERIA AND THE NOMINAL TRAJECTORY SIMULATION

There are several quantities that are useful in evaluating the performance of the guidance algorithm. The main goal of the atmospheric maneuvering is to change the inclination of the orbital plane. If the

algorithm does not guide the ERV to the desired inclination, it is not doing the job. Therefore, one of the most important quantities is the amount of inclination change that was accomplished during the atmospheric maneuver. The algorithm has been designed for a nominal plane change of 20 degrees. If the actual plane change in a test run is within 0.1 degrees of that nominal value, the test will be considered successful. The closer the inclination is to the nominal value, the better, as less fuel will be required to correct the orbit.

Another important criterion is the final apogee altitude. The algorithm has been designed for a nominal target apogee of 160 nautical miles. If the actual apogee in a test run is within 5 nautical miles of that nominal value, the test will be considered successful. Once again, the closer the apogee is to the nominal value, the better as less fuel will be required to correct the apogee.

Since the potential fuel savings is one of the main reasons for performing the maneuver, fuel use is important and is also a consideration in the performance evaluation. For each test run, the fuel required to circularize the orbit at the target apogee height is computed assuming that engine burns are made at the apogee and then at the raised perigee. Also included in this calculation is the fuel required to correct any inclination error. Comparing the total fuel required to obtain the 160

nm circular orbit to the nominal trajectory simulation run provides one measure of the algorithm performance.

In addition, a comparison with the fuel used in the optimized trajectory generated by POST for the same conditions provides an evaluation of how well the algorithm performed in comparison to the best it could be expected to perform. The only caveat being, the fuel results from POST shown in Chapter 4 and the summary of results for this chapter are for a 1976 standard atmosphere. The CSDL simulations used a 1962 standard atmosphere. These models are very similar below 290,000 feet. Therefore, the comparison between POST and the CSDL simulation fuel results while not exactly comparable should offer some valid insight.

Also computed is the fuel required to correct the perturbed orbit's longitude of the ascending node (LAN) to the nominal. Although no attempt was made to control the node shift, the node does shift during the atmosphere phase of the trajectory. This is because the inclination change was spread out across the node, and unless it was balanced evenly before and after the node there is going to be some node shift. For the CSDL nominal 80 and 125 BTU/ft²-sec trajectories the LAN shifted from zero to 3.91 and 1.44 degrees respectively. Therefore, all simulations will use this LAN as the final desired LAN. While the fuel to correct the note shift is typically small, a large value will indicate that the algorithm's performance could possibly be improved. As a point of ref-

erence, the final LAN for the POST 80 and 125 nominal trajectories (1962 atmosphere) was 3.90 and 1.44 degrees respectively.

The final important criterion used in the performance evaluation is maximum heating rate. Since there is a limit to the heating rate that the ERV can withstand, a run which allows the heating rate to exceed its limit has safety of flight problems. On the other hand, if the algorithm allows the vehicle to operated below its maximum limit, fuel efficiency will be hurt because of the correlation between heat-rate and plane change performance (6). Although exceeding the maximum heating rate limit would probably cause a much worse consequence than degraded plane change efficiency, for simplicity, an actual heating rate within 5 BTU/ft²-sec of the desired heating rate, high or low, will be considered acceptable and the test successful. As mentioned in Chapter 2, total heat load for this type of plane change is not considered a constraint and is not included as a performance criterion.

The CSDL 80 and 125 BTU/ft²-sec nominal trajectory simulation runs will be used as the primary basis for comparison. For these runs the inclination change is 20.007 and 20.006 degrees respectively, and the final apogee altitude is 158.0 and 158.5 nautical miles. The final vehicle weight in a 160 nm circular orbit with the complete plane change is 5450 and 5961 pounds respectively, and the maximum heating rate is 80 and 126 BTU/ft²-sec. For reference, Figures 6-1 thru 8 present plot

profiles for the 80 and 125 nominal synergetic plane change trajectories generated by the CSDL computer simulation using the plane change guidance algorithm. These figures should be useful for comparison with the figures of the various test runs presented in the following sections.

6.3 SIMULATION TEST RESULTS

A wide variety of off-nominal conditions are simulated to evaluate the guidance algorithm's performance. An example of the resulting trajectory plots will be presented for each type of test condition and where some new information is contained in the plotted data. Tables will summarize the test results in each subsection that follows.

6.3.1 SINGLE OFF-NOMINAL CONDITION TESTS

The following subsections will present the results for tests which involve one off-nominal condition while all other values are nominal. The tests include density biases, density shears, aerodynamic uncertainties, and single-engine failure performance.

6.3.1.1 DENSITY BIASES

The nominal density levels are multiplied by a constant factor in this set of tests to determine how thin or thick an atmosphere the guid-

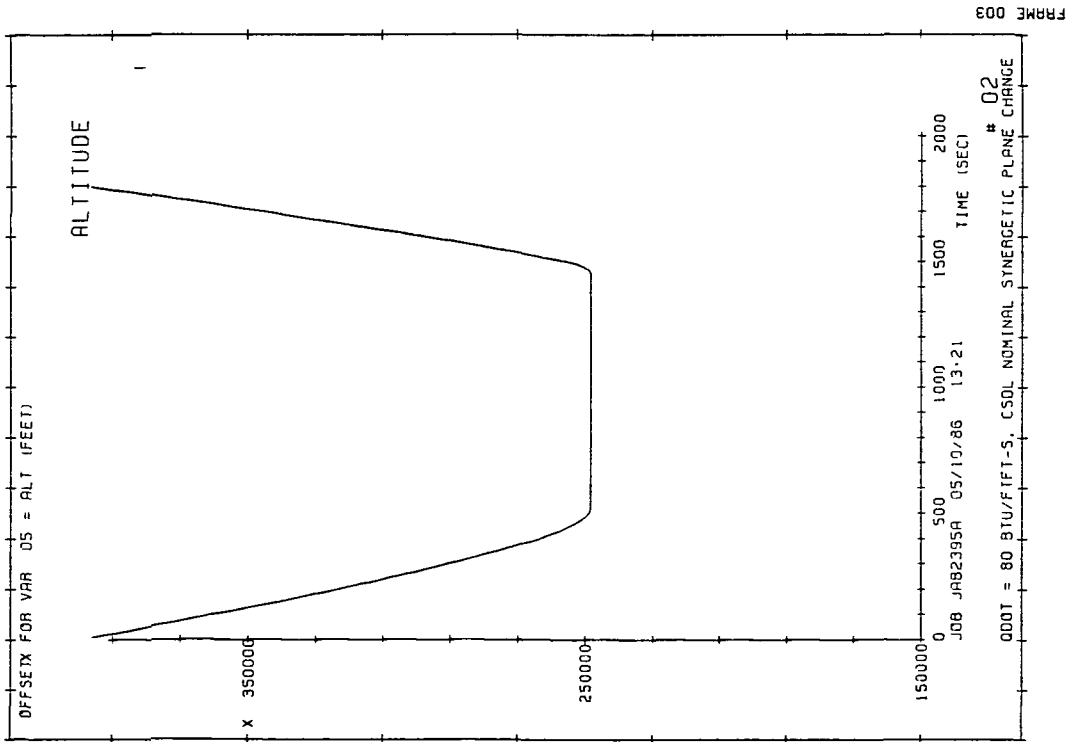
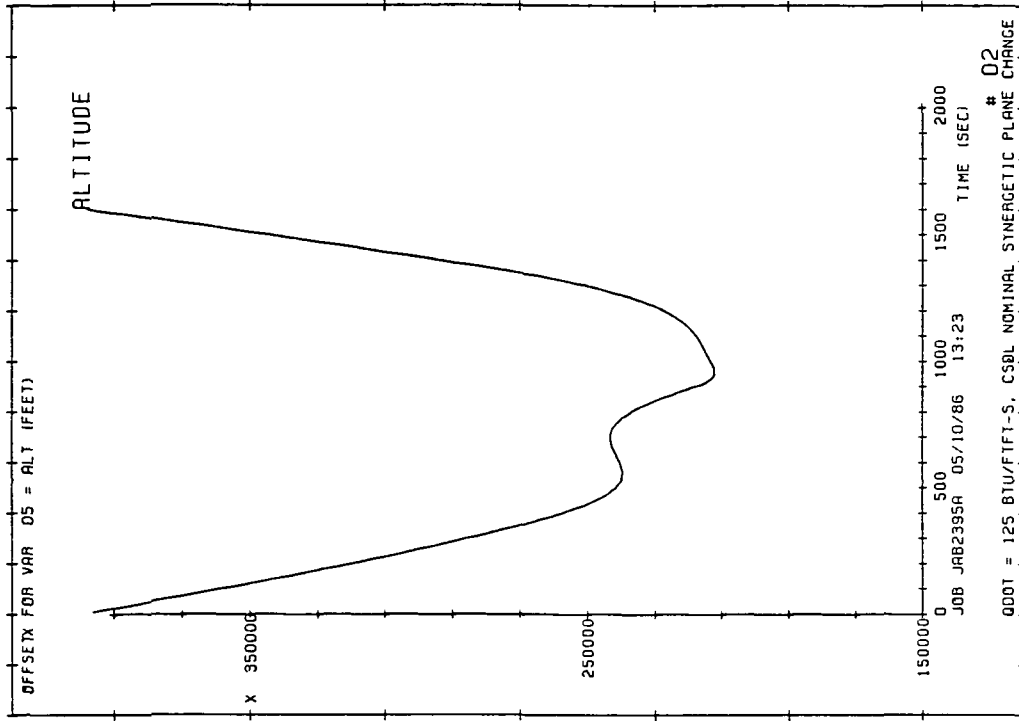
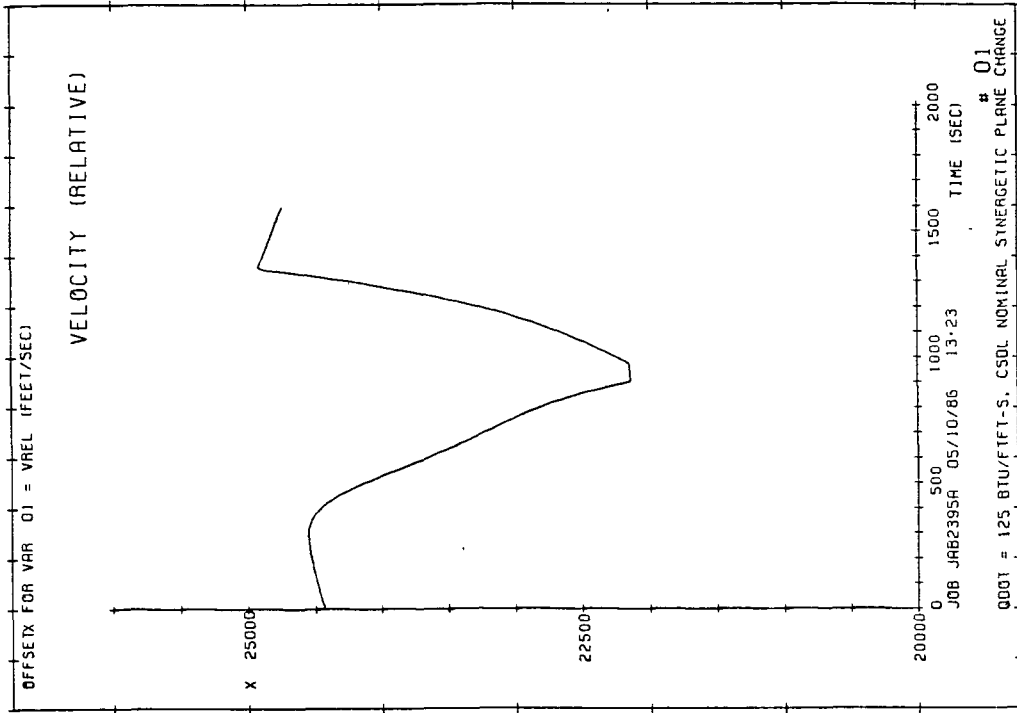
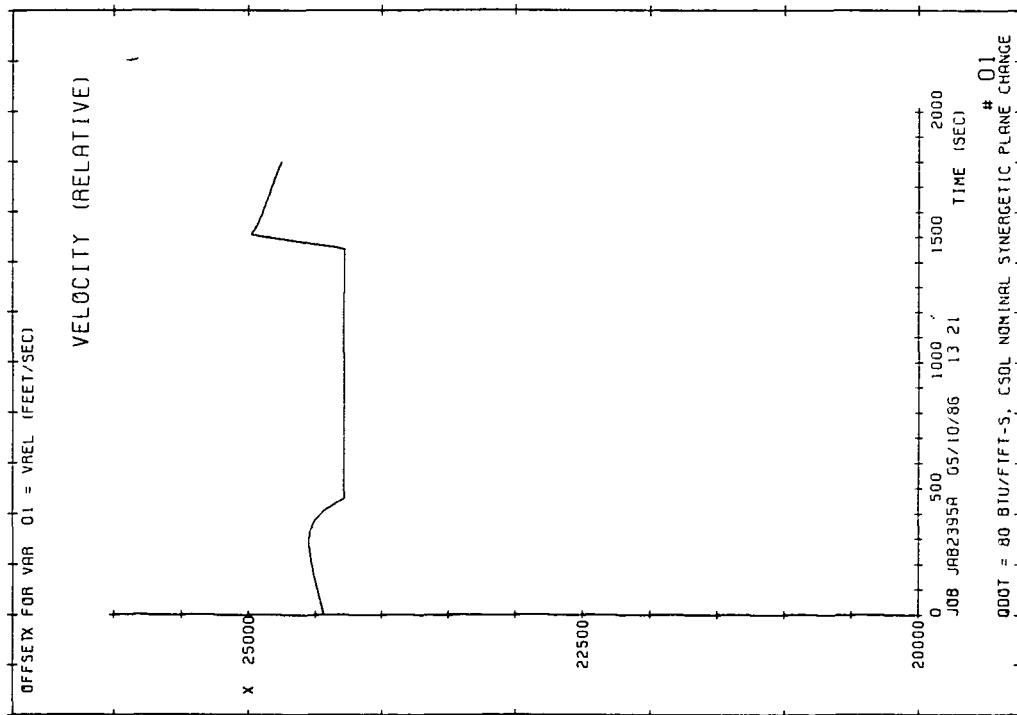


Figure 6-1. Altitude profiles for QDOT = 80 and 125, nominal conditions.

ORIGINAL PAGE IS
OF POOR QUALITY



FRAME 002



FRAME 002

Figure 6-2. Vehicle velocity profiles for QDOT = 80 and 125, nominal conditions.

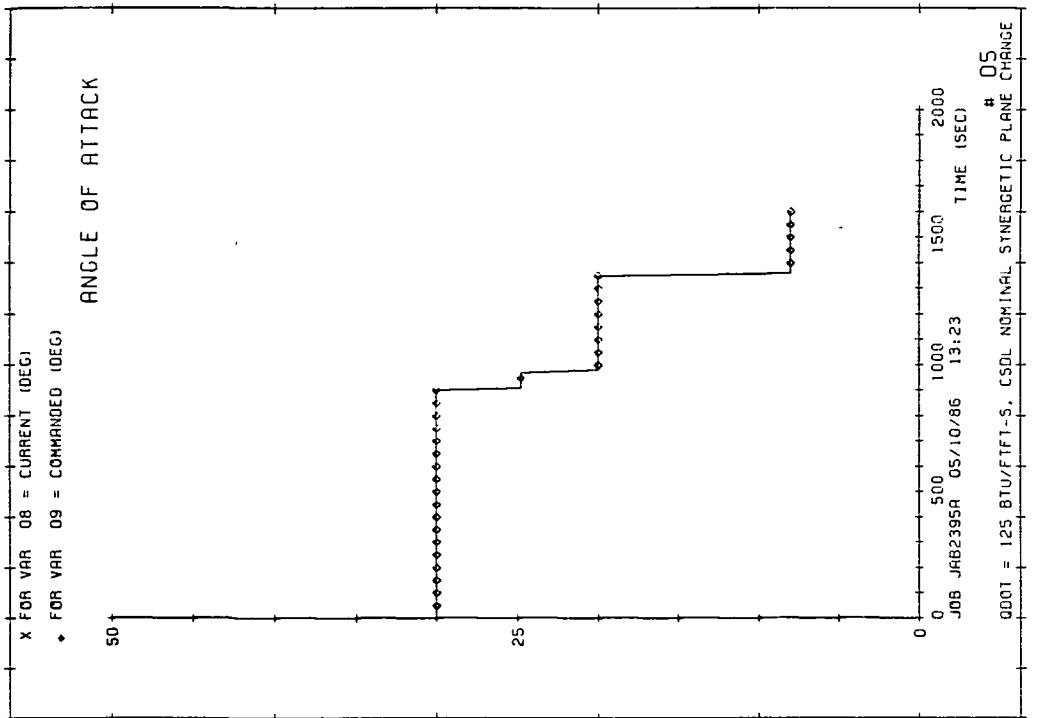
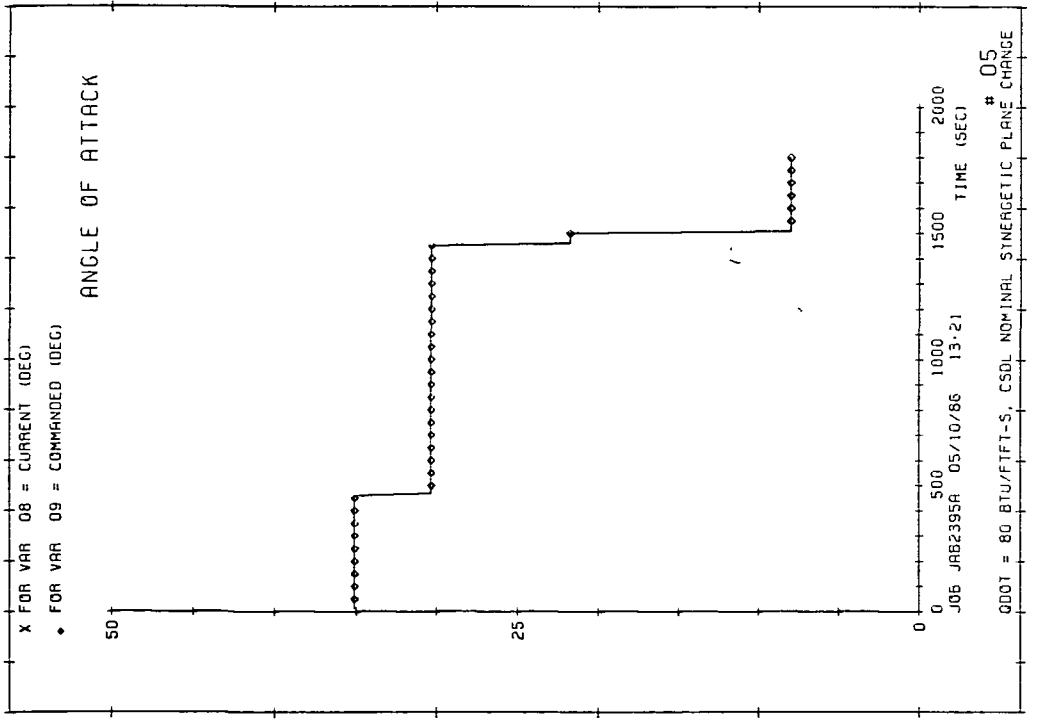


Figure 6-3. Angle-of-attack profiles for QDOT = 80 and 125, nominal conditions.

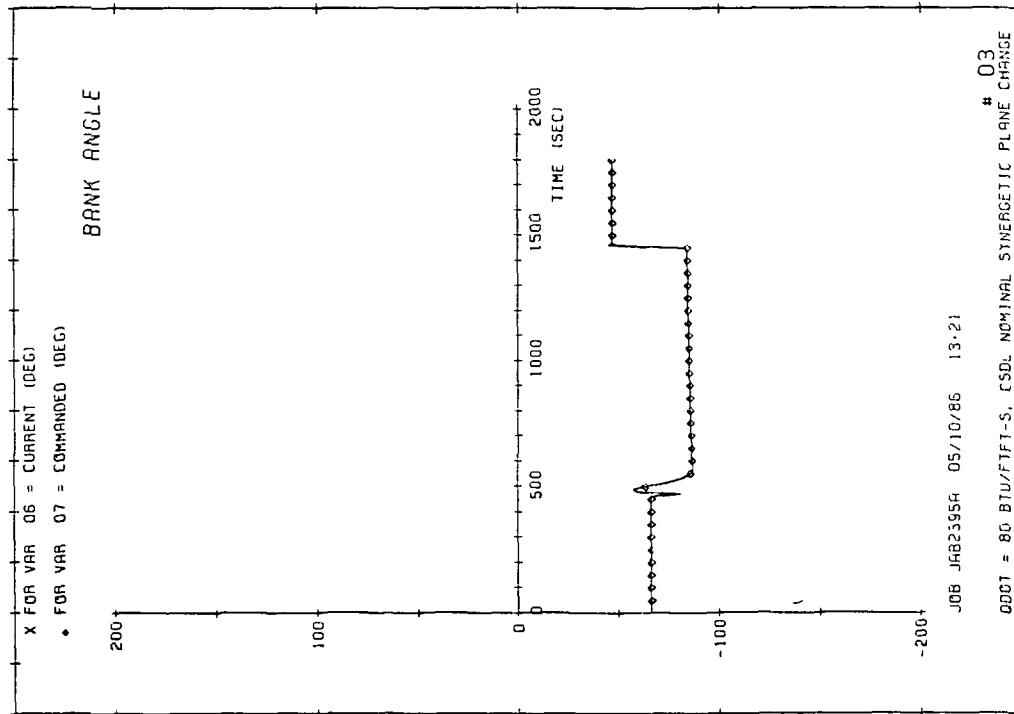
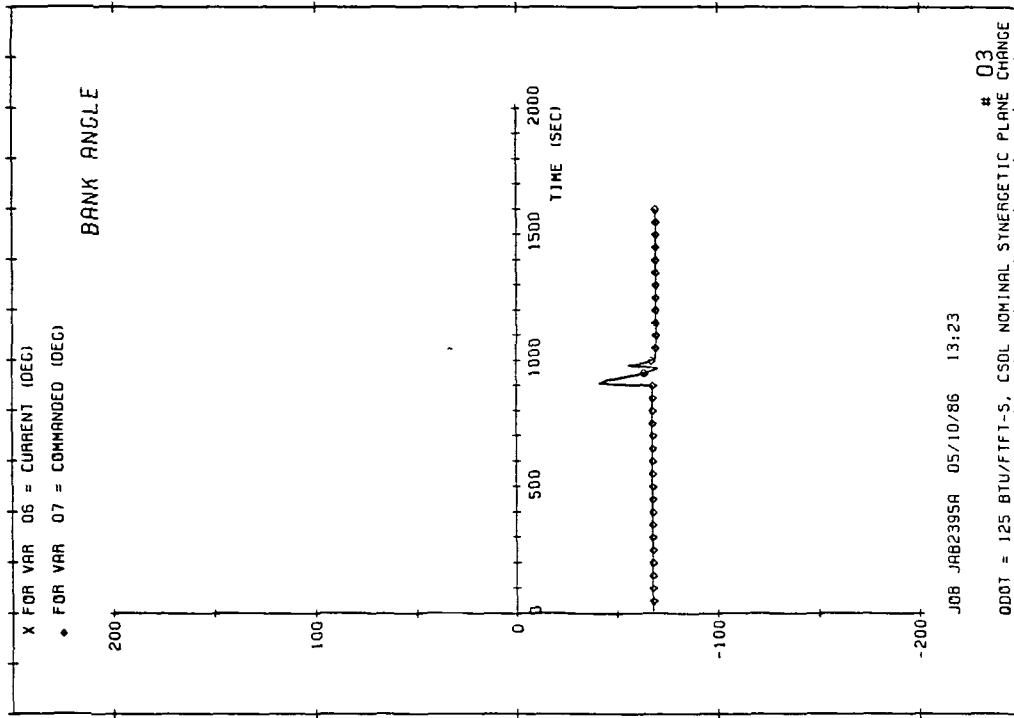
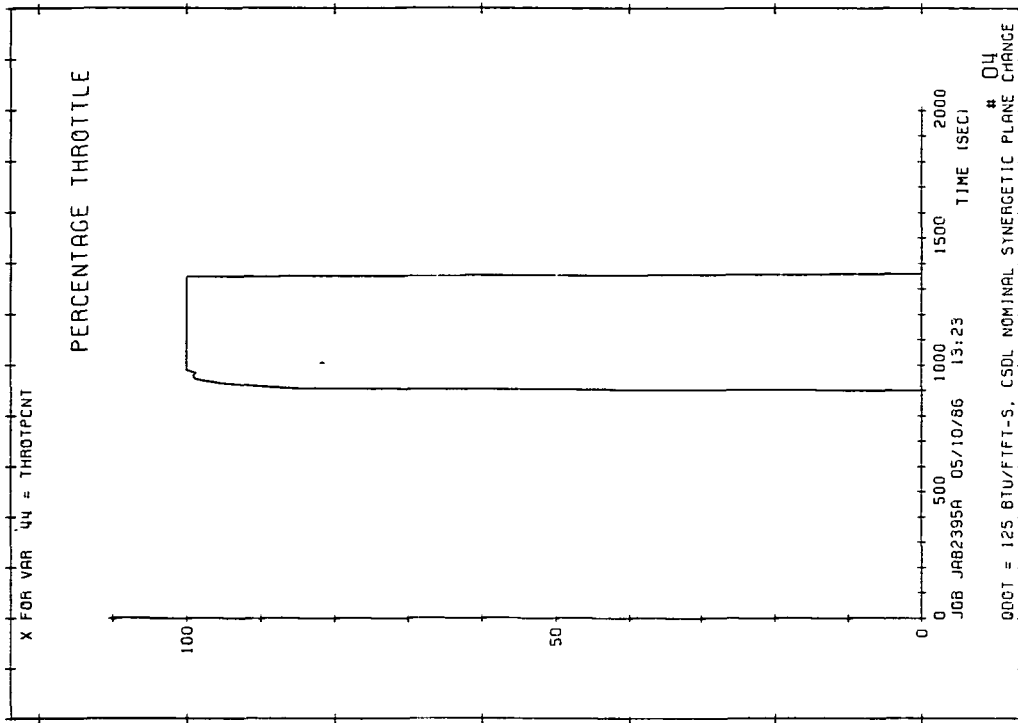
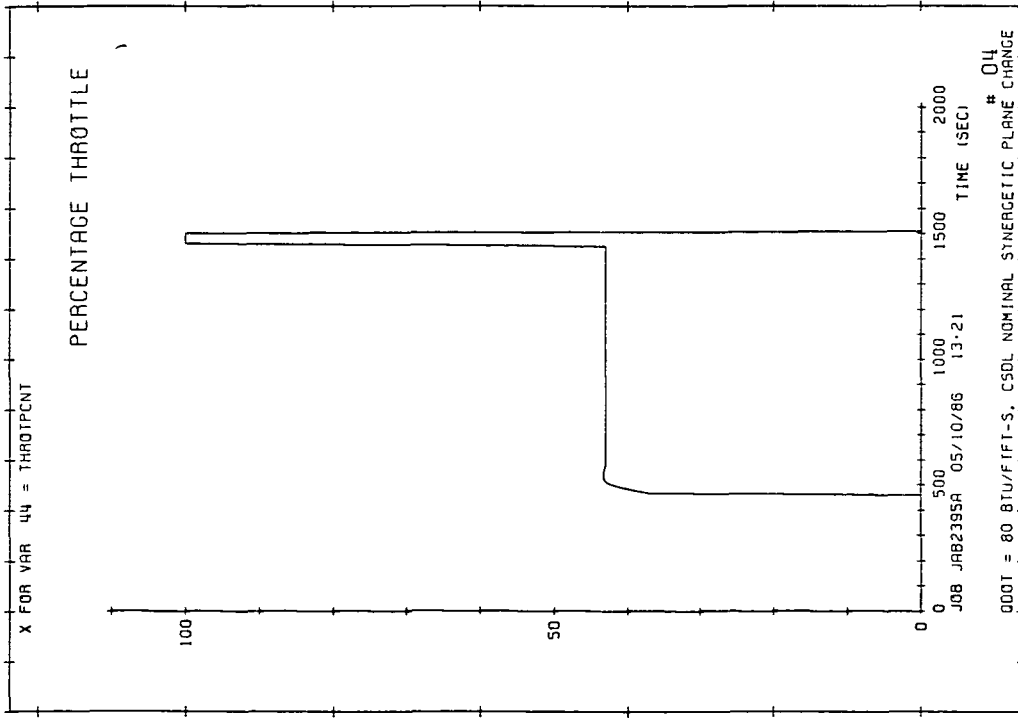


Figure 6-4. Bank angle profiles for QDOT = 80 and 125, nominal conditions.

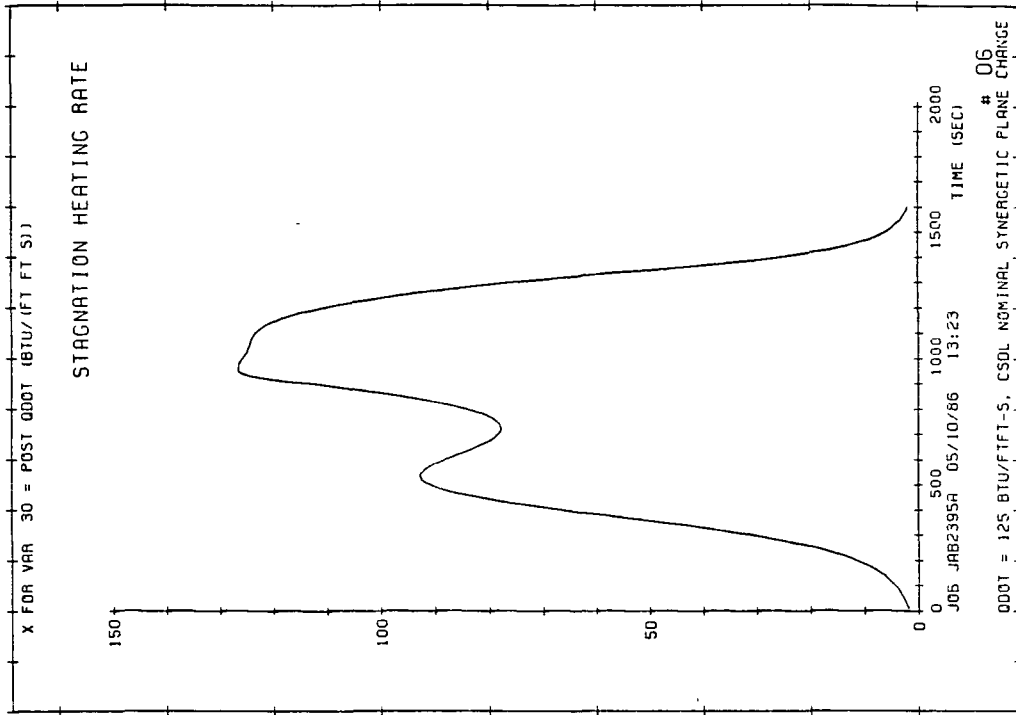


FRAME 005

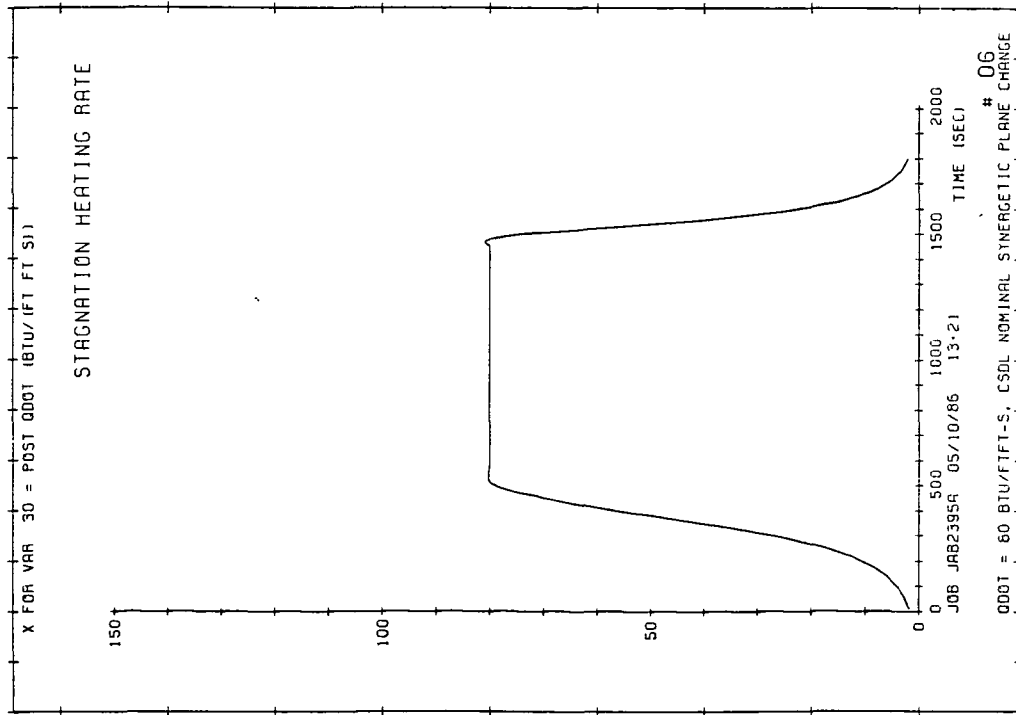


FRAME 005

Figure 6-5. Engine throttling profiles for QDOT = 80 and 125, nominal conditions.



FRAME 007



FRAME 007

Figure 6-6. Heat-rate profiles for QDOT = 80 and 125, nominal conditions.

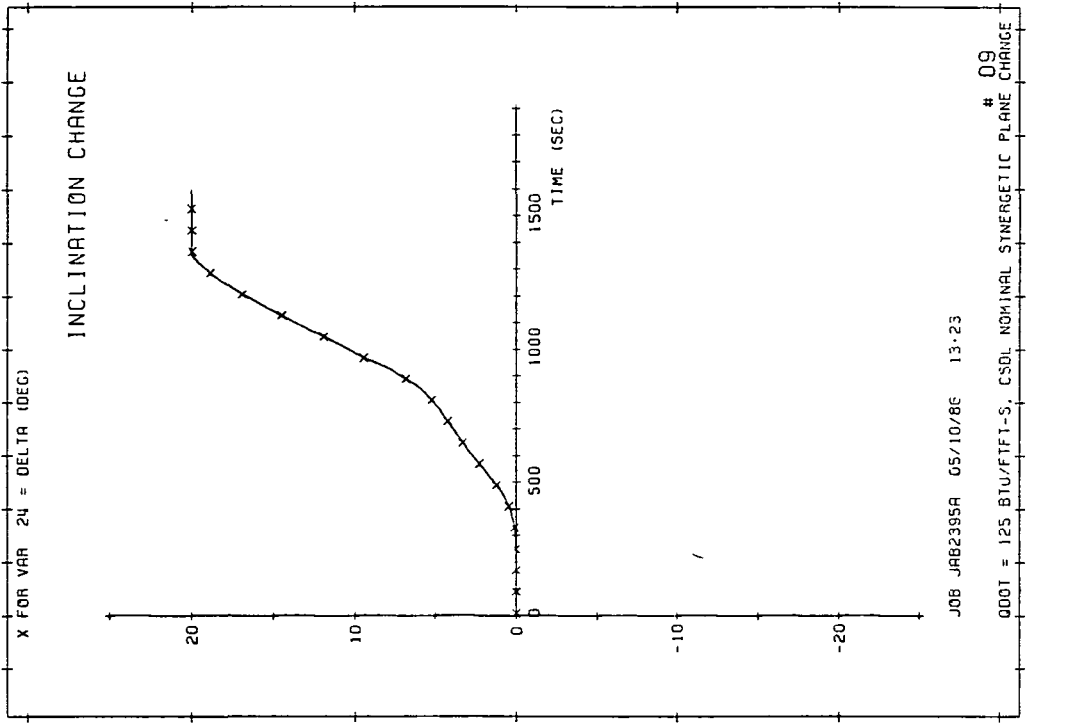
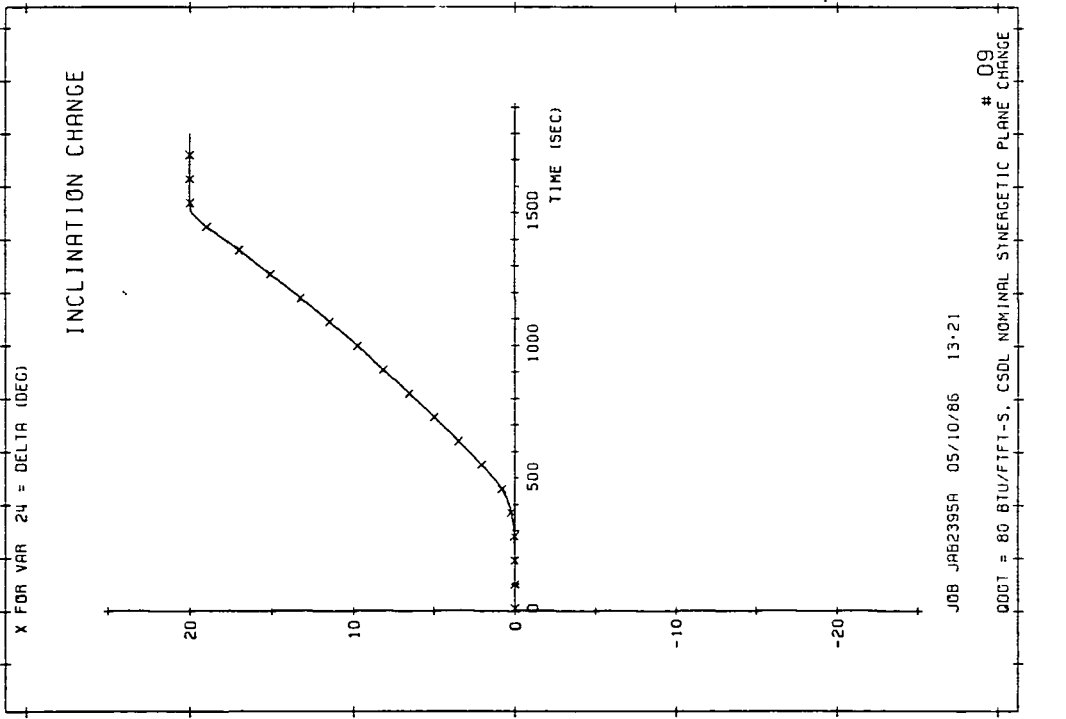
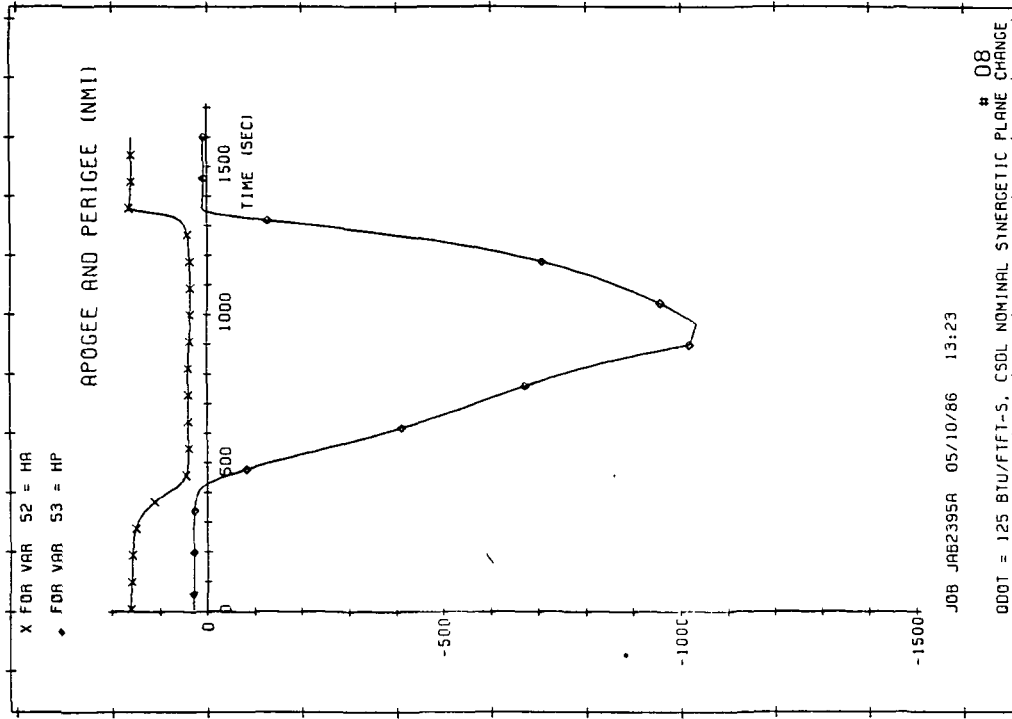
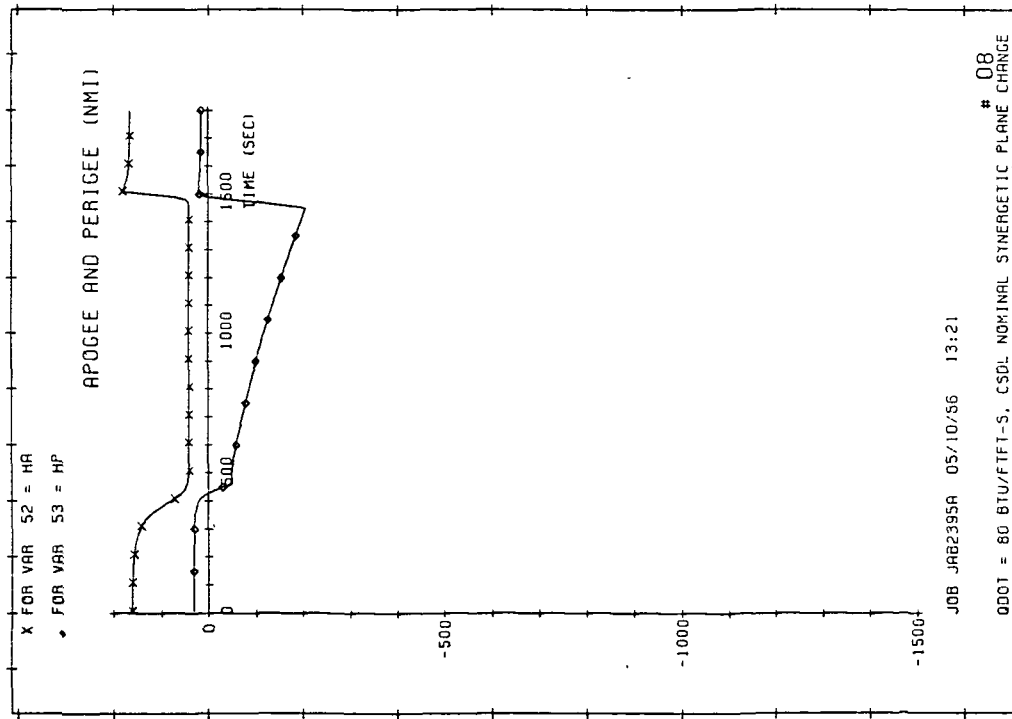


Figure 6-7. Inclination change profiles for QDOT = 80 and 125, nominal conditions.

ORIGINAL PAGE IS
OF POOR QUALITY



FRAME 009



FRAME 009

Figure 6-8. Apogee and perigee altitude profiles for QDOT = 80 and 125, nominal conditions.

ance algorithm can handle. A -30% atmosphere is one which is constantly 30% below normal density, while a +30% atmosphere is 30% more dense, or thicker, than a normal atmosphere. When the atmosphere is too thin, the ERV does not turn as fast, so the plane change tends to take longer and use more fuel. On the other hand, too thick an atmosphere turns the vehicle quicker and uses slightly less fuel. Overall, the algorithm performs excellently in atmospheres ranging from 50% of normal to 150% of normal. Table 6-1 and 2 contains the results of these test runs. Figures 6-9 thru 12 show the plot profiles for the QDOT = 80 trajectory with a +50% density bias.

From these test results two points should be noted. First, a comparison of the final vehicle weights for the CSDL and POST simulations suggests that the designed guidance algorithm performs as well or better (e.g., QDOT = 80) than POST. Recall however, from earlier in this chapter, that the CSDL and POST trajectories were generated using different atmospheric models. For the 125 trajectories, the vehicle weights compare very close. For the 80 BTU/ft²-sec trajectories there is a significant difference in vehicle weights (about 200 lbs). It should be remembered that the 80 trajectory stays significantly higher in the atmosphere (approximately 35,000 feet), and the difference between the atmospheric models is more significant for the higher altitudes. Therefore, the comparison between CSDL and POST vehicle weights may not be as valid for the 80 trajectories.

Table 6-1. Density bias test results for QDOT = 80 Btu/ft²-sec.

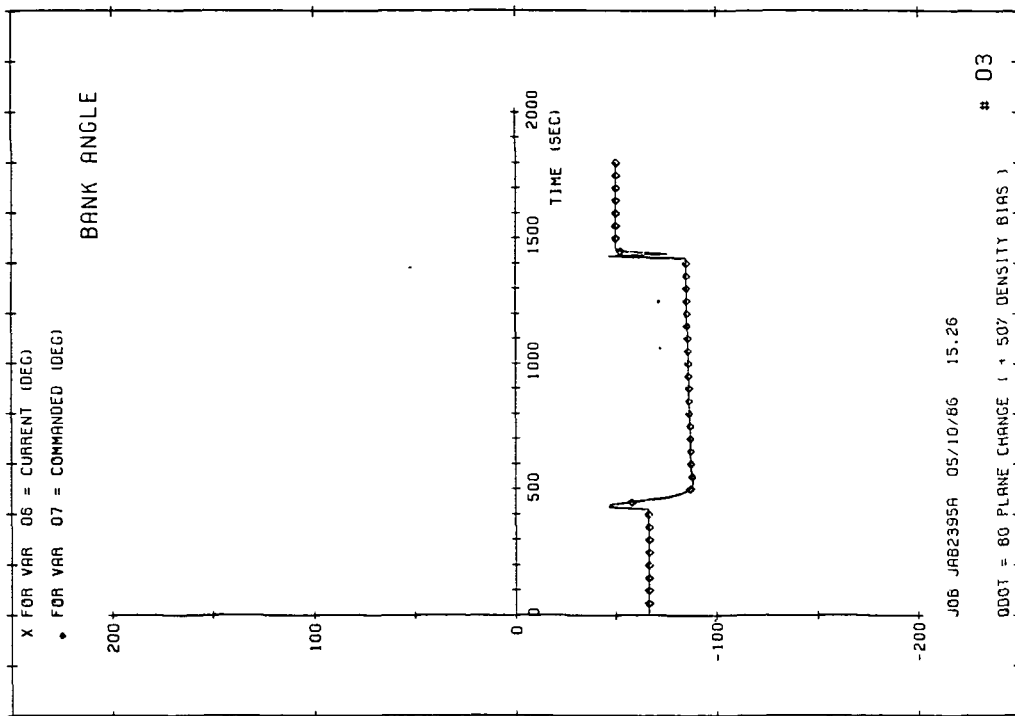
Condition	Inclination Change (deg)	Apogee Altitude (nm)	Vehicle Weight in 160 nm Circular Orbit (lbs)	"POST" Vehicle Weight in 160 nm Cir. Ob. (lbs)	LAN (deg)	Fuel to Inertial Nominal Plane (lbs)	Maximum QDOT (Btu/ft ² -sec)
Nominal	20.003	164.0	5422	5262	3.90	0	80
+30%	19.997	155.1	5427	5253	4.02	23	81
-30%	19.995	157.3	5455	5293	5.16	237	81
+50%	19.998	157.6	5441	N/A	2.99	171	80
-50%	20.004	162.0	5438	N/A	5.98	378	81

NOTE: 1. LAN - Longitude of the ascending node.
 2. N/A - Not available.

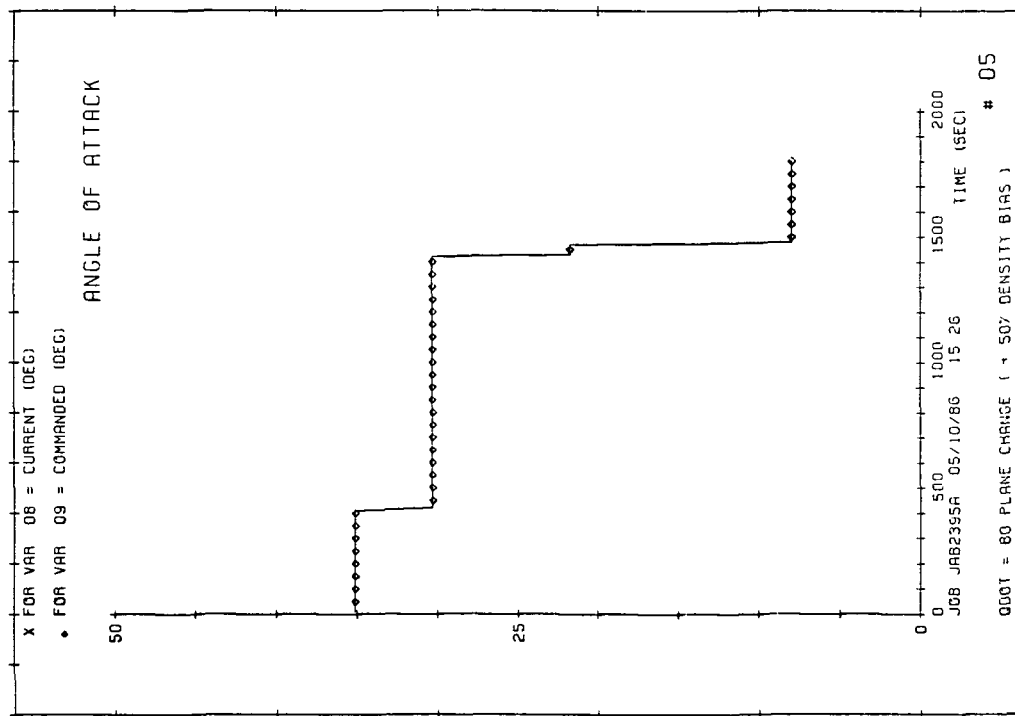
Table 6-2. Density bias test results for QDOT = 125 Btu/ft²-sec.

Condition	Inclination Change (deg)	Apogee Altitude (nm)	Vehicle Weight in 160 nm Circular Orbit (lbs)	"POST" Vehicle Weight in 160 nm Cir. Ob. (lbs)	LAN (deg)	Fuel to Inertial Nominal Plane (lbs)	Maximum QDOT (Btu/ft ² -sec)
Nominal	20.006	158.5	5961	5873	1.44	0	125
+30%	20.004	159.9	5962	5941	0.49	193	126
-30%	20.003	156.8	5926	5943	3.54	48	127
+50%	19.991	157.4	5925	N/A	-0.31	349	127
-50%	19.970	160.9	5931	N/A	3.91	448	127

NOTE: 1. LAN - Longitude of the ascending node.
 2. N/A - Not available.

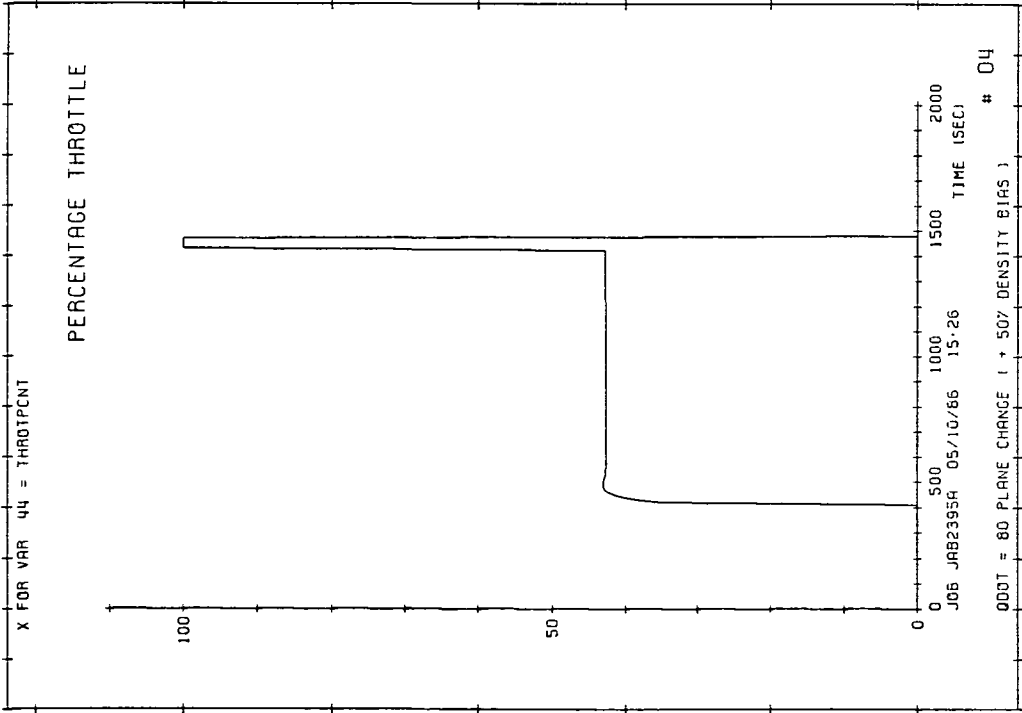


FRAME 004

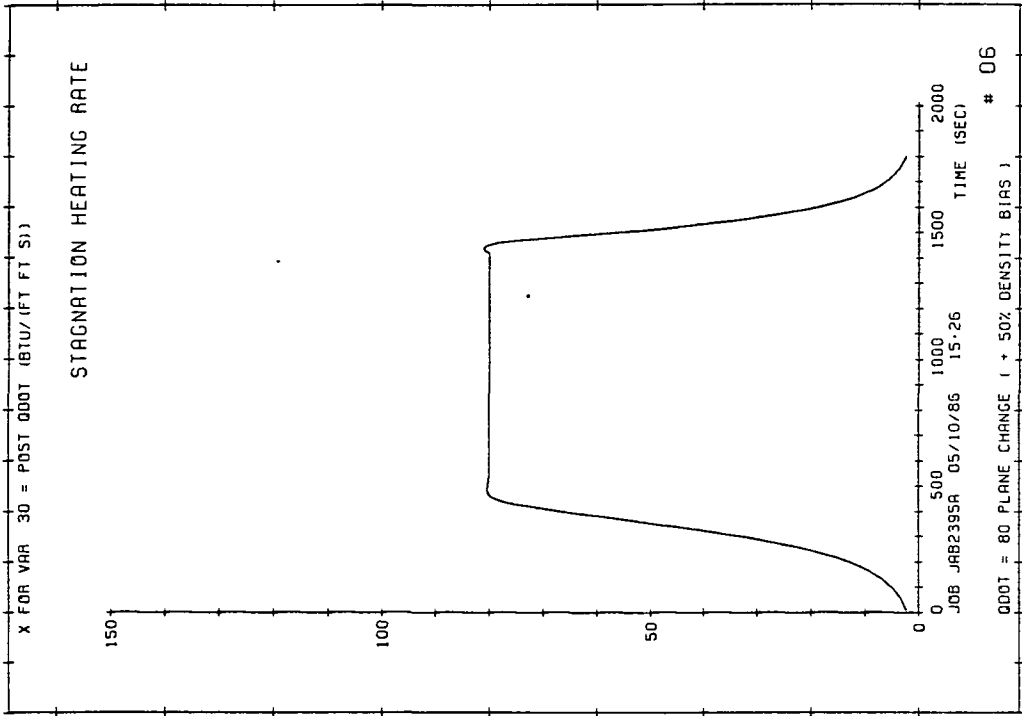


FRAME 006

Figure 6-10. Angle-of-attack and bank angle profiles for QDOT = 80, +50% density bias.

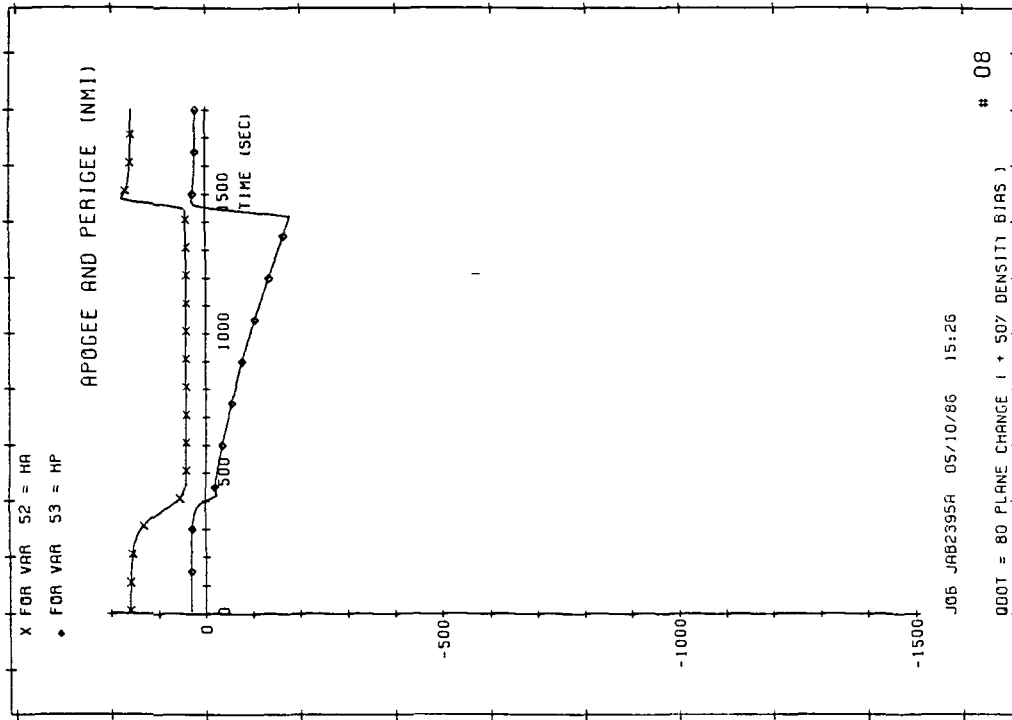


FRAME 005

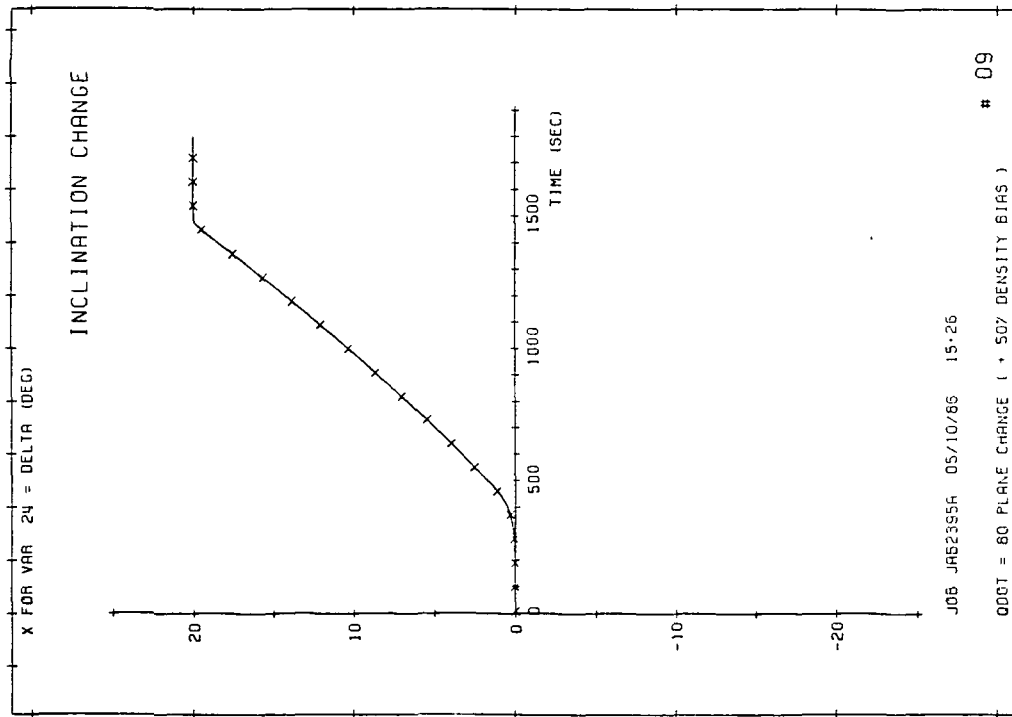


FRAME 007

Figure 6-11. Engine throttling and heat-rate profiles for QDOT = 80, +50% density bias.



FRAME 009



FRAME 010

Figure 6-12. Inclination change, apogee and perigee altitude profiles for QDOT = 80, +50% density bias.

Second, the test results for both the 80 and 125 BTU/ft²-sec trajectories indicate that as the density bias increases so does the shift in the longitude of the ascending node. The 125 trajectory shows the larger node shift reflecting its higher sensitivity to density perturbations. Still, the node shift is relatively small considering the size of the tested density biases.

6.3.1.2 DENSITY SHEARS

Density shears are introduced along the plane change trajectory to evaluate the guidance algorithm's performance flying through regions of changing density factors or levels. Two types of density shear models are used for testing, the density shear experienced by the shuttle on the STS-4 mission and a derived model. The STS-4 model is shown in Figure 6-13 and the derived model in Figure 6-14 as a normalized density verses altitude plot. The density is normalized by the 1962 standard atmospheric density. The shear models are mechanized as a table of density multipliers verses altitude.

The algorithm has no difficulty with density shears. The density shears encountered during the descending portion of the trajectory, are simply flown through, as the ERV approaches level-off, the automatic compensation of heating rate that was discussed in Chapter 4 tends to automatically adjust the cruise altitude to correct any effects caused by the density variations. Even when the shears are encountered during exit, the bank controller is easily able to correct for the density variations.

In fact, the density shears were so benign, a $\pm 30\%$ density bias was added to the STS-4 shear during cruise. The objective was to show that the guidance would respond to the changing density and guide the ERV back

STS-4 DENSITY PROFILE

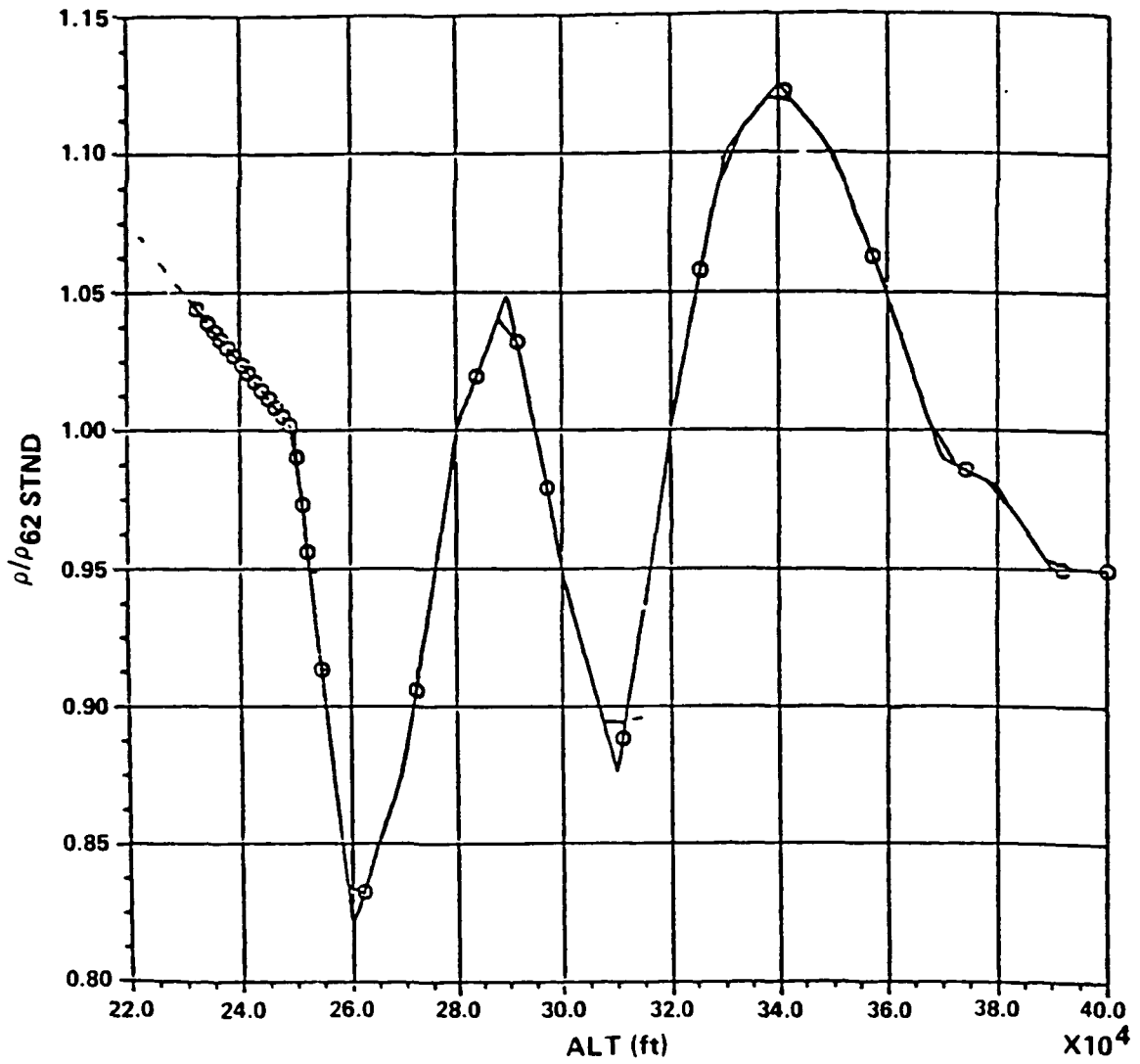


Figure 6-13. STS-4 density profile.

CSDL DENSITY SHEAR MODEL

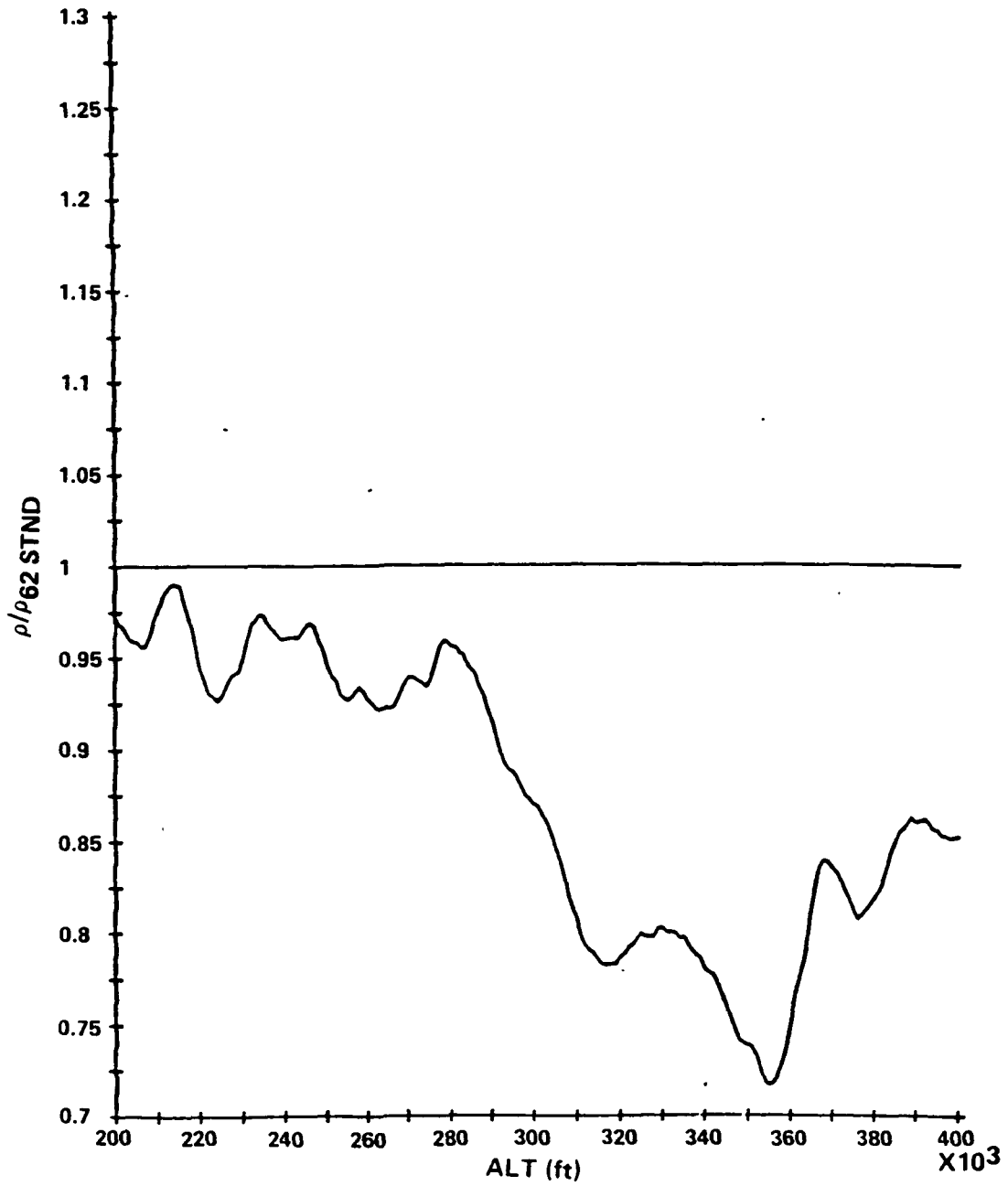


Figure 6-14. CSDL density shear model profile.

to the reference heating rate. The density bias was added as the vehicle flew below 225,000 feet. This caused a step change in density and heating rate that does not reflect real-world conditions. However, the guidance algorithm very rapidly drove the ERV back to the reference heating rate. Table 6-3 contains the results of a sample of the tested cases. The heating rate values in the parentheses are for cruise equilibrium conditions and are a better reflection of the algorithm's performance for the shear tests with the added density bias. Figures 6-15 thru 18 show profile plots for a 125 trajectory with a STS-4 density shear profile.

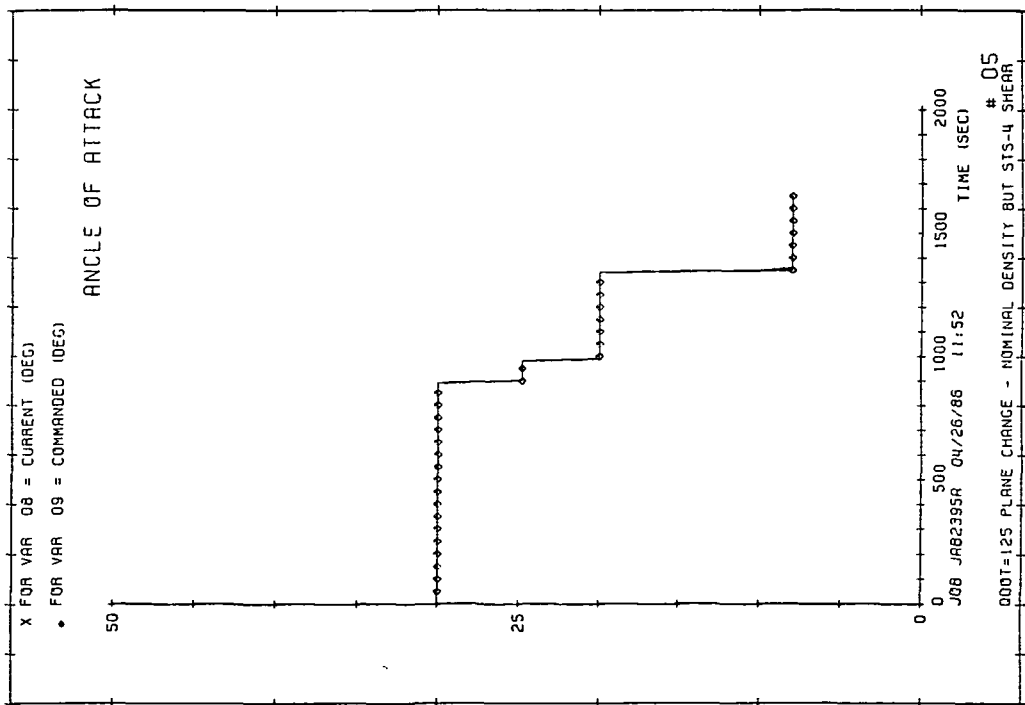
6.3.1.3 AERODYNAMIC UNCERTAINTIES

This test is useful for determining how well the guidance algorithm can perform if the vehicle's modeled aerodynamic characteristics are in error. This error is simulated by inputting a straight bias for CL and CD to be used throughout the plane change trajectory. Guidance was never given any knowledge of the CL and CD shift. While there are an unlimited possible combinations of CL and CD errors, the testing was limited to the same four combinations of $\pm 15\%$ CL and CD used in Chapter 4, plus two extreme cases of $\pm 25\%$ CL and CD error to demonstrate the robustness of the guidance system. It should be noted that the 15% cases included two cases with no net change of L/D and two cases with a L/D change (one increased and one decreased).

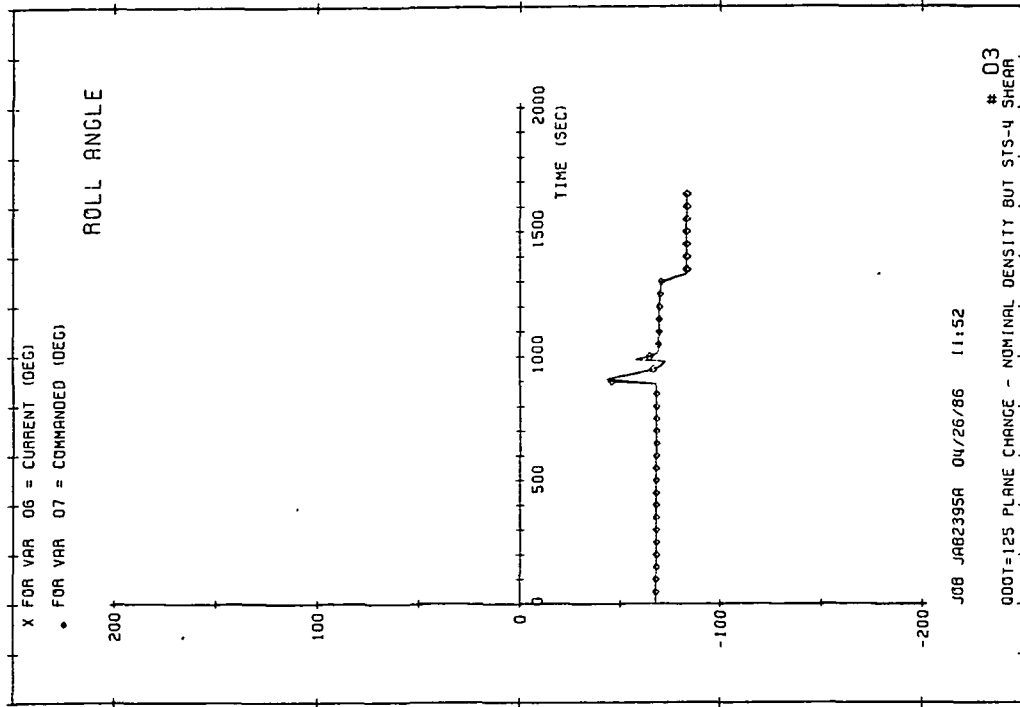
Table 6-3. Density shear test results for QDOT = 125 Btu/ft²-sec.

Condition	Inclination Change (deg)	Apogee Altitude (nm)	Vehicle Weight in 160 nm Circular Orbit (lbs)	"POST" Vehicle Weight in 160 nm Cir. Ob. (lbs)	LAN (deg)	Fuel to Inertial Nominal Plane (lbs)	Maximum QDOT (Btu/ft ² -sec)
Nominal	20.006	158.5	5961	5873	1.44	0	125
STS-4 shear	20.004	156.4	5976	N/A	1.35	18	126
STS-4 shear with +30% density bias during cruise	19.995	159.5	5972	N/A	1.20	48	130 (125)
STS-4 shear with -30% density bias during cruise	20.009	160.1	5847	N/A	1.82	74	128 (125)
Derived shear with +30% density bias during cruise	20.000	161.2	5983	N/A	1.35	18	126 (125)

NOTE: 1. LAN - Longitude of the ascending node.
 2. The heat-rate values in the parentheses are for cruise equilibrium conditions.
 3. N/A - Not available.



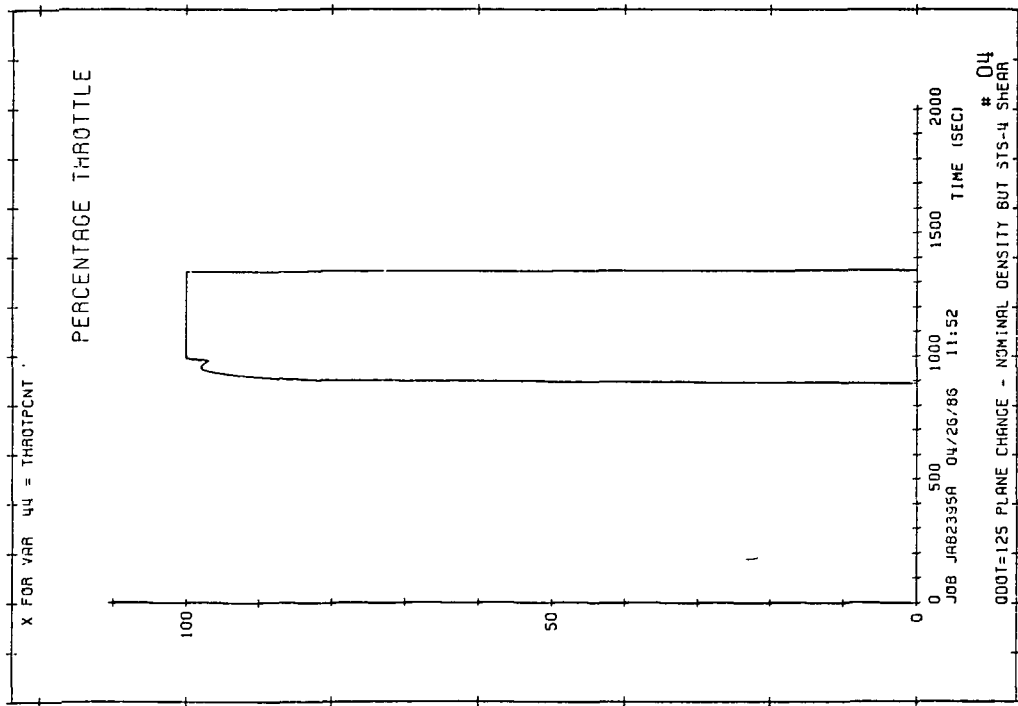
FRAME 006



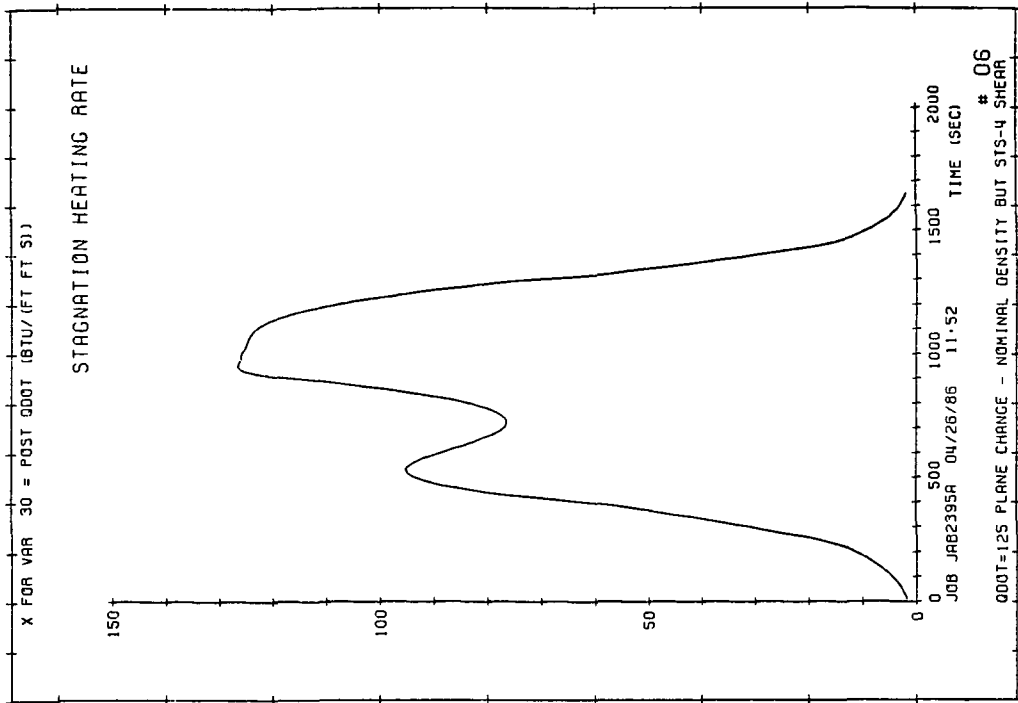
FRAME 004

Figure 6-16. Angle-of-attack and bank angle profiles for QDOT = 125, STS-4 density profile.

PRECEDING PAGE BLANK NOT FILMED



FRAME 005



FRAME 007

Figure 6-17. Engine throttling and heat-rate profiles for QDOT = 125, STS-4 density profile.

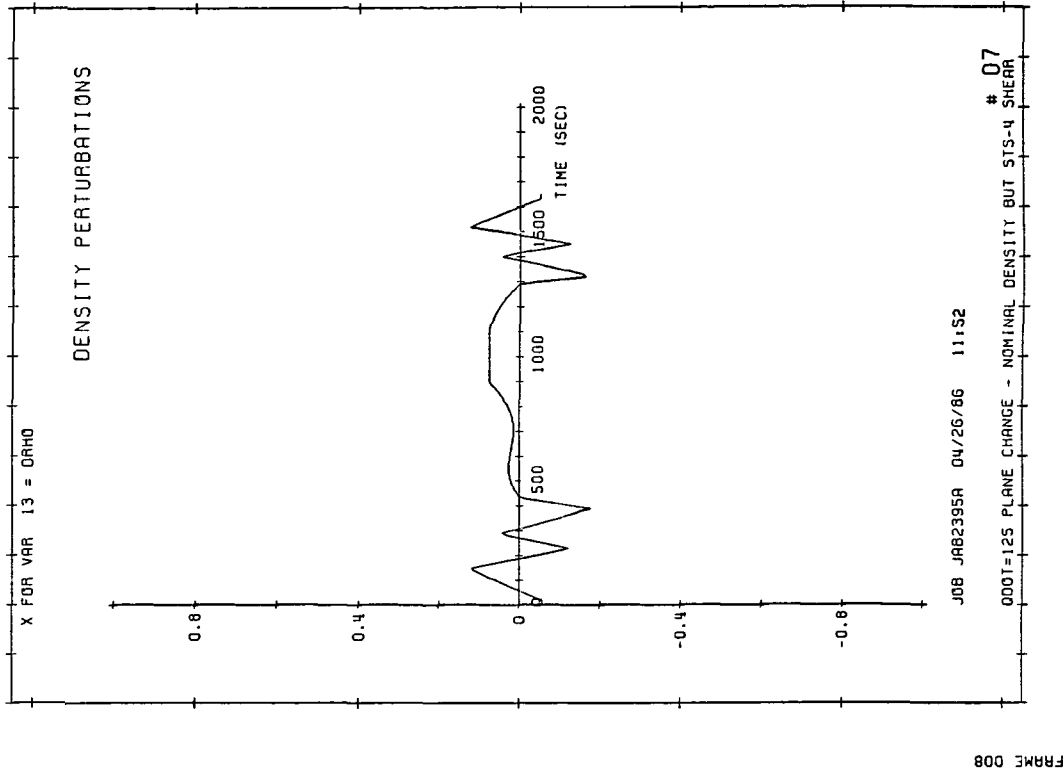
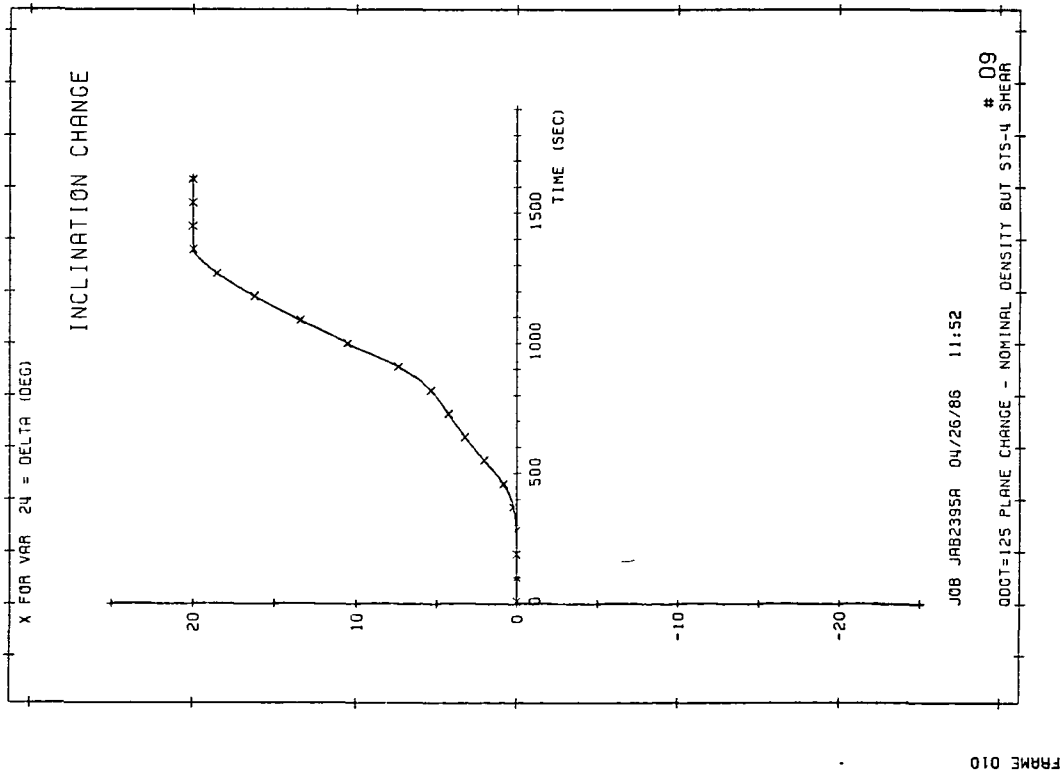


Figure 6-18. Inclination change and density perturbation profiles for QDOT = 125, STS-4 density profile.

Overall, the algorithm handled the uncertainties well and exhibited no unexpected performance loss/gain. Tables 6-4 and 5 summarize these results and offer a comparison with the performance loss/gain that was seen with POST. Figures 6-19 thru 22 show the plot profiles for a QDOT = 125 test with -25% CL and +25% CD.

Several points are worth noting:

1. The fuel usage for both the 80 and 125 trajectories was very similar to that calculated by POST under the same conditions.
2. For the performance cases with no change in L/D (e.g., +CL and +CD), the final vehicle weight is almost the same as the nominal vehicle weight for both the QDOT 80 and 125 trajectories. However, in terms of LAN shift, the results were opposite. The QDOT = 80 trajectory had a large node shift while the 125 trajectory showed almost no shift.
3. For the cases with a change in L/D (e.g., +CL and -CD), the final vehicle weight reflected that change with a corresponding increase or decrease for both QDOT = 80 and 125. However, in terms of LAN shift, the results were again opposite. The 80 trajectories showed almost no node shift while the 125 trajectories showed a large node shift.

Table 6-4. Aerodynamic uncertainty test results for QDOT = 80 Btu/ft²-sec.

Condition	Inclination Change (deg)	Apogee Altitude (nm)	Vehicle Weight in 160 nm Circular Orbit (lbs)	"POST" Vehicle Weight in 160 nm Cir. Ob. (lbs)	LAN (deg)	Fuel to Inertial Nominal Plane (lbs)	Maximum QDOT (Btu/ft ² -sec)
Nominal	20.003	164.0	5422	5262	3.90	0	80
+15% CL -15% CD	20.022	161.4	6185	6029	3.95	10	81
-15% CL +15% CD	19.982	151.5	4723	4528	4.21	62	81
+15% CL +15% CD	20.011	159.4	5517	5397	1.27	465	81
-15% CL -15% CD	19.983	164.6	5283	5120	8.18	813	81

NOTE: 1. LAN - Longitude of the ascending node.
 2. N/A - Not available.

Table 6-5. Aerodynamic uncertainty test results for QDOT = 125 Btu/ft²-sec.

Condition	Inclination Change (deg)	Apogee Altitude (nm)	Vehicle Weight in 160 nm Circular Orbit (lbs)	"POST" Vehicle Weight in 160 nm Cir. Ob. (lbs)	LAN (deg)	Fuel to Inertial Nominal Plane (lbs)	Maximum QDOT (Btu/ft ² -sec)
Nominal	20.006	158.5	5961	5873	1.44	0	125
+15% CL -15% CD	20.018	162.0	6673	6683	4.82	740	126
-15% CL +15% CD	19.992	160.8	5133	5116	-0.73	393	126
+15% CL +15% CD	20.011	158.2	5904	5892	0.70	147	127
-15% CL -15% CD	19.950	163.0	5943	5819	2.44	193	126
+25% CL -25% CD	19.999	160.0	7088	N/A	8.30	1421	126
-25% CL +25% CD	19.989	160.7	4812	N/A	-1.95	635	126

NOTE: 1. LAN - Longitude of the ascending node.
2. N/A - Not available.

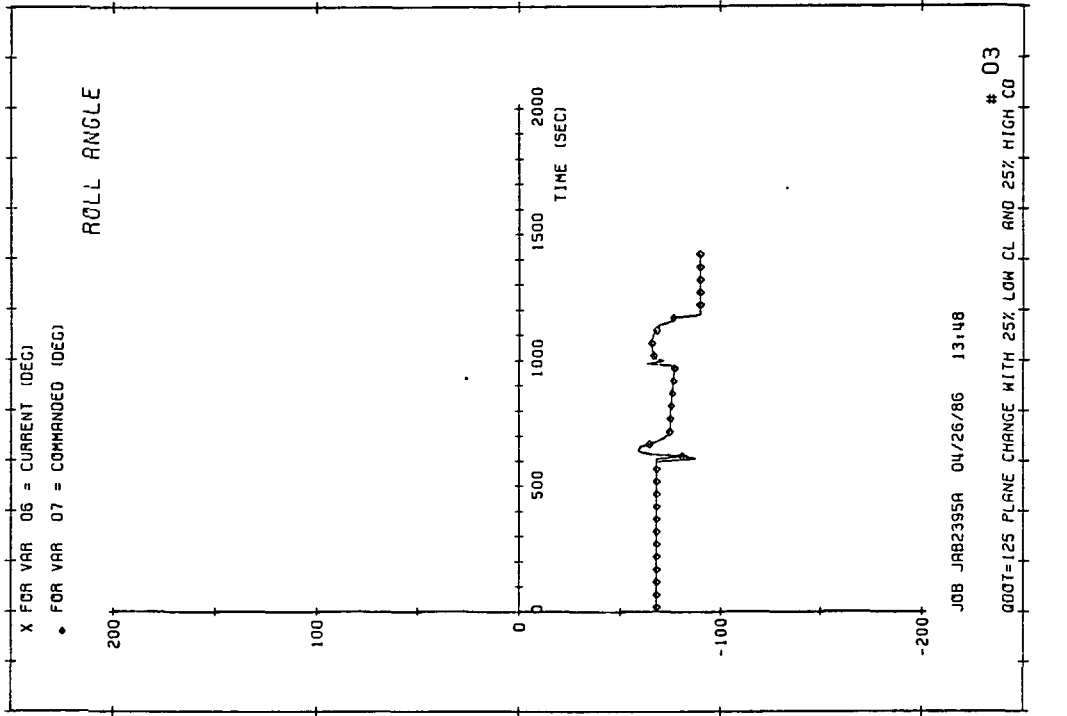
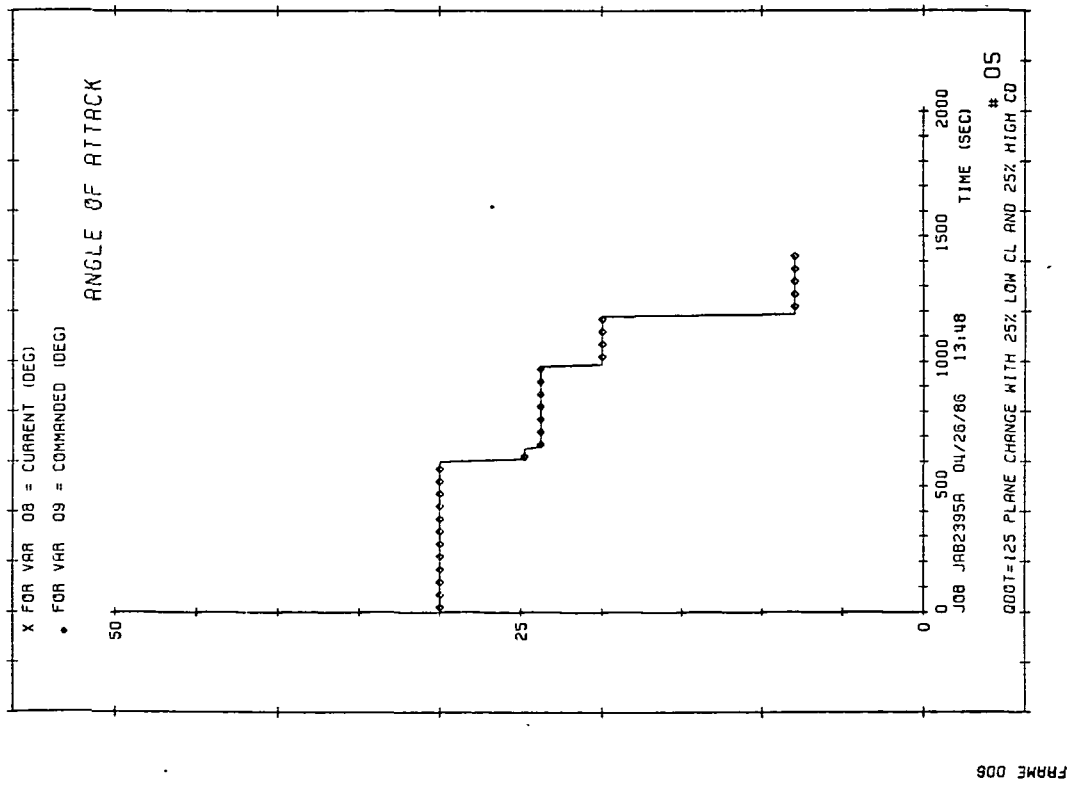
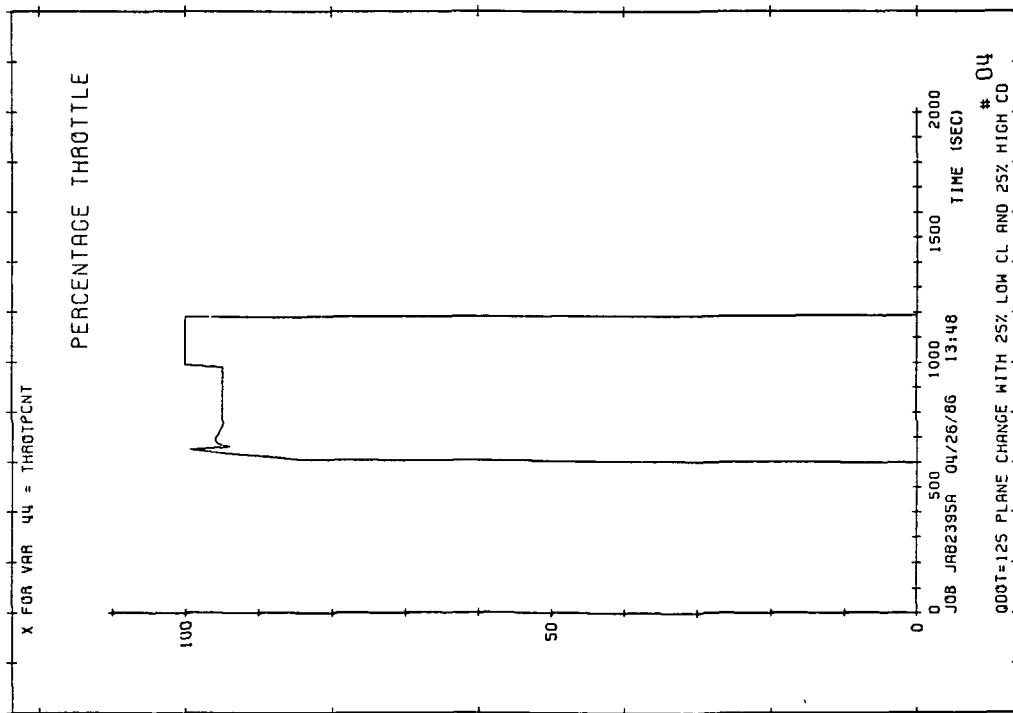
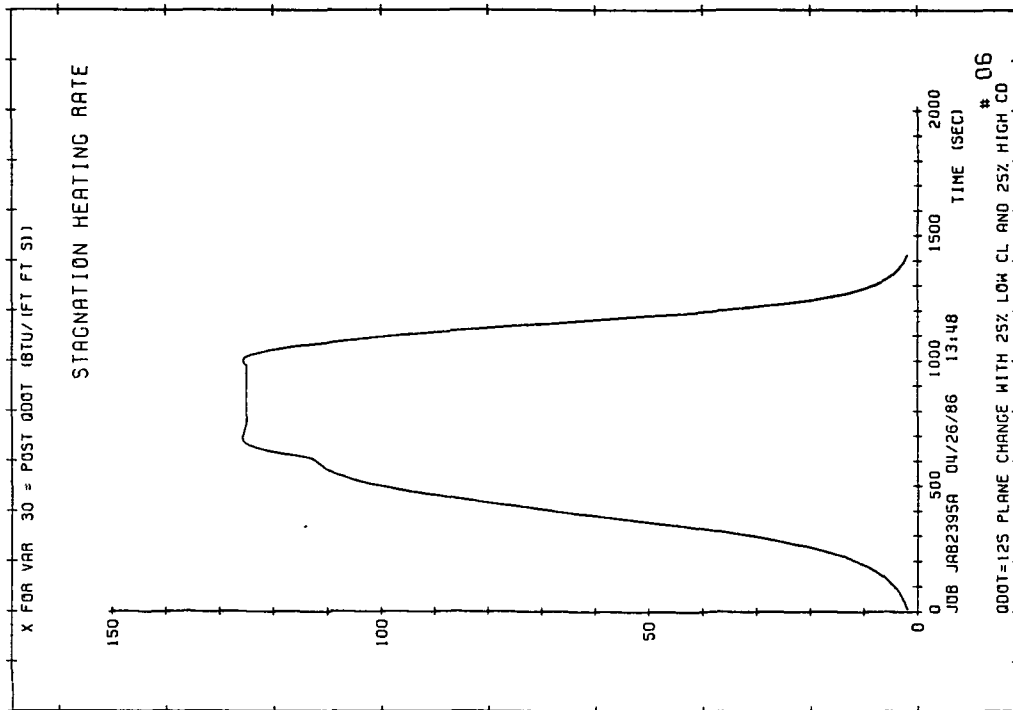


Figure 6-20. Angle-of-attack and bank angle profiles for QDOT = 125, -25% CL and +25% CD.



FRAME 005



FRAME 007

Figure 6-21. Engine throttling and heat-rate profiles for QDOT = 125, -25% CL and +25% CD.

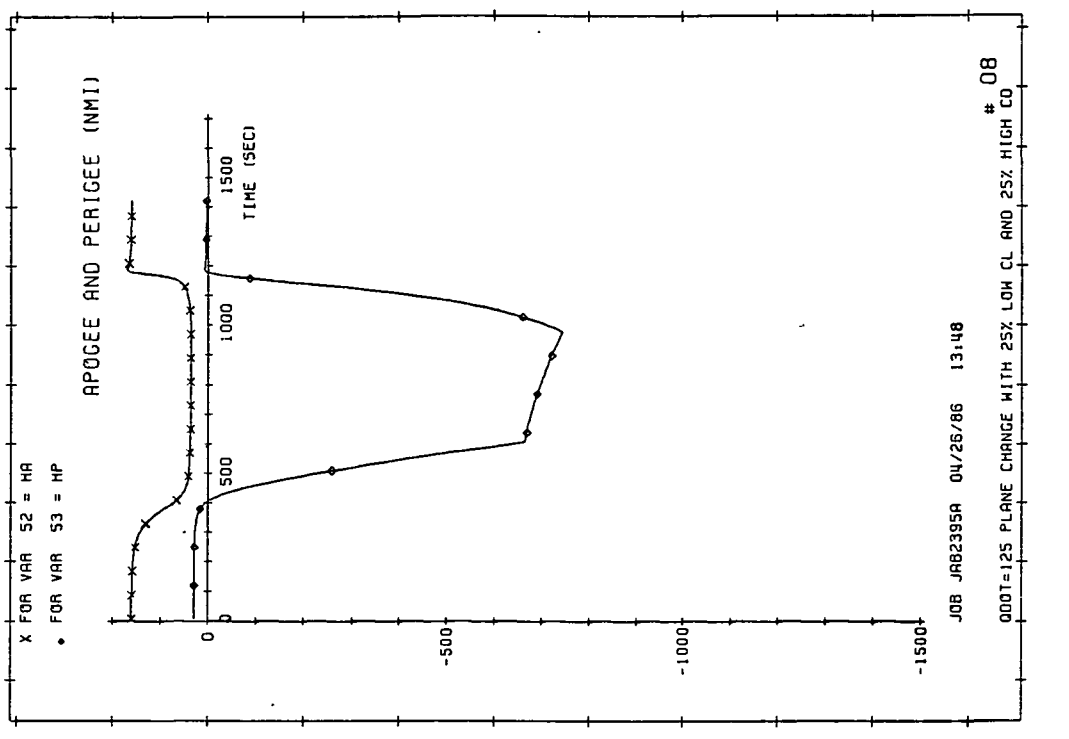
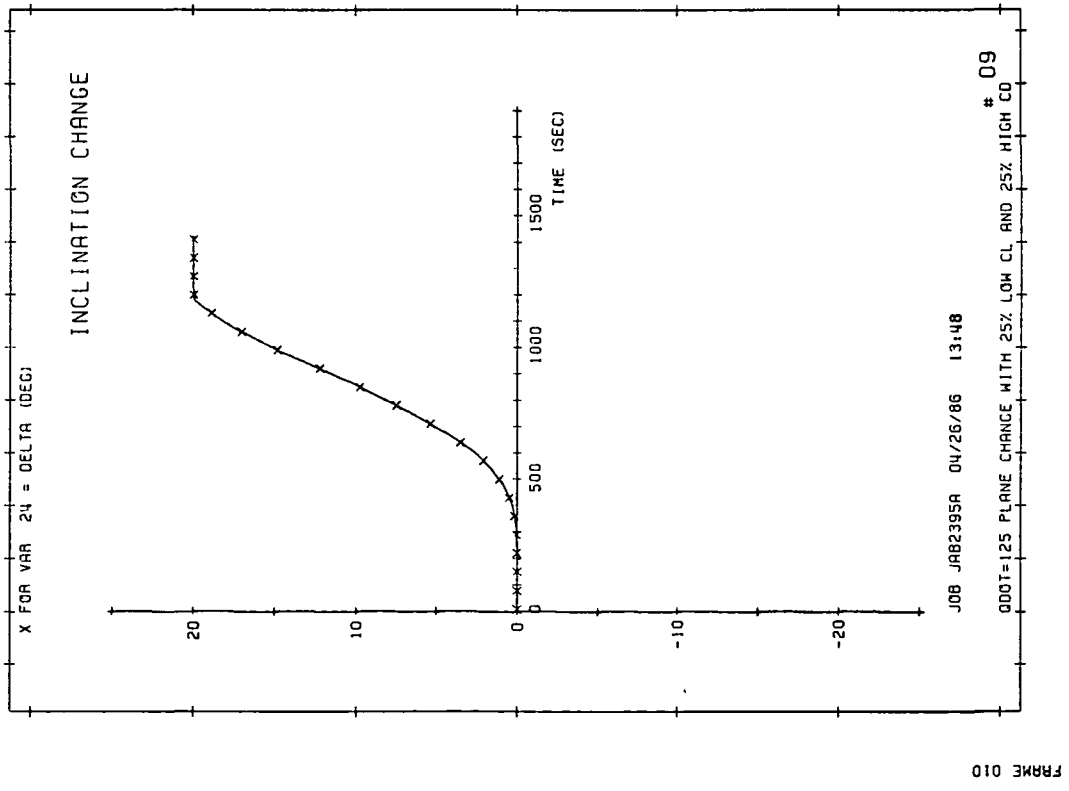


Figure 6-22. Inclination change, apogee and perigee altitude profiles for QDOT = 125, -25% CL and +25% CD.

4. The 25% low vehicle performance case (QDOT = 125) lost the characteristic "double-peak" heat-rate curve as shown in Figure 6-21. This test and one other multiple off-nominal test were the only cases that lost the "double-peak" suggesting that the 90% of maximum heat-rate was an adequate lead-point.

5. The 15% low vehicle performance case (QDOT = 80) failed to meet the apogee altitude criterion. Recall from Chapter 4 that for a heat-rate of 80 BTU/ft²-sec engine cutoff occurs much lower in the atmosphere than for a heat-rate of 125. This makes adequate compensation for large perturbations more difficult for a QDOT = 80 trajectory. Overall, the apogee error does not represent a significant fault in the guidance algorithm but some improvement might be needed.

6.3.1.4 SINGLE-ENGINE FAILURE

In this test, the algorithm's ability maintain control of the vehicle, complete the plane change and return safely to orbit is determined. Two tests are conducted with single-engine failure at a different location for each test. We felt the start of the level-off phase and the start of the exit phase represented the two worst possibilities. Guidance was given knowledge of the engine failure in both cases (i.e.,

the predictor/corrector used a reduced thrust model). Overall, the algorithm was able to compensate for the engine failure in both cases and still obtain the desired plane change and final apogee altitude. Table 6-6 summarizes the results while Figures 6-23 thru 26 show the profile plots for QDOT = 125 with single-engine failure at level-off.

Three points are worth noting:

1. The CSDL plane change algorithm was able to achieve almost the same fuel results as the POST simulation.
2. A comparison of Figure 6-1 and 6-23 shows the longer mission time for the QDOT = 125 single-engine case. The increased time to complete the mission caused a larger LAN shift than with the nominal mission. Thus, a significant fuel penalty would be paid to achieve the same orbital plane as the nominal run.
3. The QDOT = 80 case was almost totally unaffected by the single-engine failure. Although not shown, the mission time was nearly nominal and as the results show in Table 6-6 , very little LAN shift occurred.

6.3.2 MULTIPLE OFF-NOMINAL CONDITION TEST

Table 6-6. Single-engine failure test results.

Condition	Inclination Change (deg)	Apogee Altitude (nm)	Vehicle Weight in 160 nm Circular Orbit (lbs)	"POST" Vehicle Weight in 160 nm Cir. Ob. (lbs)	LAN (deg)	Fuel to Inertial Nominal Plane (lbs)	Maximum QDOT (Btu/ft ² -sec)
QDOT = 80 Nominal	20.003	164.0	5422	5262	3.90	0	80
QDOT = 80 single-engine failure at level-off	20.007	160.7	5439	N/A	3.91	6	81
QDOT = 125 Nominal	20.006	158.5	5961	5873	1.44	0	125
QDOT = 125 single-engine failure at level-off	19.995	157.2	5728	5827	3.69	438	127
QDOT = 125 single engine failure at exit	20.003	159.2	5768	5827	4.35	573	126

NOTE: 1. LAN - Longitude of the ascending node.
 2. N/A - Not available.

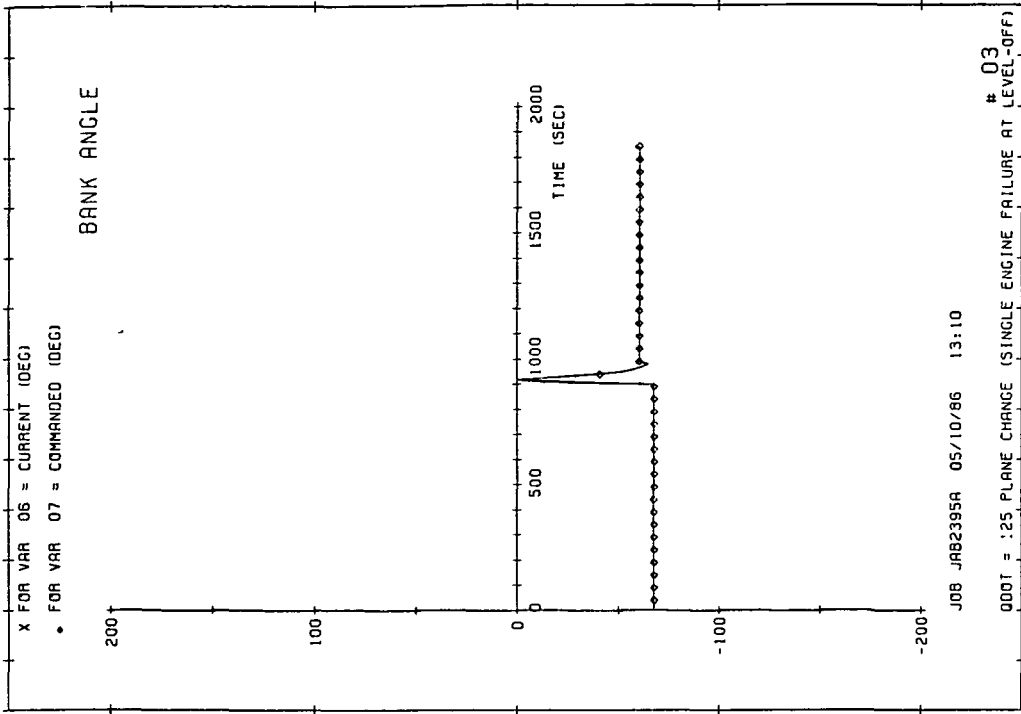
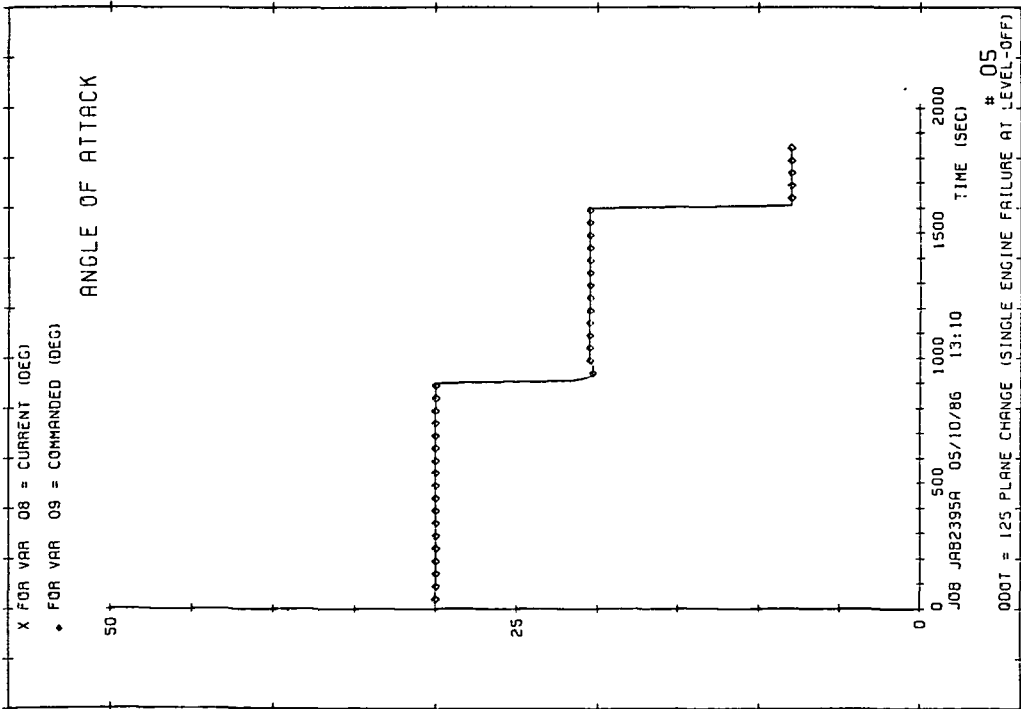
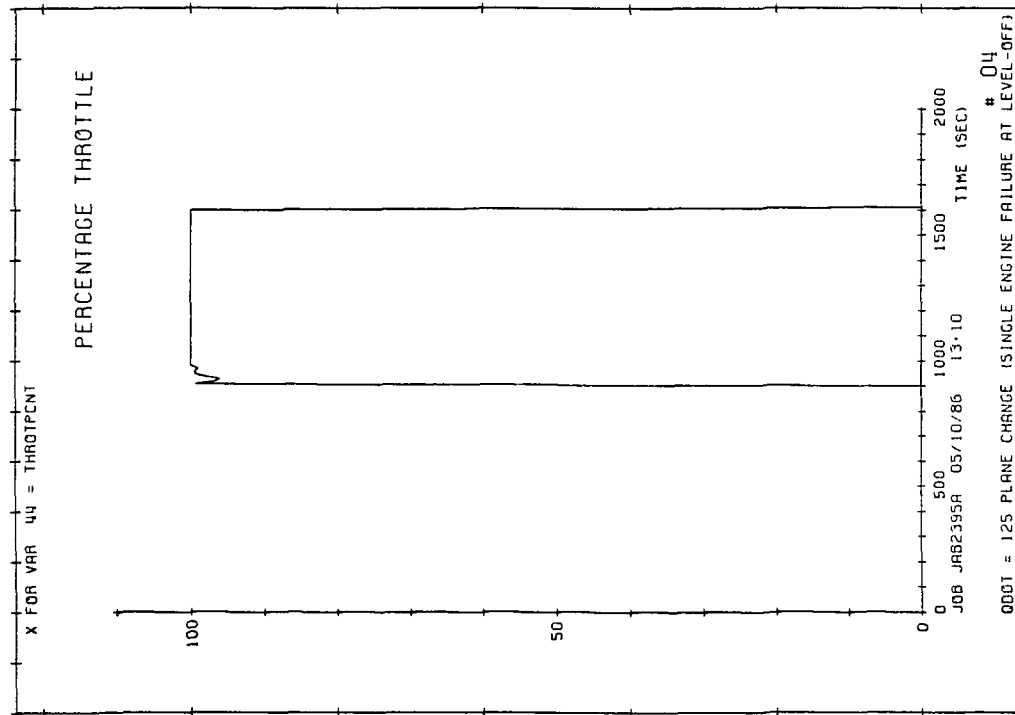
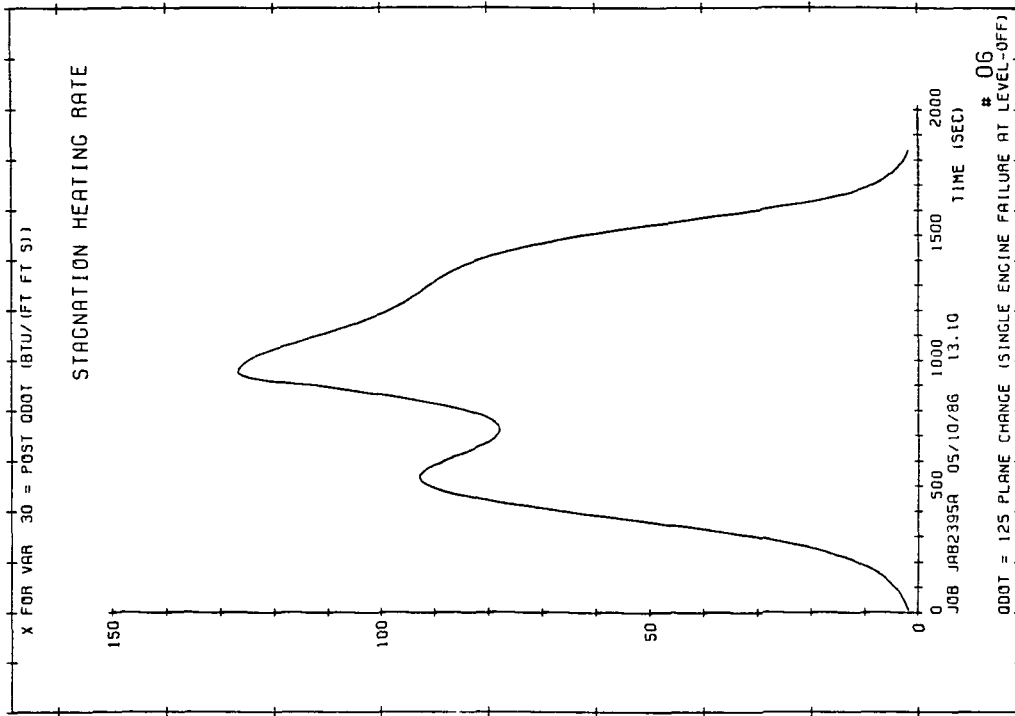


Figure 6-24. Angle-of-attack and bank angle profiles for QDOT = 125, single engine failure at level-off.



FRAME 007

FRAME 005

Figure 6-25. Engine throttling and heat-rate profiles for QDOT = 125, single-engine failure at level-off.

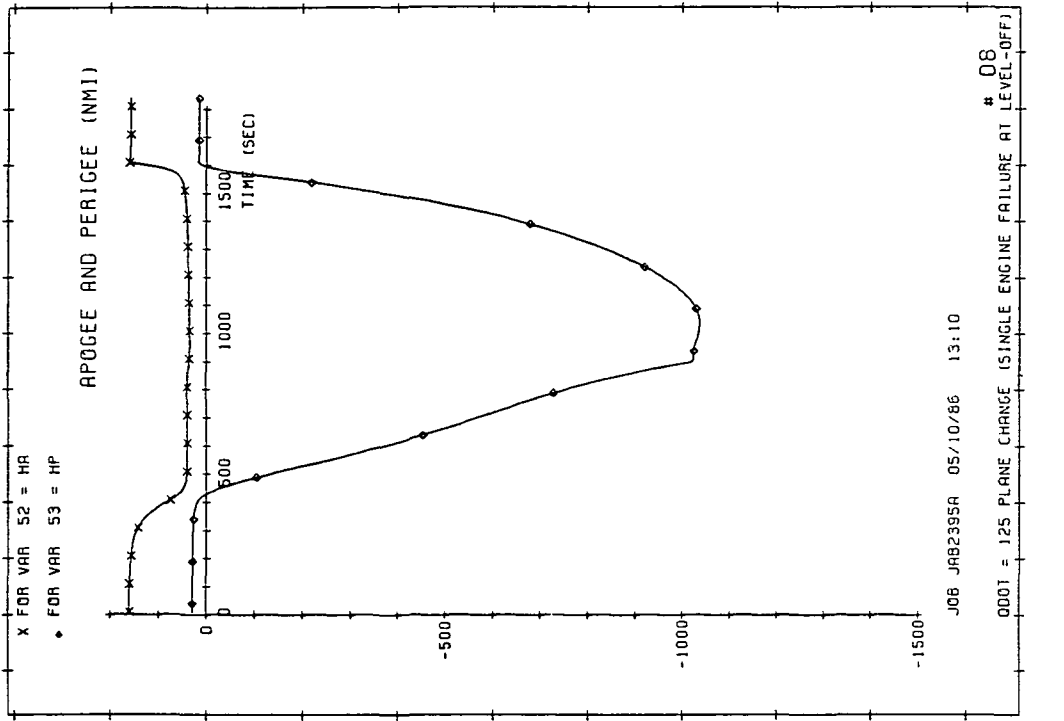
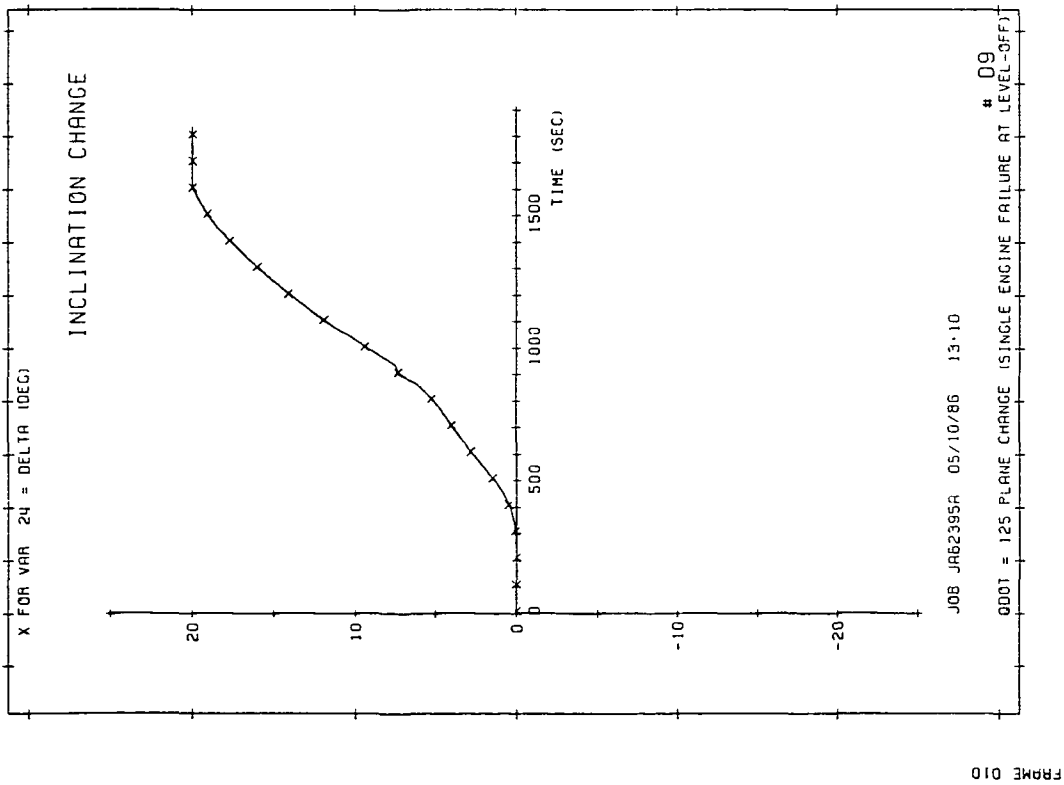


Figure 6-26. Inclination change, apogee and perigee altitude profiles for QDOT = 125, single-engine failure at level-off.

Table 6-7. Multiple off-nominal test results for QDOT = 80 Btu/ft²-sec.

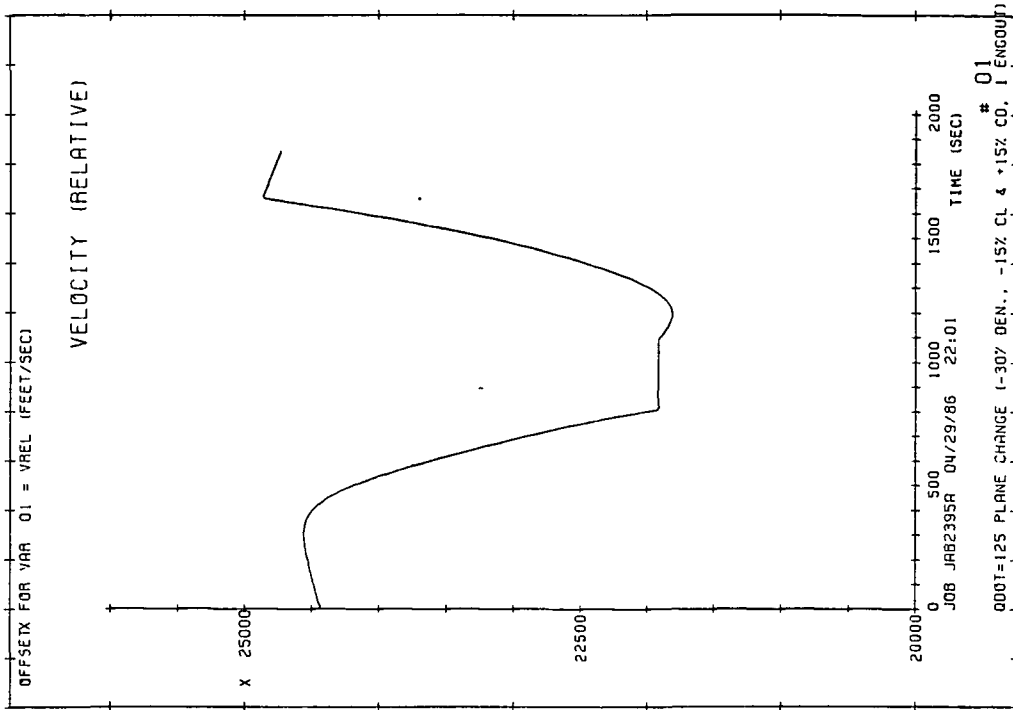
Condition	Inclination Change (deg)	Apogee Altitude (nm)	Vehicle Weight in 160 nm Circular Orbit (lbs)	"POST" Vehicle Weight in 160 nm Cir. Ob. (lbs)	LAN (deg)	Fuel to Inertial Nominal Plane (lbs)	Maximum QDOT (Btu/ft ² -sec)
Nominal	20.007	158.0	5450	5262	4.49	0	80
+30% Density -15% CL +15% CD	19.976	148.1	4675	N/A	4.53	96	80
+30% Density +15% CL -15% CD	20.027	167.4	6164	N/A	3.47	64	81
-30% Density -15% CL +15% CD	19.972	150.7	4708	N/A	5.70	313	80
+30% Density +15% CL -15% CD	20.019	165.8	6174	N/A	4.79	201	81
-30% Density -15% CL +15% CD single-engine failure	19.983	155.9	4716	N/A	5.73	296	81

NOTE: 1. LAN - Longitude of the ascending node.
2. N/A - Not available.

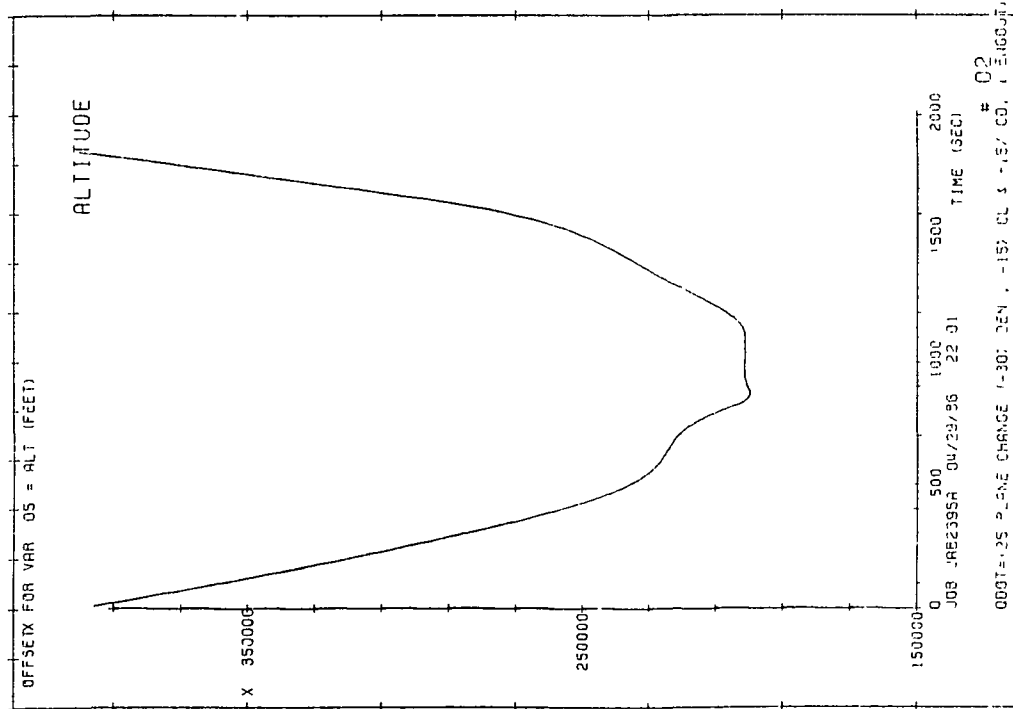
Table 6-8. Multiple off-nominal test results for QDOT = 125 Btu/ft²-sec.

Condition	Inclination Change (deg)	Apogee Altitude (nm)	Vehicle Weight in 160 nm Circular Orbit (lbs)	"POST" Vehicle Weight in 160 nm Cir. Ob. (lbs)	LAN (deg)	Fuel to Inertial Nominal Plane (lbs)	Maximum QDOT (Btu/ft ² -sec)
Nominal	20.006	158.5	5961	5873	1.44	0	125
+30% Density -15% CL +15% CD	19.997	159.6	5109	4941	-1.52	532	126
+30% Density +15% CL -15% CD	20.008	161.7	6645	6559	3.65	472	126
-30% Density -15% CL +15% CD	19.992	158.7	5136	5124	0.73	124	126
+30% Density +15% CL -15% CD	20.006	159.3	6641	6474	6.25	996	126
-30% Density -15% CL +15% CD	20.004	162.3	4696	4882	4.02	466	129
single-engine failure							
+30% density -15% CL +15% CD	19.996	160.0	4636	N/A	1.96	94	129
single-engine failure							

NOTE: 1. LAN - Longitude of the ascending node.
2. N/A - Not available.

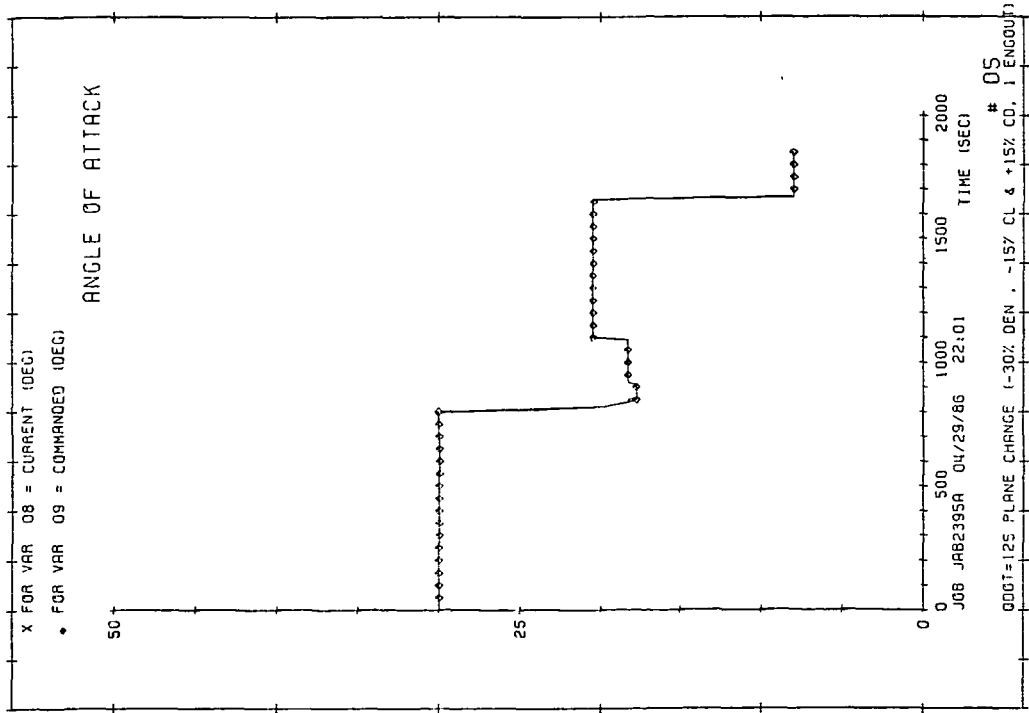


FRAME 002

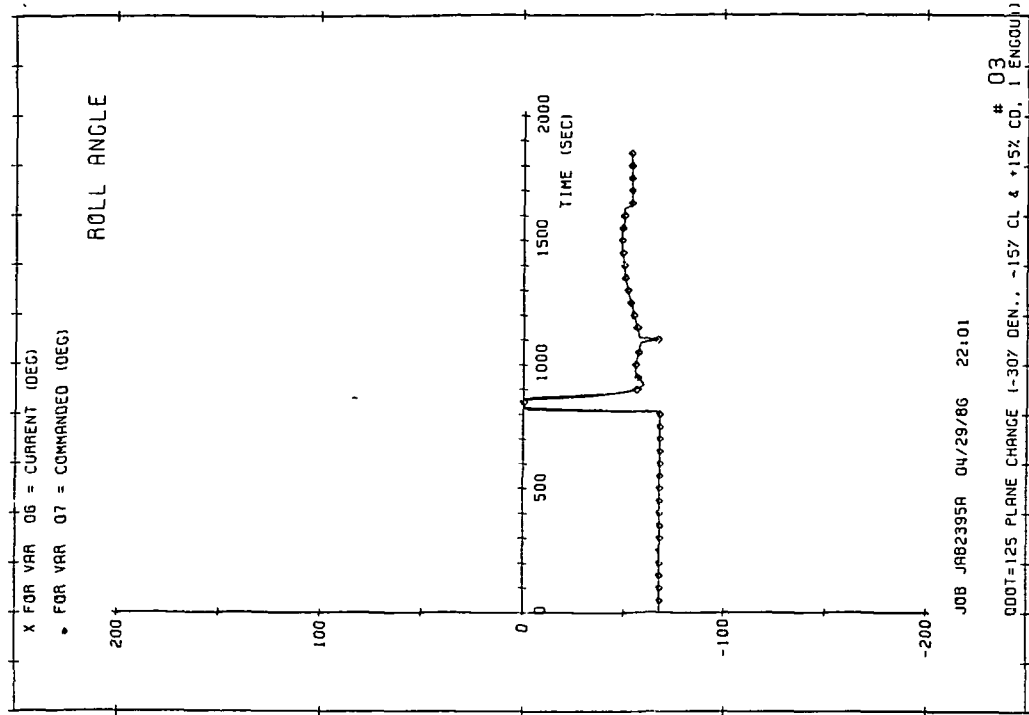


FRAME 003

Figure 6-27. Altitude and vehicle velocity profiles for QDOT = 125, -30% density, -15% CL and +15% CD, single-engine failure at level-off.

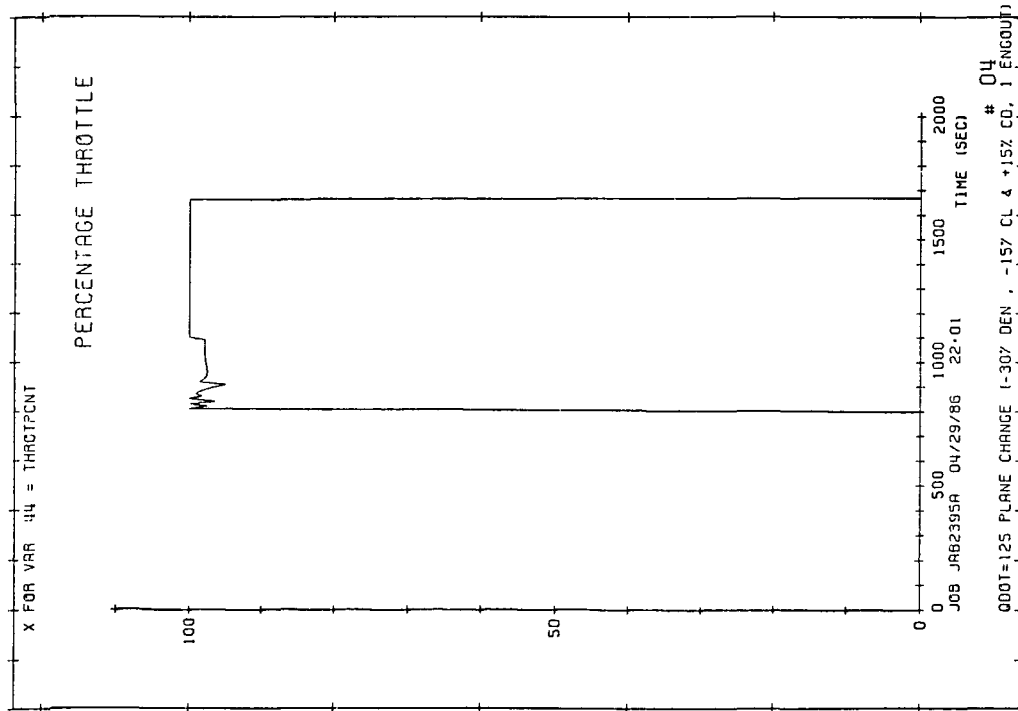


FRAME 006

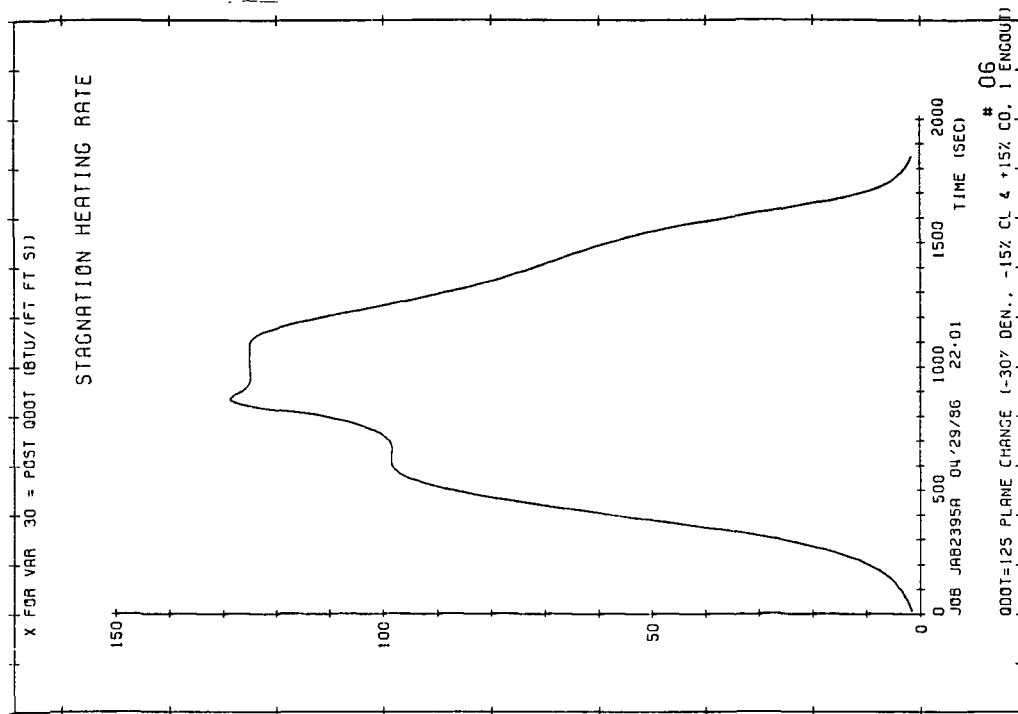


FRAME 004

Figure 6-28. Angle-of-attack and bank angle profiles for QDOT = 125, -30% density, -15% CL and +15% CD, single engine failure at level-off.



FRAME 005



FRAME 007

Figure 6-29. Engine throttling and heat-rate profiles for QDOT = 125, -30% density, -15% CL and +15% CD, single-engine failure at level-off.

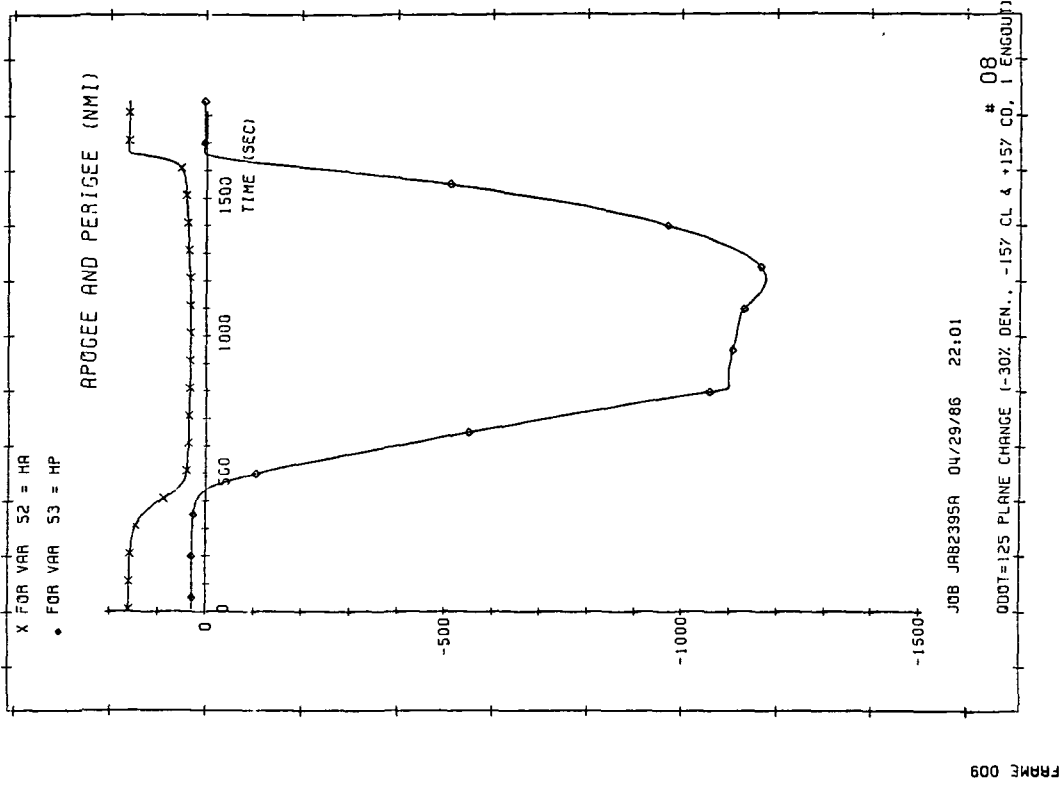
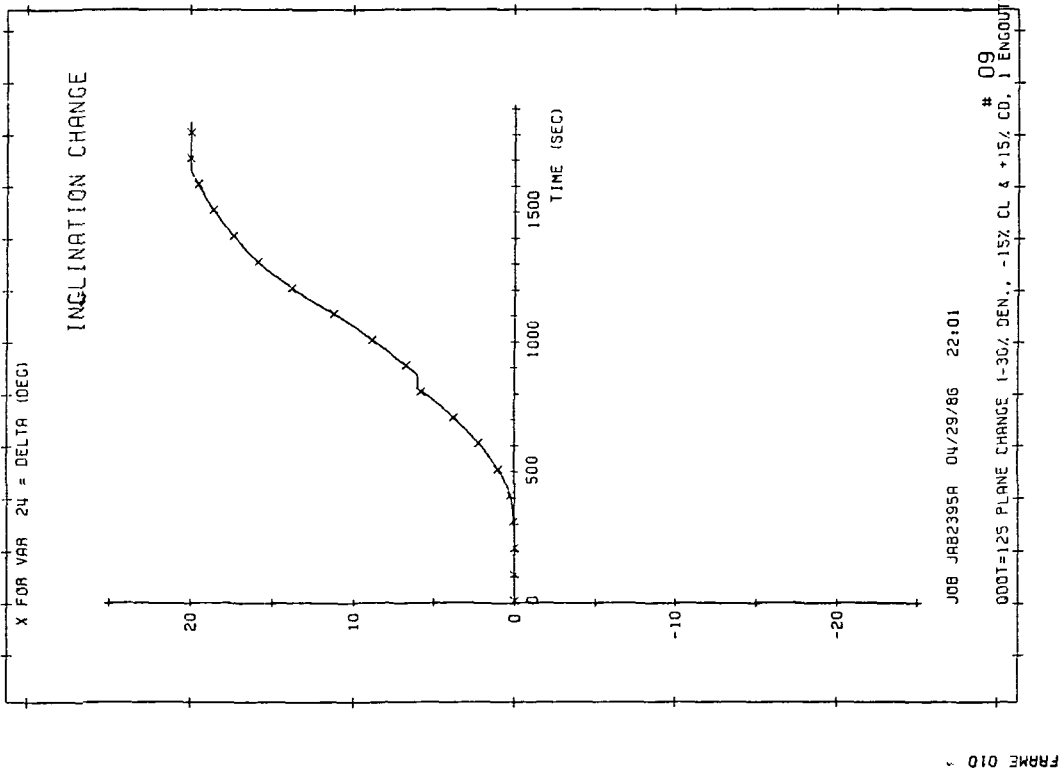


Figure 6-30. Inclination change, apogee and perigee altitude profiles for QDOT = 125, -30% density, -15% CL and +15% CD, single-engine failure at level-off.

By combining two or more of the off-nominal conditions discussed in Section 6.3.1, further tests of the algorithm's performance can be made. The purpose here is to explore the combinations which yield useful information in the determination of what the guidance algorithm can and cannot do. The results of all of the combinations tested are summarized in Table 6-7 and 8.

Several points are worth noting:

1. All the test cases that had some combination of low vehicle performance and single-engine failure (e.g., -30% density, -15% CL and +15% CD, and single-engine failure) experienced bank control saturation during level-off. Figures 6-27 thru 30 show the profile plots for one such case. The "common thread" for all cases was the significant change in cruise angle-of-attack. As a result, bank angle was saturated for about 30 seconds and a heat-rate overshoot occurred. Still, the heat-rate remained within the performance criterion. Delaying the angle-of-attack adjustment by 30 or 40 seconds after level-off would probably eliminate this bank saturation.
2. The same test cases that experienced bank saturation also lost velocity during the initial part of the exit phase. However, this loss of velocity had no significant overall effect as the vehicle was able to complete the intended maneuver.

3. Four of the five test combination cases for a heat-rate of 80 BTU/ft²-sec failed to meet the apogee altitude criterion. However, only two of these cases (+30% density with 15% low aero and -30% density with 15% low aero) were significantly outside the criterion. In addition, the combination of off-nominal conditions may be too severe of a test (i.e., unrealistic). Still, as discussed earlier, these results point out a need for improvement in the apogee altitude predictor.

4. Table 6-8 shows again how comparable the CSDL guidance system results (in terms of fuel) are to the POST results.

5. Several of the QDOT = 125 test showed a significant shift in the LAN. For the combinations involving high aero, the final vehicle weight to achieve the nominal inertial plane is almost nominal. However, for the combinations with low aero, the vehicle weight to achieve the nominal orbit was significantly below nominal.

7.2 CONCLUSIONS

1. A guidance system has been developed for the ERV synergetic plane change maneuver.

2. The recommended plane change algorithm is a hybrid of perturbation guidance and predictor/corrector guidance. Perturbation guidance is used to control heat-rate during cruise, and the predictor/corrector guidance is used to control the end-conditions.

3. The guidance system explicitly controls the end-conditions and will guide to any specified heat-rate, inclination and apogee combination.

4. The guidance system provides accurate control over heating rate within its knowledge of density and velocity. Due to the importance of heat-rate control (both from a performance and a vehicle safety point of view), an accurate, reliable measurement/estimate of density and velocity should receive top priority.

5. The guidance system has demonstrated the ability to handle $\pm 30\%$ density biases, two density shear profiles, $\pm 15\%$ aerodynamic uncertainties, a single-engine failure, and various combinations of the above.

PRECEDING PAGE BLANK NOT FILMED

The guidance system is adaptive in the sense that it will respond to these dispersions and maintain control over heat-rate and the desired targeting parameters.

6. The aerodynamic uncertainties caused the largest uncontrollable performance effect (fuel usage) and therefore represent the largest uncertainty in efficiency of the ERV synergetic plane change maneuver.

7. Simulated plane change missions using this guidance system have nearly the same total fuel usage as trajectories generated by an optimization program.

8. Overall, with this guidance algorithm in its software the ERV can be expected to accurately maneuver through the earth's atmosphere for the programmed synergetic plane change and thereby demonstrate capabilities that will be desired on future operational vehicles.

7.3 TOPICS FOR FURTHER RESEARCH

As with most all challenging tasks, time never seems available to explore all the possible options nor to deal with all the opportunities that surface during the investigation. Listed below are five such items which seem to warrant further study and/or work.

7.3.1 NODE CONTROL

While the objective of this task was to provide a guidance system to handle an ERV during a plane change, the ultimate desire will surely involve a system to maneuver into a specific inertial plane. Therefore, in addition to inclination control, control of the longitude of the ascending node would also be required. While we have addressed the node shift in Chapter 6 by including the fuel required to correct any undesired shift, it is not clear that both inclination and node can not be efficiently controlled during the atmospheric phase. In other words, would the total fuel for handling both in the atmosphere be less than the current scheme where only inclination is actively controlled in the atmosphere and any node shift is corrected on-orbit.

The current algorithm has available three possible control variables, (1) the length of the cruise phase, (2) angle-of-attack during exit, and (3) engine throttling during exit. These would seem to offer a means of controlling the node. However, it is also unclear if the added complexity is worth any possible fuel savings.

7.3.2 PLANE CHANGE TRAJECTORY IMPROVEMENTS

During our analysis of single-engine failure performance, some of our results seemed to suggest that some performance gain could be made

by allowing the thrust to vary during the exit phase. In theory, this concept could be tested with only two or three POST runs. Likewise, there are other possible parameters that have been fixed during our plane change analysis that if allowed to vary or change more often could offer some performance improvements. For example, a few POST runs were made where alpha and bank angle were allowed to change two additional times during entry, resulting in a small gain of roughly 100 pounds of fuel. Thus, it seems possible that a "more optimum" trajectory exists.

7.3.3 HEAT-RATE CONTROL

Our final scheme used a lead-point for our heat-rate controller that will still modify the first heat-rate peak under some perturbed conditions causing fuel efficiency to suffer. A method to avoid this was mentioned in Chapter 4 but never tested. Specifically it might be possible to actively control heat-rate such that the first heat-rate peak is not eliminated or significantly modified. The resulting fuel savings could be as high as 8% of the total fuel used or roughly 450 pounds for a 20 degree plane change.

7.3.4 MINIMUM FUEL

One advantage of the predictor/corrector guidance scheme is the availability of fairly accurate predictions of end-conditions like fuel

remaining. This information could be used to make adjustments to the intended trajectory (i.e., reduced the amount of desired plane change) as necessary to insure the ERV returns to orbit with the minimum required fuel.

7.3.5 APOGEE ALTITUDE CONTROL

Several of the test cases in Chapter 6 for multiple off-nominal conditions, failed to guide to the apogee altitude within the desired accuracy criterion. All of the cases were for a heat-rate of 80 BTU/ft²-sec and most of them involved off-nominal aerodynamic conditions. It might be possible to improve the apogee accuracy by providing an improved estimate of the aerodynamic characteristics to the predictor/corrector routine.

6. Powell, R.W., Naftel, J.C. Cunningham, M.J., "Performance Evaluation Of An Entry Research Vehicle," AIAA Paper No. 86-0270, AIAA 24th Aerospace Sciences Meeting, Reno, NA, January 1986.
7. Stalony-Dobrzanski, J., "Re-entry Guidance And Control Using Temperature Rate Flight Control System"
8. Bradt, J.E., Hardtla, J.W., "An Adaptive Guidance Algorithm For Aerospace Vehicles", AIAA Paper No. 85-1917.
9. Cervisi, R.T., "Analytic Solution For A Cruising Plane Change Maneuver," AIAA Paper No. 83-2095, AIAA 10th Atmospheric Flight Mechanics Conference, Gatlinburg, TN, August 1983.
10. Clauss, J.S., Jr. and Yeatman, R.D., "Effect Of Heating Restraints On Aeroglide And Aerocruise Synergetic Maneuver Performance," Journal Of Spacecraft And Rockets, Vol. 4, August 1967, pp. 1107-1109.
11. Dickmanns, E.D., "The Effect Of Finite Thrust And Heating Constraints On The Synergetic Plane Change Maneuver For A Space Shuttle Orbiter - Class Vehicle," NASA TN-D-7211, October 1973.

12. Joosten, B.K. and Pierson, B.L., "Minimum Fuel Aerodynamic Orbital Plane Change Maneuvers," AIAA Paper 81-0167, AIAA 19th Aerospace Sciences Meeting, St. Louis, Missouri, January 1981.
13. Hull, D.G., "Optimal Reentry and Plane-Change Trajectories," Paper 81-156, AAS/AIAA Astrodynamics Specialist Conference, Lake Tahoe, Nev., August 1981.
14. Ikawa, H. and Rudiger, T.F., "Synergetic Maneuvering of Winged Spacecraft For Orbital Plane Change," Journal Of Spacecraft And Rockets, Volume 19, November - December 1982, pp. 513-520.
15. Parsons, W.D., "Analytic Solution Of The Synergetic Turn," Journal Of Spacecraft And Rockets, Volume 3, No. 11, November 1966, pp1675-1678.
16. Bate, R.R., Mueller, D.D., and White, J.E., Fundamentals of Astrodynamics, Dover Publications, Inc., New York, 1971, pp. 396-407.
17. Walderg, G.D., "A Review of Aeroassisted Orbit Transfer", AIAA paper 82-1378, AIAA 9th Atmospheric Flight Mechanic Conference, San Diego, California, August 1982.

18. Candra, E. and Arthur, Paul D., "Orbit Plane Change by External Buring Aerocruise", AIAA Paper 65-21, AIAA 2nd Aerospace Sciences Meetings, New York, NY, January 1965.

19. Kriegsman, B.A., Richards, R.T., Brand, T.J., "Guidance and Navigation System Studies for Entry Research Vehicle," CSDL-P-2864, Cambridge, Massachusetts, April 1986.

20. Maslen, S.H., "Synergetic Turns with Variable Aerodynamics", Journal of Spacecraft and Rockets, Vol. 4, November 1967, pp 1475-1482, Cambridge, Massachusetts.

APPENDIX A

POST

A.1 INTRODUCTION

This appendix provides the details on the primary tool that was used to conduct the plane change analysis. The formulation of the plane change problem involves many nonlinearities, beginning with the equations of motion and heat transfer and skin temperature computations. In this situation, the value of linearized analysis is quite limited and, at times, even misleading. Therefore, most of the analysis and synthesis work was accomplished with the aid of digital simulations. Specifically, this appendix will provide details on the Program to Optimize Simulated Trajectories (POST) and an example of trajectory generation for a nominal 20 degree plane change as an illustration of POST.

A.2 POST DESCRIPTION

The following was taken almost verbatim from Reference 1. POST, a generalized point mass, discrete parameter targeting and optimization program, provides the capability to target and optimize point mass trajectories for a powered or unpowered vehicle operating near a rotating oblate planet. Developed for the vehicle analysis branch, space direc-

torate, NASA Langley Research Center by the Martin Marietta Corporation, it was intended to provide the capability to simulate and optimize ascent and reentry trajectories for shuttle type vehicles. However, the generality of the program also allows various other types of vehicles to be simulated. POST has been used successfully to solve a wide variety of atmospheric flight mechanics and orbital transfer problems. The generality of the program is evidenced by its N-phase simulation capability, which features generalized planet and vehicle models. This flexible simulation capability is augmented by an efficient discrete parameter optimization capability that includes equality and inequality constraints. POST was originally written in Fortran IV for the CDC 6000 series computers. However, it is also operational on the IBM 370, and Univac 1108 computers.

One of the key features of POST is an easy to use NAMELIST-type input procedure. This feature significantly reduces input deck set-up time (and costs) for studies that require the normal large amount of input data. In addition, the general applicability of POST is further enhanced by a general-purpose discrete parameter targeting and optimization capability. This capability can be used to solve a broad spectrum of problems related to the performance characteristics of aerospace vehicles.

The basic simulation flexibility is achieved by decomposing the trajectory into a logical sequence of simulation segments. These trajectory segments, referred to as phases, enable the trajectory analyst to model both the physical and the nonphysical aspects of the simulation accurately and efficiently. By segmenting the mission into phases, each phase can be modeled and simulated in a manner most appropriate to that particular flight regime. For example, the planet model, the vehicle model, and the simulation options can be changed in any phase to be compatible with the level of detail required in that phase.

Every computational routine in the program can be categorized according to five basic functional elements. These elements are: The planet model, the vehicle model, the trajectory simulation model, the auxiliary calculations module, and the targeting and optimization module. The planet model is composed of an oblate spheroid model, a gravitational model, an atmosphere model, and a winds model. These models define the environment in which the vehicle operates. The vehicle model comprises mass properties, propulsion, aerodynamics and aeroheating and a navigation and guidance model. These models define the basic vehicle simulation characteristics. The trajectory simulation models are the event-sequencing module that controls the program cycling, table interpolation routines, and several standard numerical integration techniques. These models are used in numerically solving the translational and rotational equations of motion. The auxiliary calculations module

provides for a wide variety of output calculations. For example, conic parameters, range calculations, and tracking data are among the many output variables computed. The targeting and optimization module provides a general discrete parameter iteration capability. The user can select the optimization variable, the dependent variables, and the independent variables from a list of more than 400 program variables. An accelerated projected gradient algorithm is used as the basic optimization technique. This algorithm is a combination of Rosen's projection method for nonlinear programming and Davidon's variable metric method for unconstrained optimization. In the targeting mode, the minimum norm algorithm is used to satisfy the trajectory constraints. The cost and constraint gradients required by these algorithms are computed as first differences calculated from perturbed trajectories. To reduce the costs of calculating numerical sensitivities, only that portion of the trajectory influenced by any particular independent variable is reintegrated on the perturbed runs. This feature saves a significant amount of computer time when targeting and optimization is performed (1). A more complete description and additional information can be found in the formulation, utilization, and programmers manuals (1), (2), and (3).

A.3 TRAJECTORY GENERATION EXAMPLE

The baseline plane change trajectories were primarily developed by R.W. Powell and J.C. Naftel of NASA Langley Research Center. However,

the author with help and assistance from Powell and Naftel made modifications and some improvements to the POST baseline trajectory input deck for his specific application. The following 14 pages are presented as an example of a POST input deck necessary to produce the nominal 20 degree plane change trajectory with a heating rate of 125 BTU/ft²-sec. The complete ERV CL and CD data is included as a part of the input deck. The data is set up in three types of tables corresponding to three correlation parameters: (1) altitude (ALTITO), (2) viscous (VINV), and (3) mach number (MACH). Each correlation parameter table is broken into a number of sections for CL and CD (e.g., ALTITO = 300,000' and 537,000'). Within each section the CL or CD values are catalogued for angles-of-attack 0 to 60 degrees (1 degree increments).

Following the input code is a brief description of the input conditions, the various phases of the trajectory, and the independent variables that were used while optimizing the amount of fuel required for the plane change along with the constraints or dependent variables that were used in generating the plane change trajectory with POST. Most of the notation used in this appendix is the same notation that is used by POST. However, where possible both the POST and the more generic notation used in the main body of this thesis is shown.

COPYRIGHT 1981 MARTIN MARIETTA CORPORATION

```

L$SEARCH
PERT= 01, .1, 3*.01, .00001, 6* 01,
PCTCC=.01,
  SRCHM=4,
  OPT=1,
  OPTVAR=6HWEIGHT,
  OPTPH=1000,
  NDEPV=3,
  DEPVR=6HINC ,6HALTA ,6HXMAX4 ,
  DEPVAL=48.5, 160, 1.0,
  DEPTL= .10, 5, .01,
  DEPPH=1000, 1000, 1000,
  NINDV=12,
  INDVR=5HCRITR, 5HCRITR, 6HALPPC1, 6HBNKPC1,
6HALPPC1, 6HDPVLS1, 5HCRITR, 5HDBANK, 6HDALPHA, 5HCRITR, 6HALPPC1, 6HBNKPC1,
  INDPH=50, 55, 100, 100, 105, 105, 180, 180, 180, 200, 200,
U=- 9, 27, 27, -64, 25, .004, 40, -66, 20, 170, 8, -50,
$
L$GENDAT
PRNC=1,
NPC(9)=1, NPC(22)=1, ETAPC(1)=0,
  TITLE=OH*ERV CRUISING SYNERGISTIC PLANE CHANGE O-DOT=125*,
  EVENT=1,
  SREF=177.40,
  LREF=25.,
  FESN=1000,
  NPC(2)=4,
  WGTSG=11430,
  NPC(1)=3,
  NPC(15)=1,
  NPC(3)=5,
  NPC(5)=0,
  NPC(8)=0,
  NPC(12)=0,
  NPC(16)=1,
  ISPV=295.0,
  DT=100,
  IGUID(1)=3, 0, 1,
  ALTP=160,
  ALTA=160,
  PINC=1000,
  NPC(25)=3,
  PRNT(91)=5HXMAX1, 5HXMIN2, 5HXMAX3, 5HXMIN4, 5HXMAX4, 5HBETAI, 6HTIMRF1, 6HVIDEAL,
6HVINV ,6HINC ,6HPSTOP ,
  MONX=6HHEATRT, 6HALTITO, 6HDYNP ,6HETA ,
  INC=28.5,
  TRUAN=150., PGCLAT=-19,
  BETA=0,
$
L$TBLMLT TVC1M=3, AE1M=3, CLM= 5, CDM=.5, CLHM=.5, CDHM=.5, CLVM=.5, CDVM=.5 $
L$TAB TABLE=5HTVC1T, 0, 1100$
L$TAB TABLE=6HAE1T , 0, 1.4 $
L$TAB
TABLE=6HCLHT , 2, 5HALPHA, 6HALTITO, 51.2, 1, 1, 1, 1, 1, 1, 1,
3.00000000E+05,
0., 1.54130435E-02, 1.00000000E+00, 2.90433333E-02,
2.00000000E+00, 4.26161832E-02, 3.00000000E+00, 5.61415108E-02,
4.00000000E+00, 6.96270748E-02, 5.00000000E+00, 8.30790323E-02,
6.00000000E+00, 1.03075910E-01, 7.00000000E+00, 1.23070807E-01,
8.00000000E+00, 1.43063966E-01, 9.00000000E+00, 1.63055590E-01,
1.00000000E+01, 1.83045852E-01, 1.10000000E+01, 2.09544373E-01,
1.20000000E+01, 2.36086535E-01, 1.30000000E+01, 2.62668672E-01,
1.40000000E+01, 2.89287518E-01, 1.50000000E+01, 3.15940152E-01,
1.60000000E+01, 3.46924729E-01, 1.70000000E+01, 3.78013237E-01,
1.80000000E+01, 4.09199247E-01, 1.90000000E+01, 4.40476852E-01,
2.00000000E+01, 4.71840614E-01, 2.10000000E+01, 5.05921147E-01,

```

ORIGINAL PAGE IS
OF POOR QUALITY

2.20000000E+01,	5 39782977E-01,	2.30000000E+01,	5.73567038E-01,	-- 62--
2.40000000E+01,	6 07475313E-01,	2.50000000E+01,	6.41499793E-01,	-- 63--
2.60000000E+01,	6.75698509E-01,	2.70000000E+01,	7.10064539E-01,	-- 64--
2.80000000E+01,	7.44588487E-01,	2.90000000E+01,	7.79261646E-01,	-- 65--
3.00000000E+01,	8.15700000E-01,	3 10000000E+01,	8.51620000E-01,	-- 66--
3.20000000E+01,	8.87540000E-01,	3.30000000E+01,	9.23460000E-01,	-- 67--
3.40000000E+01,	9.59380000E-01,	3.50000000E+01,	9.95300000E-01,	-- 68--
3.60000000E+01,	1.02692000E+00,	3.70000000E+01,	1.05854000E+00,	-- 69--
3.80000000E+01,	1.09016000E+00,	3 90000000E+01,	1.12178000E+00,	-- 70--
4.00000000E+01,	1 15340000E+00,	4.10000000E+01,	1 17780000E+00,	-- 71--
4.20000000E+01,	1.20220000E+00,	4.30000000E+01,	1.22660000E+00,	-- 72--
4 40000000E+01,	1.25100000E+00,	4.50000000E+01,	1.27540000E+00,	-- 73--
4.60000000E+01,	1.28949000E+00,	4.70000000E+01,	1.30358000E+00,	-- 74--
4.80000000E+01,	1.31767000E+00,	4.90000000E+01,	1.33176000E+00,	-- 75--
5.00000000E+01,	1.34585000E+00,			-- 76--
5.37000000E+05,				-- 77--
0	9.20449438E-03,	1.00000000E+00,	1 08389264E-02,	-- 78--
2.00000000E+00,	1 27396078E-02,	3 00000000E+00,	1 48316963E-02,	-- 79--
4.00000000E+00,	1 70659970E-02,	5.00000000E+00,	1 94088435E-02,	-- 80--
6.00000000E+00,	2.15988761E-02,	7.00000000E+00,	2.24467141E-02,	-- 81--
8.00000000E+00,	2.33543284E-02,	9.00000000E+00,	2.63200000E-02,	-- 82--
1.00000000E+01,	2.97500000E-02,	1 10000000E+01,	3.41600000E-02,	-- 83--
1.20000000E+01,	3.85700000E-02,	1 30000000E+01,	4.29800000E-02,	-- 84--
1 40000000E+01,	4.73900000E-02,	1.50000000E+01,	5.18000000E-02,	-- 85--
1 60000000E+01,	5.69150000E-02,	1.70000000E+01,	6.20300000E-02,	-- 86--
1.80000000E+01,	6.71450000E-02,	1.90000000E+01,	7.22600000E-02,	-- 87--
2.00000000E+01,	7.73750000E-02,	2 10000000E+01,	8.28600000E-02,	-- 88--
2.20000000E+01,	8.83450000E-02,	2.30000000E+01,	9.38300000E-02,	-- 89--
2 40000000E+01,	9.93150000E-02,	2.50000000E+01,	1.04800000E-01,	-- 90--
2 60000000E+01,	1.10300000E-01,	2.70000000E+01,	1.15800000E-01,	-- 91--
2.80000000E+01,	1.21300000E-01,	2.90000000E+01,	1.26800000E-01,	-- 92--
3.00000000E+01,	1 32300000E-01,	3 10000000E+01,	1.37405000E-01,	-- 93--
3.20000000E+01,	1 42510000E-01,	3.30000000E+01,	1 47615000E-01,	-- 94--
3.40000000E+01,	1.52720000E-01,	3.50000000E+01,	1.57825000E-01,	-- 95--
3.60000000E+01,	1.62160000E-01,	3.70000000E+01,	1.66495000E-01,	-- 96--
3.80000000E+01,	1 70830000E-01,	3.90000000E+01,	1.75165000E-01,	-- 97--
4.00000000E+01,	1 79500000E-01,	4.10000000E+01,	1.82705000E-01,	-- 98--
4.20000000E+01,	1 85910000E-01,	4.30000000E+01,	1.89115000E-01,	-- 99--
4 40000000E+01,	1.92320000E-01,	4.50000000E+01,	1.95525000E-01,	-- 100--
4.60000000E+01,	1.97300000E-01,	4.70000000E+01,	1.99075000E-01,	-- 101--
4.80000000E+01,	2.00850000E-01,	4.90000000E+01,	2.02625000E-01,	-- 102--
5.00000000E+01,	2.04400000E-01,			-- 103--
\$				-- 104--
L\$TAB				-- 104--
TABLE=6HCDHT ,2,5HALPHA,6HALTITO,51,2,1,1,1,1,1,1,1,				-- 105--
3.00000000E+05,				-- 106--
0	9 73826087E-02,	1.00000000E+00,	9.97333333E-02,	-- 107--
2.00000000E+00,	1 02212214E-01,	3.00000000E+00,	1.04797122E-01,	-- 108--
4 00000000E+00,	1 07470748E-01,	5.00000000E+00,	1.10219355E-01,	-- 109--
6.00000000E+00,	1 16979753E-01,	7.00000000E+00,	1.23743898E-01,	-- 110--
8 00000000E+00,	1.30511331E-01,	9.00000000E+00,	1.37281670E-01,	-- 111--
1.00000000E+01,	1 44054585E-01,	1.10000000E+01,	1 55992797E-01,	-- 112--
1.20000000E+01,	1 67867737E-01,	1 30000000E+01,	1 79684720E-01,	-- 113--
1 40000000E+01,	1 91448482E-01,	1.50000000E+01,	2.03163258E-01,	-- 114--
1 60000000E+01,	2.22711371E-01,	1.70000000E+01,	2 42151422E-01,	-- 115--
1.80000000E+01,	2.61490092E-01,	1.90000000E+01,	2.80733524E-01,	-- 116--
2.00000000E+01,	2 99887372E-01,	2.10000000E+01,	3.27071201E-01,	-- 117--
2.20000000E+01,	3.54901625E-01,	2.30000000E+01,	3.82984404E-01,	-- 118--
2 40000000E+01,	4 10871250E-01,	2.50000000E+01,	4.38574793E-01,	-- 119--
2.60000000E+01,	4.74809028E-01,	2.70000000E+01,	5.10838124E-01,	-- 120--
2.80000000E+01,	5.46673604E-01,	2 90000000E+01,	5.82326141E-01,	-- 121--
3.00000000E+01,	6.19675000E-01,	3.10000000E+01,	6.67695000E-01,	-- 122--
3.20000000E+01,	7 15715000E-01,	3.30000000E+01,	7.63735000E-01,	-- 123--
3 40000000E+01,	8 11755000E-01,	3.50000000E+01,	8.59775000E-01,	-- 124--
3.60000000E+01,	9.15945000E-01,	3.70000000E+01,	9.72115000E-01,	-- 125--
3 80000000E+01,	1 02828500E+00,	3.90000000E+01,	1.08445500E+00,	-- 126--
4.00000000E+01,	1.14062500E+00,	4.10000000E+01,	1.20373500E+00,	-- 127--
4.20000000E+01,	1.26684500E+00,	4.30000000E+01,	1.32995500E+00,	-- 128--
4.40000000E+01,	1 39306500E+00,	4.50000000E+01,	1.45617500E+00,	-- 129--
4.60000000E+01,	1.52469000E+00,	4.70000000E+01,	1.59320500E+00,	-- 130--

4.80000000E+01,	1.66172000E+00,	4.90000000E+01,	1.73023500E+00,	-- 131--
5.00000000E+01,	1.79875000E+00,			-- 132--
5.37000000E+05,				-- 133--
0.	6.84452809E-01,	1.00000000E+00,	7.03390696E-01,	-- 134--
2.00000000E+00,	7.24948627E-01,	3.00000000E+00,	7.48390113E-01,	-- 135--
4.00000000E+00,	7.73231049E-01,	5.00000000E+00,	7.99140136E-01,	-- 136--
6.00000000E+00,	8.44880153E-01,	7.00000000E+00,	9.06022390E-01,	-- 137--
8.00000000E+00,	9.66479159E-01,	9.00000000E+00,	1.02663500E+00,	-- 138--
1.00000000E+01,	1.08697500E+00,	1.10000000E+01,	1.15062500E+00,	-- 139--
1.20000000E+01,	1.21427500E+00,	1.30000000E+01,	1.27792500E+00,	-- 140--
1.40000000E+01,	1.34157500E+00,	1.50000000E+01,	1.40522500E+00,	-- 141--
1.60000000E+01,	1.46999400E+00,	1.70000000E+01,	1.53476300E+00,	-- 142--
1.80000000E+01,	1.59953200E+00,	1.90000000E+01,	1.66430100E+00,	-- 143--
2.00000000E+01,	1.72907000E+00,	2.10000000E+01,	1.79373600E+00,	-- 144--
2.20000000E+01,	1.85840200E+00,	2.30000000E+01,	1.92306800E+00,	-- 145--
2.40000000E+01,	1.98773400E+00,	2.50000000E+01,	2.05240000E+00,	-- 146--
2.60000000E+01,	2.11653500E+00,	2.70000000E+01,	2.18173000E+00,	-- 147--
2.80000000E+01,	2.24480500E+00,	2.90000000E+01,	2.30894000E+00,	-- 148--
3.00000000E+01,	2.37307500E+00,	3.10000000E+01,	2.43676000E+00,	-- 149--
3.20000000E+01,	2.50044500E+00,	3.30000000E+01,	2.56413000E+00,	-- 150--
3.40000000E+01,	2.62781500E+00,	3.50000000E+01,	2.69150000E+00,	-- 151--
3.60000000E+01,	2.75382000E+00,	3.70000000E+01,	2.81614000E+00,	-- 152--
3.80000000E+01,	2.87846000E+00,	3.90000000E+01,	2.94078000E+00,	-- 153--
4.00000000E+01,	3.00310000E+00,	4.10000000E+01,	3.06269000E+00,	-- 154--
4.20000000E+01,	3.12228000E+00,	4.30000000E+01,	3.18187000E+00,	-- 155--
4.40000000E+01,	3.24146000E+00,	4.50000000E+01,	3.30105000E+00,	-- 156--
4.60000000E+01,	3.35755500E+00,	4.70000000E+01,	3.41406000E+00,	-- 157--
4.80000000E+01,	3.47056500E+00,	4.90000000E+01,	3.52707000E+00,	-- 158--
5.00000000E+01,	3.58357500E+00,			-- 159--
\$				-- 160--
L\$TAB				-- 160--
TABLE=6HCLVT ,2.5HALPHA,6HVINV ,51,8,1,1,1,1,1,1,1,				-- 161--
5.00000000E-03,				-- 162--
0.	1.46464286E-02,	1.00000000E+00,	2.86227845E-02,	-- 163--
2.00000000E+00,	4.25473300E-02,	3.00000000E+00,	5.64287515E-02,	-- 164--
4.00000000E+00,	7.02738964E-02,	5.00000000E+00,	8.40882353E-02,	-- 165--
6.00000000E+00,	1.04420102E-01,	7.00000000E+00,	1.24748993E-01,	-- 166--
8.00000000E+00,	1.45075276E-01,	9.00000000E+00,	1.65399262E-01,	-- 167--
1.00000000E+01,	1.85721212E-01,	1.10000000E+01,	2.12207849E-01,	-- 168--
1.20000000E+01,	2.38744784E-01,	1.30000000E+01,	2.65327825E-01,	-- 169--
1.40000000E+01,	2.91953236E-01,	1.50000000E+01,	3.18617669E-01,	-- 170--
1.60000000E+01,	3.50041208E-01,	1.70000000E+01,	3.81573117E-01,	-- 171--
1.80000000E+01,	4.13206959E-01,	1.90000000E+01,	4.44936796E-01,	-- 172--
2.00000000E+01,	4.76757143E-01,	2.10000000E+01,	5.10854598E-01,	-- 173--
2.20000000E+01,	5.44962558E-01,	2.30000000E+01,	5.79199794E-01,	-- 174--
2.40000000E+01,	6.13558139E-01,	2.50000000E+01,	6.48030103E-01,	-- 175--
2.60000000E+01,	6.82654131E-01,	2.70000000E+01,	7.17458692E-01,	-- 176--
2.80000000E+01,	7.52433468E-01,	2.90000000E+01,	7.89700000E-01,	-- 177--
3.00000000E+01,	8.27800000E-01,	3.10000000E+01,	8.63905000E-01,	-- 178--
3.20000000E+01,	9.00010000E-01,	3.30000000E+01,	9.36115000E-01,	-- 179--
3.40000000E+01,	9.72220000E-01,	3.50000000E+01,	1.00832500E+00,	-- 180--
3.60000000E+01,	1.03987000E+00,	3.70000000E+01,	1.07141500E+00,	-- 181--
3.80000000E+01,	1.10296000E+00,	3.90000000E+01,	1.13450500E+00,	-- 182--
4.00000000E+01,	1.16605000E+00,	4.10000000E+01,	1.18989500E+00,	-- 183--
4.20000000E+01,	1.21374000E+00,	4.30000000E+01,	1.23758500E+00,	-- 184--
4.40000000E+01,	1.26143000E+00,	4.50000000E+01,	1.28527500E+00,	-- 185--
4.60000000E+01,	1.29905500E+00,	4.70000000E+01,	1.31283500E+00,	-- 186--
4.80000000E+01,	1.32661500E+00,	4.90000000E+01,	1.34039500E+00,	-- 187--
5.00000000E+01,	1.35417500E+00,			-- 188--
1.03000000E-02,				-- 189--
0.	1.48928571E-02,	1.00000000E+00,	2.87657296E-02,	-- 190--
2.00000000E+00,	4.25916877E-02,	3.00000000E+00,	5.63785969E-02,	-- 191--
4.00000000E+00,	7.01326577E-02,	5.00000000E+00,	8.38588235E-02,	-- 192--
6.00000000E+00,	1.04138937E-01,	7.00000000E+00,	1.24415788E-01,	-- 193--
8.00000000E+00,	1.44689774E-01,	9.00000000E+00,	1.64961229E-01,	-- 194--
1.00000000E+01,	1.85230435E-01,	1.10000000E+01,	2.11568432E-01,	-- 195--
1.20000000E+01,	2.37959444E-01,	1.30000000E+01,	2.64398919E-01,	-- 196--
1.40000000E+01,	2.90882813E-01,	1.50000000E+01,	3.17407519E-01,	-- 197--
1.60000000E+01,	3.48780309E-01,	1.70000000E+01,	3.80257749E-01,	-- 198--
1.80000000E+01,	4.11833621E-01,	1.90000000E+01,	4.43502191E-01,	-- 199--

ORIGINAL PAGE IS
OF POOR QUALITY

2.00000000E+01,	4.75258163E-01,	2.10000000E+01,	5.09193591E-01,	-- 200--
2.20000000E+01,	5.43145521E-01,	2.30000000E+01,	5.77230735E-01,	-- 201--
2.40000000E+01,	6.11440817E-01,	2.50000000E+01,	6.45768041E-01,	-- 202--
2.60000000E+01,	6.80353476E-01,	2.70000000E+01,	7.15111494E-01,	-- 203--
2.80000000E+01,	7.50032232E-01,	2.90000000E+01,	7.87275000E-01,	-- 204--
3.00000000E+01,	8.25275000E-01,	3.10000000E+01,	8.61345000E-01,	-- 205--
3.20000000E+01,	8.97415000E-01,	3.30000000E+01,	9.33485000E-01,	-- 206--
3.40000000E+01,	9.69555000E-01,	3.50000000E+01,	1.00562500E+00,	-- 207--
3.60000000E+01,	1.03714000E+00,	3.70000000E+01,	1.06865500E+00,	-- 208--
3.80000000E+01,	1.10017000E+00,	3.90000000E+01,	1.13168500E+00,	-- 209--
4.00000000E+01,	1.16320000E+00,	4.10000000E+01,	1.18726000E+00,	-- 210--
4.20000000E+01,	1.21132000E+00,	4.30000000E+01,	1.23538000E+00,	-- 211--
4.40000000E+01,	1.25944000E+00,	4.50000000E+01,	1.28350000E+00,	-- 212--
4.60000000E+01,	1.29737000E+00,	4.70000000E+01,	1.31124000E+00,	-- 213--
4.80000000E+01,	1.32511000E+00,	4.90000000E+01,	1.33898000E+00,	-- 214--
5.00000000E+01,	1.35285000E+00,			-- 215--
1.48000000E-02,				-- 216--
0.	1.48928571E-02,	1.00000000E+00,	2.87297051E-02,	-- 217--
2.00000000E+00,	4.25225253E-02,	3.00000000E+00,	5.62785680E-02,	-- 218--
4.00000000E+00,	7.00035747E-02,	5.00000000E+00,	8.37021505E-02,	-- 219--
6.00000000E+00,	1.03926982E-01,	7.00000000E+00,	1.24148841E-01,	-- 220--
8.00000000E+00,	1.44368098E-01,	9.00000000E+00,	1.64585063E-01,	-- 221--
1.00000000E+01,	1.84800000E-01,	1.10000000E+01,	2.11145700E-01,	-- 222--
1.20000000E+01,	2.37542553E-01,	1.30000000E+01,	2.63986169E-01,	-- 223--
1.40000000E+01,	2.90472643E-01,	1.50000000E+01,	3.16998496E-01,	-- 224--
1.60000000E+01,	3.48269013E-01,	1.70000000E+01,	3.79646234E-01,	-- 225--
1.80000000E+01,	4.11123819E-01,	1.90000000E+01,	4.42695922E-01,	-- 226--
2.00000000E+01,	4.74357143E-01,	2.10000000E+01,	5.08280279E-01,	-- 227--
2.20000000E+01,	5.42217826E-01,	2.30000000E+01,	5.76287000E-01,	-- 228--
2.40000000E+01,	6.10479318E-01,	2.50000000E+01,	6.44787010E-01,	-- 229--
2.60000000E+01,	6.79290655E-01,	2.70000000E+01,	7.13969013E-01,	-- 230--
2.80000000E+01,	7.48812100E-01,	2.90000000E+01,	7.85940000E-01,	-- 231--
3.00000000E+01,	8.23900000E-01,	3.10000000E+01,	8.59945000E-01,	-- 232--
3.20000000E+01,	8.95990000E-01,	3.30000000E+01,	9.32035000E-01,	-- 233--
3.40000000E+01,	9.68080000E-01,	3.50000000E+01,	1.00412500E+00,	-- 234--
3.60000000E+01,	1.03566000E+00,	3.70000000E+01,	1.06719500E+00,	-- 235--
3.80000000E+01,	1.09873000E+00,	3.90000000E+01,	1.13026500E+00,	-- 236--
4.00000000E+01,	1.16180000E+00,	4.10000000E+01,	1.18594000E+00,	-- 237--
4.20000000E+01,	1.21008000E+00,	4.30000000E+01,	1.23422000E+00,	-- 238--
4.40000000E+01,	1.25836000E+00,	4.50000000E+01,	1.28250000E+00,	-- 239--
4.60000000E+01,	1.29641000E+00,	4.70000000E+01,	1.31032000E+00,	-- 240--
4.80000000E+01,	1.32423000E+00,	4.90000000E+01,	1.33814000E+00,	-- 241--
5.00000000E+01,	1.35205000E+00,			-- 242--
2.08000000E-02,				-- 243--
0.	1.48857143E-02,	1.00000000E+00,	2.87880965E-02,	-- 244--
2.00000000E+00,	4.26460606E-02,	3.00000000E+00,	5.64669212E-02,	-- 245--
4.00000000E+00,	7.02564706E-02,	5.00000000E+00,	8.40193548E-02,	-- 246--
6.00000000E+00,	1.04186043E-01,	7.00000000E+00,	1.24351260E-01,	-- 247--
8.00000000E+00,	1.44515184E-01,	9.00000000E+00,	1.64677967E-01,	-- 248--
1.00000000E+01,	1.84839738E-01,	1.10000000E+01,	2.11148206E-01,	-- 249--
1.20000000E+01,	2.37510927E-01,	1.30000000E+01,	2.63923105E-01,	-- 250--
1.40000000E+01,	2.90380495E-01,	1.50000000E+01,	3.16879323E-01,	-- 251--
1.60000000E+01,	3.48096819E-01,	1.70000000E+01,	3.79419351E-01,	-- 252--
1.80000000E+01,	4.10840679E-01,	1.90000000E+01,	4.42355049E-01,	-- 253--
2.00000000E+01,	4.73957143E-01,	2.10000000E+01,	5.07860279E-01,	-- 254--
2.20000000E+01,	5.41777826E-01,	2.30000000E+01,	5.75827000E-01,	-- 255--
2.40000000E+01,	6.09999318E-01,	2.50000000E+01,	6.44287010E-01,	-- 256--
2.60000000E+01,	6.78723589E-01,	2.70000000E+01,	7.13332239E-01,	-- 257--
2.80000000E+01,	7.48103126E-01,	2.90000000E+01,	7.85160000E-01,	-- 258--
3.00000000E+01,	8.23050000E-01,	3.10000000E+01,	8.59080000E-01,	-- 259--
3.20000000E+01,	8.95110000E-01,	3.30000000E+01,	9.31140000E-01,	-- 260--
3.40000000E+01,	9.67170000E-01,	3.50000000E+01,	1.00320000E+00,	-- 261--
3.60000000E+01,	1.03471000E+00,	3.70000000E+01,	1.06622000E+00,	-- 262--
3.80000000E+01,	1.09773000E+00,	3.90000000E+01,	1.12924000E+00,	-- 263--
4.00000000E+01,	1.16075000E+00,	4.10000000E+01,	1.18499000E+00,	-- 264--
4.20000000E+01,	1.20923000E+00,	4.30000000E+01,	1.23347000E+00,	-- 265--
4.40000000E+01,	1.25771000E+00,	4.50000000E+01,	1.28195000E+00,	-- 266--
4.60000000E+01,	1.29589000E+00,	4.70000000E+01,	1.30983000E+00,	-- 267--
4.80000000E+01,	1.32377000E+00,	4.90000000E+01,	1.33771000E+00,	-- 268--
5.00000000E+01,	1.35165000E+00,			-- 269--

2.45000000E-02,									-- 270--
0.	1.49043165E-02,	1.00000000E+00,	2.87745553E-02,						-- 271--
2.00000000E+00,	4.25933840E-02,	3.00000000E+00,	5.63694737E-02,						-- 272--
4.00000000E+00,	7.01096489E-02,	5.00000000E+00,	8.38193548E-02,						-- 273--
6.00000000E+00,	1.04000741E-01,	7.00000000E+00,	1.24180355E-01,						-- 274--
8.00000000E+00,	1.44358409E-01,	9.00000000E+00,	1.64535082E-01,						-- 275--
1.00000000E+01,	1.84710526E-01,	1.10000000E+01,	2.11037060E-01,						-- 276--
1.20000000E+01,	2.37416705E-01,	1.30000000E+01,	2.63844748E-01,						-- 277--
1.40000000E+01,	2.90317019E-01,	1.50000000E+01,	3.16829811E-01,						-- 278--
1.60000000E+01,	3.47993097E-01,	1.70000000E+01,	3.79262375E-01,						-- 279--
1.80000000E+01,	4.10631327E-01,	1.90000000E+01,	4.42094127E-01,						-- 280--
2.00000000E+01,	4.73645392E-01,	2.10000000E+01,	5.07535986E-01,						-- 281--
2.20000000E+01,	5.41402120E-01,	2.30000000E+01,	5.75403454E-01,						-- 282--
2.40000000E+01,	6.09531081E-01,	2.50000000E+01,	6.43776860E-01,						-- 283--
2.60000000E+01,	6.78192470E-01,	2.70000000E+01,	7.12783016E-01,						-- 284--
2.80000000E+01,	7.47538288E-01,	2.90000000E+01,	7.84405000E-01,						-- 285--
3.00000000E+01,	8.22275000E-01,	3.10000000E+01,	8.58300000E-01,						-- 286--
3.20000000E+01,	8.94325000E-01,	3.30000000E+01,	9.30350000E-01,						-- 287--
3.40000000E+01,	9.66375000E-01,	3.50000000E+01,	1.00240000E+00,						-- 288--
3.60000000E+01,	1.03393000E+00,	3.70000000E+01,	1.06546000E+00,						-- 289--
3.80000000E+01,	1.09699000E+00,	3.90000000E+01,	1.12852000E+00,						-- 290--
4.00000000E+01,	1.16005000E+00,	4.10000000E+01,	1.18429000E+00,						-- 291--
4.20000000E+01,	1.20853000E+00,	4.30000000E+01,	1.23277000E+00,						-- 292--
4.40000000E+01,	1.25701000E+00,	4.50000000E+01,	1.28125000E+00,						-- 293--
4.60000000E+01,	1.29523000E+00,	4.70000000E+01,	1.30921000E+00,						-- 294--
4.80000000E+01,	1.32319000E+00,	4.90000000E+01,	1.33717000E+00,						-- 295--
5.00000000E+01,	1.35115000E+00,								-- 296--
3.73000000E-02,									-- 297--
0.	1.48971223E-02,	1.00000000E+00,	2.88954178E-02,						-- 298--
2.00000000E+00,	4.28394170E-02,	3.00000000E+00,	5.67382775E-02,						-- 299--
4.00000000E+00,	7.05992072E-02,	5.00000000E+00,	8.44279570E-02,						-- 300--
6.00000000E+00,	1.04571655E-01,	7.00000000E+00,	1.24713465E-01,						-- 301--
8.00000000E+00,	1.44853617E-01,	9.00000000E+00,	1.64992305E-01,						-- 302--
1.00000000E+01,	1.85129694E-01,	1.10000000E+01,	2.11335123E-01,						-- 303--
1.20000000E+01,	2.37593114E-01,	1.30000000E+01,	2.63899138E-01,						-- 304--
1.40000000E+01,	2.90249170E-01,	1.50000000E+01,	3.16639623E-01,						-- 305--
1.60000000E+01,	3.47718108E-01,	1.70000000E+01,	3.78900000E-01,						-- 306--
1.80000000E+01,	4.10179134E-01,	1.90000000E+01,	4.41549826E-01,						-- 307--
2.00000000E+01,	4.73006826E-01,	2.10000000E+01,	5.06972694E-01,						-- 308--
2.20000000E+01,	5.40789620E-01,	2.30000000E+01,	5.74740415E-01,						-- 309--
2.40000000E+01,	6.08816258E-01,	2.50000000E+01,	6.43009091E-01,						-- 310--
2.60000000E+01,	6.77340073E-01,	2.70000000E+01,	7.11844464E-01,						-- 311--
2.80000000E+01,	7.46512333E-01,	2.90000000E+01,	7.82590000E-01,						-- 312--
3.00000000E+01,	8.20400000E-01,	3.10000000E+01,	8.56375000E-01,						-- 313--
3.20000000E+01,	8.92350000E-01,	3.30000000E+01,	9.28325000E-01,						-- 314--
3.40000000E+01,	9.64300000E-01,	3.50000000E+01,	1.00027500E+00,						-- 315--
3.60000000E+01,	1.03183500E+00,	3.70000000E+01,	1.06339500E+00,						-- 316--
3.80000000E+01,	1.09495500E+00,	3.90000000E+01,	1.12651500E+00,						-- 317--
4.00000000E+01,	1.15807500E+00,	4.10000000E+01,	1.18241500E+00,						-- 318--
4.20000000E+01,	1.20675500E+00,	4.30000000E+01,	1.23109500E+00,						-- 319--
4.40000000E+01,	1.25543500E+00,	4.50000000E+01,	1.27977500E+00,						-- 320--
4.60000000E+01,	1.29379000E+00,	4.70000000E+01,	1.30780500E+00,						-- 321--
4.80000000E+01,	1.32182000E+00,	4.90000000E+01,	1.33583500E+00,						-- 322--
5.00000000E+01,	1.34985000E+00,								-- 323--
5.70000000E-02,									-- 324--
0.	1.52669065E-02,	1.00000000E+00,	2.90579245E-02,						-- 325--
2.00000000E+00,	4.27977440E-02,	3.00000000E+00,	5.64950000E-02,						-- 326--
4.00000000E+00,	7.01564892E-02,	5.00000000E+00,	8.37876344E-02,						-- 327--
6.00000000E+00,	1.04128818E-01,	7.00000000E+00,	1.24464626E-01,						-- 328--
8.00000000E+00,	1.44795713E-01,	9.00000000E+00,	1.65122632E-01,						-- 329--
1.00000000E+01,	1.85445852E-01,	1.10000000E+01,	2.11602557E-01,						-- 330--
1.20000000E+01,	2.37810337E-01,	1.30000000E+01,	2.64064789E-01,						-- 331--
1.40000000E+01,	2.90362002E-01,	1.50000000E+01,	3.16698491E-01,						-- 332--
1.60000000E+01,	3.47704080E-01,	1.70000000E+01,	3.78813888E-01,						-- 333--
1.80000000E+01,	4.10021703E-01,	1.90000000E+01,	4.41321795E-01,						-- 334--
2.00000000E+01,	4.72708874E-01,	2.10000000E+01,	5.06855488E-01,						-- 335--
2.20000000E+01,	5.40566855E-01,	2.30000000E+01,	5.74413238E-01,						-- 336--
2.40000000E+01,	6.08385743E-01,	2.50000000E+01,	6.42476240E-01,						-- 337--
2.60000000E+01,	6.76708562E-01,	2.70000000E+01,	7.11109952E-01,						-- 338--
2.80000000E+01,	7.45670728E-01,	2.90000000E+01,	7.80381934E-01,						-- 339--

3.00000000E+01	8.18075000E-01	3.10000000E+01	8.54015000E-01	-- 340--
3.20000000E+01	8.89955000E-01	3.30000000E+01	9.25895000E-01	-- 341--
3.40000000E+01	9.61835000E-01	3.50000000E+01	9.97775000E-01	-- 342--
3.60000000E+01	1.02932500E+00	3.70000000E+01	1.06087500E+00	-- 343--
3.80000000E+01	1.09242500E+00	3.90000000E+01	1.12397500E+00	-- 344--
4.00000000E+01	1.15552500E+00	4.10000000E+01	1.17995500E+00	-- 345--
4.20000000E+01	1.20438500E+00	4.30000000E+01	1.22881500E+00	-- 346--
4.40000000E+01	1.25324500E+00	4.50000000E+01	1.27767500E+00	-- 347--
4.60000000E+01	1.29173000E+00	4.70000000E+01	1.30578500E+00	-- 348--
4.80000000E+01	1.31984000E+00	4.90000000E+01	1.33389500E+00	-- 349--
5.00000000E+01	1.34795000E+00			-- 350--
7.44000000E-02				-- 351--
0.	1.54130435E-02	1.00000000E+00	2.90433333E-02	-- 352--
2.00000000E+00	4.26161832E-02	3.00000000E+00	5.61415108E-02	-- 353--
4.00000000E+00	6.96270748E-02	5.00000000E+00	8.30790323E-02	-- 354--
6.00000000E+00	1.03075910E-01	7.00000000E+00	1.23070807E-01	-- 355--
8.00000000E+00	1.43063966E-01	9.00000000E+00	1.63055590E-01	-- 356--
1.00000000E+01	1.83045852E-01	1.10000000E+01	2.09544373E-01	-- 357--
1.20000000E+01	2.36086535E-01	1.30000000E+01	2.62668672E-01	-- 358--
1.40000000E+01	2.89287518E-01	1.50000000E+01	3.15940152E-01	-- 359--
1.60000000E+01	3.46924729E-01	1.70000000E+01	3.78013237E-01	-- 360--
1.80000000E+01	4.09199247E-01	1.90000000E+01	4.40476852E-01	-- 361--
2.00000000E+01	4.71840614E-01	2.10000000E+01	5.05921147E-01	-- 362--
2.20000000E+01	5.39782977E-01	2.30000000E+01	5.73567038E-01	-- 363--
2.40000000E+01	6.07475313E-01	2.50000000E+01	6.41499793E-01	-- 364--
2.60000000E+01	6.75698509E-01	2.70000000E+01	7.10064539E-01	-- 365--
2.80000000E+01	7.44588487E-01	2.90000000E+01	7.79261646E-01	-- 366--
3.00000000E+01	8.15700000E-01	3.10000000E+01	8.51620000E-01	-- 367--
3.20000000E+01	8.87540000E-01	3.30000000E+01	9.23460000E-01	-- 368--
3.40000000E+01	9.59380000E-01	3.50000000E+01	9.95300000E-01	-- 369--
3.60000000E+01	1.02692000E+00	3.70000000E+01	1.05854000E+00	-- 370--
3.80000000E+01	1.09016000E+00	3.90000000E+01	1.12178000E+00	-- 371--
4.00000000E+01	1.15340000E+00	4.10000000E+01	1.17780000E+00	-- 372--
4.20000000E+01	1.20220000E+00	4.30000000E+01	1.22660000E+00	-- 373--
4.40000000E+01	1.25100000E+00	4.50000000E+01	1.27540000E+00	-- 374--
4.60000000E+01	1.28949000E+00	4.70000000E+01	1.30358000E+00	-- 375--
4.80000000E+01	1.31767000E+00	4.90000000E+01	1.33176000E+00	-- 376--
5.00000000E+01	1.34585000E+00			-- 377--
\$				-- 378--
L\$TAB				-- 378--
TABLE=6HCDVT	,2.5HALPHA,6HVINV	,51,8,1,1,1,1,1,1,1,		-- 379--
5.00000000E-03				-- 380--
0.	4.61507143E-02	1.00000000E+00	4.97237216E-02	-- 381--
2.00000000E+00	5.33939295E-02	3.00000000E+00	5.71450416E-02	-- 382--
4.00000000E+00	6.09642117E-02	5.00000000E+00	6.48411765E-02	-- 383--
6.00000000E+00	7.23717058E-02	7.00000000E+00	7.99070381E-02	-- 384--
8.00000000E+00	8.74465792E-02	9.00000000E+00	9.49898290E-02	-- 385--
1.00000000E+01	1.02536364E-01	1.10000000E+01	1.15383294E-01	-- 386--
1.20000000E+01	1.28157208E-01	1.30000000E+01	1.40864190E-01	-- 387--
1.40000000E+01	1.53509668E-01	1.50000000E+01	1.66098496E-01	-- 388--
1.60000000E+01	1.85489352E-01	1.70000000E+01	2.04759134E-01	-- 389--
1.80000000E+01	2.23915035E-01	1.90000000E+01	2.42963689E-01	-- 390--
2.00000000E+01	2.61911224E-01	2.10000000E+01	2.89909726E-01	-- 391--
2.20000000E+01	3.17964993E-01	2.30000000E+01	3.45800284E-01	-- 392--
2.40000000E+01	3.73429491E-01	2.50000000E+01	4.00865361E-01	-- 393--
2.60000000E+01	4.37095319E-01	2.70000000E+01	4.73108038E-01	-- 394--
2.80000000E+01	5.08915933E-01	2.90000000E+01	5.46885000E-01	-- 395--
3.00000000E+01	5.85725000E-01	3.10000000E+01	6.34165000E-01	-- 396--
3.20000000E+01	6.82605000E-01	3.30000000E+01	7.31045000E-01	-- 397--
3.40000000E+01	7.79485000E-01	3.50000000E+01	8.27925000E-01	-- 398--
3.60000000E+01	8.84770000E-01	3.70000000E+01	9.41615000E-01	-- 399--
3.80000000E+01	9.98460000E-01	3.90000000E+01	1.05530500E+00	-- 400--
4.00000000E+01	1.11215000E+00	4.10000000E+01	1.17629000E+00	-- 401--
4.20000000E+01	1.24043000E+00	4.30000000E+01	1.30457000E+00	-- 402--
4.40000000E+01	1.36871000E+00	4.50000000E+01	1.43285000E+00	-- 403--
4.60000000E+01	1.50210000E+00	4.70000000E+01	1.57135000E+00	-- 404--
4.80000000E+01	1.64060000E+00	4.90000000E+01	1.70985000E+00	-- 405--
5.00000000E+01	1.77910000E+00			-- 406--
1.03000000E-02				-- 407--
0.	4.65000000E-02	1.00000000E+00	5.02267470E-02	-- 408--

2.00000000E+00,	5.40437280E-02,	3.00000000E+00,	5.79358145E-02,	-- 409--
4.00000000E+00,	6.18910811E-02,	5.00000000E+00,	6.59000000E-02,	-- 410--
6.00000000E+00,	7.36945603E-02,	7.00000000E+00,	8.14946327E-02,	-- 411--
8.00000000E+00,	8.92995489E-02,	9.00000000E+00,	9.71087444E-02,	-- 412--
1.00000000E+01,	1.04921739E-01,	1.10000000E+01,	1.17909781E-01,	-- 413--
1.20000000E+01,	1.30824550E-01,	1.30000000E+01,	1.43672337E-01,	-- 414--
1.40000000E+01,	1.56458733E-01,	1.50000000E+01,	1.69188722E-01,	-- 415--
1.60000000E+01,	1.88756804E-01,	1.70000000E+01,	2.08206320E-01,	-- 416--
1.80000000E+01,	2.27544314E-01,	1.90000000E+01,	2.46777282E-01,	-- 417--
2.00000000E+01,	2.65911224E-01,	2.10000000E+01,	2.93935901E-01,	-- 418--
2.20000000E+01,	3.22015525E-01,	2.30000000E+01,	3.49874761E-01,	-- 419--
2.40000000E+01,	3.77527528E-01,	2.50000000E+01,	4.04986598E-01,	-- 420--
2.60000000E+01,	4.41277688E-01,	2.70000000E+01,	4.77358264E-01,	-- 421--
2.80000000E+01,	5.13240358E-01,	2.90000000E+01,	5.51325000E-01,	-- 422--
3.00000000E+01,	5.90200000E-01,	3.10000000E+01,	6.38550000E-01,	-- 423--
3.20000000E+01,	6.86900000E-01,	3.30000000E+01,	7.35250000E-01,	-- 424--
3.40000000E+01,	7.83600000E-01,	3.50000000E+01,	8.31950000E-01,	-- 425--
3.60000000E+01,	8.88725000E-01,	3.70000000E+01,	9.45500000E-01,	-- 426--
3.80000000E+01,	1.00227500E+00,	3.90000000E+01,	1.05905000E+00,	-- 427--
4.00000000E+01,	1.11582500E+00,	4.10000000E+01,	1.17968500E+00,	-- 428--
4.20000000E+01,	1.24354500E+00,	4.30000000E+01,	1.30740500E+00,	-- 429--
4.40000000E+01,	1.37126500E+00,	4.50000000E+01,	1.43512500E+00,	-- 430--
4.60000000E+01,	1.50422500E+00,	4.70000000E+01,	1.57332500E+00,	-- 431--
4.80000000E+01,	1.64242500E+00,	4.90000000E+01,	1.71152500E+00,	-- 432--
5.00000000E+01,	1.78062500E+00,			-- 433--
1.48000000E-02,				-- 434--
0.				-- 435--
	4.80071429E-02,	1.00000000E+00,	5.18254960E-02,	-- 436--
2.00000000E+00,	5.57384848E-02,	3.00000000E+00,	5.97305251E-02,	-- 437--
4.00000000E+00,	6.37892760E-02,	5.00000000E+00,	6.79048387E-02,	-- 438--
6.00000000E+00,	7.57605339E-02,	7.00000000E+00,	8.36205697E-02,	-- 439--
8.00000000E+00,	9.14844068E-02,	9.00000000E+00,	9.93515913E-02,	-- 440--
1.00000000E+01,	1.07221739E-01,	1.10000000E+01,	1.20327386E-01,	-- 441--
1.20000000E+01,	1.33362128E-01,	1.30000000E+01,	1.46332051E-01,	-- 442--
1.40000000E+01,	1.59242566E-01,	1.50000000E+01,	1.72098496E-01,	-- 443--
1.60000000E+01,	1.91666303E-01,	1.70000000E+01,	2.11114545E-01,	-- 444--
1.80000000E+01,	2.30450325E-01,	1.90000000E+01,	2.49680194E-01,	-- 445--
2.00000000E+01,	2.68810204E-01,	2.10000000E+01,	2.96882575E-01,	-- 446--
2.20000000E+01,	3.25012852E-01,	2.30000000E+01,	3.52927680E-01,	-- 447--
2.40000000E+01,	3.80640944E-01,	2.50000000E+01,	4.08165361E-01,	-- 448--
2.60000000E+01,	4.44432983E-01,	2.70000000E+01,	4.80489972E-01,	-- 449--
2.80000000E+01,	5.16348367E-01,	2.90000000E+01,	5.54365000E-01,	-- 450--
3.00000000E+01,	5.93250000E-01,	3.10000000E+01,	6.41560000E-01,	-- 451--
3.20000000E+01,	6.89870000E-01,	3.30000000E+01,	7.38180000E-01,	-- 452--
3.40000000E+01,	7.86490000E-01,	3.50000000E+01,	8.34800000E-01,	-- 453--
3.60000000E+01,	8.91475000E-01,	3.70000000E+01,	9.48150000E-01,	-- 454--
3.80000000E+01,	1.00482500E+00,	3.90000000E+01,	1.06150000E+00,	-- 455--
4.00000000E+01,	1.11817500E+00,	4.10000000E+01,	1.18188500E+00,	-- 456--
4.20000000E+01,	1.24559500E+00,	4.30000000E+01,	1.30930500E+00,	-- 457--
4.40000000E+01,	1.37301500E+00,	4.50000000E+01,	1.43672500E+00,	-- 458--
4.60000000E+01,	1.50579000E+00,	4.70000000E+01,	1.57485500E+00,	-- 459--
4.80000000E+01,	1.64392000E+00,	4.90000000E+01,	1.71298500E+00,	-- 460--
5.00000000E+01,	1.78205000E+00,			-- 461--
2.08000000E-02,				-- 462--
0.				-- 463--
	4.85071429E-02,	1.00000000E+00,	5.22754960E-02,	-- 464--
2.00000000E+00,	5.61427778E-02,	3.00000000E+00,	6.00926969E-02,	-- 465--
4.00000000E+00,	6.41123529E-02,	5.00000000E+00,	6.81913978E-02,	-- 466--
6.00000000E+00,	7.60105036E-02,	7.00000000E+00,	8.38319685E-02,	-- 467--
8.00000000E+00,	9.1655052E-02,	9.00000000E+00,	9.94808711E-02,	-- 468--
1.00000000E+01,	1.07307860E-01,	1.10000000E+01,	1.20477513E-01,	-- 469--
1.20000000E+01,	1.33577506E-01,	1.30000000E+01,	1.46613997E-01,	-- 470--
1.40000000E+01,	1.59592436E-01,	1.50000000E+01,	1.72517669E-01,	-- 471--
1.60000000E+01,	1.92195449E-01,	1.70000000E+01,	2.11756840E-01,	-- 472--
1.80000000E+01,	2.31208755E-01,	1.90000000E+01,	2.50557573E-01,	-- 473--
2.00000000E+01,	2.69809184E-01,	2.10000000E+01,	2.97940009E-01,	-- 474--
2.20000000E+01,	3.26127174E-01,	2.30000000E+01,	3.54099027E-01,	-- 475--
2.40000000E+01,	3.81869444E-01,	2.50000000E+01,	4.09451134E-01,	-- 476--
2.60000000E+01,	4.45758852E-01,	2.70000000E+01,	4.81857392E-01,	-- 477--
2.80000000E+01,	5.17758709E-01,	2.90000000E+01,	5.55820000E-01,	-- 478--
3.00000000E+01,	5.94750000E-01,	3.10000000E+01,	6.43020000E-01,	-- 479--
3.20000000E+01,	6.91290000E-01,	3.30000000E+01,	7.39560000E-01,	-- 480--

3.40000000E+01,	7.87830000E-01,	3.50000000E+01,	8.36100000E-01,	-- 479--
3.60000000E+01,	8.92775000E-01,	3.70000000E+01,	9.49450000E-01,	-- 480--
3.80000000E+01,	1.00612500E+00,	3.90000000E+01,	1.06280000E+00,	-- 481--
4.00000000E+01,	1.11947500E+00,	4.10000000E+01,	1.18312000E+00,	-- 482--
4.20000000E+01,	1.24676500E+00,	4.30000000E+01,	1.31041000E+00,	-- 483--
4.40000000E+01,	1.37405500E+00,	4.50000000E+01,	1.43770000E+00,	-- 484--
4.60000000E+01,	1.50667000E+00,	4.70000000E+01,	1.57564000E+00,	-- 485--
4.80000000E+01,	1.64461000E+00,	4.90000000E+01,	1.71358000E+00,	-- 486--
5.00000000E+01,	1.78255000E+00,			-- 487--
2.45000000E-02,				-- 488--
0.	5.04093525E-02,	1.00000000E+00,	5.41193531E-02,	-- 489--
2.00000000E+00,	5.79274271E-02,	3.00000000E+00,	6.18170335E-02,	-- 490--
4.00000000E+00,	6.57751529E-02,	5.00000000E+00,	6.97913978E-02,	-- 491--
6.00000000E+00,	7.76864198E-02,	7.00000000E+00,	8.55846154E-02,	-- 492--
8.00000000E+00,	9.34856061E-02,	9.00000000E+00,	1.01389071E-01,	-- 493--
1.00000000E+01,	1.09294737E-01,	1.10000000E+01,	1.22491232E-01,	-- 494--
1.20000000E+01,	1.35621351E-01,	1.30000000E+01,	1.48690983E-01,	-- 495--
1.40000000E+01,	1.61705342E-01,	1.50000000E+01,	1.74669057E-01,	-- 496--
1.60000000E+01,	1.94365100E-01,	1.70000000E+01,	2.13944403E-01,	-- 497--
1.80000000E+01,	2.33413925E-01,	1.90000000E+01,	2.52780084E-01,	-- 498--
2.00000000E+01,	2.72048805E-01,	2.10000000E+01,	3.00102821E-01,	-- 499--
2.20000000E+01,	3.28310495E-01,	2.30000000E+01,	3.56304214E-01,	-- 500--
2.40000000E+01,	3.84098074E-01,	2.50000000E+01,	4.11704959E-01,	-- 501--
2.60000000E+01,	4.47978283E-01,	2.70000000E+01,	4.84045016E-01,	-- 502--
2.80000000E+01,	5.19917214E-01,	2.90000000E+01,	5.57760000E-01,	-- 503--
3.00000000E+01,	5.96650000E-01,	3.10000000E+01,	6.44910000E-01,	-- 504--
3.20000000E+01,	6.93170000E-01,	3.30000000E+01,	7.41430000E-01,	-- 505--
3.40000000E+01,	7.89690000E-01,	3.50000000E+01,	8.37950000E-01,	-- 506--
3.60000000E+01,	8.94565000E-01,	3.70000000E+01,	9.51180000E-01,	-- 507--
3.80000000E+01,	1.00779500E+00,	3.90000000E+01,	1.06441000E+00,	-- 508--
4.00000000E+01,	1.12102500E+00,	4.10000000E+01,	1.18460000E+00,	-- 509--
4.20000000E+01,	1.24817500E+00,	4.30000000E+01,	1.31175000E+00,	-- 510--
4.40000000E+01,	1.37532500E+00,	4.50000000E+01,	1.43890000E+00,	-- 511--
4.60000000E+01,	1.50785500E+00,	4.70000000E+01,	1.57681000E+00,	-- 512--
4.80000000E+01,	1.64576500E+00,	4.90000000E+01,	1.71472000E+00,	-- 513--
5.00000000E+01,	1.78367500E+00,			-- 514--
3.73000000E-02,				-- 515--
0.	5.85093525E-02,	1.00000000E+00,	6.21791644E-02,	-- 516--
2.00000000E+00,	6.59517871E-02,	3.00000000E+00,	6.98098804E-02,	-- 517--
4.00000000E+00,	7.37397961E-02,	5.00000000E+00,	7.77306452E-02,	-- 518--
6.00000000E+00,	8.53133196E-02,	7.00000000E+00,	9.28991535E-02,	-- 519--
8.00000000E+00,	1.00487762E-01,	9.00000000E+00,	1.08078820E-01,	-- 520--
1.00000000E+01,	1.15672052E-01,	1.10000000E+01,	1.28862930E-01,	-- 521--
1.20000000E+01,	1.41983550E-01,	1.30000000E+01,	1.55039968E-01,	-- 522--
1.40000000E+01,	1.68037564E-01,	1.50000000E+01,	1.80981132E-01,	-- 523--
1.60000000E+01,	2.00718211E-01,	1.70000000E+01,	2.20337697E-01,	-- 524--
1.80000000E+01,	2.39846600E-01,	1.90000000E+01,	2.59251385E-01,	-- 525--
2.00000000E+01,	2.78558020E-01,	2.10000000E+01,	3.06362929E-01,	-- 526--
2.20000000E+01,	3.34612147E-01,	2.30000000E+01,	3.62652763E-01,	-- 527--
2.40000000E+01,	3.90498522E-01,	2.50000000E+01,	4.18161983E-01,	-- 528--
2.60000000E+01,	4.54441482E-01,	2.70000000E+01,	4.90508689E-01,	-- 529--
2.80000000E+01,	5.26375762E-01,	2.90000000E+01,	5.63435000E-01,	-- 530--
3.00000000E+01,	6.02300000E-01,	3.10000000E+01,	6.50525000E-01,	-- 531--
3.20000000E+01,	6.98750000E-01,	3.30000000E+01,	7.46975000E-01,	-- 532--
3.40000000E+01,	7.95200000E-01,	3.50000000E+01,	8.43425000E-01,	-- 533--
3.60000000E+01,	8.99865000E-01,	3.70000000E+01,	9.56305000E-01,	-- 534--
3.80000000E+01,	1.01274500E+00,	3.90000000E+01,	1.06918500E+00,	-- 535--
4.00000000E+01,	1.12562500E+00,	4.10000000E+01,	1.18903500E+00,	-- 536--
4.20000000E+01,	1.25244500E+00,	4.30000000E+01,	1.31585500E+00,	-- 537--
4.40000000E+01,	1.37926500E+00,	4.50000000E+01,	1.44267500E+00,	-- 538--
4.60000000E+01,	1.51152000E+00,	4.70000000E+01,	1.58036500E+00,	-- 539--
4.80000000E+01,	1.64921000E+00,	4.90000000E+01,	1.71805500E+00,	-- 540--
5.00000000E+01,	1.78690000E+00,			-- 541--
5.70000000E-02,				-- 542--
0.	7.91273381E-02,	1.00000000E+00,	8.18231806E-02,	-- 543--
2.00000000E+00,	8.46373891E-02,	3.00000000E+00,	8.75500000E-02,	-- 544--
4.00000000E+00,	9.05453001E-02,	5.00000000E+00,	9.36107527E-02,	-- 545--
6.00000000E+00,	1.00210031E-01,	7.00000000E+00,	1.06818543E-01,	-- 546--
8.00000000E+00,	1.13435165E-01,	9.00000000E+00,	1.20058947E-01,	-- 547--
1.00000000E+01,	1.26689083E-01,	1.10000000E+01,	1.39894716E-01,	-- 548--

ORIGINAL PAGE IS
OF POOR QUALITY

1.20000000E+01,	1.53029614E-01,	1.30000000E+01,	1.66099872E-01,	-- 549--
1.40000000E+01,	1.79110908E-01,	1.50000000E+01,	1.92067547E-01,	-- 550--
1.60000000E+01,	2.11730466E-01,	1.70000000E+01,	2.31279783E-01,	-- 551--
1.80000000E+01,	2.50722271E-01,	1.90000000E+01,	2.70064175E-01,	-- 552--
2.00000000E+01,	2.89311263E-01,	2.10000000E+01,	3.16470018E-01,	-- 553--
2.20000000E+01,	3.44728057E-01,	2.30000000E+01,	3.72772850E-01,	-- 554--
2.40000000E+01,	4.00618446E-01,	2.50000000E+01,	4.28277686E-01,	-- 555--
2.60000000E+01,	4.64530231E-01,	2.70000000E+01,	5.00577188E-01,	-- 556--
2.80000000E+01,	5.36430331E-01,	2.90000000E+01,	5.72100550E-01,	-- 557--
3.00000000E+01,	6.10875000E-01,	3.10000000E+01,	6.59000000E-01,	-- 558--
3.20000000E+01,	7.07125000E-01,	3.30000000E+01,	7.55250000E-01,	-- 559--
3.40000000E+01,	8.03375000E-01,	3.50000000E+01,	8.51500000E-01,	-- 560--
3.60000000E+01,	9.07825000E-01,	3.70000000E+01,	9.64150000E-01,	-- 561--
3.80000000E+01,	1.02047500E+00,	3.90000000E+01,	1.07680000E+00,	-- 562--
4.00000000E+01,	1.13312500E+00,	4.10000000E+01,	1.19624500E+00,	-- 563--
4.20000000E+01,	1.25936500E+00,	4.30000000E+01,	1.32248500E+00,	-- 564--
4.40000000E+01,	1.38560500E+00,	4.50000000E+01,	1.44872500E+00,	-- 565--
4.60000000E+01,	1.51744500E+00,	4.70000000E+01,	1.58616500E+00,	-- 566--
4.80000000E+01,	1.65488500E+00,	4.90000000E+01,	1.72360500E+00,	-- 567--
5.00000000E+01,	1.79232500E+00,			-- 568--
7.44000000E-02,				-- 569--
0,	9.73826087E-02,	1.00000000E+00,	9.97333333E-02,	-- 570--
2.00000000E+00,	1.02212214E-01,	3.00000000E+00,	1.04797122E-01,	-- 571--
4.00000000E+00,	1.07470748E-01,	5.00000000E+00,	1.10219355E-01,	-- 572--
6.00000000E+00,	1.16979753E-01,	7.00000000E+00,	1.23743898E-01,	-- 573--
8.00000000E+00,	1.30511331E-01,	9.00000000E+00,	1.37281670E-01,	-- 574--
1.00000000E+01,	1.44054585E-01,	1.10000000E+01,	1.55992797E-01,	-- 575--
1.20000000E+01,	1.67867737E-01,	1.30000000E+01,	1.79684720E-01,	-- 576--
1.40000000E+01,	1.91448482E-01,	1.50000000E+01,	2.03163258E-01,	-- 577--
1.60000000E+01,	2.22711371E-01,	1.70000000E+01,	2.42151422E-01,	-- 578--
1.80000000E+01,	2.61490092E-01,	1.90000000E+01,	2.80733524E-01,	-- 579--
2.00000000E+01,	2.99887372E-01,	2.10000000E+01,	3.27071201E-01,	-- 580--
2.20000000E+01,	3.54901625E-01,	2.30000000E+01,	3.82984404E-01,	-- 581--
2.40000000E+01,	4.10871250E-01,	2.50000000E+01,	4.38574793E-01,	-- 582--
2.60000000E+01,	4.74809028E-01,	2.70000000E+01,	5.10838124E-01,	-- 583--
2.80000000E+01,	5.46673604E-01,	2.90000000E+01,	5.82326141E-01,	-- 584--
3.00000000E+01,	6.19675000E-01,	3.10000000E+01,	6.67695000E-01,	-- 585--
3.20000000E+01,	7.15715000E-01,	3.30000000E+01,	7.63735000E-01,	-- 586--
3.40000000E+01,	8.11755000E-01,	3.50000000E+01,	8.59775000E-01,	-- 587--
3.60000000E+01,	9.15945000E-01,	3.70000000E+01,	9.72115000E-01,	-- 588--
3.80000000E+01,	1.02828500E+00,	3.90000000E+01,	1.08445500E+00,	-- 589--
4.00000000E+01,	1.14062500E+00,	4.10000000E+01,	1.20373500E+00,	-- 590--
4.20000000E+01,	1.26684500E+00,	4.30000000E+01,	1.32995500E+00,	-- 591--
4.40000000E+01,	1.39306500E+00,	4.50000000E+01,	1.45617500E+00,	-- 592--
4.60000000E+01,	1.52469000E+00,	4.70000000E+01,	1.59320500E+00,	-- 593--
4.80000000E+01,	1.66172000E+00,	4.90000000E+01,	1.73023500E+00,	-- 594--
5.00000000E+01,	1.79875000E+00,			-- 595--
\$				-- 596--
L\$TAB				-- 596--
TABLE=6HCLT	,2,5HALPHA,6HMACH	,51,5,1,1,1,1,1,1,1,		-- 597--
2.00000000E+00,				-- 598--
0,	1.50099291E-02,	1.00000000E+00,	2.89746738E-02,	-- 599--
2.00000000E+00,	4.28950063E-02,	3.00000000E+00,	5.67781969E-02,	-- 600--
4.00000000E+00,	7.06300112E-02,	5.00000000E+00,	8.44550802E-02,	-- 601--
6.00000000E+00,	1.04932768E-01,	7.00000000E+00,	1.25406276E-01,	-- 602--
8.00000000E+00,	1.45876120E-01,	9.00000000E+00,	1.66342736E-01,	-- 603--
1.00000000E+01,	1.86806494E-01,	1.10000000E+01,	2.13501041E-01,	-- 604--
1.20000000E+01,	2.40249601E-01,	1.30000000E+01,	2.67047553E-01,	-- 605--
1.40000000E+01,	2.93890793E-01,	1.50000000E+01,	3.20775655E-01,	-- 606--
1.60000000E+01,	3.52517061E-01,	1.70000000E+01,	3.84367397E-01,	-- 607--
1.80000000E+01,	4.16320651E-01,	1.90000000E+01,	4.48371244E-01,	-- 608--
2.00000000E+01,	4.80513993E-01,	2.10000000E+01,	5.15038280E-01,	-- 609--
2.20000000E+01,	5.49448757E-01,	2.30000000E+01,	5.83997671E-01,	-- 610--
2.40000000E+01,	6.18675980E-01,	2.50000000E+01,	6.53475410E-01,	-- 611--
2.60000000E+01,	6.88337692E-01,	2.70000000E+01,	7.23384751E-01,	-- 612--
2.80000000E+01,	7.58606494E-01,	2.90000000E+01,	7.95500000E-01,	-- 613--
3.00000000E+01,	8.33875000E-01,	3.10000000E+01,	8.70115000E-01,	-- 614--
3.20000000E+01,	9.06355000E-01,	3.30000000E+01,	9.42595000E-01,	-- 615--
3.40000000E+01,	9.78835000E-01,	3.50000000E+01,	1.01507500E+00,	-- 616--
3.60000000E+01,	1.04627500E+00,	3.70000000E+01,	1.07747500E+00,	-- 617--

3.80000000E+01	1.10867500E+00	3.90000000E+01	1.13987500E+00	-- 618--
4.00000000E+01	1.17107500E+00	4.10000000E+01	1.19453000E+00	-- 619--
4.20000000E+01	1.21798500E+00	4.30000000E+01	1.24144000E+00	-- 620--
4.40000000E+01	1.26489500E+00	4.50000000E+01	1.28835000E+00	-- 621--
4.60000000E+01	1.30180500E+00	4.70000000E+01	1.31526000E+00	-- 622--
4.80000000E+01	1.32871500E+00	4.90000000E+01	1.34217000E+00	-- 623--
5.00000000E+01	1.35562500E+00			-- 624--
4.00000000E+00				-- 625--
0.	1.50142857E-02	1.00000000E+00	2.89755020E-02	-- 626--
2.00000000E+00	4.28866499E-02	3.00000000E+00	5.67561237E-02	-- 627--
4.00000000E+00	7.05905405E-02	5.00000000E+00	8.43951872E-02	-- 628--
6.00000000E+00	1.04803473E-01	7.00000000E+00	1.25209091E-01	-- 629--
8.00000000E+00	1.45612371E-01	9.00000000E+00	1.66013591E-01	-- 630--
1.00000000E+01	1.86412987E-01	1.10000000E+01	2.13041412E-01	-- 631--
1.20000000E+01	2.39718792E-01	1.30000000E+01	2.66441048E-01	-- 632--
1.40000000E+01	2.93204541E-01	1.50000000E+01	3.2006015E-01	-- 633--
1.60000000E+01	3.51643699E-01	1.70000000E+01	3.83391185E-01	-- 634--
1.80000000E+01	4.15242169E-01	1.90000000E+01	4.47190821E-01	-- 635--
2.00000000E+01	4.79231741E-01	2.10000000E+01	5.13595007E-01	-- 636--
2.20000000E+01	5.47888405E-01	2.30000000E+01	5.82316391E-01	-- 637--
2.40000000E+01	6.16870327E-01	2.50000000E+01	6.51542300E-01	-- 638--
2.60000000E+01	6.86340645E-01	2.70000000E+01	7.21322823E-01	-- 639--
2.80000000E+01	7.56478773E-01	2.90000000E+01	7.93540000E-01	-- 640--
3.00000000E+01	8.31850000E-01	3.10000000E+01	8.68195000E-01	-- 641--
3.20000000E+01	9.04540000E-01	3.30000000E+01	9.40885000E-01	-- 642--
3.40000000E+01	9.77230000E-01	3.50000000E+01	1.01357500E+00	-- 643--
3.60000000E+01	1.04486500E+00	3.70000000E+01	1.07615500E+00	-- 644--
3.80000000E+01	1.10744500E+00	3.90000000E+01	1.13873500E+00	-- 645--
4.00000000E+01	1.17002500E+00	4.10000000E+01	1.19355000E+00	-- 646--
4.20000000E+01	1.21707500E+00	4.30000000E+01	1.24060000E+00	-- 647--
4.40000000E+01	1.26412500E+00	4.50000000E+01	1.28765000E+00	-- 648--
4.60000000E+01	1.30118000E+00	4.70000000E+01	1.31471000E+00	-- 649--
4.80000000E+01	1.32824000E+00	4.90000000E+01	1.34177000E+00	-- 650--
5.00000000E+01	1.35530000E+00			-- 651--
6.00000000E+00				-- 652--
0.	1.49071429E-02	1.00000000E+00	2.88626506E-02	-- 653--
2.00000000E+00	4.27687657E-02	3.00000000E+00	5.66337693E-02	-- 654--
4.00000000E+00	7.04641892E-02	5.00000000E+00	8.42652406E-02	-- 655--
6.00000000E+00	1.04558611E-01	7.00000000E+00	1.24850753E-01	-- 656--
8.00000000E+00	1.45141818E-01	9.00000000E+00	1.65431935E-01	-- 657--
1.00000000E+01	1.85721212E-01	1.10000000E+01	2.12278975E-01	-- 658--
1.20000000E+01	2.38885159E-01	1.30000000E+01	2.65535730E-01	-- 659--
1.40000000E+01	2.92227089E-01	1.50000000E+01	3.18956015E-01	-- 660--
1.60000000E+01	3.50492985E-01	1.70000000E+01	3.82136286E-01	-- 661--
1.80000000E+01	4.13879816E-01	1.90000000E+01	4.45717928E-01	-- 662--
2.00000000E+01	4.77645392E-01	2.10000000E+01	5.11832959E-01	-- 663--
2.20000000E+01	5.45994252E-01	2.30000000E+01	5.80290090E-01	-- 664--
2.40000000E+01	6.14711666E-01	2.50000000E+01	6.49250924E-01	-- 665--
2.60000000E+01	6.83931330E-01	2.70000000E+01	7.18792582E-01	-- 666--
2.80000000E+01	7.53824783E-01	2.90000000E+01	7.90945000E-01	-- 667--
3.00000000E+01	8.29125000E-01	3.10000000E+01	8.65310000E-01	-- 668--
3.20000000E+01	9.01495000E-01	3.30000000E+01	9.37680000E-01	-- 669--
3.40000000E+01	9.73865000E-01	3.50000000E+01	1.01005000E+00	-- 670--
3.60000000E+01	1.04158500E+00	3.70000000E+01	1.07312000E+00	-- 671--
3.80000000E+01	1.10465500E+00	3.90000000E+01	1.13619000E+00	-- 672--
4.00000000E+01	1.16772500E+00	4.10000000E+01	1.19142500E+00	-- 673--
4.20000000E+01	1.21512500E+00	4.30000000E+01	1.23882500E+00	-- 674--
4.40000000E+01	1.26252500E+00	4.50000000E+01	1.28622500E+00	-- 675--
4.60000000E+01	1.29981500E+00	4.70000000E+01	1.31340500E+00	-- 676--
4.80000000E+01	1.32699500E+00	4.90000000E+01	1.34058500E+00	-- 677--
5.00000000E+01	1.35417500E+00			-- 678--
8.00000000E+00				-- 679--
0.	1.49071429E-02	1.00000000E+00	2.88311647E-02	-- 680--
2.00000000E+00	4.27069521E-02	3.00000000E+00	5.65425922E-02	-- 681--
4.00000000E+00	7.03444595E-02	5.00000000E+00	8.41176471E-02	-- 682--
6.00000000E+00	1.04463800E-01	7.00000000E+00	1.24806882E-01	-- 683--
8.00000000E+00	1.45147273E-01	9.00000000E+00	1.65485293E-01	-- 684--
1.00000000E+01	1.85821212E-01	1.10000000E+01	2.12333412E-01	-- 685--
1.20000000E+01	2.38894971E-01	1.30000000E+01	2.65501778E-01	-- 686--
1.40000000E+01	2.92150162E-01	1.50000000E+01	3.18836842E-01	-- 687--

1.60000000E+01,	3.50096610E-01,	1.70000000E+01,	3.81553468E-01,	-- 688--
1.80000000E+01,	4.13196102E-01,	1.90000000E+01,	4.45014047E-01,	-- 689--
2.00000000E+01,	4.76997611E-01,	2.10000000E+01,	5.11435919E-01,	-- 690--
2.20000000E+01,	5.45741749E-01,	2.30000000E+01,	5.80022658E-01,	-- 691--
2.40000000E+01,	6.14280219E-01,	2.50000000E+01,	6.48515876E-01,	-- 692--
2.60000000E+01,	6.83160000E-01,	2.70000000E+01,	7.17986112E-01,	-- 693--
2.80000000E+01,	7.52983810E-01,	2.90000000E+01,	7.90275000E-01,	-- 694--
3.00000000E+01,	8.28400000E-01,	3.10000000E+01,	8.64545000E-01,	-- 695--
3.20000000E+01,	9.00690000E-01,	3.30000000E+01,	9.36835000E-01,	-- 696--
3.40000000E+01,	9.72980000E-01,	3.50000000E+01,	1.00912500E+00,	-- 697--
3.60000000E+01,	1.04068500E+00,	3.70000000E+01,	1.07224500E+00,	-- 698--
3.80000000E+01,	1.10380500E+00,	3.90000000E+01,	1.13536500E+00,	-- 699--
4.00000000E+01,	1.16692500E+00,	4.10000000E+01,	1.19068500E+00,	-- 700--
4.20000000E+01,	1.21444500E+00,	4.30000000E+01,	1.23820500E+00,	-- 701--
4.40000000E+01,	1.26196500E+00,	4.50000000E+01,	1.28572500E+00,	-- 702--
4.60000000E+01,	1.29943500E+00,	4.70000000E+01,	1.31314500E+00,	-- 703--
4.80000000E+01,	1.32685500E+00,	4.90000000E+01,	1.34056500E+00,	-- 704--
5.00000000E+01,	1.35427500E+00,			-- 705--
1.00000000E+01,				-- 706--
0.	1.46464286E-02,	1.00000000E+00,	2.86227845E-02,	-- 707--
2.00000000E+00,	4.25473300E-02,	3.00000000E+00,	5.64287515E-02,	-- 708--
4.00000000E+00,	7.02738964E-02,	5.00000000E+00,	8.40882353E-02,	-- 709--
6.00000000E+00,	1.04440102E-01,	7.00000000E+00,	1.24788993E-01,	-- 710--
8.00000000E+00,	1.45135276E-01,	9.00000000E+00,	1.65479262E-01,	-- 711--
1.00000000E+01,	1.85821212E-01,	1.10000000E+01,	2.12313412E-01,	-- 712--
1.20000000E+01,	2.38854971E-01,	1.30000000E+01,	2.65441778E-01,	-- 713--
1.40000000E+01,	2.92070162E-01,	1.50000000E+01,	3.18736842E-01,	-- 714--
1.60000000E+01,	3.50153402E-01,	1.70000000E+01,	3.81680000E-01,	-- 715--
1.80000000E+01,	4.13310099E-01,	1.90000000E+01,	4.45037670E-01,	-- 716--
2.00000000E+01,	4.76857143E-01,	2.10000000E+01,	5.10974085E-01,	-- 717--
2.20000000E+01,	5.45100290E-01,	2.30000000E+01,	5.79354606E-01,	-- 718--
2.40000000E+01,	6.13728943E-01,	2.50000000E+01,	6.48215876E-01,	-- 719--
2.60000000E+01,	6.82840000E-01,	2.70000000E+01,	7.17646112E-01,	-- 720--
2.80000000E+01,	7.52623810E-01,	2.90000000E+01,	7.89895000E-01,	-- 721--
3.00000000E+01,	8.28000000E-01,	3.10000000E+01,	8.64125000E-01,	-- 722--
3.20000000E+01,	9.00250000E-01,	3.30000000E+01,	9.36375000E-01,	-- 723--
3.40000000E+01,	9.72500000E-01,	3.50000000E+01,	1.00862500E+00,	-- 724--
3.60000000E+01,	1.04015000E+00,	3.70000000E+01,	1.07167500E+00,	-- 725--
3.80000000E+01,	1.10320000E+00,	3.90000000E+01,	1.13472500E+00,	-- 726--
4.00000000E+01,	1.16625000E+00,	4.10000000E+01,	1.19009500E+00,	-- 727--
4.20000000E+01,	1.21394000E+00,	4.30000000E+01,	1.23778500E+00,	-- 728--
4.40000000E+01,	1.26163000E+00,	4.50000000E+01,	1.28547500E+00,	-- 729--
4.60000000E+01,	1.29923500E+00,	4.70000000E+01,	1.31299500E+00,	-- 730--
4.80000000E+01,	1.32675500E+00,	4.90000000E+01,	1.34051500E+00,	-- 731--
5.00000000E+01,	1.35427500E+00,			-- 732--
\$				-- 733--
L\$TAB				-- 733--
TABLE=6HCDDT	,2.5HALPHA,6HMACH	,51,5,1,1,1,1,1,1,		-- 734--
2.00000000E+00,				-- 735--
0	5.20985816E-02,	1.00000000E+00,	5.53389880E-02,	-- 736--
2.00000000E+00,	5.86878545E-02,	3.00000000E+00,	6.21274259E-02,	-- 737--
4.00000000E+00,	6.56436220E-02,	5.00000000E+00,	6.92251337E-02,	-- 738--
6.00000000E+00,	7.62035138E-02,	7.00000000E+00,	8.31889150E-02,	-- 739--
8.00000000E+00,	9.01804686E-02,	9.00000000E+00,	9.71774437E-02,	-- 740--
1.00000000E+01,	1.04179221E-01,	1.10000000E+01,	1.16369186E-01,	-- 741--
1.20000000E+01,	1.28481663E-01,	1.30000000E+01,	1.40523278E-01,	-- 742--
1.40000000E+01,	1.52499923E-01,	1.50000000E+01,	1.64416854E-01,	-- 743--
1.60000000E+01,	1.83271095E-01,	1.70000000E+01,	2.01992603E-01,	-- 744--
1.80000000E+01,	2.20588705E-01,	1.90000000E+01,	2.39066199E-01,	-- 745--
2.00000000E+01,	2.57431399E-01,	2.10000000E+01,	2.84744086E-01,	-- 746--
2.20000000E+01,	3.12418214E-01,	2.30000000E+01,	3.39869521E-01,	-- 747--
2.40000000E+01,	3.67112563E-01,	2.50000000E+01,	3.94160656E-01,	-- 748--
2.60000000E+01,	4.30299405E-01,	2.70000000E+01,	4.66208161E-01,	-- 749--
2.80000000E+01,	5.01899489E-01,	2.90000000E+01,	5.39060000E-01,	-- 750--
3.00000000E+01,	5.77775000E-01,	3.10000000E+01,	6.26310000E-01,	-- 751--
3.20000000E+01,	6.74845000E-01,	3.30000000E+01,	7.23380000E-01,	-- 752--
3.40000000E+01,	7.71915000E-01,	3.50000000E+01,	8.20450000E-01,	-- 753--
3.60000000E+01,	8.77890000E-01,	3.70000000E+01,	9.35330000E-01,	-- 754--
3.80000000E+01,	9.92770000E-01,	3.90000000E+01,	1.05021000E+00,	-- 755--
4.00000000E+01,	1.10765000E+00,	4.10000000E+01,	1.17231500E+00,	-- 756--

ORIGINAL PAGE IS
OF POOR QUALITY

4.20000000E+01,	1.23698000E+00,	4.30000000E+01,	1.30164500E+00,	-- 757--
4.40000000E+01,	1.36631000E+00,	4.50000000E+01,	1.43097500E+00,	-- 758--
4.60000000E+01,	1.50058500E+00,	4.70000000E+01,	1.57019500E+00,	-- 759--
4.80000000E+01,	1.63980500E+00,	4.90000000E+01,	1.70941500E+00,	-- 760--
5.00000000E+01,	1.77902500E+00,			-- 761--
4.00000000E+00,				-- 762--
0.	5.01285714E-02,	1.00000000E+00,	5.34331727E-02,	-- 763--
2.00000000E+00,	5.68429723E-02,	3.00000000E+00,	6.03403329E-02,	-- 764--
4.00000000E+00,	6.39113514E-02,	5.00000000E+00,	6.75449198E-02,	-- 765--
6.00000000E+00,	7.46608989E-02,	7.00000000E+00,	8.17812121E-02,	-- 766--
8.00000000E+00,	8.89053233E-02,	9.00000000E+00,	9.60327813E-02,	-- 767--
1.00000000E+01,	1.03163203E-01,	1.10000000E+01,	1.15574824E-01,	-- 768--
1.20000000E+01,	1.27911396E-01,	1.30000000E+01,	1.40179175E-01,	-- 769--
1.40000000E+01,	1.52383737E-01,	1.50000000E+01,	1.64530075E-01,	-- 770--
1.60000000E+01,	1.83630995E-01,	1.70000000E+01,	2.02600462E-01,	-- 771--
1.80000000E+01,	2.21446024E-01,	1.90000000E+01,	2.40174659E-01,	-- 772--
2.00000000E+01,	2.58792833E-01,	2.10000000E+01,	2.86355912E-01,	-- 773--
2.20000000E+01,	3.14182761E-01,	2.30000000E+01,	3.41789781E-01,	-- 774--
2.40000000E+01,	3.69191082E-01,	2.50000000E+01,	3.96399589E-01,	-- 775--
2.60000000E+01,	4.32534376E-01,	2.70000000E+01,	4.68438861E-01,	-- 776--
2.80000000E+01,	5.04125652E-01,	2.90000000E+01,	5.41535000E-01,	-- 777--
3.00000000E+01,	5.80250000E-01,	3.10000000E+01,	6.28555000E-01,	-- 778--
3.20000000E+01,	6.76860000E-01,	3.30000000E+01,	7.25165000E-01,	-- 779--
3.40000000E+01,	7.73470000E-01,	3.50000000E+01,	8.21775000E-01,	-- 780--
3.60000000E+01,	8.79060000E-01,	3.70000000E+01,	9.36345000E-01,	-- 781--
3.80000000E+01,	9.93630000E-01,	3.90000000E+01,	1.05091500E+00,	-- 782--
4.00000000E+01,	1.10820000E+00,	4.10000000E+01,	1.17278000E+00,	-- 783--
4.20000000E+01,	1.23736000E+00,	4.30000000E+01,	1.30194000E+00,	-- 784--
4.40000000E+01,	1.36652000E+00,	4.50000000E+01,	1.43110000E+00,	-- 785--
4.60000000E+01,	1.50059000E+00,	4.70000000E+01,	1.57008000E+00,	-- 786--
4.80000000E+01,	1.63957000E+00,	4.90000000E+01,	1.70906000E+00,	-- 787--
5.00000000E+01,	1.77855000E+00,			-- 788--
6.00000000E+00,				-- 789--
0.	4.95500000E-02,	1.00000000E+00,	5.29691566E-02,	-- 790--
2.00000000E+00,	5.64894710E-02,	3.00000000E+00,	6.00939834E-02,	-- 791--
4.00000000E+00,	6.37693243E-02,	5.00000000E+00,	6.75048128E-02,	-- 792--
6.00000000E+00,	7.47755056E-02,	7.00000000E+00,	8.20481720E-02,	-- 793--
8.00000000E+00,	8.93225679E-02,	9.00000000E+00,	9.65984878E-02,	-- 794--
1.00000000E+01,	1.03875758E-01,	1.10000000E+01,	1.16507664E-01,	-- 795--
1.20000000E+01,	1.29066269E-01,	1.30000000E+01,	1.41557683E-01,	-- 796--
1.40000000E+01,	1.53987351E-01,	1.50000000E+01,	1.66360150E-01,	-- 797--
1.60000000E+01,	1.85640707E-01,	1.70000000E+01,	2.04793324E-01,	-- 798--
1.80000000E+01,	2.23825344E-01,	1.90000000E+01,	2.42743561E-01,	-- 799--
2.00000000E+01,	2.61554266E-01,	2.10000000E+01,	2.89342649E-01,	-- 800--
2.20000000E+01,	3.17297990E-01,	2.30000000E+01,	3.45039520E-01,	-- 801--
2.40000000E+01,	3.72581234E-01,	2.50000000E+01,	3.99935934E-01,	-- 802--
2.60000000E+01,	4.36150653E-01,	2.70000000E+01,	4.72136528E-01,	-- 803--
2.80000000E+01,	5.07906087E-01,	2.90000000E+01,	5.45600000E-01,	-- 804--
3.00000000E+01,	5.84400000E-01,	3.10000000E+01,	6.32815000E-01,	-- 805--
3.20000000E+01,	6.81230000E-01,	3.30000000E+01,	7.29645000E-01,	-- 806--
3.40000000E+01,	7.78060000E-01,	3.50000000E+01,	8.26475000E-01,	-- 807--
3.60000000E+01,	8.83385000E-01,	3.70000000E+01,	9.40295000E-01,	-- 808--
3.80000000E+01,	9.97205000E-01,	3.90000000E+01,	1.05411500E+00,	-- 809--
4.00000000E+01,	1.11102500E+00,	4.10000000E+01,	1.17535000E+00,	-- 810--
4.20000000E+01,	1.23967500E+00,	4.30000000E+01,	1.30400000E+00,	-- 811--
4.40000000E+01,	1.36832500E+00,	4.50000000E+01,	1.43265000E+00,	-- 812--
4.60000000E+01,	1.50203500E+00,	4.70000000E+01,	1.57142000E+00,	-- 813--
4.80000000E+01,	1.64080500E+00,	4.90000000E+01,	1.71019000E+00,	-- 814--
5.00000000E+01,	1.77957500E+00,			-- 815--
8.00000000E+00,				-- 816--
0.	4.74642857E-02,	1.00000000E+00,	5.0882463E-02,	-- 817--
2.00000000E+00,	5.44096725E-02,	3.00000000E+00,	5.80122235E-02,	-- 818--
4.00000000E+00,	6.16830180E-02,	5.00000000E+00,	6.54117647E-02,	-- 819--
6.00000000E+00,	7.28820838E-02,	7.00000000E+00,	8.03572239E-02,	-- 820--
8.00000000E+00,	8.78365886E-02,	9.00000000E+00,	9.53196760E-02,	-- 821--
1.00000000E+01,	1.02806061E-01,	1.10000000E+01,	1.1555479E-01,	-- 822--
1.20000000E+01,	1.28231739E-01,	1.30000000E+01,	1.40840937E-01,	-- 823--
1.40000000E+01,	1.53388510E-01,	1.50000000E+01,	1.65879323E-01,	-- 824--
1.60000000E+01,	1.85226780E-01,	1.70000000E+01,	2.04447009E-01,	-- 825--
1.80000000E+01,	2.23547314E-01,	1.90000000E+01,	2.42534451E-01,	-- 826--

```

2.00000000E+01, 2.61414676E-01, 2.10000000E+01, 2.89349726E-01, -- 827--
2.20000000E+01, 3.17344993E-01, 2.30000000E+01, 3.45120284E-01, -- 828--
2.40000000E+01, 3.72689491E-01, 2.50000000E+01, 4.00065361E-01, -- 829--
2.60000000E+01, 4.36315319E-01, 2.70000000E+01, 4.72348038E-01, -- 830--
2.80000000E+01, 5.08175933E-01, 2.90000000E+01, 5.46165000E-01, -- 831--
3.00000000E+01, 5.85025000E-01, 3.10000000E+01, 6.33440000E-01, -- 832--
3.20000000E+01, 6.81855000E-01, 3.30000000E+01, 7.30270000E-01, -- 833--
3.40000000E+01, 7.78685000E-01, 3.50000000E+01, 8.27100000E-01, -- 834--
3.60000000E+01, 8.83965000E-01, 3.70000000E+01, 9.40830000E-01, -- 835--
3.80000000E+01, 9.97695000E-01, 3.90000000E+01, 1.05456000E+00, -- 836--
4.00000000E+01, 1.11142500E+00, 4.10000000E+01, 1.17568000E+00, -- 837--
4.20000000E+01, 1.23993500E+00, 4.30000000E+01, 1.30419000E+00, -- 838--
4.40000000E+01, 1.36844500E+00, 4.50000000E+01, 1.43270000E+00, -- 839--
4.60000000E+01, 1.50199500E+00, 4.70000000E+01, 1.57129000E+00, -- 840--
4.80000000E+01, 1.64058500E+00, 4.90000000E+01, 1.70988000E+00, -- 841--
5.00000000E+01, 1.77917500E+00, -- 842--
1.00000000E+01, -- 843--
0, 4.59507143E-02, 1.00000000E+00, 4.95037216E-02, -- 844--
2.00000000E+00, 5.31539295E-02, 3.00000000E+00, 5.68850416E-02, -- 845--
4.00000000E+00, 6.06842117E-02, 5.00000000E+00, 6.45411765E-02, -- 846--
6.00000000E+00, 7.20717058E-02, 7.00000000E+00, 7.96070381E-02, -- 847--
8.00000000E+00, 8.71465792E-02, 9.00000000E+00, 9.46898290E-02, -- 848--
1.00000000E+01, 1.02236364E-01, 1.10000000E+01, 1.15083294E-01, -- 849--
1.20000000E+01, 1.27857208E-01, 1.30000000E+01, 1.40564190E-01, -- 850--
1.40000000E+01, 1.53209668E-01, 1.50000000E+01, 1.65798496E-01, -- 851--
1.60000000E+01, 1.85172401E-01, 1.70000000E+01, 2.04423723E-01, -- 852--
1.80000000E+01, 2.23559745E-01, 1.90000000E+01, 2.42587184E-01, -- 853--
2.00000000E+01, 2.61512245E-01, 2.10000000E+01, 2.89488701E-01, -- 854--
2.20000000E+01, 3.17520457E-01, 2.30000000E+01, 3.45329910E-01, -- 855--
2.40000000E+01, 3.72931099E-01, 2.50000000E+01, 4.00336907E-01, -- 856--
2.60000000E+01, 4.36587057E-01, 2.70000000E+01, 4.72622878E-01, -- 857--
2.80000000E+01, 5.08456617E-01, 2.90000000E+01, 5.46455000E-01, -- 858--
3.00000000E+01, 5.85325000E-01, 3.10000000E+01, 6.33755000E-01, -- 859--
3.20000000E+01, 6.82185000E-01, 3.30000000E+01, 7.30615000E-01, -- 860--
3.40000000E+01, 7.79045000E-01, 3.50000000E+01, 8.27475000E-01, -- 861--
3.60000000E+01, 8.84350000E-01, 3.70000000E+01, 9.41225000E-01, -- 862--
3.80000000E+01, 9.98100000E-01, 3.90000000E+01, 1.05497500E+00, -- 863--
4.00000000E+01, 1.11850000E+00, 4.10000000E+01, 1.17599000E+00, -- 864--
4.20000000E+01, 1.24013000E+00, 4.30000000E+01, 1.30427000E+00, -- 865--
4.40000000E+01, 1.36841000E+00, 4.50000000E+01, 1.43255000E+00, -- 866--
4.60000000E+01, 1.50182000E+00, 4.70000000E+01, 1.57109000E+00, -- 867--
4.80000000E+01, 1.64036000E+00, 4.90000000E+01, 1.70963000E+00, -- 868--
5.00000000E+01, 1.77890000E+00, -- 869--
ENDPHS=1 $ -- 870--
L$GENDAT -- 870--
EVENT=50,CRITR=5HGCLAT,ENDPHS=1,ETAPC(1)=1,NENG=1,NPC(21)=1, -- 871--
ALPPC(1)=180., -- 872--
NPC(2)=1,DT=1, -- 873--
$ -- 874--
L$GENDAT -- 874--
EVENT=55,NPC(2)=4,DT=100,CRITR=6HALTP,VALUE=28.8348843,ETAPC(1)=0,ENDPHS=1 $ -- 875--
L$GENDAT -- 875--
EVENT=100,CRITR=6HALTITO,VALUE=400000,ENDPHS=1,PRNC=1,NPC(12)=1, -- 876--
PINC=100, -- 877--
IGUID=0,1,0,IGUID(6)=1,0,1,NPC(15)=1,DT=1,NPC(2)=1,NPC(5)=4, -- 878--
ALPPC(1)=37.0010556,BNKPC(1)=-69.2957708, -- 879--
NPC(8)=-2,NPC(5)=4,DTIMR=1,BETA=0., -- 880--
$ -- 881--
L$GENDAT -- 881--
EVENT=105,CRITR=6HHEATRT,PINC=20,VALUE=115,IGUID(6)=1,0,4, -- 882--
NPC(9)=1,NPC(22)=1,PRNC=1, -- 883--
NDEPVS=1,DEPVS=5HVELAD,DEPTLS=.00001,INDVRS=6HETAPC1, -- 884--
US=.1,MAXITS=10, -- 885--
DGF(3)=6HHEATRT,IDGF(3)=1,KDG(3)=30,KRG(3)=2000, -- 886--
$ -- 887--
L$BLMLT $ -- 887--
L$TAB TABLE=5HGDF3T,1,5HTDURP,5,1,1,1, -- 888--
0,115,15,120,30,124,60,125,1000,125 $ -- 888--
L$TAB TABLE=6HGNMN3T,0,-180$ -- 888--
L$TAB TABLE=6HGNMX3T,0,0$ -- 888--

```

```
L$TAB TABLE=6HGNDM3T,0,-70.000000,ENDPHS=1 $ -- 888--
L$GENDAT -- 888--
  EVENT=180,CRITR=6HINC ,ENDPHS=1,NDEPVS=0, -- 889--
  IGUID(6)=3,0,3,DBANK=0,DALPHA=12 $ -- 890--
L$GENDAT -- 890--
  EVENT=190,CRITR=5HTDURP,PINC=1000,VALUE=10,ETAPC(1)=1,ENDPHS=1 $ -- 891--
L$GENDAT -- 891--
  EVENT=200,CRITR=6HALTA ,ENDPHS=1,DT=10,IGUID(6)=1,0,1, -- 892--
  ETAPC(1)=0, -- 893--
  PRNC=10, -- 894--
  $ -- 895--
L$GENDAT -- 895--
  EVENT=210,CRITR=6HALTITO,VALUE=400000,NPC(2)=4,DT=100,NPC(5)=0,NPC(8)=0, -- 896--
  ENDPHS=1 $ -- 897--
L$GENDAT -- 897--
  EVENT=220,CRITR=6HGAMMAI,VALUE=0,NPC(2)=1,DT=1,ETAPC(1)=1, -- 898--
  IGUID=3,0,1,ALPPC(1)=0,BETPC(1)=0,BNKPC(1)=0,ENDPHS=1 $ -- 899--
L$GENDAT -- 899--
  EVENT=1000,CRITR=6HVELI ,VALUE=25354.1388,ENDPHS=1,ENDPRB=1,ENDJOB=1 $ -- 900--
```

A.3.1 INPUT FILE DESCRIPTION

A.3.1.1 INPUT CONDITIONS

The following is a list of the input conditions for the nominal plane change trajectory.

Initial inclination = 28.5 degrees

Initial Orbit altitude = 160 nautical mile circular orbit

True anomaly (Truan) = 150 degrees

Vehicle Model:

Reference Surface Area (SREF) = 177.4 square feet

Reference length (LREF) = 25 feet

Initial weight (WGTSG) = 11,430 pounds

Engine ISP (ISPV) = 295.0 seconds

Coefficients of lift (CL) and drag (CD) as a function of angle-of-attack and a correlation parameter of either altitude (ALTI-TO), viscous interaction (VINV), or mach number (MACH).

Spherical, rotating earth model.

1976 standard atmospheric model

A.3.1.2 TRAJECTORY PHASES

The trajectory has 11 different phases called events and are numbered: 1,50,55,100,105,180,190,200,210,220, and 1000. Each phase represents a change in either the vehicle and/or the environmental conditions. The following is a list of the events and their purpose. Most of these phases are shown on Figure A-4.

<u>Event Number</u>	<u>Purpose</u>
1	Sets initial conditions
50	Starts deorbit burn at best point
55	Stops deorbit burn at best point
100	Turns on atmosphere at 400,000 feet
105	Starts level-off based on heat-rate
180	Starts exit based on best inclination

190	Completes the exit set-up by going 100% throttle
200	Cuts-off engines based on desired apogee altitude
210	Turns off atmosphere at 400,00 feet
220	Starts circularization burn
1000	Stops circularization burn when a 160 nautical mile circular orbit is obtained.

A.3.1.3 INDEPENDENT VARIABLES

POST has been given a number of parameters which it can vary to optimize the problem. There are 12 variables that are what we call exterior parameters and two interior parameters. These variables are listed below with the associated phase/event numbers and a brief description.

Exterior Independent Variables <u>Names</u>	Event <u>Number</u>	<u>Description</u>
GCLAT	50	Geocentric latitude for deorbit burn
ALTP	55	Perigee altitude to stop burn
ALPPC1	100	Entry angle-of-attack
BANKPC1	100	Entry bank angle
ALPPC1	105	Level-off angle-of-attack
DEPVLSI	105	Cruise acceleration
INC	180	Exit inclination
DBANK	180	Exit bank angle
DALPHA	180	Exit angle-of-attack
ALTA	200	Apogee altitude for engine cut-off
ALPPC1	200	Angle-of-attack after engine cut-off
BANKPC1	200	Bank angle after engine cut-off

Interior Independent Variables <u>Names</u>	Event <u>Number</u>	<u>Description</u>
ETAPC1	105	Throttle % to maintain cruise acceleration
BANK	105	Bank angle to maintain heating rate

A.3.2 OUTPUT DESCRIPTION

As might be expected, POST has the capacity to generate a large amount of output data and plot information. Included below are samples of the output data and generated plots from our sample trajectory.

A.3.2.1 OUTPUT DATA

Figures A-1 thru 3 present a sample from the output data file for the nominal 20 degree plane change. Figure A-1 presents the 270 parameters offered as nominal output. Specifically, the parameters are for the start of phase 105 (cruise phase). Figure A-2 presents the same parameter for the end of the trajectory (last frame of phase 220 and first and only frame of phase 1000). Figure A-3 provides a summary of the trajectory to include the independent variable values (u), the end condition errors (e), the optimization parameter value (P1) and a targeting parameter (P2).

A.3.2.2 TRAJECTORY PLOTS

Shown in Figures A-4 thru 12 are the baseline trajectory plots generated by POST for a heat-rate of 80 and 125 BTU/ft²-sec. The plots for QDOT = 125 were generated with the trajectory generation input deck shown in Section A.3. The Figures present a time history of altitude above the planet, relative atmospheric vehicle velocity, angle-of-attack, bank angle, Engine throttle percentage, heat-rate, heat load, and

```

TIME 3.15651252E+03 TIMES 0.0000000E+00 TDURP 0.0000000E+00 DENS 2.48395801E-07 PRES 1.75212314E-01 ATEM 4.10919271E+02
ALTI TO 2.19239772E+05 GCRAD 2.11429808E+07 GDLAT 2.91114254E+00 GCLAT 2.91114254E+00 LONGI 1.24636213E+00
VELI 2.38132756E+04 GAMMAI -5.20940850E-01 AZVELI 5.58096784E+01 XI 2.11126969E+07 VVI -1.32404687E+03 AXI -2.72027918E+01
VELR 2.25561480E+04 GAMMAR -5.49975448E-01 AZVELR 5.36109237E+01 YI 4.59339544E+05 VVI 1.96727987E+04 AYI -8.25469947E+00
VELA 2.25561480E+04 GAMMAA -5.49975448E-01 AZVELA 5.36109237E+01 ZI 1.07389361E+06 VZI 1.33529018E+04 AZI 8.59503417E+00
GAMAD -2.23431086E-04 AZVAD -2.89567229E-02 DWNRRG 3.76344707E+03 CRRNG -1.92910126E+02 DPRNG1 3.76624497E+03 DPRNG2 3.76624497E+03
THRUST 2.42694464E+03 WEIGHT 1.11452486E+04 WDOT 8.22942554E+00 WEICON 2.84751380E+02 WPROP -2.84751380E+02 ASMG 4.16007477E-01
ETA 7.35660768E-01 ETAL 7.35660768E-01 IPNULL 0.0000000E+00 IYNUL 0.0000000E+00 INCPCH 0.0000000E+00 INCYAW 0.0000000E+00
FTXB 2.42694464E+03 FAXB -5.60164069E+02 AXB 5.38900479E+00 ALPHA 2.50000000E+01 ALPDDT 0.0000000E+00 ALPTOT 2.50000000E+01
FTYB 0.0000000E+00 FAYB 0.0000000E+00 AYB 0.0000000E+00 BETA -1.01073179E-15 BETDDT 0.0000000E+00 QALPHA 1.57973461E+03
FTZB 0.0000000E+00 FAZB -4.24409298E+03 AZB -1.22518081E+01 BNKANG -7.00000109E+01 BNKDOT 0.0000000E+00 QALTOT 1.57973461E+03
CA 4.99709388E-02 CD 2.05294734E-01 DRAG 2.30131225E+03 ROLI -1.76495396E+02 YAWR 2.99798031E+01 ROLBD 3.22430843E-02
CN 3.78605700E-01 CL 3.22014663E-01 LIFT 3.60971895E+03 YAWI 5.05287674E+01 PITR 7.80706947E+00 PITBD 7.65339218E-03
CY 0.0000000E+00 HEATRT 1.1500000E+02 TLHEAT 5.53099485E+04 PITI 5.61503158E+01 ROLR -7.15210934E+01 YAWBD -6.40075654E-02
DYNP 6.31893846E+01 MACH 2.26982809E+01 REYND 4.51671331E+05 ASXI 4.23251599E+00 ASYI -7.57077548E+00 ASZI 1.01939856E+01
XMAX1 1.15000000E+02 XMIN2 2.19239772E+05 XMAX3 6.31893846E+01 XMIN4 0.0000000E+00 XMAX4 1.0000000E+00 BETAI 7.78729433E-01
XIMRF1 9.68991962E+02 VIDEAL 2.39449204E+02 VINV 2.26687557E-02 INC 3.42990093E+01

*** PHASE 105.000 ***
TIME 3.15651252E+03 TIMES 0.0000000E+00 TDURP 0.0000000E+00 DENS 2.48395801E-07 PRES 1.75212314E-01 ATEM 4.10919271E+02
ALTI TO 2.19239772E+05 GCRAD 2.11429808E+07 GDLAT 2.91114254E+00 GCLAT 2.91114254E+00 LONGI 1.24636213E+00
VELI 2.38132756E+04 GAMMAI -5.20940850E-01 AZVELI 5.58096784E+01 XI 2.11126969E+07 VVI -1.32404687E+03 AXI -2.72027918E+01
VELR 2.25561480E+04 GAMMAR -5.49975448E-01 AZVELR 5.36109237E+01 YI 4.59339544E+05 VVI 1.96727987E+04 AYI -8.25469947E+00
VELA 2.25561480E+04 GAMMAA -5.49975448E-01 AZVELA 5.36109237E+01 ZI 1.07389361E+06 VZI 1.33529018E+04 AZI 8.59503417E+00
GAMAD -2.23431086E-04 AZVAD -2.89567229E-02 DWNRRG 3.76344707E+03 CRRNG -1.92910126E+02 DPRNG1 3.76624497E+03 DPRNG2 3.76624497E+03
THRUST 2.42694464E+03 WEIGHT 1.11452486E+04 WDOT 8.22942554E+00 WEICON 2.84751380E+02 WPROP -2.84751380E+02 ASMG 4.16007477E-01
ETA 7.35660768E-01 ETAL 7.35660768E-01 IPNULL 0.0000000E+00 IYNUL 0.0000000E+00 INCPCH 0.0000000E+00 INCYAW 0.0000000E+00
FTXB 2.42694464E+03 FAXB -5.60164069E+02 AXB 5.38900479E+00 ALPHA 2.50000000E+01 ALPDDT 0.0000000E+00 ALPTOT 2.50000000E+01
FTYB 0.0000000E+00 FAYB 0.0000000E+00 AYB 0.0000000E+00 BETA -1.01073179E-15 BETDDT 0.0000000E+00 QALPHA 1.57973461E+03
FTZB 0.0000000E+00 FAZB -4.24409298E+03 AZB -1.22518081E+01 BNKANG -7.00000109E+01 BNKDOT 0.0000000E+00 QALTOT 1.57973461E+03
CA 4.99709388E-02 CD 2.05294734E-01 DRAG 2.30131225E+03 ROLI -1.76495396E+02 YAWR 2.99798031E+01 ROLBD 3.22430843E-02
CN 3.78605700E-01 CL 3.22014663E-01 LIFT 3.60971895E+03 YAWI 5.05287674E+01 PITR 7.80706947E+00 PITBD 7.65339218E-03
CY 0.0000000E+00 HEATRT 1.1500000E+02 TLHEAT 5.53099485E+04 PITI 5.61503158E+01 ROLR -7.15210934E+01 YAWBD -6.40075654E-02
DYNP 6.31893846E+01 MACH 2.26982809E+01 REYND 4.51671331E+05 ASXI 4.23251599E+00 ASYI -7.57077548E+00 ASZI 1.01939856E+01
XMAX1 1.15000000E+02 XMIN2 2.19239772E+05 XMAX3 6.31893846E+01 XMIN4 0.0000000E+00 XMAX4 1.0000000E+00 BETAI 7.78729433E-01
XIMRF1 9.68991962E+02 VIDEAL 2.39449204E+02 VINV 2.26687557E-02 INC 3.42990093E+01

*** ELLIPTIC ORBIT ***
TIME 3.15651252E+03 TIMES 0.0000000E+00 TDURP 0.0000000E+00 DENS 2.48395801E-07 PRES 1.75212314E-01 ATEM 4.10919271E+02
ALTI TO 2.19239772E+05 GCRAD 2.11429808E+07 GDLAT 2.91114254E+00 GCLAT 2.91114254E+00 LONGI 1.24636213E+00
VELI 2.38132756E+04 GAMMAI -5.20940850E-01 AZVELI 5.58096784E+01 XI 2.11126969E+07 VVI -1.32404687E+03 AXI -2.72027918E+01
VELR 2.25561480E+04 GAMMAR -5.49975448E-01 AZVELR 5.36109237E+01 YI 4.59339544E+05 VVI 1.96727987E+04 AYI -8.25469947E+00
VELA 2.25561480E+04 GAMMAA -5.49975448E-01 AZVELA 5.36109237E+01 ZI 1.07389361E+06 VZI 1.33529018E+04 AZI 8.59503417E+00
GAMAD -2.23431086E-04 AZVAD -2.89567229E-02 DWNRRG 3.76344707E+03 CRRNG -1.92910126E+02 DPRNG1 3.76624497E+03 DPRNG2 3.76624497E+03
THRUST 2.42694464E+03 WEIGHT 1.11452486E+04 WDOT 8.22942554E+00 WEICON 2.84751380E+02 WPROP -2.84751380E+02 ASMG 4.16007477E-01
ETA 7.35660768E-01 ETAL 7.35660768E-01 IPNULL 0.0000000E+00 IYNUL 0.0000000E+00 INCPCH 0.0000000E+00 INCYAW 0.0000000E+00
FTXB 2.42694464E+03 FAXB -5.60164069E+02 AXB 5.38900479E+00 ALPHA 2.50000000E+01 ALPDDT 0.0000000E+00 ALPTOT 2.50000000E+01
FTYB 0.0000000E+00 FAYB 0.0000000E+00 AYB 0.0000000E+00 BETA -1.01073179E-15 BETDDT 0.0000000E+00 QALPHA 1.57973461E+03
FTZB 0.0000000E+00 FAZB -4.24409298E+03 AZB -1.22518081E+01 BNKANG -7.00000109E+01 BNKDOT 0.0000000E+00 QALTOT 1.57973461E+03
CA 4.99709388E-02 CD 2.05294734E-01 DRAG 2.30131225E+03 ROLI -1.76495396E+02 YAWR 2.99798031E+01 ROLBD 3.22430843E-02
CN 3.78605700E-01 CL 3.22014663E-01 LIFT 3.60971895E+03 YAWI 5.05287674E+01 PITR 7.80706947E+00 PITBD 7.65339218E-03
CY 0.0000000E+00 HEATRT 1.1500000E+02 TLHEAT 5.53099485E+04 PITI 5.61503158E+01 ROLR -7.15210934E+01 YAWBD -6.40075654E-02
DYNP 6.31893846E+01 MACH 2.26982809E+01 REYND 4.51671331E+05 ASXI 4.23251599E+00 ASYI -7.57077548E+00 ASZI 1.01939856E+01
XMAX1 1.15000000E+02 XMIN2 2.19239772E+05 XMAX3 6.31893846E+01 XMIN4 0.0000000E+00 XMAX4 1.0000000E+00 BETAI 7.78729433E-01
XIMRF1 9.68991962E+02 VIDEAL 2.39449204E+02 VINV 2.26687557E-02 INC 3.42990093E+01

*** VELOCITY LOSSES ***
TIME 3.15651252E+03 TIMES 0.0000000E+00 TDURP 0.0000000E+00 DENS 2.48395801E-07 PRES 1.75212314E-01 ATEM 4.10919271E+02
ALTI TO 2.19239772E+05 GCRAD 2.11429808E+07 GDLAT 2.91114254E+00 GCLAT 2.91114254E+00 LONGI 1.24636213E+00
VELI 2.38132756E+04 GAMMAI -5.20940850E-01 AZVELI 5.58096784E+01 XI 2.11126969E+07 VVI -1.32404687E+03 AXI -2.72027918E+01
VELR 2.25561480E+04 GAMMAR -5.49975448E-01 AZVELR 5.36109237E+01 YI 4.59339544E+05 VVI 1.96727987E+04 AYI -8.25469947E+00
VELA 2.25561480E+04 GAMMAA -5.49975448E-01 AZVELA 5.36109237E+01 ZI 1.07389361E+06 VZI 1.33529018E+04 AZI 8.59503417E+00
GAMAD -2.23431086E-04 AZVAD -2.89567229E-02 DWNRRG 3.76344707E+03 CRRNG -1.92910126E+02 DPRNG1 3.76624497E+03 DPRNG2 3.76624497E+03
THRUST 2.42694464E+03 WEIGHT 1.11452486E+04 WDOT 8.22942554E+00 WEICON 2.84751380E+02 WPROP -2.84751380E+02 ASMG 4.16007477E-01
ETA 7.35660768E-01 ETAL 7.35660768E-01 IPNULL 0.0000000E+00 IYNUL 0.0000000E+00 INCPCH 0.0000000E+00 INCYAW 0.0000000E+00
FTXB 2.42694464E+03 FAXB -5.60164069E+02 AXB 5.38900479E+00 ALPHA 2.50000000E+01 ALPDDT 0.0000000E+00 ALPTOT 2.50000000E+01
FTYB 0.0000000E+00 FAYB 0.0000000E+00 AYB 0.0000000E+00 BETA -1.01073179E-15 BETDDT 0.0000000E+00 QALPHA 1.57973461E+03
FTZB 0.0000000E+00 FAZB -4.24409298E+03 AZB -1.22518081E+01 BNKANG -7.00000109E+01 BNKDOT 0.0000000E+00 QALTOT 1.57973461E+03
CA 4.99709388E-02 CD 2.05294734E-01 DRAG 2.30131225E+03 ROLI -1.76495396E+02 YAWR 2.99798031E+01 ROLBD 3.22430843E-02
CN 3.78605700E-01 CL 3.22014663E-01 LIFT 3.60971895E+03 YAWI 5.05287674E+01 PITR 7.80706947E+00 PITBD 7.65339218E-03
CY 0.0000000E+00 HEATRT 1.1500000E+02 TLHEAT 5.53099485E+04 PITI 5.61503158E+01 ROLR -7.15210934E+01 YAWBD -6.40075654E-02
DYNP 6.31893846E+01 MACH 2.26982809E+01 REYND 4.51671331E+05 ASXI 4.23251599E+00 ASYI -7.57077548E+00 ASZI 1.01939856E+01
XMAX1 1.15000000E+02 XMIN2 2.19239772E+05 XMAX3 6.31893846E+01 XMIN4 0.0000000E+00 XMAX4 1.0000000E+00 BETAI 7.78729433E-01
XIMRF1 9.68991962E+02 VIDEAL 2.39449204E+02 VINV 2.26687557E-02 INC 3.42990093E+01

PERIOD 6.97555403E+01 ARGP 1.82180432E+02
ANGMOM 5.03510441E+11 PGERAD 1.56822865E+07
TIMTP 3.41050826E+01 TIMSP 3.56504577E+01
DVCIR 2.00091793E+03 VCIRC 2.58014609E+04
VIDEAL 2.39449204E+02 DLI 2.19919267E+03

```

Figure A-1. Sample of POST output data for cruise phase.

```

TIME 5 35886173E+03 TIMES 1.81259768E+01 TDURP 1.81259768E+01 DENS 220.000 ***
ALTTD 1.00139091E+06 GCRAD 2.19271319E+07 GDLAT 2.25497481E+01 GCLAT 2.25497481E+01 LONG 0.00000000E+00 ATEM 0.00000000E+00
VELI 2.53541388E+04 GAMMAI -1.32816417E-02 AZVELI 1.31918351E+02 XI -1.89675864E+07 VXI -1.26877243E+04 AXI 1.26877243E+04 AXI 1.59494233E+02
VELR 2.42753802E+04 GAMMAR -1.38718564E-02 AZVELR 1.34247476E+02 YI 7.09386596E+06 VYI -1.53970256E+04 AYI -2.00857262E+01
VELA 2.42753802E+04 GAMMAA -1.38718564E-02 AZVELA 1.34247476E+02 ZI 8.40873634E+06 VZI -1.56456259E+04 AZI -2.20127297E+01
GAMAD 9.33649011E-05 AZVAD 2.04638864E-02 DWNRRG 1.22650400E+04 CRRNG -3.36747426E+02 DPRNG1 9.33740531E+03 DPRNG2 1.23014705E+04
THRUST 3.30000000E+03 WEIGHT 6.07479559E+03 WDOT 1.11864407E+01 WEICON 5.35520441E+03 WPROP -5.35520441E+03 ASMG 5.43228155E-01
ETA 1.00000000E+00 ETAL 1.00000000E+00 IPNULL 0.00000000E+00 IYNUL 0.00000000E+00 INCPCH 0.00000000E+00 INCYAW 0.00000000E+00
FTXB 3.30000000E+03 FAXB 0.00000000E+00 AXB 1.74778227E+01 ALPHA 6.01684138E-04 ALPDDT 0.00000000E+00 ALPTOT 2.32912487E+00
FTYB 0.00000000E+00 FAYB 0.00000000E+00 AYB 0.00000000E+00 BETA 2.32912487E+00 BETDDT 0.00000000E+00 QALPHA 0.00000000E+00
FTZB 0.00000000E+00 FAZB 0.00000000E+00 AZB 0.00000000E+00 BNKANG -5.64214245E-04 BNKDDT 0.00000000E+00 QALPHA 0.00000000E+00
CA 0.00000000E+00 CD 0.00000000E+00 DRAG 0.00000000E+00 ROLI -1.30020739E+02 YAWR 1.31918351E+02 ROLBD 0.00000000E+00
CN 0.00000000E+00 CL 0.00000000E+00 LIFT 0.00000000E+00 YAWI -1.05861702E+01 PITR -1.32816417E-02 PITBD 0.00000000E+00
CY 0.00000000E+00 HEATRI 1.80637950E+00 TLHEAT 1.06542009E+05 PIII -8.88744015E+01 ROLR 0.00000000E+00 YAWBD 0.00000000E+00
DYNP 0.00000000E+00 MACH 0.00000000E+00 REYND 0.00000000E+00 ASXI -8.74625626E+00 ASVI -1.06139074E+01 ASZI -1.07852796E+01
XMAX1 1.26289990E+02 XMIN2 2.14636897E+05 XMAX3 7.62016080E+01 XMIN4 0.00000000E+00 XMAX4 1.00000000E+00 BETAI 0.00000000E+00
TIMRF1 3 17134117E+03 VIDEAL 5 99940456E+03 VINV 2.68834538E+00 INC 4.65904147E+01

```

```

*** PHASE 220.000 ***
1.81259768E+01 DENS 0.00000000E+00 PRES 0.00000000E+00 ATEM 0.00000000E+00
2.25497481E+01 GCLAT 2.25497481E+01 LONG 0.00000000E+00 PRES 0.00000000E+00 ATEM 0.00000000E+00
1.31918351E+02 XI -1.89675864E+07 VXI -1.26877243E+04 AXI 1.26877243E+04 AXI 1.59494233E+02
1.34247476E+02 YI 7.09386596E+06 VYI -1.53970256E+04 AYI -2.00857262E+01
1.34247476E+02 ZI 8.40873634E+06 VZI -1.56456259E+04 AZI -2.20127297E+01
1.22650400E+04 CRRNG -3.36747426E+02 DPRNG1 9.33740531E+03 DPRNG2 1.23014705E+04
5.35520441E+03 WPROP -5.35520441E+03 ASMG 5.43228155E-01
0.00000000E+00 IYNUL 0.00000000E+00 INCPCH 0.00000000E+00 INCYAW 0.00000000E+00
1.74778227E+01 ALPHA 6.01684138E-04 ALPDDT 0.00000000E+00 ALPTOT 2.32912487E+00
0.00000000E+00 BETA 2.32912487E+00 BETDDT 0.00000000E+00 QALPHA 0.00000000E+00
0.00000000E+00 BNKANG -5.64214245E-04 BNKDDT 0.00000000E+00 QALPHA 0.00000000E+00
0.00000000E+00 ROLI -1.30020739E+02 YAWR 1.31918351E+02 ROLBD 0.00000000E+00
0.00000000E+00 YAWI -1.05861702E+01 PITR -1.32816417E-02 PITBD 0.00000000E+00
1.06542009E+05 PIII -8.88744015E+01 ROLR 0.00000000E+00 YAWBD 0.00000000E+00
0.00000000E+00 ASXI -8.74625626E+00 ASVI -1.06139074E+01 ASZI -1.07852796E+01
7.62016080E+01 XMIN4 0.00000000E+00 XMAX4 1.00000000E+00 BETAI 0.00000000E+00
2.68834538E+00 INC 4.65904147E+01

```

```

*** ELLIPTIC ORBIT ***
1 74598915E+02 ECCEN 1 36468159E-03 INC 4.65904147E+01 PERIOD 9 08092521E+01 ARGP 1.57930609E+02
3.50206887E+02 LAN 2.62283294E+00 ANGMOM 5.55943531E+11 PGERAD 2.19266965E+07
1.58400130E+01 PGLON 1.67053981E+02 ARGV 1.48137496E+02 TIMTP 2.46358953E+00 TIMSP 8.83456626E+01
3.50233460E+02 PGVEL 2.53546416E+04 APVEL 2.52855339E+04 DVCIR 1.80164945E+01 VCIRC 2.53371072E+04
3.49598502E+02 APLON 3 35428917E+02

```

```

*** VELOCITY LOSSES ***
1.48044466E+00 GLR 2.56900505E+01 VIDEAL 5.99940456E+03 DLI 5.02093197E+03
3.56809423E+01
END OF PHASE 220 000
ESN = 1000.000 FESN= 1000.000
TIME = 5.35886173E+03
NORMAL TERMINATION

```

Figure A-2. Sample of POST output data for circularization phase.

ERV CRUISING SYNERGISTIC PLANE CHANGE 0-DOT=125

PROBLEM NO. 1

*** NOMINAL FUNCTION EVALUATION

INDVR	CRITR	CRITR	ALPPC1	ALPPC1	DPVLS1
	CRITR	DBANK	DALPHA	ALPPC1	BNKPC1
INDPH	50.000	55.000	100.000	105.000	105.000
	180.000	180.000	180.000	200.000	200.000
U(I)	-9 00000000E-01	2.70000000E+01	2.70000000E+01	2.50000000E+01	4.00000000E-03
	4 00000000E+01	-6.60000000E+01	2.00000000E+01	8.00000000E+00	-5.00000000E+01

U=-9.00000000E-01, 2.70000000E+01, 2.70000000E+01, -6.40000000E+01,
 2.50000000E+01, 4.00000000E-03, 4.00000000E+01, -6.60000000E+01,
 2.00000000E+01, 1.70000000E+02, 8.00000000E+00, -5.00000000E+01,

WE(I) -1.90958535E+01 2.91978298E+00 0.00000000E+00
 DEPVR INC ALTA XMAX4
 DEPPH 1000.000 1000.000 1000.000
 E(I.) -1.90958535E+00 1 45989149E+01 0.00000000E+00
 P1 -6.07479559E+03

OPTVAR WEIGHT
 OPTPH 1000.000
 OPTVL 6 07479559E+03
 P2 3 73176753E+02

Figure A-3. Sample of POST trajectory summary.

inclination for the nominal conditions. The time reference for the plots ($t=0$) is atmospheric interface at 400,000 feet. The phase/event divisions and numbers are shown on the altitude time history.

ORIGINAL PAGE IS
OF POOR QUALITY

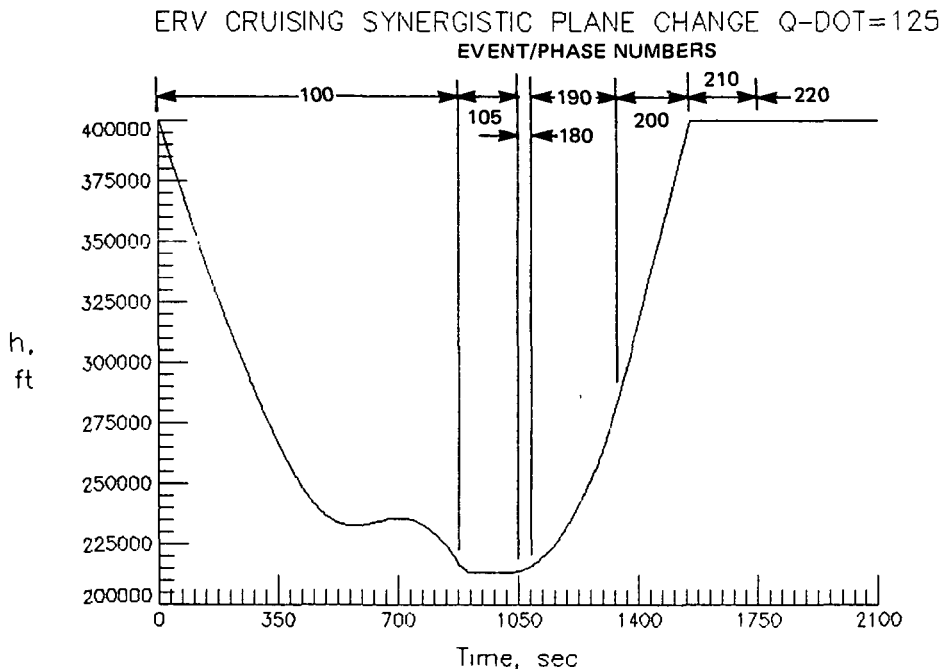
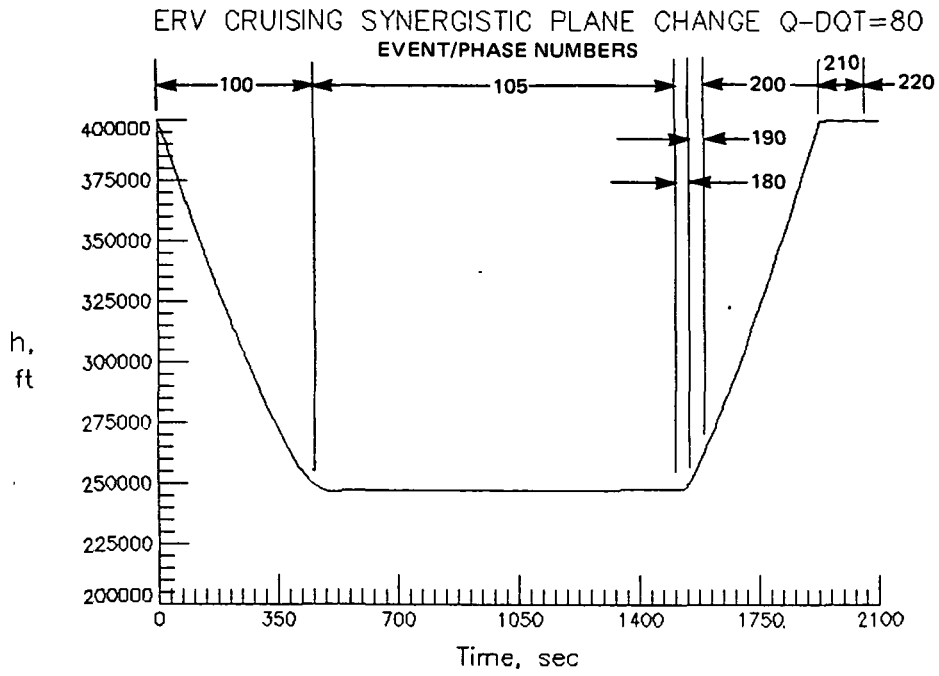
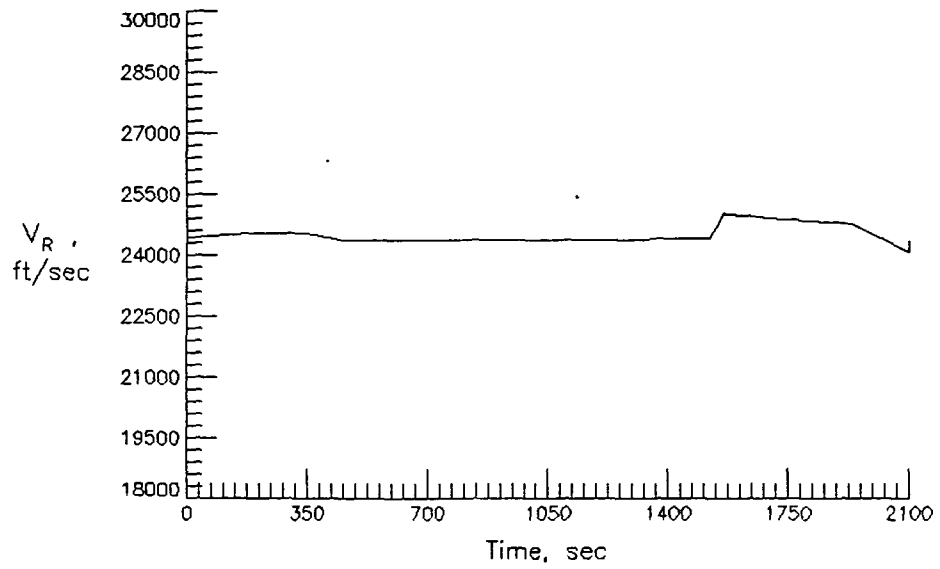


Figure A-4. Baseline altitude profiles.

ERV CRUISING SYNERGISTIC PLANE CHANGE $\dot{Q}=80$



ERV CRUISING SYNERGISTIC PLANE CHANGE $\dot{Q}=125$

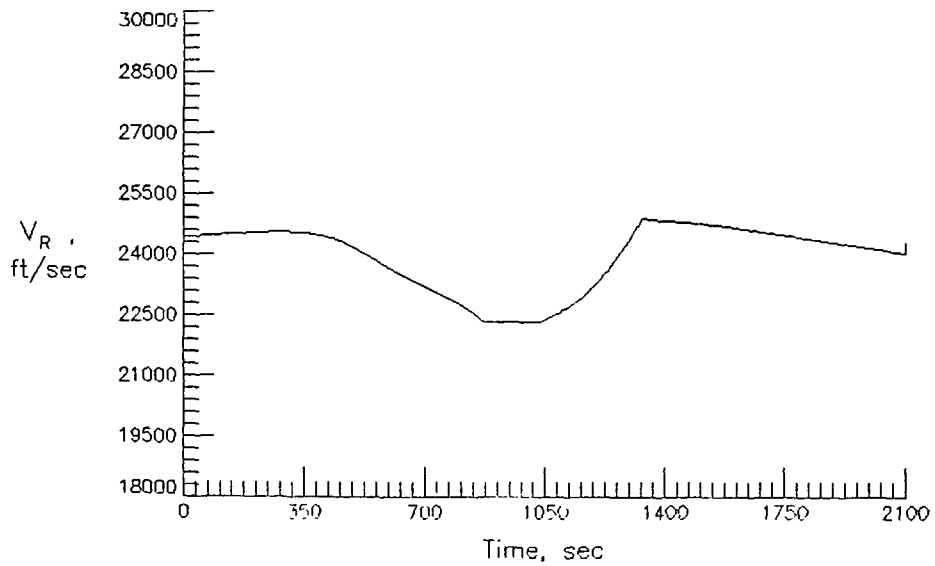
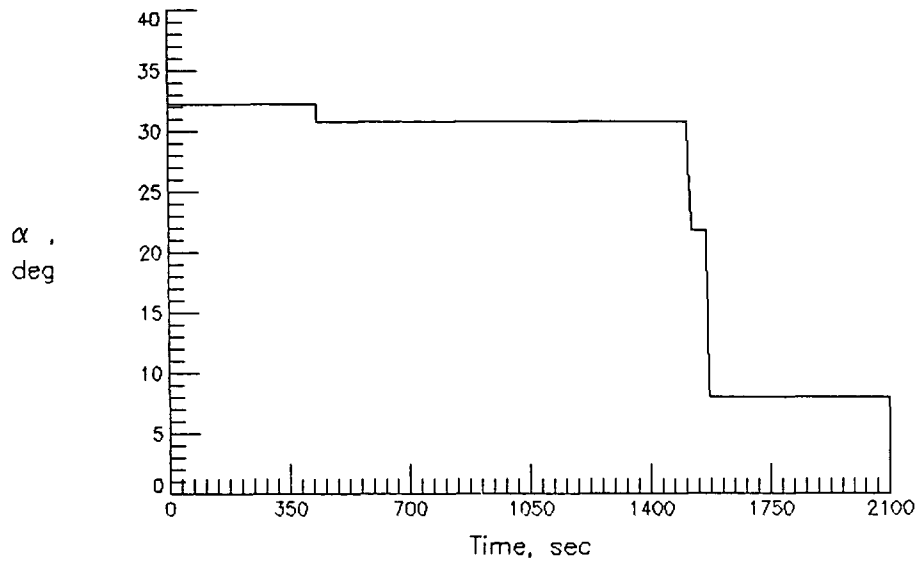


Figure A-5. Baseline vehicle velocity relative to the atmosphere profiles.

ERV CRUISING SYNERGISTIC PLANE CHANGE Q-DOT=80



ERV CRUISING SYNERGISTIC PLANE CHANGE Q-DOT=125

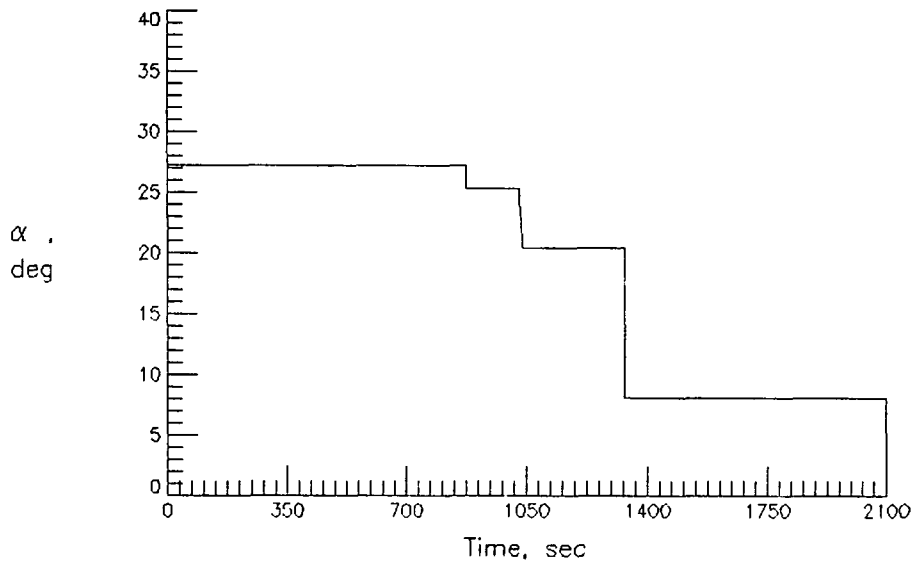
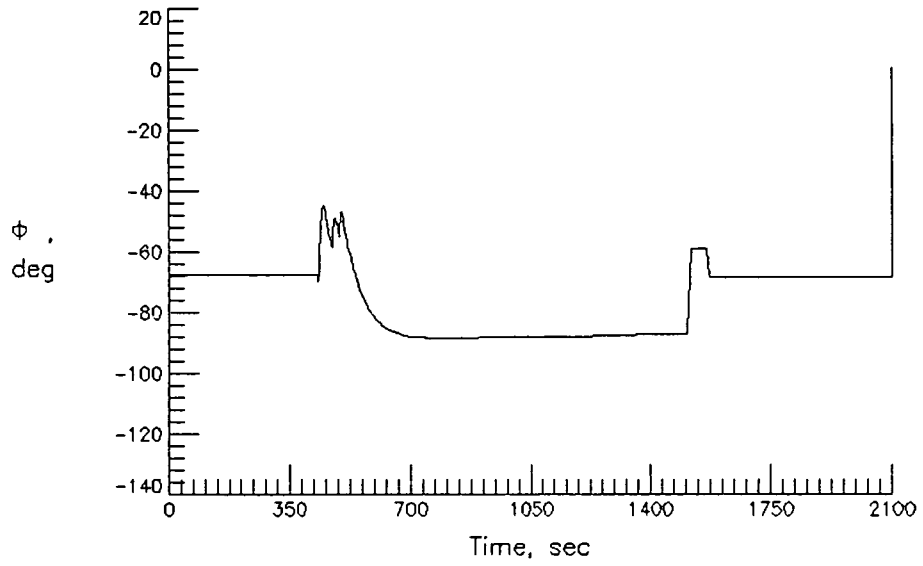


Figure A-6. Baseline angle-of-attack profiles.

ERV CRUISING SYNERGISTIC PLANE CHANGE Q-DOT=80



ERV CRUISING SYNERGISTIC PLANE CHANGE Q-DOT=125

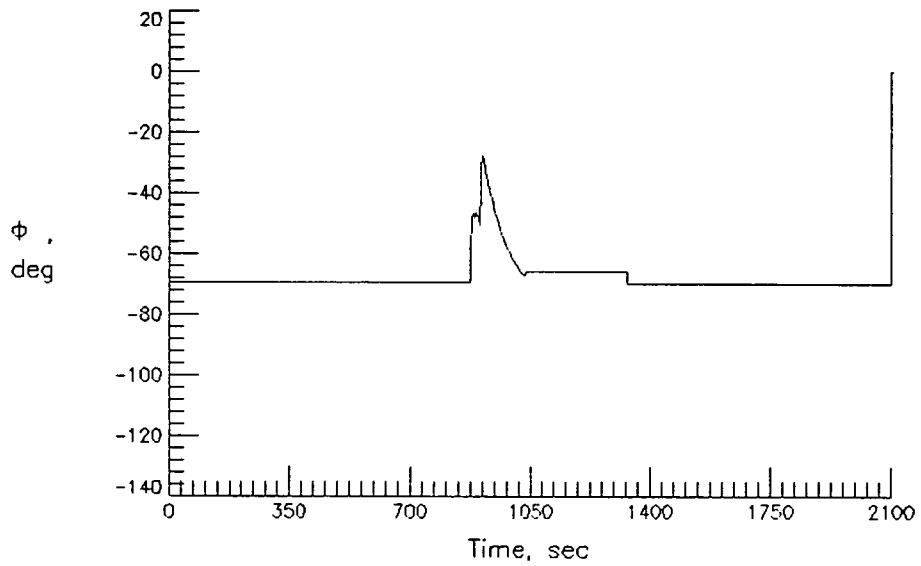
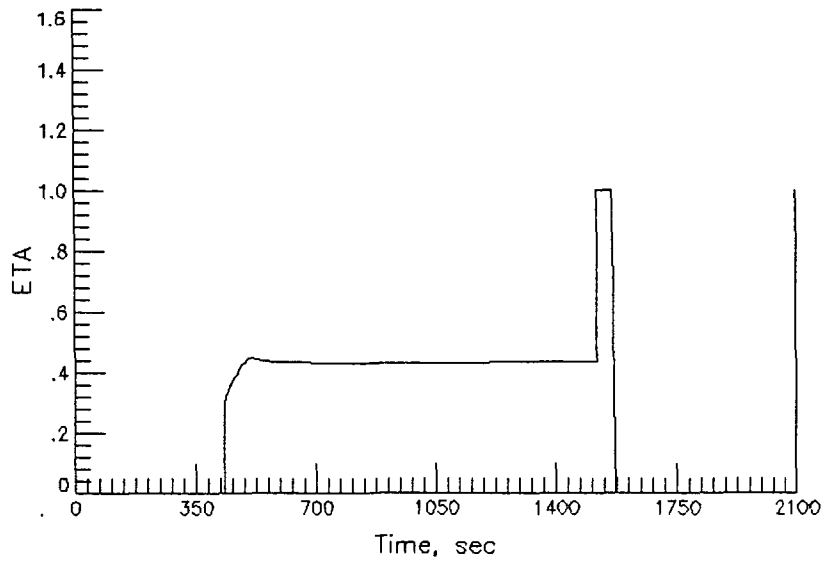


Figure A-7. Baseline bank angle profiles.

ERV CRUISING SYNERGISTIC PLANE CHANGE $\dot{Q}=80$



ERV CRUISING SYNERGISTIC PLANE CHANGE $\dot{Q}=125$

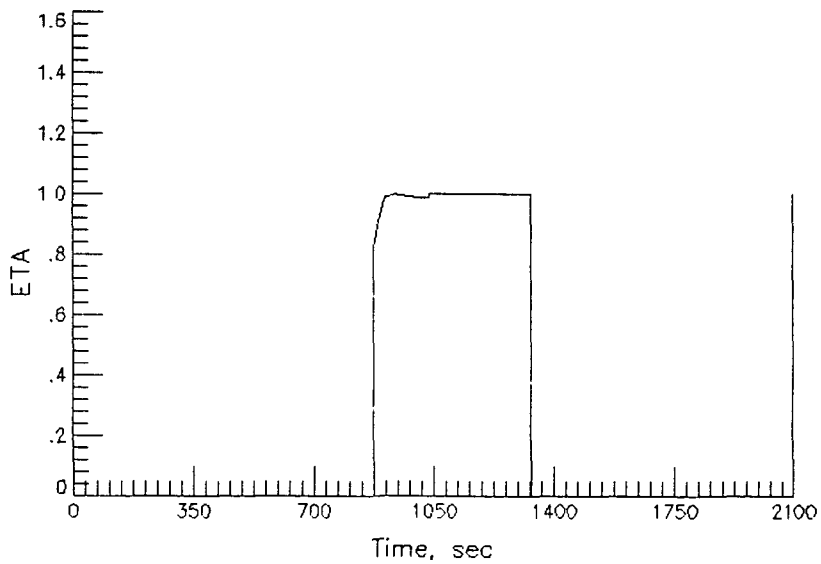
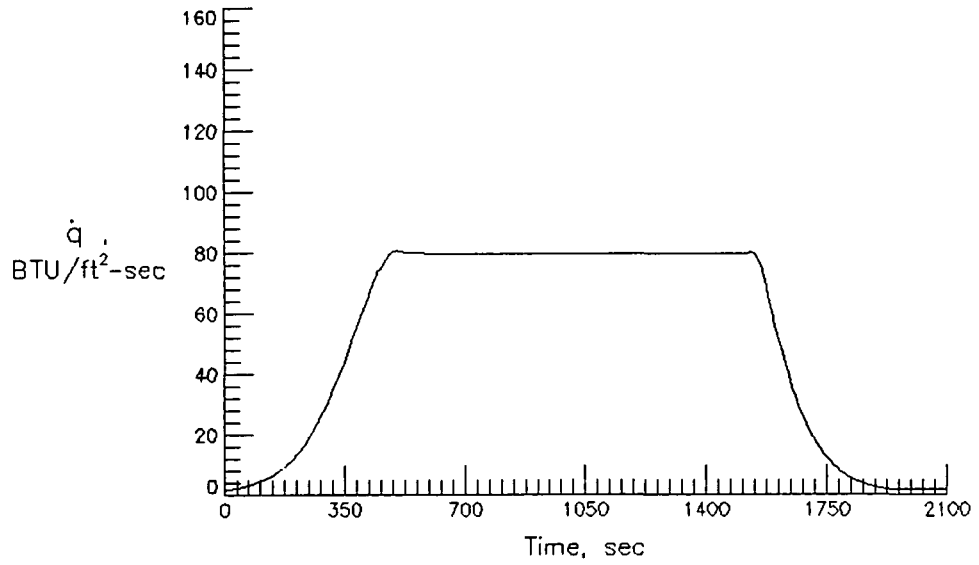


Figure A-8. Baseline engine throttling profiles (1.0 = maximum).

ERV CRUISING SYNERGISTIC PLANE CHANGE Q-DOT=80



ERV CRUISING SYNERGISTIC PLANE CHANGE Q-DOT=125

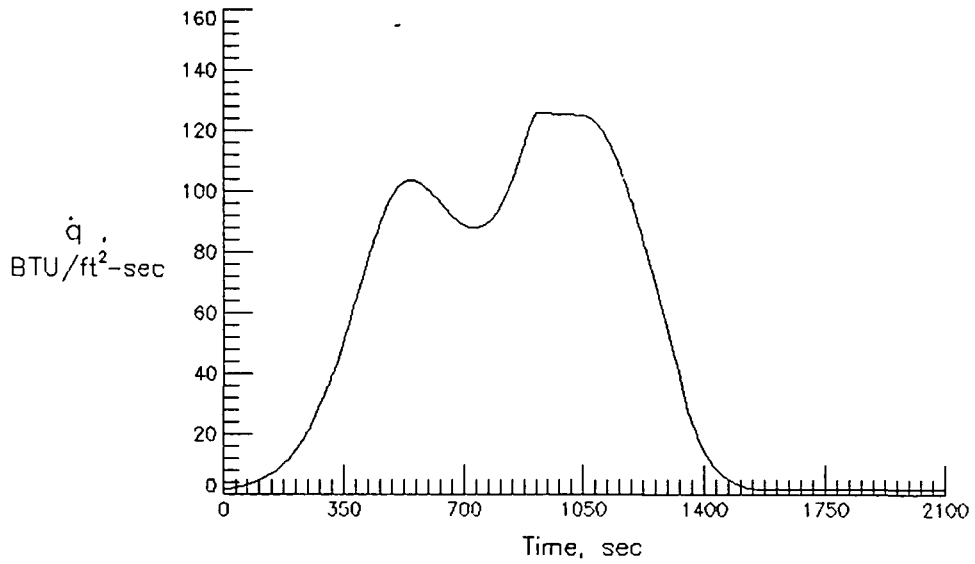
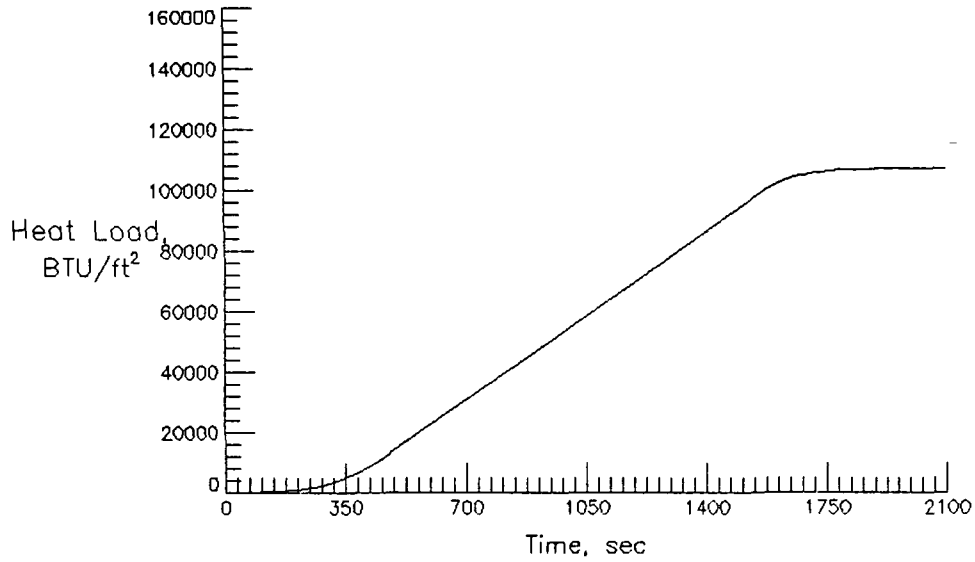


Figure A-9. Baseline heat-rate profiles.

ORIGINAL PAGE IS
OF POOR QUALITY

ERV CRUISING SYNERGISTIC PLANE CHANGE $\dot{Q}=80$



ERV CRUISING SYNERGISTIC PLANE CHANGE $\dot{Q}=125$

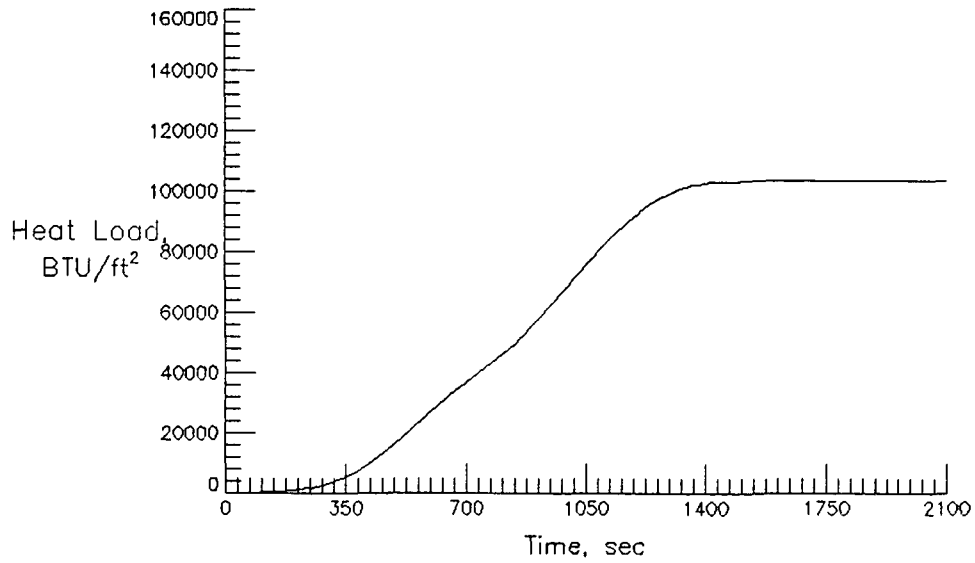
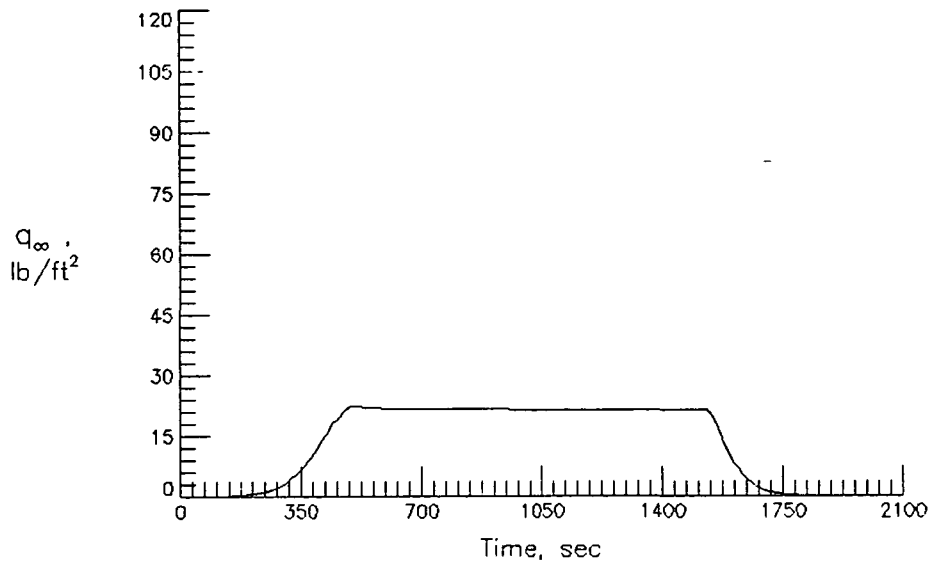


Figure A-10. Baseline heat-load profiles.

ERV CRUISING SYNERGISTIC PLANE CHANGE Q-DOT=80



ERV CRUISING SYNERGISTIC PLANE CHANGE Q-DOT=125

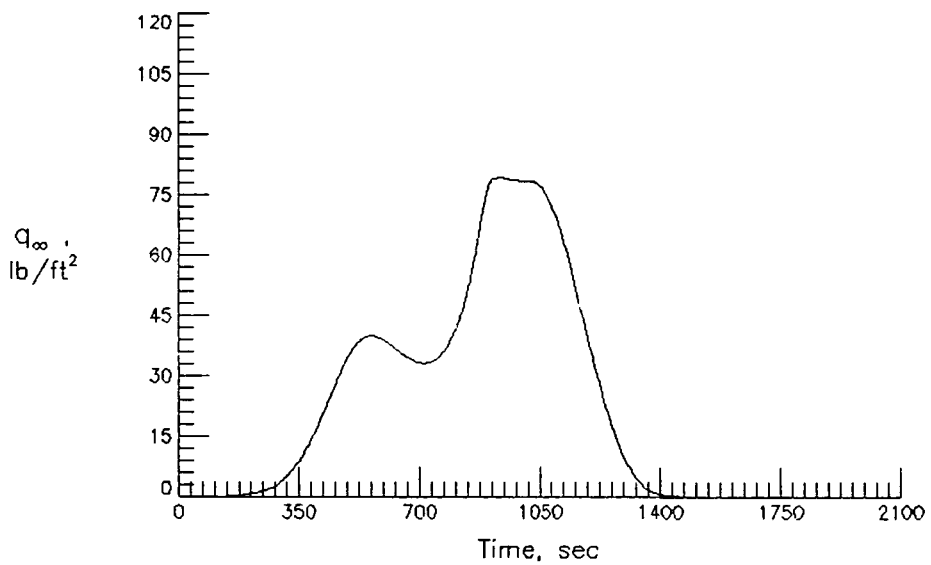
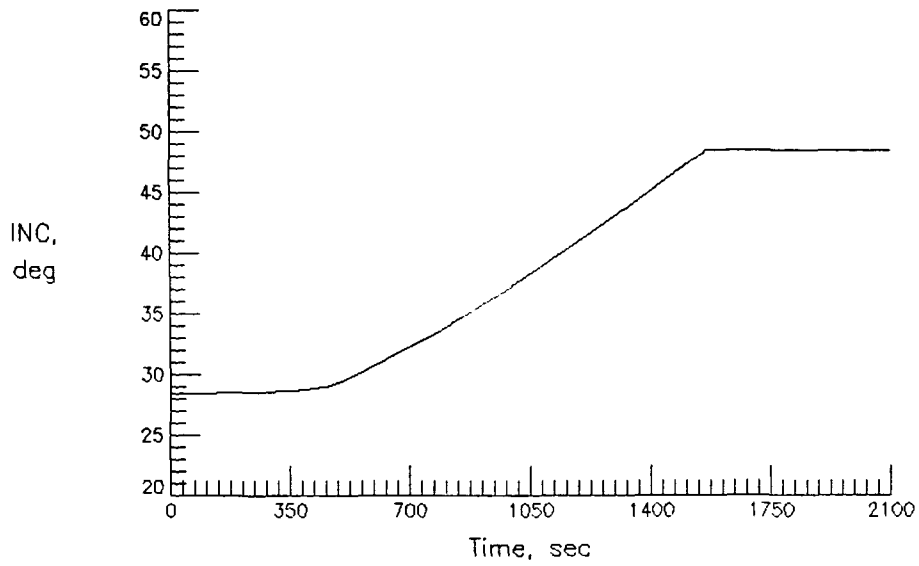


Figure A-11. Baseline dynamic pressure profiles.

ERV CRUISING SYNERGISTIC PLANE CHANGE $\dot{Q}=80$



ERV CRUISING SYNERGISTIC PLANE CHANGE $\dot{Q}=125$

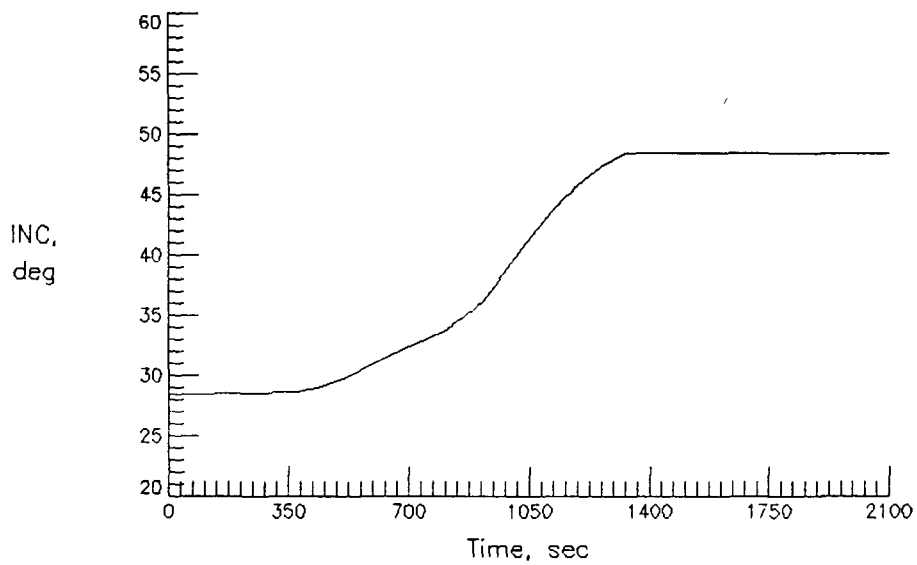


Figure A-12. Baseline inclination angle profiles.

APPENDIX B

DRAPER ERV COMPUTER SIMULATOR AND GUIDANCE ALGORITHM

B.1 SIMULATOR DESCRIPTION

The ERV simulator is a three degree-of-freedom (point mass) simulator used to simulate the atmospheric phase of an orbital plane change maneuver. A fourth order Runge-kutta integrator is used to integrate the vehicle state. A spherical earth gravity model and a 1962 standard atmospheric model are used. Bank angle, angle-of-attack, and throttle are controllable with bank angle and angle-of-attack being rate limited. Thrust is modeled as a force along the ERV's longitudinal axis through the center of gravity. Complete ERV CL and CD data including viscous interaction effects are used.

B.2 SIMULATOR AND GUIDANCE ALGORITHM COMPUTER PROGRAM

The computer program for the CSDL ERV simulation and guidance algorithm actually consists of a control program and a plot program that collects and uses 14 other programs to generate the trajectory data and plot information. While some of the programs were developed or modified

by the author for his own application, most of the code was modified and or developed by R. Richards based on previous in-house computer simulators at C.S Draper Laboratory (19).

The software is written in MAC, a language developed at and used only at Draper Laboratory. It is an excellent language for dealing with vector and matrix quantities and operations. However, because of the unique language in which the software is written and because the total collection of code is nearly 300 pages, the actual code is not included (The computer code can be obtained though by contacting the CSDL NASA Department, Guidance and Navigation Division, 10E).

To provide at least a basic understanding of the ERV computer simulator and guidance program, a listing and brief description of the programs used are shown below. Figure B-1 provides a top level flowchart showing how the programs are grouped and connected.

1. Control Program: Provides a top-level input/output control channel for the various subprograms. Allows for easy changes in vehicle and atmospheric conditions (e.g., density, aerodynamic, and engine performance) by the operator.
2. Plot Program: Uses data collected by the control program to plot various trajectory parameters (e.g., altitude, velocity, and heat-rate).

3. Driver Program: Reads data from the control program and calculates the initial vehicle state to be used by the other subprograms. Also collects information from the other programs and prints the desired output.

4. ERV Simulator Program: Uses the initial ERV state information along with atmospheric, vehicle performance, and guidance information to estimate the current vehicle state.

5. Guidance Program: Provides the guidance information produced by the guidance algorithm described in Chapter 5. Outputs include the commanded angle-of-attack, bank angle, and throttle setting.

6. Predictor/Corrector Program: Predictor/corrector algorithm for the guidance program. Outputs include the estimated final inclination change, apogee altitude, and final vehicle weight.

7. Conic Program: Performs the conic calculations for the predictor/corrector and simulator program.

8. Kepler Program: Solves the Kepler problem for the conic program.

9. Atmosphere Program: Provides the atmospheric model data (e.g., density, temperature, and dynamic pressure) for the various subprograms.

10. CLCD Driver Program: Provides the ERV aerodynamic data to the simulator program. Interpolates the vehicle's CL/CD data based on angle-of-attack and a correlation parameter of either altitude, viscous, or mach number.

11. VINV Programs: Calculates the viscous correlation parameter values for the CLCD Driver program.

12. DATA, DATA 1,2 and 3: Contains the tables of ERV aerodynamic data.

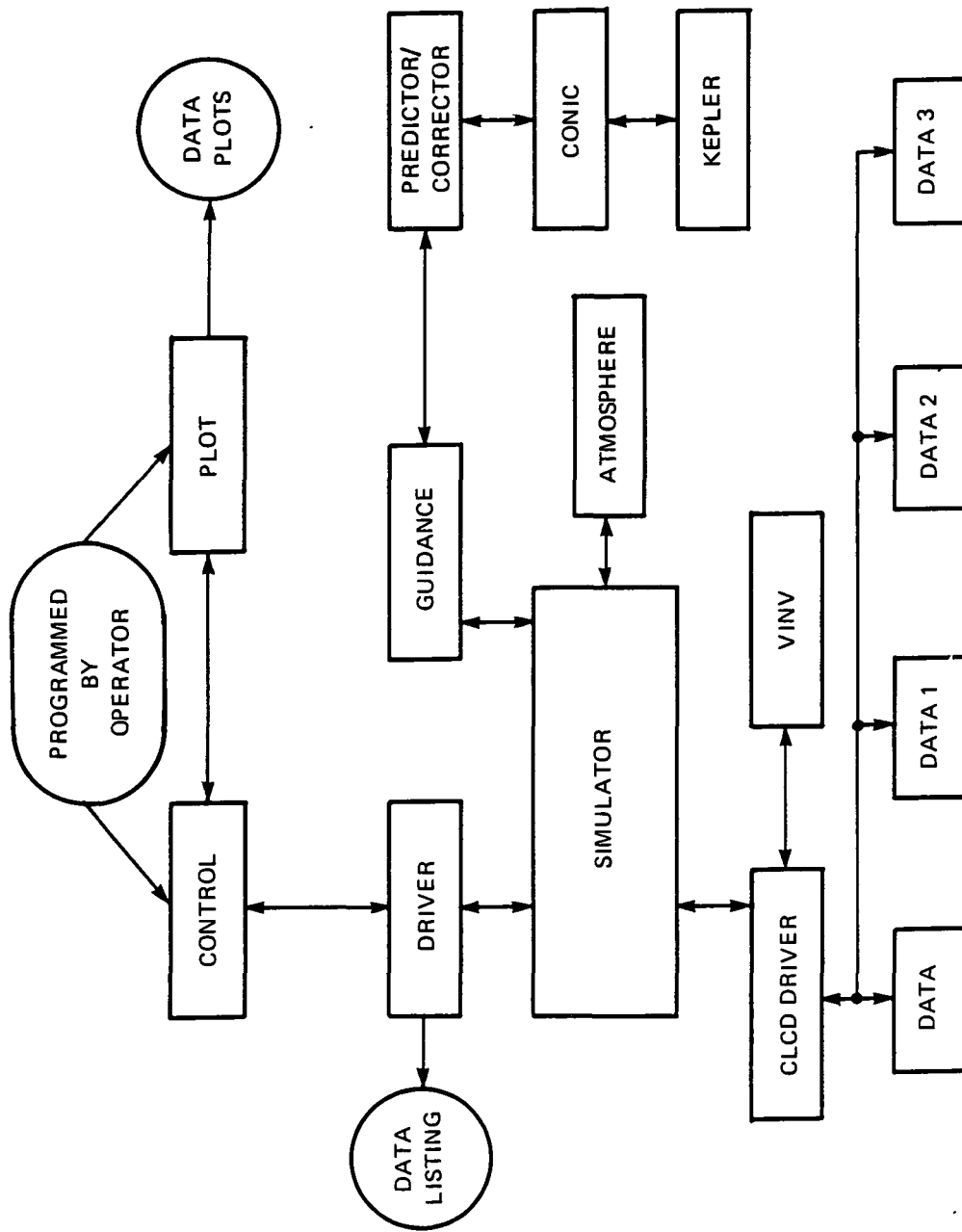


Figure B-1. ERV top-level computer simulation and guidance algorithm flowchart.